Mechanism of IKK activation by the Kaposi's sarcoma-associated herpesvirus protein vFLIP and its cellular homologues

Mehdi Baratchian

Thesis submitted to the University College London
for the degree of Doctor of Philosophy
2014

Division of Infection and Immunity
University College London

DECLARATION

I, Mehdi Baratchian, confirm the work presented in this thesis is my own. Where information has been derived from other sources, I confirm that this has been indicated in the thesis. No part of this thesis has been or is currently being submitted for any other degree in this university or elsewhere.

آدمی چون کشتی است و بادبان

تا کی آرد باد را آن بادران

مولانا

ABSTRACT

Activation of the NF-κB pathway is linked to cancer development and progression. Kaposi's sarcoma-associated herpesvirus (KSHV/HHV8) encodes vFLIP which binds to the NEMO/IKKγ subunit of IKK and constitutively activates NF-κB, leading to tumourigenesis. Cellular FLIPs, which share sequence homology with KSHV vFLIP and induce NF-κB activation, are upregulated in a variety of malignancies and are therefore promising targets for anti-cancer therapies. The cFLIP family consists of three splice variant isoforms ($cFLIP_L$, $cFLIP_S$ and $cFLIP_R$) and two proteolytic fragments (p43-FLIP and p22-FLIP). Much is known about how cFLIPs regulate apoptosis but the mechanisms by which they activate NF-κB are not well understood. Potential similarities to vFLIP-induced activation have been suggested but not investigated.

Here we show that, unlike KSHV vFLIP, cFLIP variants are not found in stable complexes with NEMO and all require upstream events to mediate signalling to IKK. By mutational analysis on NEMO and protein expression knockdowns, we demonstrate that all cFLIP isoforms require the ubiquitin binding domain (UBD) of NEMO while it is redundant for vFLIP's function. Similarly, our data reveals that TAK1 is essential for induction of IKK by cFLIP isoforms but not vFLIP. We further show that different cFLIP isoforms have different requirements for IKK activation. While $cFLIP_L$ needs LUBAC to activate NF-κB, $cFLIP_S$ and p22-FLIP require FADD and RIP1. Contrary to existing reports, our results suggest that processing of $cFLIP_L$ to p22-FLIP or p43-FLIP fragments by caspase-8 is not necessary for its IKK activation. Finally, we propose that vFLIP-mediated activation of IKK is most likely to occur through induction of multimerisation and re-orientation of the IKK complexes within higher order IKK assemblies that lead to autophosphorylation of the enzymatic subunits, IKKα and β.

In conclusion, the work in this thesis provides evidence that vFLIP, $cFLIP_L$, $cFLIP_S$ and p22-FLIP have specific and different mechanisms of inducing IKK activation. This has implications for the design of therapeutics to block pathological NF-κB activation in viral and non-viral tumours.

ACKNOWLEDGEMENTS

First and foremost, I am deeply grateful to Mary Collins for supervising this PhD. Her constant encouragement, guidance, patience and support from the first time I met her in Tehran has gone beyond my expectations. Without her help, this would have not been possible.

It has been a privilege to be part of the Collins lab and I would like to thank all the past and present members of the lab. An especially big thank you to David Escors for training me during the early stages of my PhD and his great advice during the past four years. Christopher Bricogne's help and friendship are highly valued legacies of our time in the UCL Cancer Institute and I will fondly remember our 8 pm discussions in the lab. I also owe many thanks to fellow colleagues: Doug, Fred, Sean, Khaled, Gary, Chris and Kam for providing a fantastic environment to work in and for many scientific and non-scientific discussions we have had over these years.

A word of thanks goes to my MPhil/PhD examiners -Mahdad Noursadeghi and Pablo Rodriguez- for their advice. I also gratefully acknowledge the funding from UCL graduate school which made this PhD possible.

I am eternally grateful to my parents Rafat and Zaman, my sister Sima, my brother Mohammad Reza and my nephews Sina and Taha for their love, support and belief in me. In particular, my late father who has been and always will remain my source of inspiration in life. To him, I dedicate this thesis.

I am also indebted to my parents in-law, Hoda and Imad, for their unconditional love and support throughout.

An enormous thank you to my cousin Mohamad Alimohamadian for everything he has done for me. You are a great friend and have always been close to me in spite of distance.

Last but not least, to my best friend and wife Maha, not enough words can describe how grateful I am. You have been a constant source of strength and happiness for me and have always changed me for the better. I love you.

TABLE OF CONTENTS

LIST OF FIGURES

LIST OF TABLES

ABBREVIATIONS

aa	amino acid
aka	also known as
Atg	autophagy-related protein
ATP	adenosine 5'-triphosphate
BCA	bicinchoninic acid
BSA	bovine serum albumin
CC	coiled coil
CD	cluster of differentiation
cDNA	complementary DNA
cFLIP	cellular FLICE-like inhibitory protein
cIAP	cellular inhibitor of apoptosis
CMV	cytomegalovirus
cPPT	central polypurine tract
CYLD	cylindromatosis protein
DED	death effector domain
DISC	death-inducing signalling complex
DMEM	Dulbecco's modified Eagle's medium
DNA	deoxyribonucleic acid
dNTP	deoxynucleotide triphosphates
DR	death receptor
DTT	dithiothreitol
DUB	deubiquitinase
E1	ubiquitin-activating enzyme
E2	ubiquitin-conjugating enzyme
E3	ubiquitin ligase
ECL	enhanced chemiluminescence
EDTA	ethylenediaminetetraacetic acid
EGTA	ethylene glycol-bis(-aminoethyl ether)-N,N,N',N'-tetra acetic acid
ERK	extracellular signal-regulated kinase
FBS	foetal bovine serum
FLICE	Fas-associated death domain-like interleukin-1β-converting enzyme
FW	forward primer
GAPDH	glyceraldehyde-3-phosphate dehydrogenase
GFP	green fluorescent protein
GST	glutathione-S-transferase
HIV	human immunodeficiency virus
HLX	helical domain
HOIL-1L	longer isoform of heme-oxidised IRP2 ubiquitin ligase-1
HOIP	HOIL-1L interacting protein
HRP	horseradish peroxidase

HSP	heat shock protein
$Hygo^R$	hygromycin resistance gene
IB	immunoblotting
Ig	immunoglobulin
IKK-K	IKK-activating kinase
IL-1	interleukin-1
IP	immunoprecipitation
IκB	inhibitor of κB
JNK	Jun N-terminal kinase
KA	kinase assay
Kb	kilobases
KD	knockdown
kDa	kilodalton
KO	knockout
LB	Luria Bertani
LPS	lipopolysaccharide
LTR	long terminal repeat
LUBAC	linear ubiquitin chain assembly complex
LV	lentiviral vector
LZ	leucine zipper
M	molar
MAPK	mitogen-activated protein kinase
MEF	mouse embryonic fibroblasts
MEKK3	mitogen-activated protein/ERK kinase kinase 3
MOI	multiplicity of infection
mRNA	messenger RNA
mTOR	mammalian target of rapamycin
NBD	NEMO binding domain
NEMO	NF-κB essential modulator
NF-κB	nuclear factor κB
NIK	NF-κB inducing kinase
^oC	degrees Celsius
OD	optical density
OE-PCR	overlap extension-PCR
OIS	oncogene-induced senescence
PAGE	polyacrylamide gel electrophoresis
PBS	phosphate buffered saline
PCR	polymerase chain reaction
PMA	phorbol 12-myristate 13-acetate
PMSF	phenylmethanesulfonyl fluoride
PP2A	protein phosphatase type2A
$Puro^R$	puromycin resistance gene
PVDF	polyvinylidene difluoride
qPCR	quantitative PCR

RIP	receptor-interacting protein
RMPI	Roswell Park Memorial Institute medium
RNA	ribonucleic acid
RPM	revolutions per minute
RS	reverse primer
RT	reverse transcriptase
RT	room temperature
SFFV	spleen focus-forming virus
SHARPIN	SHANK-associated RH domain interacting protein
shRNA	short hairpin RNA
SIN	self-inactivating vector
siRNA	small interfering RNA
SMAC	second mitochondria-derived activator of caspases
SP	stapled peptide
TAK1	TGF-β-activated kinase 1
TCR	T cell receptor
TEMED	tetramethylethylenediamine
TGF-β	transforming growth factor-β
TLR	Toll-like receptor
TNF	tumour necrosis factor
TRAF	TNF receptor-associated factor
TRAIL	TNF-related apoptosis-inducing ligand
U	unit
UBAN	ubiquitin-binding in ABIN and NEMO
UBD	ubiquitin binding domain
UV	ultraviolet
vFLIP	viral FLICE-like inhibitory protein
VSV-G	vesicular stomatitis virus-glycoprotein
WT	wild-type
ZF	zinc finger

CHAPTER

1

INTRODUCTION

1.1 NF-κB signalling pathway: an overview

Nuclear Factor-κB (NF-κB) is one of the crucial signalling pathways which regulates a wide variety of physiological processes such as innate and adaptive immunity, proliferation, differentiation and cell death. In 1986, NF-κB was identified in David Baltimore's laboratory as an inducible nuclear protein which binds to specific DNA sequences within κ light chain enhancer in B cells, referred to as κB sites (Sen and Baltimore, 1986a, 1986b). Extensive research over the past 27 years has revealed an enormous number of biological roles for this pathway in almost all cell types. The activation of NF-κB is strictly controlled at multiple levels by positive and negative regulatory elements whose malfunction can give rise to various pathologies, notably inflammatory diseases and cancers (Oeckinghaus et al., 2011).

In the following sections, I provide a brief description of NF-κB signalling components and their mechanisms of action.

1.1.1 NF-κB related proteins

In resting conditions, NF-κB is sequestered in cell cytoplasm by inhibitor of κB (IκB). Upon activation by various stimuli such as IL-1 or TNFα, the IκB is phosphorylated by IκB kinase (IKK) complex leading to its ubiquitination and subsequent proteasomal degradation. The released NF-κB is further regulated by post-translational modifications and migrates to nucleus where it promotes the transcription of target genes. In principle, three major families of protein form the backbone of NF-κB signalling network: NF-κB transcription factors, IκB family and IKK complex (Hayden and Ghosh, 2008).

1.1.1.1 NF-κB transcription factors

In mammals, NF-κB family consists of five transcription factors: RelA (p65), RelB, c-Rel, NF-κB1 (p105/p50) and NF-κB2 (p100/p52) encoded by *RELA*, *RELB*, *REL*, *NFKB1* and *NFKB2* genes, respectively (Gilmore, 2006) (Figure 1.1A). Except for RelA, transcription of the other subunits is upregulated by NF-κB, producing a positive feedback loop on stimulated cells (Huxford et al., 2011). Synthesised as large precursor proteins, p105 and p100 undergo proteolytic processing to generate the transcriptionally active mature polypeptides, p50 and p52, respectively (Ghosh et al., 1998). Processing of

p105 occurs constitutively (Karin and Ben-Neriah, 2000; Lin et al., 1998), whereas p100 processing is mediated through regulated signals (Liou et al., 1994).

All members of the NF-κB family share a conserved N-terminal region of roughly 300 amino acids, known as the rel homology domain (RHD) which is responsible for hetero- and homo-dimerisation, nuclear localisation, DNA binding and association with IκBs (Hayden and Ghosh, 2004). In RelA, RelB and c-Rel, the RHD is followed by a transcription activation domain (TAD) which mediates their association with trans-acting factors leading to positive regulation of gene expression (Hayden and Ghosh, 2008). On the contrary, p50 and p52 which lack a TAD fail to mediate transcription as homo-dimers and may act as repressors unless hetero-dimerised with one of the TAD containing NF-κB subunits or other cofactor-recruiting proteins (Hayden and Ghosh, 2008; Zhong et al., 2002). Some studies, however, suggest that these homo-dimers are able to mediate activation through interaction with nuclear IκB proteins which can act as coactivators (Smale, 2012). Unlike the Rel proteins, p100 and p105 precursors contain an ankyrin repeat domain (ARD) in their carboxy terminal halves, similar to that found in the IκB family (Hoffmann et al., 2006). RelB is unique in that it contains a further N-terminal lucine zipper-like (LZ) motif which - in addition to the TAD - is necessary for its full activation (Hayden and Ghosh, 2008).

Through combinatorial interactions, NF-κB subunits can form up to 15 distinct homo- and hetero-dimers (Gilmore, 2006). Although 12 out of the 15 possible dimers have been identified in various tissues, other yet undetected dimers may exit in some specific cellular conditions (Huxford et al., 2011). RelA: p50 is the most abundant of NF-κB dimers, identified in almost all cell types (Oeckinghaus and Ghosh, 2009). The composition of NF-κB dimers can vary depending on cell type, stimulus and duration of signalling (Sen and Smale, 2009). In addition to the combinatorial specificity, various post-translational modifications of NF-κB polypeptides as well as diverse interactions with other coactivators contribute further to remarkable complexity of cell- and stimuli-specific NF-κB responses (Sen and Smale, 2009).

1.1.1.2 IκB family

IκBs consist of structurally related proteins, characterised by the presence of a conserved ARD that mediates their interaction with NF-κB subunits (Li et al., 2006a; Zheng et al., 2011). Based on their subcellular localisation as well as functional and

structural characteristics, the IκB family can be subdivided into two groups of typical and atypical IκBs (Figure 1.1B).

IκBα, Iκβ and IκBε represent the typical cytoplasmic IκBs that function in part by masking the nuclear localisation sequence (NLS) of NF-κB polypeptides - contained within the RHD - and therefore, inhibit their nuclear translocation (Vallabhapurapu and Karin, 2009). In case of IκBα, the NLS masking is incomplete but a nuclear export sequence (NES) within IκBα mediates quick export of NF-κB:IκBα complexes from the nucleus. This leads to continuous shuttling of the complexes between cytoplasm and nucleus. Upon stimulation-induced degradation of IκBα, this balance shifts in favour of nuclear localisation and leads to transactivation (Hayden and Ghosh, 2008). Selective binding of the typical IκBs to specific homo- or hetero-dimers ties them to their distinct functions(Malek et al., 2001; Tran et al., 1997). Discrete degradation dynamics as well as different stimuli-dependant expression modes contribute further to specificity of their transcriptional activities (Hinz et al., 2012).

The atypical IκBs consist of IκBζ, IκBη, IκBNS and B cell lymphoma-3 (Bcl-3) that all predominantly reside in the cell nucleus. Nuclear IκBs can bind to DNA-bound NF-κB, inhibit their degradation and mediate their interaction with various cofactors resulting in positive or negative regulation of transcription (Ghosh and Hayden, 2008). Expression of atypical IκBs, except for IκBη, is limited in resting cells but can be greatly induced upon NF-κB stimulation (Hinz et al., 2012).

Through their C-terminal ankyrin repeat motifs, NF-κB precursors p100 and p105 can also function as IκB-like proteins, sequestering their dimeric partners in the cytoplasm (Naumann et al., 1993a, 1993b) (Figure 1.1B). In contrast to typical IκBs which demonstrate subunit-specific inhibitory function, p105 binds to and inhibits all NF-κB subunits including its own processed form, p50. Recent studies have shown that multiple units of p100 and p105 can form large complexes (referred to as IκBsomes) that contain various NF-κB subunits. Different structural organisation and subunit binding preferences of atypical IκBs suggests that they might have distinct kinetic properties in activation and post-induction termination of NF-κB signalling as compared with typical IκBs (Huxford et al., 2011).

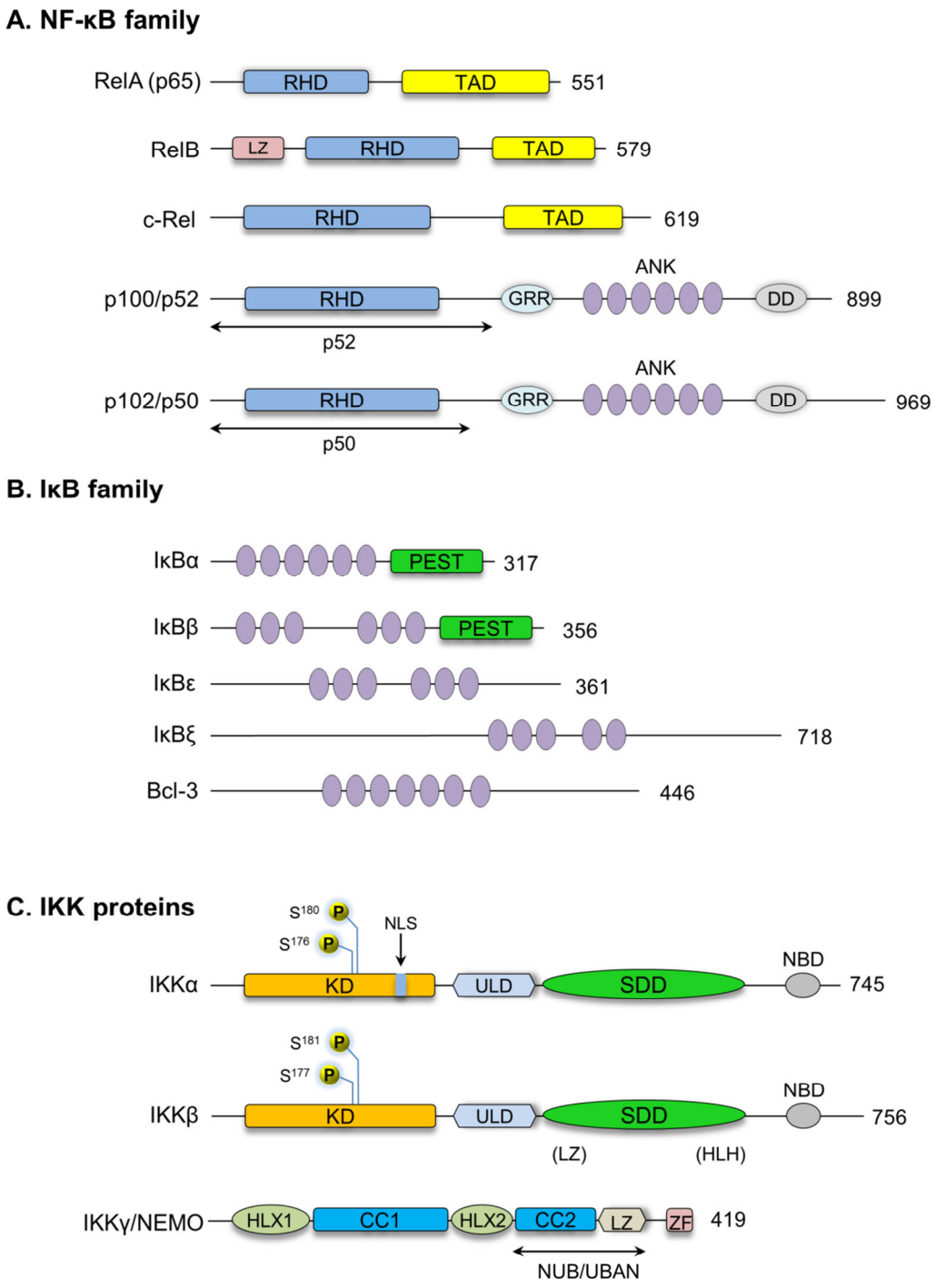

Figure 1.1. Molecular architecture of the NF-κB, IκB and IKK family members. The number of amino acids in each human protein is indicated on the right. **A)** All members of the NF-κB share a rel homology domain (RHD) that is required for their dimerisation, nuclear localisation, DNA binding and sequestration of IκBs. In RelA, RelB and c-Rel, this domain is followed by a transactivation domain (TAD) that mediates transcription initiation at κB sites-containing promoters. RelB additionally harbours a

leucine zipper domain in its N-terminus that is required for its maximal activity. The RHD in the p100 and p105 precursors is followed by a glycine-rich region (GRR), ankryin repeat motifs (ANK) and a C-terminal death domain (DD). The p52 and p50 subunits are shown below the p100 and p105 structures, generated after their proteolysis. **B)** IκB family members are characterised by the presence of multiple ANK motifs which mediate interactions with NF-κB dimers. IκBα and IκBβ contain an additional C-terminal PEST domain (sequences rich in proline (P), glutamate (E), serine (S), and threonine (T) residues) that is important for normal protein turnover. **C)** The core IKK complex consists of the enzymatic subunits, IKKα and IKKβ, and the regulatory subunit, NEMO. Serine residues within the activation loop of the IKKα/β kinase domain (KD) that undergo phosphorylation have been indicated. The previously designated leucine zipper (LZ) and helix-loop-helix (HLH) regions are shown in parentheses. ULD: ubiquitin-like domain, SDD: scaffold/dimerisation domain, NBD: NEMO-binding domain, HLX: helical domain, CC: coiled coli.

1.1.1.3 IκB kinase complex

The IκB Kinase complex is the master regulator of the NF-κB signalling and consists of two enzymatic subunits: IKKα (IKK1) and IKKβ (IKK2) as well as a regulatory subunit known as NF-κB essential modulator (NEMO) or IKKγ (Scheidereit, 2006) (Figure 1.1C). Several biochemical studies on purified IKK complex have proposed a 2:1:1 ratio of the subunits where a dimer of NEMO associates with 1 IKKα hetero-dimerised with 1 IKKβ. However, other combinations of IKK core complex have also been suggested to exist, including the homodimers of IKKα and IKKβ either associated with or distinct from NEMO or separate (Liu et al., 2012). *In vitro* experiments provide evidence that IKK complexes can further assemble to form high-order structures through multimerisation (Drew et al., 2007). This can explain the high molecular weight of the endogenous IKK complexes (700-900 kDa) when separated by gel filtration chromatography. However, it is thought that the elongated shape of NEMO may also be the reason for the apparent molecular weight of IKK (Hayden and Ghosh, 2008).

1.1.1.3.1 The catalytic subunits

IKKα and IKKβ are structurally very similar and share 51% amino acid sequence homology (Mercurio et al., 1997). Both kinases contain an N-terminal kinase domain

(KD) -with two serine residues within the activation loop (S176 and S180 for IKKα, S177 and S181 for IKKβ) that require phosphorylation for the kinase activity, followed by a dimerisation domain and a C-terminal NEMO binding domain (NBD)(Israël, 2010; Liu et al., 2012; Scheidereit, 2006) (Figure 1.1C). IKKα, but not IKKβ, has a putative nuclear localisation signal (NLS) that has been linked to its NF-κB-independent nuclear activities (Sil et al., 2004).

Crystal structures of IKKβ (from human and *Xenopus laevis*) were recently resolved, leading to a significant progress in understanding the domain organisation and function of this enzyme (Liu et al., 2013; Polley et al., 2013; Xu et al., 2011). Based on these studies, IKKβ has a trimodular architecture comprising the N-terminal KD, a central ubiquitin-like domain (ULD) and C-terminal elongated α-helical scaffold/dimerisation domain (SDD) (Figure 1.1C). Interestingly, neither of the previously predicted helix-loop-helix (HLH) and leucine zipper (LZ) motifs form these structures but they are part of the SDD (Xu et al., 2011). The ULD is required for catalytic activity of IKKβ and, together with SDD, is involved in determining the substrates specificity towards IκBα. The SDD mediates dimersiation of IKKβ which is required for kinase activation, but not important for maintaining the kinase activity once the activation loop is phosphorylated (Xu et al., 2011).

In both IKKα and IKKβ, the NBD contains a shared six amino acid sequence (LDWSWL) that is necessary for their interaction with NEMO (May et al., 2002). Cell permeable peptides containing this sequence have been utilised to specifically disrupt IKK-NEMO interaction and prevent cytokine-induced NF-κB activation. Interestingly, competition assays using the peptide mimic of the NBD indicate a considerably weaker interaction of NEMO with IKKα compared to IKKβ (May, 2000). The higher affinity of IKKβ might be due to a unique 12 amino acid region that is not found in IKKα. This extension occurs immediately after the NBD and contains five negatively charged glutamic acid residues (Delhase, 1999). Remarkably, swapping the C-termini of IKKα and IKKβ generates an IKKα with IKKβ-like behaviour. These results suggest that differences in the NEMO binding affinity of IKKα and IKKβ might be responsible for their distinct functions (Kwak, 2000).

1.1.1.3.2 NEMO/IKKγ

The regulatory subunit of IKK complex, NEMO, is a 49 kDa polypeptide predicted to have two helical (HLX) domains interleaved with two coiled-coil (CC) domains, followed by a leucine zipper motif and a C-terminal zinc finger (ZF) (Zheng et al., 2011)(Figure 1.1C). Unlike IKKα and IKKβ, NEMO lacks any intrinsic enzymatic activity. The N-terminal region of NEMO (amino acids 40-120 contained within HLX1 region) mediates its binding to the C-termini of the catalytic subunits (May, 2000). The CC2 domain together with the adjacent LZ form the ubiquitin binding domain of NEMO, generally referred to as the NUB (NEMO ubiquitin binding), CoZi (coil-zipper domain) or UBAN (ubiquitin-binding in ABIN and NEMO)(Bloor et al., 2008; Ea et al., 2006; Wu et al., 2006a). The ZF motif was suggested by a recent study to be required for directing the substrate-specificity of IKKβ towards IκBα (Schröfelbauer et al., 2012). This domain has also been implicated in enhancing affinity of NEMO for binding to ubiquitin chains (Laplantine et al., 2009).

Except for the C-terminus, the α-helical sequence of NEMO is capable of forming coiled-coil structure either alone or in association with a partner protein. The CC regions of NEMO are disrupted in multiple points by amino acids out of coiled-coil register. These breaks can serve as docking sites for interaction with various regulatory proteins and the flexible nature of CC region enhances the efficiency of these interactions (Ghosh et al., 2012).

NEMO is encoded by the *IKKBG* gene located on the chromosome X. In humans, amorphic mutations of NEMO that lead to a lack of NEMO-dependant NF-κB activation are lethal in males but in females cause the disease incontinentia pigmenti (IP). IP is characterised by abnormalities of skin, hair, teeth, nails, and in some cases, neurological complications (Berlin et al., 2002). Hypomorphic mutations of NEMO that result in a weakened, but not obliterated, NF-κB induction have been associated with the X-linked recessive disease of anhidrotic ectodermal dysplasia associated with immunodeficiency (EDA-ID) in males. Symptoms of EDA-ID include severe defects in immunological functions, sparse hair, dental defects and hypohydrosis (Döffinger et al., 2001). Mutations in NEMO have been also identified in patients with Mendelian susceptibility to mycobacterial disease (MSMD) who have recurrent infections with bacteria of the tuberculosis family (Al-Muhsen and Casanova, 2008).

1.1.1.3.3 Other IKK-associated components

Apart from IKKα, IKKβ, and IKKγ which form the core of IKK complex, other proteins have been also reported to participate in the architecture and function of the complex. The chaperones heat shock protein 90 (HSP90) and HSP70 are two such components detected in association with the IKK complex. HSP90 constitutively associates with IKK through its co-chaperone Cdc-37 and has been suggested to stabilise the complex through facilitating its folding. Inhibition of HSP90 by Geldanamycin (an ATPase inhibitor of HSP90) suppresses NF-κB signalling in response to various stimuli such as IL-1, TNFα and PMA (Broemer et al., 2004; Chen et al., 2002). Unlike HSP90, HSP-70 appears to function as a NEMO interacting inhibitor of the IKK through preventing the formation of the complex (Ran et al., 2004). Another component that associates with IKK and regulates its function is a 105-kDa protein, ELKS (a protein rich in glutamate (E), leucine (L), lysine (K) and serine (S)). Immunodepletion analyses suggested that ELKS is a stoichiometric component of IKK (Häcker and Karin, 2006). siRNA-mediated knockdown of ELKS results in reduced levels of IKK activation in response to TNFα and IL-1. Recent studies support a role for ELKS in ATM- and NEMO-dependent NF-κB activation in response to genotoxic stress induced by DNA double stranded breaks (Hadian and Krappmann, 2011; Yang et al., 2011). Although the association of ELKS, HSP90 and HSP70 with IKK have been well-established, the detailed mechanisms by which they regulate IKK have yet to be identified.

1.1.2 Two pathways to NF-κB

Numerous receptor-mediated cascades that lead to activation of NF-κB are classified into two major pathways, the canonical (or classical) and the non-canonical (or alternative) NF-κB pathway. These pathways are distinct in respect to the triggering stimuli, the IKK components involved and the targeted NF-κB subunits.

1.1.2.1 Canonical NF-κB pathway

The canonical pathway is triggered by a broad range of stimuli including inflammatory cytokines (such as IL-1, TNFα, etc), pathogen-associated molecular patterns (PAMPs) and antigen receptors (Bonizzi and Karin, 2004). This pathway is mainly activated through phosphorylation of IκBs at serine residues (equivalent to Ser32 and Ser36 of IκBα) by IKKβ in a NEMO-dependant manner. The phospho-IκBs are then recognised and polyubiquitinated (at residues equivalent to Lys21 and Lys22 of IκBα) by

the E3 ubiquitin ligase complex $SCF^{\beta TRCP}$ (Skp1, Cdc53/Cullin1 and F-box protein β transducin repeat-containing protein). Subsequently, the K48-linked polyubiquitin chains mark IκB for degradation by 26S proteasome resulting in the release and nuclear translocation of RelA-containing NF-κB heterodimers, most commonly RelA:50 dimers (Vallabhapurapu and Karin, 2009) (Figure 1.2, left).

Although IKKβ appears to be the predominant kinase of the canonical NF-κB pathway, several lines of evidence support a role for IKKα in this pathway. For example, receptor activator of NF-κB (RANK)-induced classical NF-κB activation in mammary cells depends on IKKα as the key kinase (Cao et al., 2001). Furthermore, IL-1 (but not TNFα)-induced canonical NF-κB induction has been shown to be intact in IKKβ deficient MEF cells (Solt et al., 2007). A recent study showed that IKKα is also involved in negative regulation of classical pathway through phosphorylating Tax1-binding protein 1 (TAX1BP1) and recruitment of the A20 deubiquitinase complex to IKK (Shembade et al., 2011). These findings indicate that IKKα may be involved in both activation and deactivation of canonical NF-κB signalling in response to at least a subset of stimuli.

The ultimate outcome of the canonical pathway is transcriptional activation of the genes that are mainly involved in innate immunity such as pro-inflammatory cytokines (e.g., IL-1, IL-2, IL-6, TNF), chemokines (e.g.,CCL2, CCL3, CXCL8), leukocyte adhesion molecules (e.g., E-selectin, ICAM-1, and VCAM-1), and multiple pro-survival and anti-apoptotic genes (e.g., Bcl-2, Bcl-XL, XIAP) (Bonizzi and Karin, 2004). Substantial increase in susceptibility to infections in conditional IKKβ or RelA KO mice reveals the importance of canonical pathway in immune functions (Pasparakis et al., 2006).

1.1.2.2 Alternative NF-κB pathway

Unlike the canonical NF-κB pathway, the non-canonical NF-κB pathway is activated by a limited number of receptors that belong to the TNF receptor superfamily. These include CD40, lymphotoxin β receptor (LTβR), B-cell activating factor receptor (BAFFR), CD27, RANK, and Fn14 (Razani et al., 2011). Although most signals that activate canonical NF-κB pathway do not activate the non-canonical pathway, the non-canonical signals are able to activate both pathways (Bonizzi and Karin, 2004).

The alternative NF-κB pathway strictly relies on IKKα and appears to be independent of IKKβ and NEMO (Senftleben et al., 2001) (Figure 1.2, right). Activation

of IKKα by NF-κB-inducing kinase (NIK), a member of the mitogen-associated protein 3 kinase (MAP3K) family, is an absolute requirement for switching on the non-canonical pathway (Xiao et al., 2001a, 2004). In resting cells, NIK is constitutively synthesised but cannot be detected due to a rapid degradation mediated by an E3 ubiquitin ligase complex composed of TNFα receptor associated factor-2 (TRAF2), TRAF3, cellular inhibitor of apoptosis-1 (cIAP1) and cIAP2 (Qing et al., 2005; Zarnegar et al., 2008). Evidences suggest that cIAP1/2 are responsible for the K48-linked ubiquitination of NIK while TRAF2 and TRAF3 cooperate to recruit NIK to cIAPs. Upon receptor ligation, the TRAF/cIAP complex is recruited to the receptor whereupon cIAP1/2 synthesises K48-linked Ub chains on TRAF3 instead of NIK. The subsequent degradation of TRAF3 results in the accumulation of NIK that in turn phosphorylates and activates IKKα (Vallabhapurapu et al., 2008; Zarnegar et al., 2008). The activated IKKα then phosphorylates p100 (at ser866 and ser870) and marks it for proteasomal degradation, resulting in the release of the p52: RelB heterodimers that translocate to the nucleus and bind to the relevant DNA sequences (Senftleben et al., 2001; Xiao et al., 2004). The activated IKKα also phosphorylates NIK that leads to its destabilisation and downregulation of downstream signalling events (Razani et al., 2010).

Biological roles of the alternative pathway that are mainly in regulating adoptive immunity include development of secondary lymphoid organs, B-cell maturation and survival, thymic epithelial cell differentiation, dendritic cells (DC) maturation and the osteoclastogenesis. Moreover, recent studies suggest a role or this pathway in regulating T-cell differentiation (Sun, 2012).

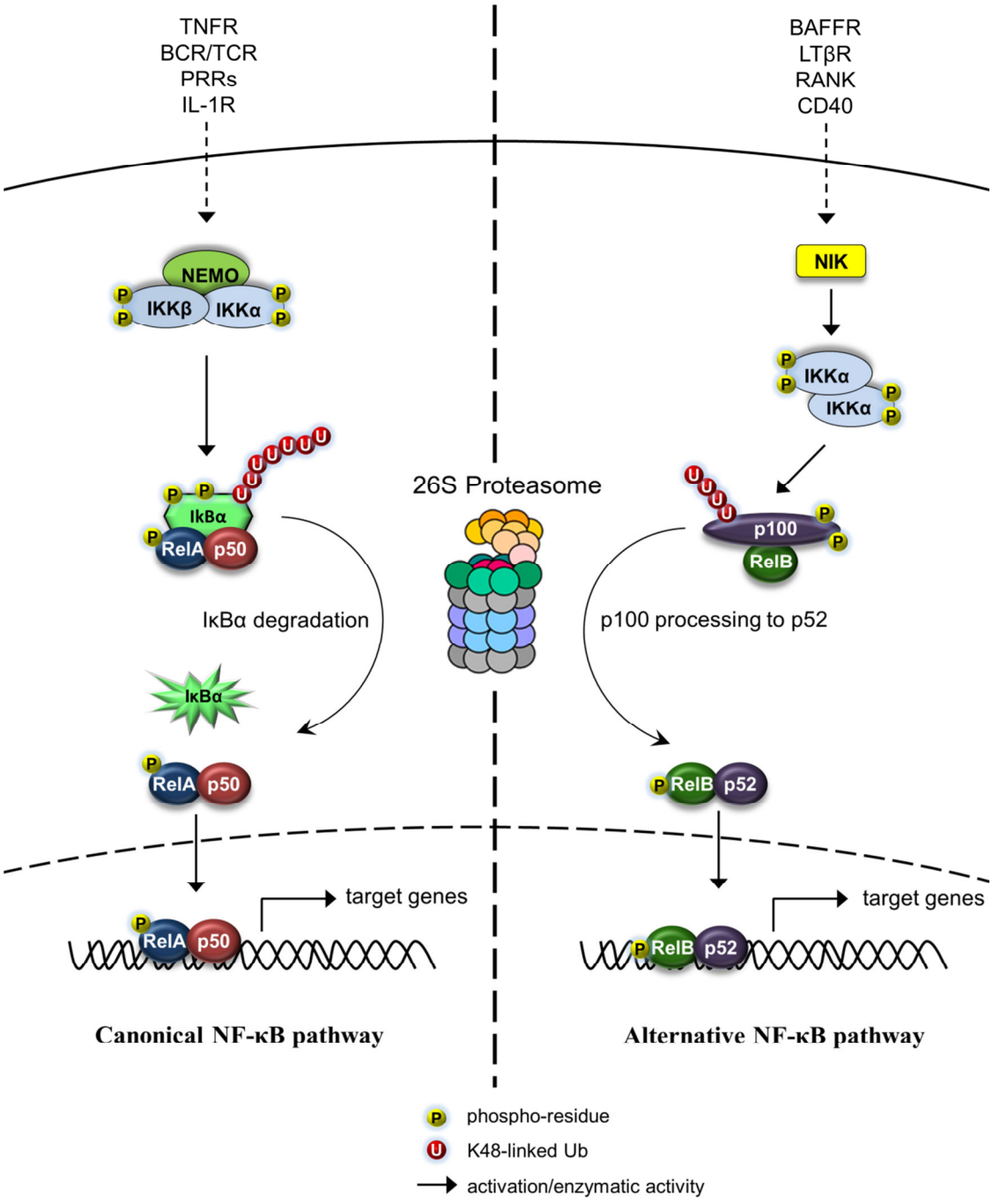

Figure 1.2. A simplified scheme of the canonical and alternative NF-κB activation pathways. Canonical pathway (right) is induced by a diverse range of surface receptors (e.g, TNFR or TLR) which converge on the tripartite IKK complex, comprising IKKα, IKKβ and NEMO. IKK activity results in phosphorylation of the IκB, followed by its K48-ubiquitination and proteasomal degradation. This leads to liberation of the Rel:p50 dimers which can then translocate to nucleus and induce plethora of target genes. Unlike the canonical cascade, the alternative pathway (right) is induced by a small subset of receptors and depends on the NIK-mediated phosphorylation and activation of IKKα homo-dimers. Activated IKKα phosphorylates p100 to induce its partial proteolysis to p52 subunit. Transcriptionally active p52 preferentially hetero-dimerises with RelB to migrate into the nucleus and initiate transcription of target genes.

1.2 Mechanisms behind positive and negative regulation of IKK

To become active, the IKK complex requires phosphorylation of the T loop serines of at least one of the kinases. Similar to other kinases, this phosphorylation is more likely to confer activation through inducing conformational changes in the activation loop (Hayden and Ghosh, 2008). Mutation of these serines (S176 and S180 on IKKα, and S177 and S181 on IKKβ) to alanine prevents kinase activity of the IKK while replacement with phosphomimetic glutamates renders them constitutively active (Mercurio et al., 1997). The exact mechanisms by which the kinase subunits are phosphorylated remain controversial to date. However, three major activation mechanisms have been proposed:

(i) Direct phosphorylation of the kinase subunits by upstream IKK-activating kinases (IKK-K)

(ii) Trans-autophosphorylation of IKK induced by oligomerisation

(iii) Trans-autophosphorylation of IKK induced by conformational changes through protein-protein interaction or posttranslational modifications

These mechanisms are not mutually exclusive and might integrate in various cell- and pathway-specific manners (Häcker and Karin, 2006). Regulation of these mechanisms and the relevant responsible components including various kinases, phosphatases, adaptor proteins and polyubiquitin chains are the subject of the following discussions.

1.2.1 IKK-activating kinases

The role of NIK for the phosphorylation and activation of IKKα in the alternative NF-κB pathway provided compelling evidence for the existence and function of IKK-Ks (Senftleben et al., 2001). Other studies have suggested a role for several other members of the MAP3K family as IKK-Ks in the canonical pathway. The most notable IKK-K is transforming growth factor-β kinase-1 (TAK1, aka MAP3K7) that was initially proposed to activate NF-κB through phosphorylating NIK (Ninomiya-Tsuji et al., 1999). Later on, *in vitro* experiments showed that TAK1, alongside its regulatory cofactors TAK1-binding protein1 (TAB1) and TAB2, can directly phosphorylate IKKβ on the activation loop in a ubiquitin-dependent manner (Wang et al., 2001). In cells, TAB2 or its homologues TAB3, but not TAB1, link TAK1 to upstream components by binding to K63-linked polyubiquitin chains on TRAF6 (in IL-1 signalling) or TRAF2 and RIP1 (in TNFα signalling) (Ea et al., 2006; Ishitani et al., 2003; Takaesu et al., 2000). This bridging is

mediated by a highly conserved C-terminal zinc finger domain on TAB2/3 (Kanayama et al., 2004). The mechanisms by which K63 ubiquitin chains induce TAK1 activation are not well-understood. However, it has been postulated that TAB2/3 binding to ubiquitin chains facilitates oligomerisation of TAK1 complexes leading to autophosphorylation and activation of TAK1 (Chen et al., 2006). In support of this hypothesis, TAK1 becomes phosphorylated at threonine187 within its activation loop and a mutation of this residue blocks its kinase activity (Singhirunnusorn et al., 2005).

siRNA-mediated silencing of TAK1 as well as studies with deletion mutants of functional domains indicated that TAK1 is required for NF-κB activation (Besse et al., 2007; Takaesu et al., 2003). Furthermore, analysis of MEFs derived from TAK1-deficient mice supported a role for this enzyme in IKK activation by stimuli such as IL-1 and TNFα. Nevertheless, animal studies suggest that TAK1 might be dispensable *in vivo*, at least in some cell types. For instance, absence of TAK1 does not impair BCR-induced NF-κB activation (Sato et al., 2005). In addition, deletion of TAK1 blocks TCR induced NF-κB signalling in thymocytes, but not in effector T cells (Liu et al., 2006; Wan et al., 2006). Based on these results, it seems plausible that the requirement for TAK1 to activate IKK may be cell type-specific.

Other studies have provided a role for mitogen-activated protein/ERK kinase kinase 3 (MEKK3, aka MAP3K3) as an IKK-K. Initial studies with *MEKK3*$^{-/-}$ fibroblasts suggested its importance in TNFα-induced NF-κB activation downstream of TRAF2 and RIP1. These cells showed reduced levels of IκBα degradation and the p65/p50 DNA binding in gel shift assays was severely impaired in response to TNFα. Since MEKK3 physically interacted with RIP1, it was proposed to mediate RIP1 signalling to IKK (Yang et al., 2001a). Later, Blonksa et al., were able to restore NF-κB activation in RIP1-defiecient cells using a fusion protein composed of full length MEKK3 and RIP1 death domain (Blonska et al., 2005). This protein could directly associate with TRADD, indicating that RIP1 is likely responsible for recruiting MEKK3 to the TNFα receptor complex.

MEKK3 is also implicated in IKK activation by IL-1R/TLR pathways and lysophosphatidic acid (LPA) (Huang et al., 2004b; Sun et al., 2009a). Similar to TAK1, MEKK3 interacts with TRAF6 upon induction of IL-1R/TLR pathways (Huang et al., 2004b). Yao et al., described independent pathways for IL-1 induced NF-κB activation by TAK1 and MEKK3. The TAK1-mediated pathway was shown to result in activation of

IKKβ, followed by IκBα phosphorylation and degradation; whereas the MEKK3-dependent pathway led to NF-κB activation by NEMO phosphorylation and IKKα activation resulting in IκBα phosphorylation and dissociation from NF-κB subunits without its degradation (Yao et al., 2007). LPA-induced IKK activation, on the other hand, appears to be dependent on MEKK3, but not TAK1 (Sun et al., 2009a). Despite these findings, the physiologic importance of MEKK3 in NF-κB pathways has yet to be determined *in vivo*. Animal studies are partially hindered by the fact that MEKK3 knockout mice die at embryonic day 11 due to defects in angiogenesis and cardiovascular development (Yang et al., 2000).

Two other MAP3Ks, MEKK1 and MEKK2, also exhibit ability to activate the IKK complex. Overexpression of MEKK1 and MEKK2 results in phosphorylation of IKKα/β in cells (Lee et al., 1997, 1998; Zhao, 1999). Although recombinant MEKK1 is shown to activate IKKs *in vitro*, there is no evidence for direct phosphorylation of IKKs by MEKK2. An analysis of biphasic cytokine-induced NF-κB activation demonstrated a mechanism in which MEKK2 regulates delayed NF-κB responses by assembling into IκBβ:NF-κB/IKK complexes; while MEKK3 inducibly associates with IκBα:NF-κB/IKK complexes and mediates rapid activation of NF-κB (Schmidt et al., 2003).

Taken together, results from different studies suggest that IKK-Ks might have either redundant roles, cooperate to signal to IKK or function in distinct NF-κB pathways. Depending on the cell- and pathway-specific conditions, all three possibilities may exist. That being said, the exact role of IKK-Ks in IKK activation is still a matter for debate. Considering that IKK complexes can be activated by artificially enforced oligomerisation *in vitro* (Tang et al., 2003), IKK-Ks may contribute to amplification of IKK activity where it has been already initiated by trans-autophosphorylation. These functions, nevertheless, might be interchangeable in cells.

Attempts to identify additional IKK-phosphorylating kinases have been hampered in part by the limitations of siRNA screenings. This is due to the fact that achieving complete protein knockdown in the whole cell population is almost impossible and the residual expression of a kinase is often sufficient to activate a signalling pathway normally (Liu et al., 2012).

1.2.2 IKK-regulating phosphatases

Negative regulation of the MAPK signalling pathways by numerous MAPK phosphatases (MKPs) is well-established (Liu et al., 2007). By contrast, only a few phosphatases have been implicated in the modulation and termination of NF-κB pathway. The most prominent of all is a ubiquitously expressed serine/threonine phosphatase known as protein phosphatase type2A (PP2A). PP2A exists as heterotrimeric holoenzymes composed of one catalytic C subunit (PP2Acα or β isoforms) and a scaffolding A subunit (PR65α or β) which together form the core dimer, as well as a regulatory B subunit (Janssens and Goris, 2001). There are at least 18 regulatory B subunits whose binding to the 'AC' core is speculated to control PP2A substrate selectivity, catalytic activity and subcellular localisations (Cho and Xu, 2007).

Several early studies associated PP2A activity with down-regulation of NF-κB on the observation that treatment with PP2A inhibitors enhanced IKK activation and blocked RelA phosphorylation in response to cytokines (DiDonato et al., 1997; Maggirwar, 1995; Yang et al., 2001b). In addition, recombinant PP2A could inhibit IKK activity and dephosphorylate RelA *in vitro* (DiDonato et al., 1997; Li et al., 2006b). In agreement with these findings, a more recent study demonstrated that siRNA-mediated silencing of various catalytic and regulatory PP2A subunits results in prolonged TNFα-induced NF-κB activation. Using co-immunoprecipitation and *in vitro* phosphatase assays, distinct PP2A complexes including PP2Acβ/PP2R1A , PP2Acα/PP2R1B and PP2Acα/PP2R1A/PP2R5C were detected to associate with and dephosphorylate IKKβ (on S181), RelA (on S536) and TRAF2 (on T117), respectively (Li et al., 2006b). In T-cells, through the regulatory subunit PP2R1A, PP2A interacts with Carma1 and removes the PKCθ-dependent phosphorylation of this protein on serine 645, thereby inhibiting the TCR-induced IKK activation (Eitelhuber et al., 2011). These results suggest that different combinations of PP2A holoenzymes may operate at different levels of the NF-κB pathway.

Although dephosphorylation of IKKβ by PP2A has been reported by multiple research groups (Hong et al., 2007; Prajapati et al., 2004; Witt et al., 2009), some contradictory reports also exist. In a study by Sun et al., PP2A did not target IKKβ but rather dephosphorylated the upstream IKK-K, MEKK3. PP2A was shown to physically bind to phosphorylated MEKK3 and specifically dephosphorylate it on threonine516 and serine520 (Sun et al., 2010). Another study from the same group described the

magnesium-dependant phosphatases PPM1A and PPM1B, but not PP2A, as IKKβ phosphatases in the TNFα-induced NF-κB pathway (Sun et al., 2009b).

Interestingly, PP2A is also implicated in positive regulation of the IKK activity (Kray et al., 2005). This is presumably mediated by reversing the inhibitory phosphorylation of NEMO and IKKβ following stimulus-dependant NF-κB activation (See 3.1.1.2). PP2A was detected in stable complexes with NEMO in resting conditions and the deletion of the putative PP2A-binding region on CC1 region of NEMO (amino acids 121-179) resulted in reduced IKKβ phosphorylation and activation in response to TNF-α (Kray et al., 2005). The discrepancies in the reported functions of PP2A and other IKK-regulating phosphatases may be explained by the distinct patterns of the phosphatase expression and/or substrate-specificity within different NF-κB pathways and cell types.

PP1 is another phosphatase demonstrated to associate with and dephosphorylate IKKβ. The adaptor protein CUE domain-containing 2 (CUEDC2) mediates this interaction by recruiting GADD34, a regulatory subunit of PP1, to the IKK complex (Li et al., 2008a). Formation of the ternary complex of IKK/PP1/CUEDC2 was shown to retain IKK in an inactive, non-phosphorylated state but following TNFα stimulation, IKK was transiently dissociated from complex and bound to TRAF2, indicating that PP1 is likely responsible for controlling basal levels of IKK activity..

A recent siRNA screen conducted to identify NF-κB modulating phosphatases in T-cells pulled out PP4R1A as another negative regulator of IKK. PP4R1 which stably and specifically binds to the catalytic subunit PP4c was shown to associate with IKK complex subsequent to TCR-induced NF-κB activation and direct PP4c to dephosphorylate and deactivate IKK complex (Brechmann et al., 2012). Interestingly, PP4c has been linked to positive regulation of NF-κB based on the evidence that it can remove inhibitory phosphate groups from threonine435 of RelA (Yeh et al., 2004). Since PP4c subunit participates in a wide collection of PP4 holoenzymes, the associated regulatory subunits most likely determine the functional outcome of the phosphatase in NF-κB pathways (Chowdhury et al., 2008; Gingras et al., 2005; Lee et al., 2010).

Wild-type p53-induced phosphatase1 (WIP1), which belongs to the magnesium dependent PP2C family of phosphatases, was found to directly interact with RelA and dephosphorylate it on serine536 in response to TNFα stimulation. WIP1 can also

dephosphorylate p38, which appears to be important for induction of a subset of NF-κB target genes such as *IL-6*, *ICAM*, and *IRF1*. Mice lacking WIP1 were reported to have hyperactivated immune responses based on the evidence that following LPS challenge, splenocytes of $WIP1^{-/-}$ mice produced higher levels of κB-dependent inflammatory cytokines, compared with $WIP1^{+/-}$ animals (Chew et al., 2009). However, in contrast to these results, Choi et al., showed that both T- and B-cells exhibit compromised functions in WIP1-deficient mice (Choi et al., 2002).

A few other phosphatases such as Shp-2, PP6c and PTPN21, have been associated with negative regulation of the NF-κB pathway (Li et al., 2006b; Stefansson and Brautigan, 2006; You et al., 2001). However, more work is needed to elucidate distinct roles of these and other NF-κB-regulating phosphatases, in tissue- and pathway-specific conditions.

1.2.3 Ubiquitin-mediated control of IKK

The ability to bind to ubiquitin chains, in free form or conjugated to other proteins, serves as a major mechanism in activating IKK. Ubiquitin-mediated control of IKK that in large depends on NEMO has been suggested to be involved in all possible IKK activation processes of oligomerisation, conformational change induction and recruiting IKK-Ks.

1.2.3.1 The ubiquitin system

Ubiquitin (Ub) is a highly conserved 76 amino acid protein that is expressed in all eukaryotic cells (Hershko and Ciechanover, 1998). The term 'Ubiquitination' or 'Ubiquitiylation' refers to the covalent attachment of ubiquitin molecules to target proteins that is executed by a concerted action of three enzymes (Hoeller et al., 2006). First, the E1 ubiquitin-activating enzyme is loaded with ubiquitin through formation of a thio-ester bond between the C-terminal Glycine of the ubiquitin and the catalytic site Cysteine of E1. The activated ubiquitin is then discharged onto the active site of a ubiquitin-conjugating enzyme (E2), generating an E2-ubiquitin thiol-ester. Finally, an E3 ubiquitin ligase transfers the ubiquitin molecule to the target protein by forming an isopeptide bond between C-terminal carboxyl group of the ubiquitin and the ε-amino group of a lysine residue on a target protein (Ciechanover et al., 1982; Hershko, 1983; Hershko et al., 1983). Interestingly, some proteins without lysine residues have been also

found to be ubiquitinated. In these cases, serine or threonine residues are likely to participate in conjugation to ubiquitin (Cadwell and Coscoy, 2005; Wang et al., 2007b).

To date, two E1s and approximately 50 E2s have been identified in mammals. E3s constitute the largest and the most diverse group of ubiquitin editing enzymes with over 600 members (Bhoj and Chen, 2009; Malynn and Ma, 2010). The E3 enzymes are classified into two families: the really interesting new gene (RING)-type and homologous to the E6-associated protein C terminus (HECT)-type E3 ligases (Bernassola et al., 2008; Petroski and Deshaies, 2005). The HECT-type ligases contain a conserved cysteine residue at the C-terminal part of the HECT motif that forms a thiol-ester bond with ubiquitin. HECT-domain bound ubiquitin can be transferred directly onto target protein (Pickart, 2001). Unlike HECT-type E3s, members of the RING-type family do not appear to form thiol-ester intermediates; instead they serve as scaffolds that bring the E2 and the target protein into close proximity. The RING finger domain contains a conserved pattern of cysteine and histidine residues whose folding allows coordination of two zinc cations (Deshaies and Joazeiro, 2009).

Substrate proteins can be modified either by a single ubiquitin molecules (monoubiquitination) or ubiquitin polymers (polyubiquitination) (Haglund and Dikic, 2005). Each type of modification leads to a distinct regulatory fate. Monoubiquitination has been shown to regulate receptor endocytosis, vesicle sorting, gene silencing and DNA repair events [reviewed in (Hicke, 2001)] . It has been also implicated in regulating enzymatic activity of IKKβ (Carter et al., 2005) and transcriptional activity of the viral oncoprotein HTLV-1 Tax (Gatza and Marriott, 2006; Gatza et al., 2007). Ubiquitin harbours seven lysine residues (K6, K11, K27, K29, K33, K48 and K63) all of which can serve as ubiquitin acceptor sites, promoting formation of seven distinct polyubiquitin chains. In addition, ubiquitin linkages can be formed in a head-to-tail configuration through the N-terminal amino group, to produce so called 'linear' or 'M1-linked' ubiquitin chains (Komander, 2009). Depending on the linkage type, ubiquitin chains adopt distinct structural and functional characteristics (Pickart and Fushman, 2004). Based on the early studies on K48-linked ubiquitin chains, the ubiquitin system was thought to be merely in charge of proteasomal degradation, however the identification and study of other linkage types has revealed diverse biological roles of ubiquitin. All eight types of ubiquitin linkages have been detected *in vivo* and are suggested to regulate functions such as DNA repair (K63), protein interactions (K33), signalling pathway activation (K63, K27, K11, linear),

trafficking (K63) and the well-known proteasomal degradation (K48 , K11, K29) (Behrends and Harper, 2011).

To recognise the signals encoded by ubiquitin moieties, cells have developed a series of modular motifs known as ubiquitin binding domains (UBD) that non-covalently bind to different forms of ubiquitin and transduce their signals into specific cellular pathways (Hicke et al., 2005). Using biochemical and bioinformatics approaches more than 150 types of UBDs have been identified to date. These domains are quite diverse in size (20-150 amino acids), structure and the functions of the UBD-containing proteins (Dikic et al., 2009). UBDs exist in E3s, deubiquitinases and binding adaptor proteins and contribute to their specificity. Most often, the binding affinity of the UBDs and ubiquitin are relatively low (about 10-500 μM) (Hicke et al., 2005). Nevertheless, specific mutations of UBDs, which disrupt ubiquitin binding, lead to impairment of protein function *in vivo* indicating the physiologic importance of these weak interactions (Ea et al., 2006; Kanayama et al., 2004; Wu et al., 2006a).

Most UBDs show little discrimination between different linkages; although some prefer a certain type of polyubiquitin chains (Haglund and Dikic, 2005). For example, the NZF domain of TAB preferentially binds to K63-linked chains; this binding is essential for TAK1 activation (Kanayama et al., 2004; Komander et al., 2009). On the other hand, UBAN domain which is present in proteins such as NEMO, optineurin and A20-binding inhibitor of NF-κB (ABIN), shows high affinities towards linear polyubiquitin chains (Nagabhushana et al., 2011; Nanda et al., 2011; Rahighi et al., 2009).

Ubiquitination processes are employed at multiple stages of both canonical and non-canonical NF-κB pathways. Indeed, cooperative functions of numerous ubiquitin editing enzymes, ubiquitin-binding proteins and different polyubiquitin chains appear to be essential for both negative and positive regulation of NF-κB pathway.

1.2.3.2 Roles of the linear and K63-linked PolyUb chains in IKK activation

Much of our understanding of how polyubiquitin chains activate IKK comes from studying TNF and IL-1 receptor induced NF-κB signalling. In TNF signalling, following the trimerisation of the receptor by TNF, adapter protein (TRADD) (Hsu et al., 1995) and RIP1 (Hsu et al., 1996a) are recruited the to the death domain of TNF receptor (TNFR). TRADD then mediates recruitment of E3 ubiquitin ligase TRAF2 (and TRAF5)(Ermolaeva et al., 2008; Tsao et al., 2000) which in turn provides a platform for

binding of two more E3s, cIAP1 and cIAP2 (Mace et al., 2010; Vince et al., 2009). Next, cIAPs synthesise K63-linked ubiquitin chains on RIP1 (and cIAPs themselves)(Bertrand et al., 2008; Varfolomeev et al., 2008) that serve as a scaffold to bring IKK and TAK1 to close proximity via binding to UBD of their respective subunits, NEMO and TAB2 (or TAB3). K63-linked ubiquitin chains are especially important for TAK1-TAB recruitment and activation since the regulatory subunit TAB2 binds specifically to this type of linkages and not any other (Kulathu et al., 2009).

Similarly, K63 polyubiquitin chains play an essential role in IL-1 and Toll-like receptor (TLR) induced NF-κB activation. Upon IL1R/TLR ligation, adapter protein MyD88 is recruited to the receptor complex which further associates with IRAK1 and IRAK4 via another adaptor protein TRAF-interacting protein with a forkhead-associated domain (TIFA) (Chen, 2012). IRAK1 induces K63-linked autoubiquitination of TRAF6 which depends on the E2 complex, Ubc13/Uev1A E2s (Deng et al., 2000; Lamothe et al., 2007). Activated TRAF6 also catalyses unanchored K63-ubiquitin chains which together with TRAF6-bound ubiquitin chains can recruit TAK1 and IKK, thereby facilitating phosphorylation of IKK by TAK1 (Wang et al., 2001).

Initially, it was thought that UBAN domain of NEMO specifically binds to K63-ubiquitinated components. However, several groups later showed that UBAN is able to discriminate linear and K63-linked Ub chains and remarkably, has 100-fold higher affinity for the first of these (Lo et al., 2009; Rahighi et al., 2009). In keeping with these studies, later a 600 kDa E3 ubiquitin ligase complex, so called LUBAC (linear ubiquitin binding assembly complex) was reported to mediate linear chains synthesis (Kirisako et al., 2006) and activate NF-κB independent of K63 ubiquitination (Tokunaga et al., 2009). LUBAC is composed of three subunits: HOIL-1L (longer isoform of heme-oxidised IRP2 ubiquitin ligase-1), SHARPIN (SHANK-associated RH domain interacting protein) and the catalytic subunit HOIP (HOIL-1L interacting protein) (Gerlach et al., 2011; Ikeda et al., 2011; Kirisako et al., 2006; Tokunaga et al., 2011). Generation of linear linkages is determined by LUBAC independent of the E2 involved. To date, LUBAC is the only known E3 capable of synthesising linear polyubiquitin chains (Iwai et al., 2014).

An interesting recent study showed that most of linear ubiquitin chains formed in response to IL-1 are covalently conjugated to K63-linked ubiquitin oligomers. Furthermore, it was demonstrated that while HOIL-1L preferentially binds to linear chains, the catalytic subunit HOIP specifically interacts with K63-linked ubiquitin chains

as the preferred substrate (Emmerich et al., 2013). These findings indicate that the K63-linked ubiquitin chains formed by upstream E3s like TRAFs and cIAPs might serve as a platform for recruitment of other regulators such as TAK1 and LUBAC. The linear ubiquitin oligomers synthesised by LUBAC can then associate strongly with NEMO and put IKK into a context where it can be phosphorylated by upstream kinases like TAK1, MEKK2 or MEKK3.

Alternatively, ubiquitin binding of NEMO may promote IKK activation through oligomerisation or inducing conformational changes, leading to trans-autophosphorylation of the kinase subunits. The latter hypothesis is supported by the notion that the recognition of linear di-ubiquitin by UBAN of NEMO induces straightening of the coiled-coil region (Rahighi et al., 2009). This conformational alteration may then extend towards N-terminus and provide enzymatic subunits with optimal positioning for trans-phosphorylation. Interestingly, mutating K270 of murine NEMO (equivalent to K277 of human NEMO) can overcome the requirement for ubiquitin binding and renders the IKK complex constitutively active in the absence of any inflammatory stimuli (Bloor et al., 2008). It is possible that the K270A NEMO mimics the conformational changes induced by the ubiquitin binding to WT NEMO. Collectively, these findings propose a model in which NEMO keeps the catalytic subunits in an inactive conformation and ubiquitin binding induces a conformational change that removes this inhibition to promote activation of IKKs by upstream kinases or trans-autophosphorylation.

Besides binding to ubiquitin chains, NEMO is also directly ubiquitinated by LUBAC at lysine residues K285 and K309 (Tokunaga et al., 2009). Reconstitution of NEMO-deficient cells with K285R/K309R double mutant NEMO did not rescue NF-κB activation in response or IL-1 or LUBAC overexpression. Since K309 is located within UBAN, its ubiquitination prevents binding to linear chains while in case of K285, theoretically conjugation and binding to linear polyubiquitin can coexist (Rahighi et al., 2009). However, because of the parallel nature of binding, the UBAN motif of NEMO is unlikely to recognize linear chains in *cis* and binds to ubiquitin chains of another NEMO molecule which may lead to oligomerisation-induced activation of IKK (Iwai and Tokunaga, 2009).

The significance of ubiquitin chain binding and conjugation in canonical NF-κB pathways manifests both in human genetics and mouse models. Mutations in the UBAN

domain of NEMO (D311N, D311G) with deleterious effects on ubiquitin binding ability of NEMO have been associated with EDA-ID (Döffinger et al., 2001; Hubeau et al., 2011). In addition, cpdm (chronic proliferatory dermatitis in mice) mice, which have mutations in the *Sharpin* gene (*Sharpin* $^{cpdm/cpdm}$), develop inflammatory disorders, severe skin lesions and defects in secondary lymphoid organs (Gerlach et al., 2011; Seymour et al., 2007). Cells derived from SHARPIN deficient as well as HOIL-1 knockout mice are sensitive to TNFα-induced apoptosis and have defects in NF-κB activation (Tokunaga et al., 2009, 2011).

1.2.3.3 DUBs and the negative regulation of IKK

Deubiquitinases (DUBs) are a group of cysteine- or metallo-proteases that reverse the activity of E3s by cleaving ubiquitin moieties form target proteins (Harhaj and Dixit, 2011). Counter-regulation of ubiquitination processes by E3s and DUBs plays a crucial role in the regulation of NF-κB pathway and thereby, innate and adoptive immune responses (Sun, 2008). Approximately 100 DUBs are encoded in the human genome which are classified into five families based on the domain structure: ubiquitin-specific proteases (USPs), ubiquitin C-terminal hydrolases (UCHs), ovarian tumour proteases (OTUs), Machado–Joseph disease protein domain proteases (MJDs) and the JAB1/PAB1/MPN domain-containing metallo-enzymes (JAMMs) (Nijman et al., 2005). Similar to E3s, DUBs display intrinsic specificity towards different types of linkages. Recognition and recruitment of various linkages is mainly mediated by UBD of the DUBs but in some cases depends on the ubiquitin-binding adapter proteins or selectivity of the catalytic core (Komander, 2010; Komander and Barford, 2008; Komander et al., 2008). Several DUBs have been implicated in the negative regulation of IKK including CYLD, A20, cellular zinc finger anti-NF-κB (Cezanne), ubiquitin-specific protease 11(USP11), USP15 and USP21.

CYLD was originally identified as a tumour suppressor since the mutation of the encoding *cylindromatosis* gene predisposes individuals for familial cylindromatosis, a genetic disorder characterised by benign tumours of skin (Bignell et al., 2000). DUB activity of this enzyme is mediated by its C-terminal USP domain (Komander et al., 2008). siRNA-mediated knockdown of CYLD enhances NF-κB activation in response to inflammatory stimuli while overexpression of CYLD, but not the mutants lacking DUB activity, reduces NF-κB activation (Kovalenko et al., 2003; Trompouki et al., 2003). Several studies show that CYLD deficient mice are highly susceptible to chemically induced colitis as well as

colon and skin tumours (Reiley et al., 2006; Zhang et al., 2006). CYLD also plays an important role in T-cell development and activation, by regulating lymphocyte-specific protein tyrosin kinase (LCK), an important kinase in T cell receptor signalling (Reiley et al., 2006). CYLD has been demonstrated to target multiple components of the NF-κB pathway for deubiquitination such as NEMO (Kovalenko et al., 2003; Saito et al., 2004), TRAF2 (Brummelkamp et al., 2003), TRAF6 (Jin et al., 2008), RIP1 (Wright et al., 2007), TAK1(Reiley et al., 2007), LCK (Reiley et al., 2006) and the NF-κB subunit co-activator Bcl-3 (Massoumi et al., 2006). CYLD directly interacts with NEMO and TRAF2; however, in certain pathways, it requires ubiquitin-binding adaptor proteins to ensure target specificity. Optineurin and p62 have been suggested to link CYLD with RIP1 and TRAF6, respectively (Jin et al., 2008; Nagabhushana et al., 2011).

In vitro experiments indicate that CYLD preferentially removes linear and K63-linked ubiquitin chains compared to K48-linked oligomers (Komander et al., 2009). Results from two other studies show that CYLD cleaves K48-linked ubiquitin chains of some targets both *in vitro* (Stokes et al., 2006) and *in vivo* (Reiley et al., 2006). Taken together, it is possible that linkage-specificity of CYLD is determined in part by the target proteins.

A20, also known as TNFα-induced protein 3 (TNFAIP3), is an NF-κB inducible protein that contains an N-terminal OTU domain and seven C-terminal zinc fingers (Krikos et al., 1992). A20-deficient mice die prematurely due to extensive inflammation of numerous organs including liver, kidneys, intestines and bone marrow (Lee et al., 2000). These mice are also highly susceptible to sublethal doses of LPS and TNF-α, indicating the substantial role of A20 in terminating inflammatory stimuli. In humans, polymorphisms of the A20 gene have been associated with multiple autoimmune diseases such as systemic lupus erythematous, Crohn's disease, psoriasis and rheumatoid arthritis (Arsenescu et al., 2008; Fung et al., 2009; Musone et al., 2008; Nair et al., 2009; Thomson et al., 2007). Furthermore, inactivating mutations of A20 are found in a large number of human lymphomas (Honma et al., 2009; Kato et al., 2009).

The unique feature of A20 is that it harbours both DUB and E3 activities which are mediated by the OTU and ZF4 domains, respectively (Wertz et al., 2004). In TNFR1 signalling, A20 first removes the K63-linked ubiquitin chains from RIP1, it then synthesises K48-linked ubiquitin polymers on RIP1 which marks it for proteasomal degradation (Wertz et al., 2004). An alternative mechanism has been described for A20

inhibition of the IL-1R/TLR pathways, whereby it blocks TRAF6 ubiquitination by disrupting its association with the E2 enzymes, Ubc13 and UbcH5C (Shembade et al., 2010). Similarly, A20 can inhibit TRAF2 and cIAPs by promoting disassembly of the E2:E3 complexes and triggering ubiquitin-mediated proteasomal degradation of the E2 enzymes. These functions depend on both ZF4 and OTU catalytic domains (Bosanac et al., 2010; Shembade et al., 2010; Wertz et al., 2004). Interestingly, two groups showed that overexpression of A20 mutant (C103A) lacking DUB activity blocks NF-κB activation as efficiently as WT-A20 (Evans et al., 2004; Li et al., 2008b). Consistent with these findings, a recent study demonstrated a non-catalytic mechanism of IKK inhibition by A20 (Skaug et al., 2011). Skaug et al., showed that linear and K63-linked ubiquitin chains on NEMO recruit A20 (via its ZF4 and ZF7) to the IKK complex which then can inhibit phosphorylation of IKK by TAK1, without reducing RIP1 ubiquitination. A20 can also bind directly to the N-terminal region of NEMO; this weak interaction is further stabilised by the interactions between A20 and polyubiquitin chains (Skaug et al., 2011). It is possible that A20 binding to NEMO blocks the IKK oligomersiation or reverses the conformational changes required for the activation of IKK. Taken together, these results suggest that A20 might utilise distinct mechanisms to terminate IKK activation in different NF-κB pathways.

Although A20 and CYLD have many overlapping targets, no obvious functional redundancy exists between these two DUBs. This is presumably due to the distinct temporal order of their function during inflammatory responses (Sun, 2008). While CYLD blocks spontaneous activation of NF-κB, A20 is induced upon NF-κB activation and is crucial to terminate the pathway in a negative feedback loop. Phosphorylation of CYLD by IKK has been shown to be required for TRAF2 ubiquitination and activation of NF-κB and JNK pathways (Reiley et al., 2005). Therefore, phosphorylation-dependant inactivation of CYLD might provide a window for NF-κB activation before signal-induced termination by A20. Linkage type specificity is another key difference between CYLD and A20. *In vitro* studies suggest that A20 preferentially cleaves K48-linked polyubiquitin chains (Komander and Barford, 2008; Lin et al., 2008) while CYLD hydrolyses both linear and K63-linked oligomers (Komander et al., 2008, 2009). In cells, A20 might depend on ubiquitin-binding protein adaptors such as TAX1BP1 and the ABIN-1 to ensure specificity (Mauro et al., 2006; Shembade et al., 2007; De Valck et al., 1999).

In addition to CYLD and A20, other DUBs have been also described to play a role in negative regulation of the NF-κB pathway [reviewed in (Sun, 2008)]. For instance, Cezanne inhibits TNFα-induced IKK activation by promoting deubiquitination of the TNFR- associated RIP1. Similar to A20, Cezanne is rapidly induced in response to TNF-α, although unlike A20, its DUB activity is essential for mediating the inhibitory functions (Enesa et al., 2008; Evans et al., 2003). Recently, Cezanne was reported to preferentially hydrolyse K11-linked ubiquitin oligomers (Bremm et al., 2010); how this function of Cezanne might regulate the NF-κB pathway still remains unknown. USP21 is another DUB which inhibits TNFα-induced IKK activity by also removing polyubiquitin chains from RIP1 (Xu et al., 2010). Clearly, IKK regulating DUBs share many overlapping targets; however the linkage type-specificity and the distinct temporal order of activity might account for their specific functions.

1.3 FLICE-Like Inhibitory Proteins

The first members of the FLICE-like inhibitory protein (FLIP) family were identified as viral genome products (vFLIPs), following a bioinformatic search conducted to recognise death effector domain (DED)-containing proteins that function as apoptosis regulators (Thome et al., 1997). Soon after, a consensus sequence from the viral FLIPs was used to screen human expressed sequence tags and several human homologues were identified, collectively named as cellular FLIPs (cFLIPs)(Irmler et al., 1997). All members of the FLIP family harbour two tandem DEDs in their N-terminal region, similar to that found in caspase-8 and caspase-10 (Fig 1.3). As suggested by structural properties of FLIPs, the initial bioactivity reported was an ability to interact with FADD (Fas-associated protein with death domain) and inhibit apoptosis induced by multiple death receptors (Bertin et al., 1997; Hu et al., 1997a; Irmler et al., 1997; Thome et al., 1997). However, since their discovery, many other biological roles have been described for different FLIPs. In the following sections, I will review the structure and multi-faceted regulatory functions of the cellular and viral FLIPs with a particular emphasis on KSHV vFLIP.

1.3.1 Viral FLIPs

Viral FLIPs are present in several γ-herpesviruses and the human molluscipoxvirus (Figuire 1.3A). The vFLIP-encoding γ-herpesviruses consist of bovine herpesvirus-4

(BHV-4), herpesvirus samiri (HSV), equine herpes virus-2 (EHV-2), rhesus monkey rhadinovirus (RRV) and the Kaposi's sarcoma-associated herpesvirus (KSHV). The genome of molluscum contagiosum virus (MCV) encodes two distinct vFLIPs: MC159 and the closely related MC160 (Searles et al., 1999; Thome et al., 1997). Unlike cFLIPs, the amino terminal DEDs of different vFLIPs are not identical and contain variable amino acid sequences (Figure 1.4). Furthermore, none of the vFLIPs contain a caspase-8-like domain; instead, the serial DEDs are extended by C-terminal tails of variable lengths.

During the early stages of a viral infection, death receptor-induced cell death can effectively demolish the infected cells. Not surprisingly, viruses have evolved various strategies (e.g., expressing vFLIPs) to resist cell death and thereby, facilitate the viral propagation and persistence. The ability of vFLIPs to effectively inhibit apoptotic pathways not only results in persistent infection, but also transforms the host cells (Thome et al., 1997). KSHV vFLIP is a notable example of a viral oncoprotein that plays indispensable roles in tumourigensis of the associated virus.

1.3.1.1 Kaposi's sarcoma-associated virus

KSHV (also known as human herpesvirus-8 (HHV-8)) is the causative agent of Kaposi's sarcoma (KS), a neoplasm of lymphatic endothelial cells. KS is the most common type of malignancy in HIV patients, although it occurs in other immunosuppressive conditions like organ transplant. KSHV is also associated with two B-cell lymphoproliferative diseases, primary effusion lymphoma (PEL) and multicentric Castleman's disease (MCD) (Mesri et al., 2010). Similar to the life cycle of other herpesviruses, KSHV displays both lytic and latent modes of infection. Expression of lytic genes (such as vIL-6, vIRFs, vCCLs and vGPCR) have been documented to contribute to KSHV oncogenicity by initiating the host signalling cascades involved in secretion of cell growth factors. However, KSHV genes pivotal for the viral genomic persistence and cellular transformation are mainly found among those expressed during latent infection (Wen and Damania, 2010). Indeed, KSHV infection is predominantly latent in the associated malignancies. Three KSHV genes are abundantly expressed in the latent mode of infection: vCyclin, latency-associated nuclear antigen (LANA) and vFLIP. These genes are encoded in one tricistronic transcript driven by a single promoter and collectively provide cells with proangiogenic and inflammatory signals, anti-apoptotic abilities as well as enhanced proliferative and growth signals [reviewed in (Cesarman, 2014)].

1.3.1.2 KSHV vFLIP

KSHV vFLIP (also known as K13) is a 188 amino acid protein encoded by ORF71 and shares 33% sequence homology with the cellular homologues. It is a potent and specific activator of the NF-κB pathway (Chaudhary et al., 1999; Matta and Chaudhary, 2004) but also interferes with several other pathways such as autophagy, MAPK and death inducing signalling cascades (See 1.3.3-1.3.6) . Expression of vFLIP induces transcription of up to 200 NF-κB target genes, most notably cFLIP which can further enhance evasion of death receptor induced apoptosis (Punj et al., 2009). Our group has previously shown that NF-κB-mediated secretion of growth factors enables vFLIP to protect cells from detachment-induced apoptosis, or anoikis (Efklidou et al., 2008).

Accumulating evidence support a role for vFLIP in KSHV-associated tumourigenesis through constitutive activation of NF-κB (Ballon et al., 2011; Baud and Karin, 2009; Chugh et al., 2005; Sun et al., 2003). A recent study on transgenic vFLIP knock-in mice indicated that expression of vFLIP in B cells is sufficient to induce B-cell malignancies *in vivo* (Ballon et al., 2011) . Furthermore, vFLIP accelerated the process of lymphomagenesis in Myc-transgenic mice which overexpress Myc in lymphoid organs (Ahmad et al., 2010). In agreement with these findings, pharmacologic or genetic inhibition of vFLIP-induced NF-κB activation leads to apoptosis in PEL cells (Godfrey et al., 2005; Guasparri et al., 2004; Keller et al., 2000). Besides anti-apoptotic effects, vFLIP-mediated NF-κB activation suppresses the lytic reactivation of the KSHV and thereby, further contributes to maintenance of latent infection (Ye et al., 2008).

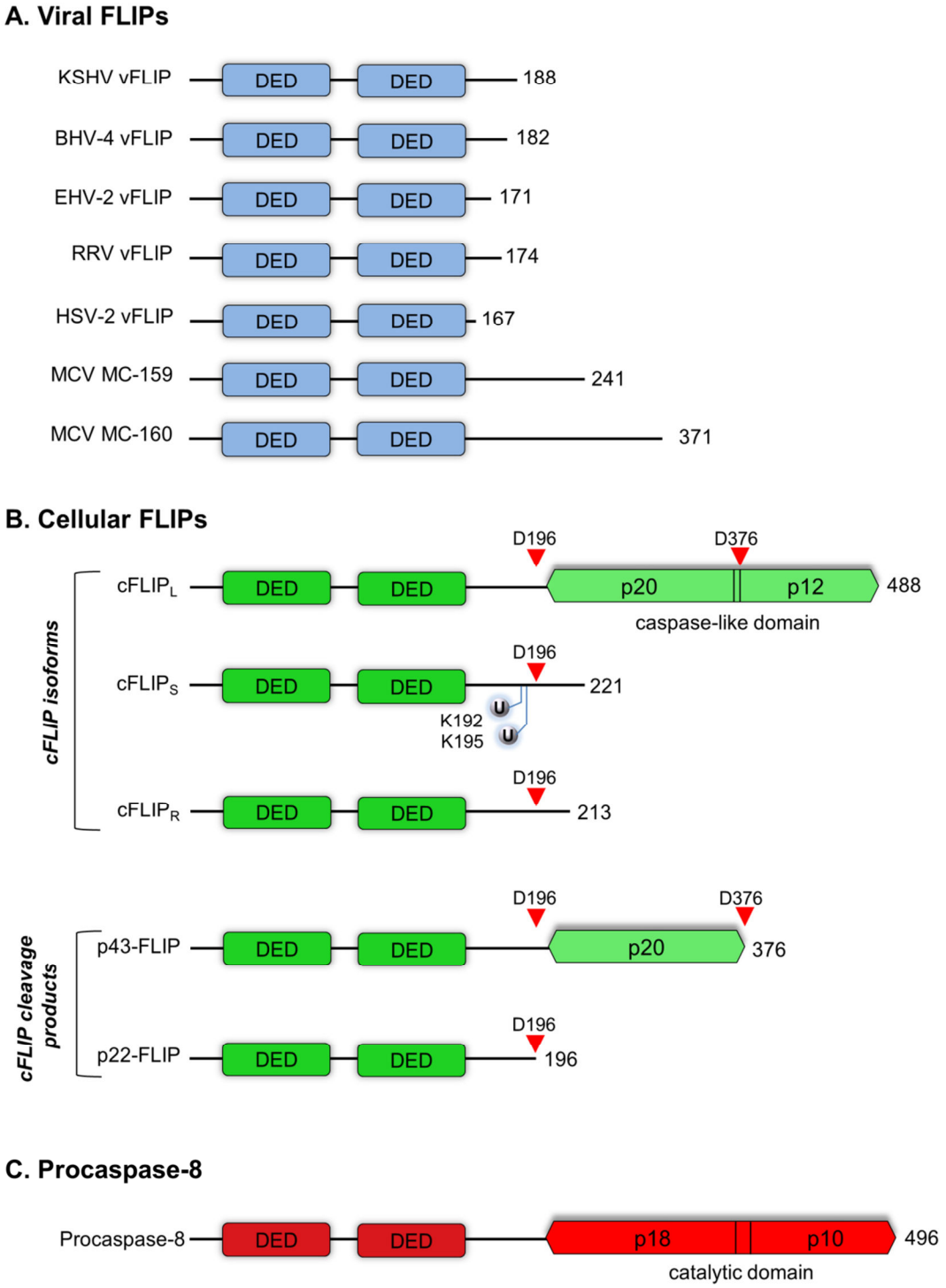

Figure 1.3. Viral and cellular FLIP proteins. A) Viral FLIPs are encoded by several γ-herpesviruses and the human molluscipoxvirus (MCV). Unlike cFLIPs which share a common N-terminal sequence of 202aa, tandem DEDs of different vFLIPs are not identical and contain variable amino acid sequences. **B)** From 13 splice variants of the *cFLAR* gene, only three are translated to protein which consist of a long isoform (FLIP$_L$) and two short variants (cFLIP$_S$ and cFLIP$_R$). cFLIP$_L$ (55kD) is structurally similar to procaspase-8 (C) but its C-terminal caspase domain is enzymatically inactive due to lack of a crucial catalytic cysteine. The N-terminal DEDs of cFLIP$_S$, but not cFLIP$_L$ or vFLIPs,

are followed by a unique 19 amino acid sequence which plays an important role in ubiquitination of $cFLIP_S$ (at the indicated K192 and K195 residues) and its subsequent degradation. Upon interaction with caspase-8, $cFLIP_L$ can further be cleaved at positions D196 or D376 to produce p22- and p43-FLIP fragments, respectively. p22-FLIP is also a cleavage product of $FLIP_{S/R}$. **C)** Domain organisation of procaspase-8

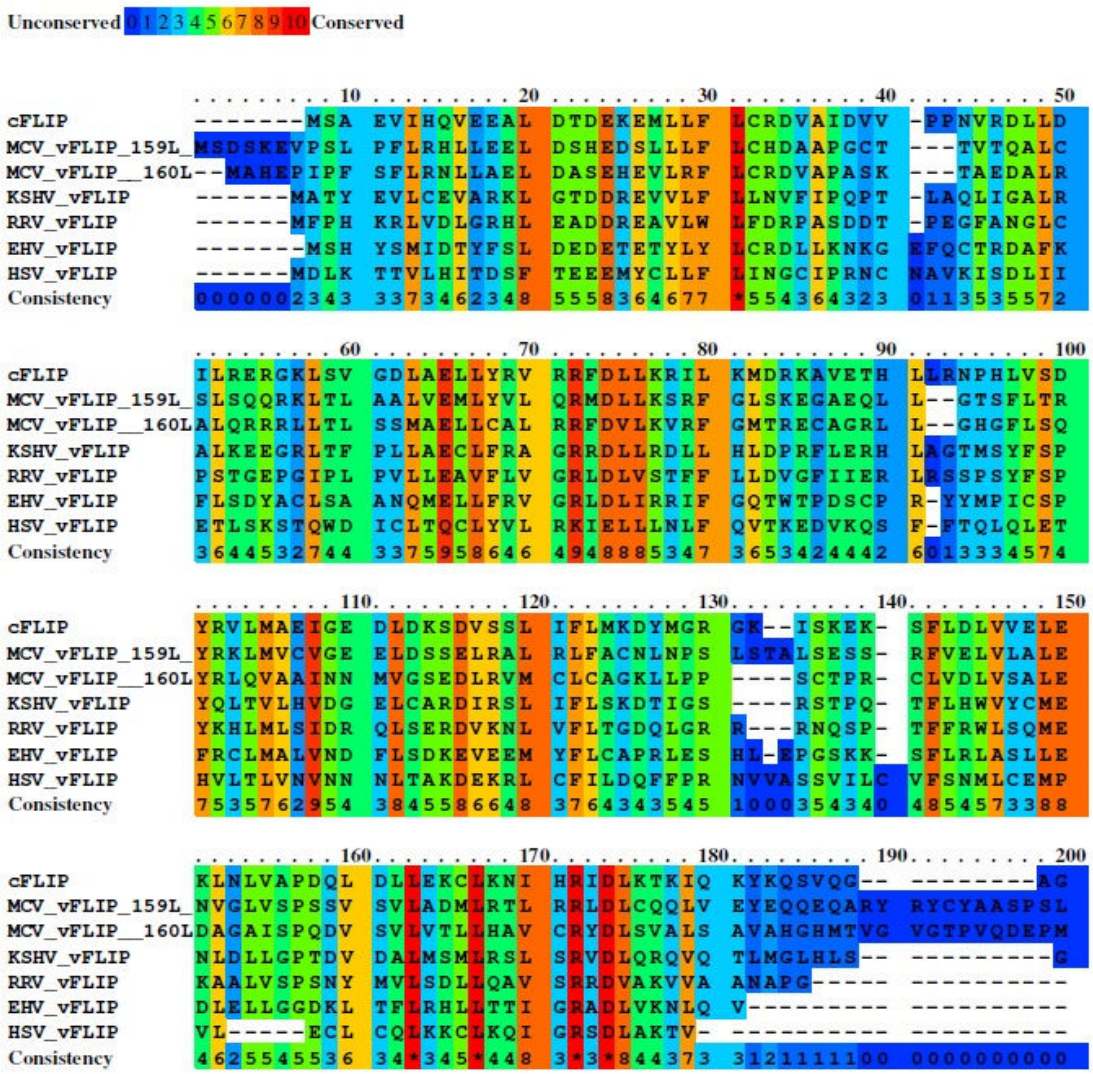

Figure 1.4. Amino acid sequence alignment of the cellular and viral FLIPs. Amino acid sequences of the shown FLIP proteins were retrieved from NCBI protein database (*http://www.ncbi.nlm.nih.gov/protein*) and aligned using PRALINE multiple sequence alignment software. Residues are colour-coded for the rank of conservation. The accession numbers for the protein sequences used for alignment were: cFLIP BAB32551.1, KSHV vFLIP AAD46498.1, RRV vFLIP AAF60069.1, HSV vFLIP CAC84369.1, EHV vFLIP NP_042671.1, MCV vFLIP 159 NP_044110.1, MCV vFLIP160 NP_044111.1.

1.3.2 Cellular FLIPs

In 1997, cellular FLIP proteins were independently identified by several groups and therefore, are recognised by other names such as MRIT (Han et al., 1997), Usurpin (Rasper et al., 1998), iFLICE (Hu et al., 1997b), FLAME1 (Srinivasula et al., 1997), CLARP (Inohara et al., 1997), CASH (Goltsev et al., 1997) and Casper (Shu et al., 1997).

1.3.2.1 cFLIP isoforms and cleavage products

Cellular FLIP is encoded by the *CFLAR* gene (CASP8 and FADD-like apoptosis regulator), located on the human chromosome 2q33-34, close to caspase-8 and caspase-10 genes. Proximity of these genes suggests that cFLIP may have emerged by duplication of procaspase-8/10 genes (Han et al., 1997; Inohara et al., 1997; Rasper et al., 1998; Srinivasula et al., 1997). To date, up to 13 splice variants of human cFLIP have been identified at mRNA level, three of which are expressed as proteins: Long isoform ($cFLIP_L$: 55kDa), short isoform ($cFLIP_S$: 26kDa) and cFLIP Raji ($cFLIP_R$, 24kDa) first isolated from human Burkitt's lymphoma B-cell line, Raji (Golks et al., 2005; Irmler et al., 1997) (Figure 1.3B). Unlike humans, mice do not express $FLIP_S$ and contain only two isoforms of $FLIP_L$ and $FLIP_R$ (Ueffing et al., 2008).

The *CFLAR* gene contains 14 exons and the initially transcribed precursor mRNA undergoes alternative splicing to generate transcripts for different cFLIP isoforms. Inclusion of exon7 which harbours a stop codon, results in translation of $cFLIP_S$, while skipping this exon generates $FLIP_L$-encoding mRNA. Translation of a small part of intron6 generates the shortest isoform, $FLIP_R$ (Djerbi et al., 2001). Recently, a single nucleotide polymorphism (SNP) of the 3' splice consensus of intron6 was identified controlling expression of $FLIP_S$ or $FLIP_R$. Interestingly, the splice-dead SNP which causes the expression of $FLIP_R$ is present at higher frequencies in transformed B cell lines and is also associated with an increased risk of follicular lymphoma in humans (Ueffing et al., 2009).

All cFLIP isoforms share an identical N-terminal sequence of 202 amino acids, which includes two DEDs, but have different C-terminal ends. The overall structure of $cFLIP_S$ is similar to vFLIPs but it contains a unique 19 amino acid C-terminal tail that is responsible for its ubiquitination and proteasomal degradation (Poukkula et al., 2005). In $cFLIP_L$, the tandem DEDs are followed by a caspase-like domain (CLD; composed of p20 and p12) that is similar to the catalytic domain of procaspase-8/10 (Figure 1.3C).

However, this domain is catalytically inactive due to substitution of several amino acids essential for the caspase activity, including a cysteine in the Gln-Ala-Cys-X-Gly motif and a histidine in the His-Gly motif (Budd et al., 2006).

In addition to the natural isoforms, two N-terminal cleavage products of cellular FLIPs have been detected in cells. Caspase-mediated cleavage of the cFLIP at positions D376 (on $FLIP_L$) and D196 (on all isoforms), generates the proteolytic fragments p43-FLIP (43kDa) and p22-FLIP (22kDa), respectively (Figure 1.3B) (Golks et al., 2006; Kataoka and Tschopp, 2004; Scaffidi et al., 1999).

1.3.2.2 Transcriptional and translational control of cFLIPs

Expression of cFLIP proteins is tightly regulated in normal cells. This is achieved through numerous regulatory mechanisms at the transcriptional, translational and post-translational levels (Safa et al., 2008). Several transcription factors are known to modulate the transcriptional activity of the *CFLAR* gene. NF-κB, CREB, FoxO, p63, p53, EGR1, NFAT, hnRNP K, AR and sp1 are among those which induce cFLIP transcription, while c-myc, Foxo3a, c-Fos, IRF5 and sp3 repress it (Shirley and Micheau, 2010). NF-κB activation is one the main inducers of cFLIPs; these proteins, in turn, elicit the NF-κB pathway, generating a positive feedback loop on stimulated cells (Micheau et al., 2001).

Little is known about isoform-specific regulation of cFLIP transcription, although some scattered reports exist. For instance, the AP-1 complex has been shown to repress $cFLIP_L$ expression (Li et al., 2007), while E21F, a transcription factor involved in control of cell cycle, inhibits the expression of $cFLIP_S$ (Salon et al., 2006). Furthermore, an siRNA screening aimed at characterising the targets of p63 suggested that this protein upregulates $cFLIP_R$ transcription, while suppressing that of $cFLIP_S$ without altering the transcription levels of $cFLIP_L$ (Borrelli et al., 2009).

The short isoform is shown to be regulated at translational level as well. Panner et al., demonstrated that in glioblastoma multiforme (GBM) cells, activation of the Akt/mTOR/S6K1 pathway results in polyribosomal accumulation of $cFLIP_S$ mRNA and therefore, increased expression of $FLIP_S$. Inhibition of mTOR or its target S6K1 supressed translation of $cFLIP_S$, but not $cFLIP_L$, and led to TRAIL-sensitisation of GBM cells (Panner et al., 2005). An mTOR-independent pathway has been also described to regulate $cFLIP_S$ translation. In this pathway, activation of Ral and its effector protein

RalBP1, inhibits cdc42-mediated activation of S6K1 and thereby, down-regulates the expression of $FLIP_S$ (Panner et al., 2006).

1.3.2.3 Post-translational regulation of cFLIPs

Cellular FLIPs exhibit a relatively short half-life. This has been indicated by rapid depletion of these proteins following treatment of cells with the inhibitor of protein synthesis cycloheximide (Kreuz and Siegmund, 2001; Micheau et al., 2001). Vice versa, cFLIPs are found to accumulate quickly in response to proteasome inhibitors such as MG-132, lactacystin, epoxomicin and bortezomib/Velcade® (Chang et al., 2006; Fukazawa et al., 2001; Kim et al., 2002; Perez et al., 2003). Post-translational modifications, most notably ubiquitination and phosphorylation, play crucial roles in regulating the turnover rate of different cFLIPs.

cFLIP proteins are predominantly degraded via the ubiquitin-proteasome degradation system. $cFLIP_S$ is particularly more prone to ubiquitination and displays a considerably shorter half-life compared with $cFLIP_L$ (Poukkula et al., 2005; Schmitz et al., 2004). This is largely due to the unique 19 amino acid C-terminal sequence of $cFLIP_S$ that facilitates its ubiquitination at lysine residues 192 and 195, marking this protein for proteasomal degradation (Poukkula et al., 2005); the stability of $cFLIP_R$ is similar to $cFLIP_S$ (Golks et al., 2005; Ueffing et al., 2008). Both proteins have been shown to be targeted by the E3 ubiquitin ligase c-Cbl (Kundu et al., 2009; Zhao et al., 2013), although the E3 responsible for the ubiquitination of K192/195 residues remains to be identified. TNFα-mediated JNK1 (Jun N-terminal Kinase1) activation can enhance $cFLIP_L$ degradation by inducing the E3 ubiquitin ligase Itch (Chang et al., 2006). The caspase-like domain of $FLIP_L$ is necessary for interaction with Itch, highlighting once more the importance of C-terminal sequences of cFLIP isoforms in determining their stability.

Phosphorylation events are also central to regulation of cFLIP levels. PKC phosphorylates cFLIP proteins at serine193 (Kaunisto et al., 2009). This results in decreased ubiquitination of all isoforms, although it only prolongs the half-lives of $cFLIP_S$ and $cFLIP_R$. Since site-specific mutation of S193 does not affect recruitment of different isoforms to the DISC (death inducing signalling complex), PKC-mediated cFLIP phosphorylation may regulate apoptotic pathways only via rapid changes in $cFLIP_S$ levels (Kaunisto et al., 2009). This seems to be different from calcium/calmodulin-dependent kinaseII (CaMKII)-mediated phosphorylations of cFLIP proteins (at a residue other than

S193) which block DISC recruitment of both short and long isoforms (Yang et al., 2003). Recently, serine273 of $cFLIP_L$ was shown to be targeted by PI3K/Akt. Phosphorylation of $cFLIP_L$-S273 following TNFα-induced macrophage activation resulted in ubiquitination and proteasomal degradation of $cFLIP_L$ (Shi et al., 2009). This $cFLIP_L$ ubiquitinaton, however, was not dependent on JNK/Itch. Phosphorylation of $cFLIP_S$ is found to be crucial for mycobacterium tuberculosis-induced cell death in murine macrophages. M.tb-mediated TNF activation induces p38 and Abl, which in turn phosphorylate $cFLIP_S$ on Ser4 and Tyr211, respectively. This facilitates recognition of $FLIP_S$ by the E3 ubiquitin ligase c-Cbl, leading to its degradation and initiation of apoptosis (Kundu et al., 2009). Taken together, these studies elucidate how the cross-talk between phosphorylation and ubiquitination events results in quick isoform-specific changes in cFLIP levels. This provides cells with a crucial ability to generate rapid responses to cellular distress.

1.3.3 Regulation of cell death pathways by FLIPs

Controlling the delicate balance between cell death and survival pathways is essential for development and homeostasis of multi-cellular organisms. To achieve this, cells have evolved numerous regulatory proteins such as FLIP, which can promote or inhibit demolition of cells in a certain set of conditions. Cell death can occur through several distinct routes (e.g, apoptosis, necrosis and autophagy-related cell death) and remarkably, FLIP proteins have been documented to be involved in regulation of all these types of cell demise.

1.3.3.1 Extrinsic and intrinsic apoptotic pathways

Apoptosis is a programmed mode of cell death that enables multicellular organisms to dispose of unwanted cells with minimum damage to neighbouring cells (Taylor et al., 2008). Precise regulation of apoptosis is central to the development, differentiation and homeostasis of tissues. Apoptotic signalling pathways are classified into two distinct types: intrinsic pathways induced by factors such as DNA damage, UV or γ-radiation, chemotherapeutic drugs and cytokine deprivation (Figure 1.5, left), and extrinsic pathways initiated by death receptors (DR) (Krammer et al., 2007; Lavrik et al., 2005) (Figure 1.5, right).

Proteins of the DR family belong to the TNFR superfamily. To date, eight members of this family have been described: TNFR1 (also known as DR1, p55, p60 and

CD120a), CD95 (also known as DR2, Fas and APO-1), DR3 (also known as APO-3, LARD, TRAMP and WSL1), TNF-related apoptosis inducing ligand receptor1 (TRAILR1; also known as DR4 and APO-2), TRAILR2 (also known as DR5, KILLER and TRICK2), DR6, ectodysplasin A receptor (EDAR) and nerve growth factor receptor (NGFR) (Lavrik et al., 2005). DR family are characterised by the presence of a C-terminal sequence of 80-100 amino acids, called the death domain (DD) that is responsible for transducing the apoptotic signals. Indeed, homotypic DD interactions connect DRs to adaptor proteins FADD and TRADD (Guicciardi and Gores, 2009).

Upon ligation of CD95, TRAILR1 or TRAILR2, a multiprotein complex is formed near the plasma membrane known as death-inducing signalling complex (DISC). This complex is composed of DR, FADD, cFLIP and precursors of two initiator caspases: procaspase-8 and procaspase-10. While FADD and DR interact via DDs, cFLIP or procaspase-8/10 are recruited to FADD via the DEDs of each protein. Activation of the initiator caspases following DISC formation, results in the induction of effector caspases (caspase-3, -6 and -7), which in turn proteolyse a wide array of substrates leading to dismantling and packaging of cells into apoptotic bodies (Figure 1.5, right).

In the intrinsic pathway, also known as the mitochondrial pathway, death signals are initiated by mitochondrial membrane permeabilisation (MMP) (Martinou and Green, 2001). Anti-apoptotic members of the Bcl-2 family (such as Bcl-2, Bcl-XL, BCL-W and MCL1), preserve the integrity of outer mitochondrial membrane by inhibiting the oligomerisation of proapoptotic Bcl-2 members, BAX and BAK. Upon arrival of a death signal, antiapoptotic Bcl-2 proteins are inhibited by Bcl-2 homology3(BH3)-only proteins (eg., BID, BAD, BIM and BMF) (Kuwana et al., 2005; Letai et al., 2002). This leads to formation of BAX-BAK oligomers within the outer membrane that allows for efflux of intermembrane space proteins such as cytochrome C, SMAC/DIABLO and AIF (apoptosis-inducing factor). Once released form mitochondria, cytochrome C mediates assembly of a caspase activation complex known as the apoptosome. This complex consists of about seven molecules of apoptotic protease-activating protein-1 (APAF1) and the same number of initiator procapspase-9. Similar to events followed by DISC assembly, activation of caspase-9 within the apoptosome induces a cascade of effector caspases that culminates in cell death (Taylor et al., 2008) (Figure 1.5, left). In some conditions, extrinsic death signals can activate the intrinsic pathway through caspase-8 mediated cleavage of the BH3-only family member, BID (BH-3 interacting domain death agonist). Truncated BID (tBID) can then promote release of intermembrane space proteins resulting in apoptosome formation and cellular demolition (Korsmeyer et al., 2000).

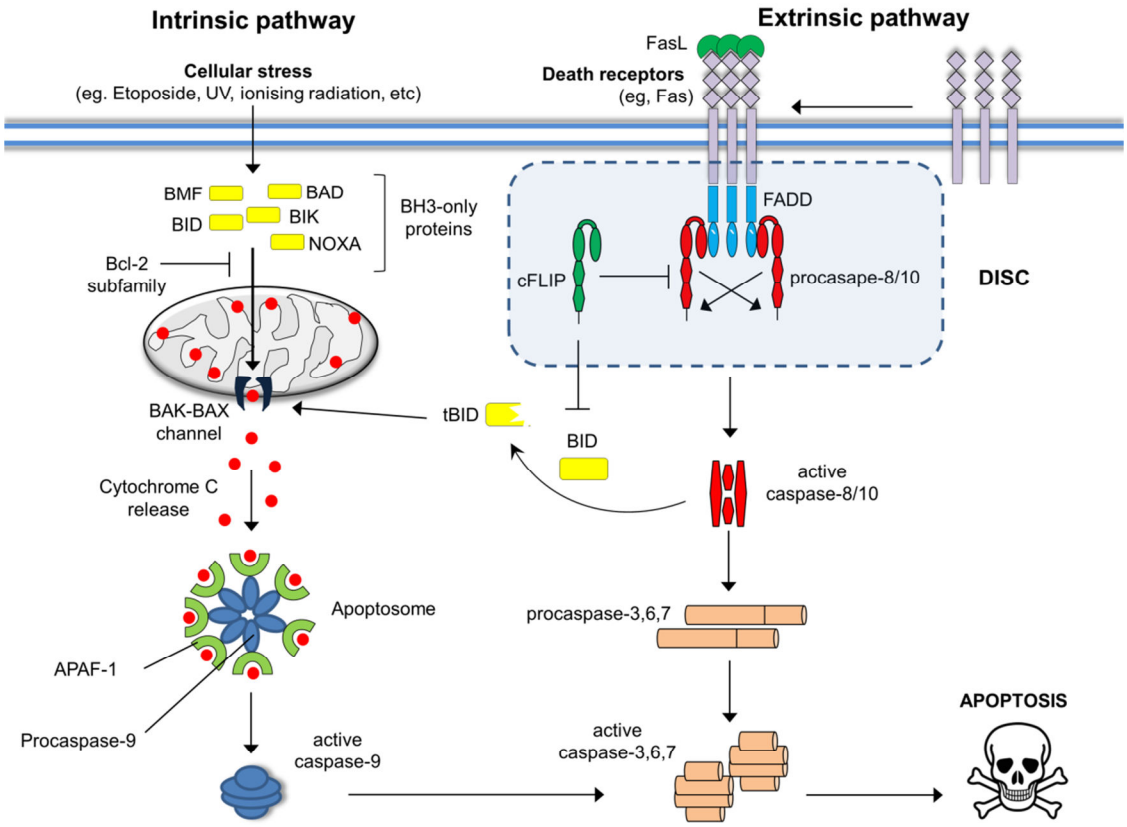

Figure 1.5. Extrinsic and intrinsic cell death pathways. Extrinsic apoptotic pathway (right) commences by engagement of death receptors (DRs) with their cognate ligands which then leads to recruitment of adaptor proteins (e.g, FADD and TRADD) and formation of DISC, consisting of DR, FADD, procaspase-8/10 and cFLIP isoforms. Autoprocessing and activation of the initiator procaspase-8/10, promotes the activation of downstream caspases, such as caspase-3, 6 and 7, for the execution of apoptosis. The extrinsic pathway is mainly under the control of cFLIP family which fine-tune the activity of initiator caspases at the DISC. In the intrinsic pathway (left) various stimuli such as UV or chemotherapeutic agents which provoke cell stress and damage activate one or more members of the BH3-only proteins. This in turn induces the assembly of BAK-BAX oligomers within mitochondrial outer membranes, leading to release of intermembrane proteins such as cytochrome C which promotes the assembly of apoptosome. Activation of caspase-9 within this complex then propagates a cascade of caspase activation, similar to final steps of the extrinsic pathway. Caspase-8-mediated cleavage of BID to generate tBID can link the extrinsic pathway to the mitochondrial cell death cascade; cFLIP can also inhibit this step.

Deregulation of cell death pathways resulting from insufficient or excessive apoptosis form the basis of multiple human disease such as neurodegenerative disorders, autoimmunity and cancer (Green and Evan, 2002; Vaux and Flavell, 2000). Therefore, apoptotic pathways are tightly controlled at multiple levels. For instance, members of the cIAP family, including NIAP, XIAP and cIAP1/2 have been shown to directly inhibit caspase-3,-7 and -9 (Liston et al., 1996). As mentioned above, proteins of the Bcl-2 family modulate the mitochondrial death programs. At the DISC level, apoptotic signals are regulated by FLIP proteins that facilitate or inhibit the activation of casapase-8. Nonetheless, DISC formation does not always result in cell death but it can be also directed to switch on several survival and proliferative pathways like NF-κB or MAPK. Remarkably, a collective body of research shows that FLIPs also play crucial roles in regulation of the DR-induced non-apoptotic pathways (Oztürk et al., 2012).

1.3.3.2 Roles of FLIPs in apoptosis

Procaspase-8 activation, which is pivotal for DR-induced apoptosis, occurs through an "induced proximity" mechanism where DR-mediated homo-dimerisation of procaspase-8 leads to its self-cleavage and release of fully active catalytic subunits (p10 and p18) (Chang et al., 2003). Similar to procaspase-8, FLIPs are recruited to DISC-associated FADD via homotypic DED interactions. Hence, the anti-apoptotic function of FLIP proteins relies on their ability to restrain FADD-mediated homo-dimerisation and activation of procaspase-8 molecules (Krueger et al., 2001b).

Although viral FLIPs, $cFLIP_R$ and $cFLIP_S$ have been well-established as potent inhibitors of procaspase-8 activation (Golks et al., 2005; Krueger et al., 2001a; Thome et al., 1997), function of $cFLIP_L$ has been inconsistently reported to be either pro-apoptotic (Goltsev et al., 1997; Han et al., 1997; Inohara et al., 1997; Shu et al., 1997) or anti-apoptotic (Irmler et al., 1997; Rasper et al., 1998; Srinivasula et al., 1997). The pro-apoptotic role of $cFLIP_L$ is supported by the phenotype of cFLIP null mice which resembles that of mice lacking caspase-8 or FADD. These mice die at embryonic day 10.5 with impaired heart, vascular and haematopoietic development, suggesting a function for $cFLIP_L$ that is similar to FADD or caspase-8 (Yeh et al., 2000). Furthermore, expression of $cFLIP_L$ at physiological levels is suggested to mediate apoptosis by formation of catalytically active $cFLIP_L$/caspase-8 heterodimers (Chang et al., 2002; Micheau et al., 2002). Nevertheless, the pro-apoptotic role of $cFLIP_L$ disagrees with the observation that $cFLIP_L$-specific knockdown cells or MEFs lacking cFLIP are highly susceptible to DR-

induced cell death compared with WT cells (Sharp et al., 2005; Yeh et al., 2000). In addition, ectopic expression of $cFLIP_L$ at high levels is found to inhibit procaspase-8 activation via competing for FADD binding (Scaffidi et al., 1999).

Despite these contradictory reports, several studies have now elucidated that depending on its expression levels $cFLIP_L$ can either promote or inhibit apoptosis (Chang et al., 2002; Fricker et al., 2010; Neumann et al., 2010). A recent study by Fricker et al., analysed the relationship between amounts of $cFLIP_L$ and the regulation of CD95-induced cell death, using mathematical modelling combined with quantitative western blotting. The authors demonstrated that $cFLIP_L$ blocks apoptosis when highly overexpressed, whereas its moderate expression can promote cell death when accompanied with strong stimulation of CD95 or in the presence of high levels of $cFLIP_{S/R}$ (Fricker et al., 2010). Therefore, the $cFLIP_L$ role at the DISC is not only dose-dependent but also may rely on other factors such as signal strength and the levels of other cFLIP isoforms.

Biochemical assays as well as crystal structure studies on vFLIP MC159 propose that viral and cellular FLIPs may use different mechanisms to inhibit caspase-8 activation. The homotypic interactions between FADD-DED and procaspase-8-DED2 or cFLIP-DED2 are mediated through a highly conserved hydrophobic patch (Berglund et al., 2000; Carrington et al., 2006; Eberstadt et al., 1998). In pull-down experiments, cFLIP competes away procaspase-8 in binding to FADD. In contrast, MC159 cannot compete procaspase-8 away and binds to FADD-DED through an extensive area outside the hydrophobic patch interface (Yang et al., 2005). Therefore, MC159 (and perhaps other vFLIPs) may disrupt DISC assembly by preventing FADD-DED self-association rather than inhibiting procapase-8 binding (Yu and Shi, 2008). Overexpression of isolated FADD-DED or tandem DEDs of procaspase-8 results in self-assembly to produce long cytoplasmic filaments (also known as death effector filaments) which can induce apoptosis independent of death receptors (Siegel et al., 1998). Unlike these proapoptotic DEDs, which are found highly aggregated *in vitro*, isolated tandem DEDs from MC159 or EHV-2 vFLIP E8 do not form filaments in cell culture and appear as monomers *in vitro* (Li et al., 2006a; Yang et al., 2005). Indeed, these viral DEDs can effectively block self-assembly of DEDs from FADD or procaspase-8 to form death filaments (Siegel et al., 1998). Whether other viral FLIPs use the same DISC-inhibition strategy still remains unanswered.

1.3.3.3 Roles of FLIPs in necroptosis

Regulated necrosis, referred to as necroptosis, is an alternative form of cell death that occurs when caspase-8 activity is inhibited and it depends on kinase activity of RIP1 and RIP3 (Cho et al., 2009; He et al., 2009; Zhang et al., 2009a). The embryonic lethality observed in *FADD* $^{-/-}$ and *CASP-8*$^{-/-}$ mice can be rescued by additional deletion of the kinases RIP1 or RIP3, indicating that FADD and caspase-8 inhibit the RIP1/3-mediated cell death during embryonic development (Kaiser et al., 2011; Oberst et al., 2011; Zhang et al., 2011).

Although necroptosis has evolved as an immune defence mechanism against intracellular infections, it has been also implicated in causation of several pathologies such as ischemia–reperfusion injury, neurological and myocardial disease (Linkermann and Green, 2014). Necroptotic signalling cascades can be initiated by stimulation of DRs, TLRs, genotoxic drugs and some viral and bacterial pathogens (e.g. human simplex virus-type1 and vaccinia virus) (Vanlangenakker et al., 2012). Similar to their role in apoptosis, cFLIP proteins can regulate necroptosis in an isoform-specific manner.

Evidence for modulation of necroptosis by FLIP proteins (and a connection between apoptosis and necroptosis) comes from the detection of a cytoplasmic complex, termed the ripoptosome, induced by treatments of human tumour cells that deplete or inhibit cIAP proteins (Feoktistova et al., 2011; Tenev et al., 2011a). This depletion leads to the formation of a RIP1/FADD/procaspase-8 complex. cIAPs inhibit formation of this complex by ubiquitinating RIP1 that leads to ubiquitin-mediated recruitment of several kinases required for NF-κB activation (Bertrand et al., 2008; Varfolomeev et al., 2008). CYLD-mediated deubiquitination of RIP1, on the other hand, enables the kinase activity of RIP1 and necrosome assembly (Wang et al., 2008). In the absence of FLIP proteins, procaspase-8 molecules homodimerise in ripoptosome, promoting cell death by apoptosis. Recruitment of $cFLIP_L$ to this complex leads to partial caspase-8 activation, not enough to induce apoptosis, but sufficient to cleave RIP kinases and disassemble the ripoptosome, resulting in cell survival (Boatright et al., 2004; Oberst et al., 2011; Pop et al., 2011). $cFLIP_S$, on the other hand, blocks caspase-8 activation and facilitates cell death through necroptosis (Feoktistova et al., 2011) (Figure 1.6). Similarly, vFLIP MC159 shifts the outcome of ripoptosome toward necroptosis (Feoktistova et al., 2012). Roles of other viral FLIPs, however, have yet to be examined.

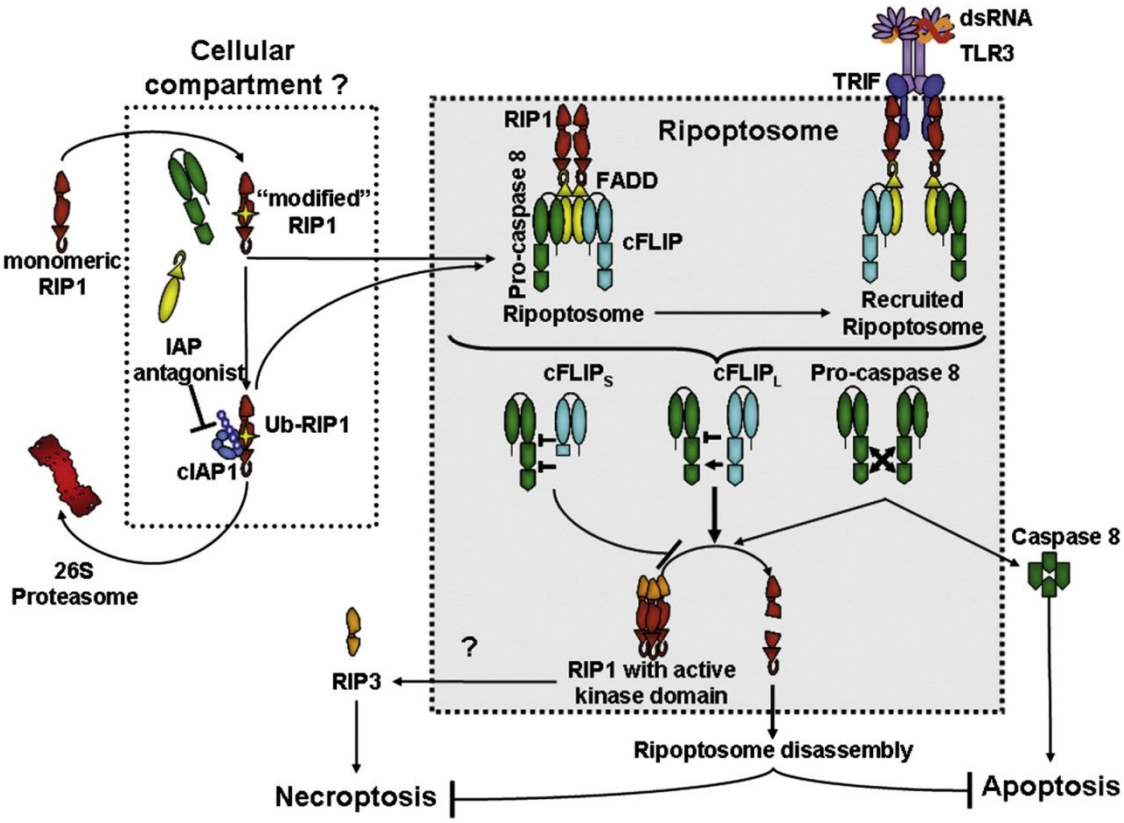

Figure 1.6. FLIP proteins regulate the activity of the ripoptosome complex. Under baseline conditions, a small proportion of RIP1 is persistently modified to active conformation. This modified RIP1, also called open conformation, is targeted for Ub-mediated degradation by cIAPs. Upon depletion of cIAPs by genotoxic stress, accumulation of modified RIP1 promotes formation of a ripoptosome signalling complex which consists of RIP1, FADD, caspase-8/10 and cFLIP isoforms. Different compositions of the caspase-8 and cFLIP isoforms bring about different levels of ripoptosome-associated caspase-8 activity and therefore, lead to different cell death responses. Procaspase-8 dimerisation within the complex forms active caspase-8 and results in cell death via apoptosis. However, $cFLIP_L$ within the ripoptosome decreases the caspase-8 activity to levels which are not sufficient for its apoptotic function but still can inactivate the modified RIP1 and therefore, cause ripoptosme disassembly. In the presence of $cFLIP_S$, procaspase-8 remains non-functional and so, active RIP1 accumulation which is followed by the recruitment of RIP3 brings about cell death via necroptosis [Reproduced from (Feoktistova et al., 2011) with a permission from the author].

1.3.4 Regulation of autophagy pathways by FLIPs

Autophagy is a homeostatic process in which cytosolic materials such as proteins, organelles and pathogens are engulfed into double-membraned vesicles, termed the autophagosome, and then delivered to lysosome for degradation. Depending on the cellular conditions, the processed constituents can then be disposed of or recycled if needed. The latter provides cells with a mechanism of adaptation to starvation (Ryter et al., 2013). Autophagy can be also induced by factors such as hypoxia, and endoplasmic reticulum stress as well as exposure to a wide range of chemical and physical agents. Although autophagy is primarily a cytoprotective pathway, its uncontrolled upregulation can lead to cell death (Shintani and Klionsky, 2004). Too much or too little autophagy has been implicated in several human pathologies including neurodegeneration, myopathies, cancer, heart and liver disease (Mizushima et al., 2008).

The core autophagic machinery comprises of the well-conserved family of autophagy-related (Atg) proteins. Molecular regulation of autophagy pathway occurs at three steps: (i) initiation, (ii) nucleation of an isolation membrane and (iii) elongation and completion of autophagosomes. Activation of ULK1 complex (ULK1, Atg13 and FIP200), which on resting conditions is inhibited by mTOR complex1, triggers the autophagy cascade. Next, the classIII PI3K complex (Beclin 1, hVps34, Atg14) mediates nucleation of autophagosomal membranes. The elongation and closure of the autophagosomal vesicles is dependent on the Atg5/Atg12/Atg16 complex and the ubiquitin-like protein, LC3. Unlike the first complex which dissociates from autophagosome once it is fully formed, LC3-phosphatidyl ethanolamine conjugates (aka LC-II) remain attached to vesicles. Attachment of phosphatidyl ethanolamine molecules to LC3 is mediated by Atg4 cysteine protease, Atg3 E2-like enzyme and Atg7 E1-like enzyme (Pyo et al., 2012).

A screen conducted to identify KSHV proteins that could inhibit autophagy-mediated cell death, pulled out vFLIP. KSHV vFLIP, HVS vFLIP, MC159L, $cFLIP_L$ and $cFLIP_S$ all inhibit autophagy. The FLIP proteins interact with the Atg3, preventing LC3 conjugation to phosphatidyl ethanolamine and attachment to membranes for autophagic vesicle expansion (Lee et al., 2009) (Figure 1.7).

During KSHV latency, deregulation of cell proliferation by vCyclin elicits DNA damage responses which, if unchecked, can promote autophagy and oncogene-induced senescence (OIS) (Koopal et al., 2007; Verschuren et al., 2002). By countering the v-

cyclin-induced autophagy, vFLIP plays an indispensable role in prevention of OIS, permitting the expansion of abnormal cells (Leidal et al., 2012).

KSHV vFLIP mutants deficient in NEMO- or FADD-binding are capable of blocking autophagy (Lee et al., 2009; Leidal et al., 2012). Hence, the anti-autophagic role of vFLIP appears to be mediated by a unique motif, independent of its ability to induce NF-κB or block apoptosis. Indeed, Atg3-binding region of KSHV vFLIP was mapped to DED1 α2 helix (aa 20-29) and DED2 α4 helix (aa 128-139). Introducing peptides derived from these motifs can effectively block Atg3-vFLIP interaction without interrupting that of Atg3-LC3, leading to growth inhibition and autophagy-mediated cell death (Lee et al., 2009).

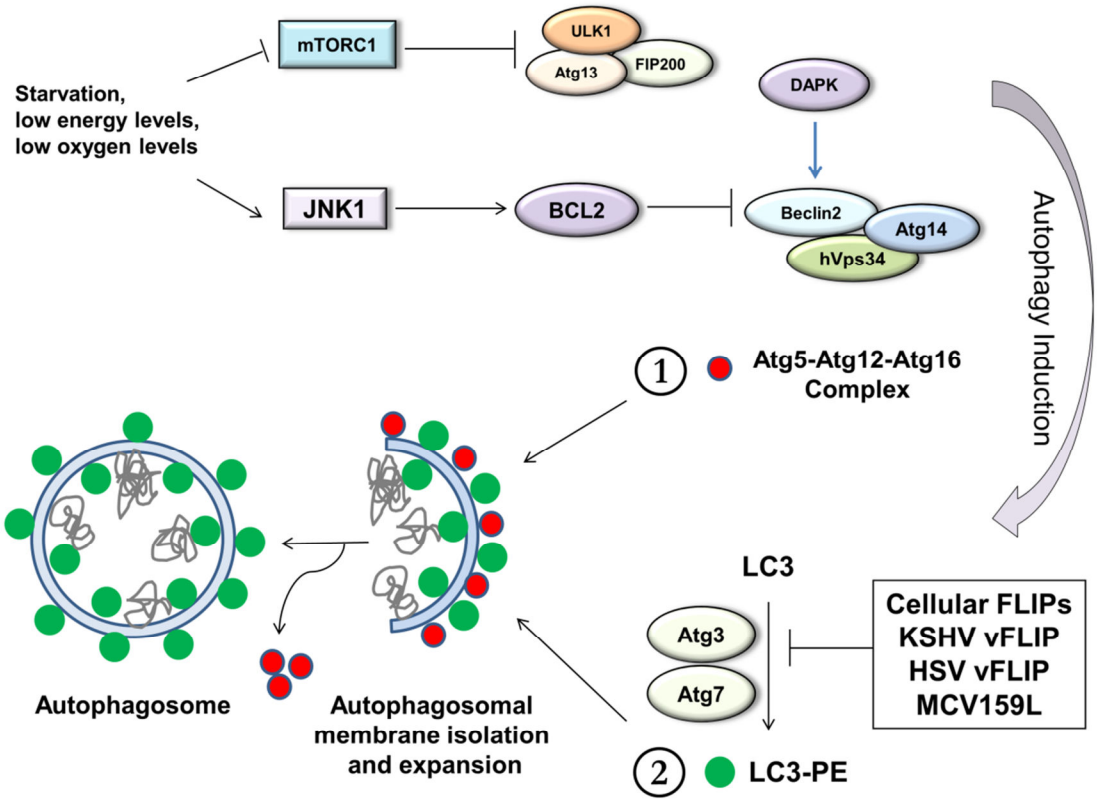

Figure 1.7. Cellular and viral FLIPs block autophagy. Autophagy is a homeostatic mechanism which is activated in response to various conditions such as absence of the amino acids, growth factors or oxygen. During starvation, mTORC1 that represses autophagy in normal conditions is inhibited which in turn causes ULK1 complex (ULK1, Atg13, FIP200) activation. Autophagy initiation is also dependent on other complex (Beclin 1, hVps34, Atg14) crucial for nucleation of autophagosomal membranes. The nucleation complex is activated through JNK1-mediated phosphorylation and subsequent inactivation of its inhibitory protein Bcl-2. The elongation and closure of the autophagosomal vesicles is dependent on the Atg5/Atg12/Atg16 complex and LC3. Unlike the first complex which dissociates from autophagosome once it is fully formed, LC3-phosphatidyl ethanolamine (PE) conjugates remain attached to vesicles. Attachment of PE molecules to LC3 is mediated by Atg3 E2-like enzyme and Atg7 E1-like enzyme. Cellular and viral FLIPs have been shown to supress autophagy by preventing the Atg3-LC3 interaction.

1.3.5 Regulation of NF-κB pathways by FLIPs

The ability of cFLIP proteins to activate NF-κB was initially demonstrated using overexpression experiments (Chaudhary et al., 2000; Hu et al., 2000). Later on, $cFLIP_L$ was found to mediate NF-κB activation following CD95 stimulation through a mechanism involving the recruitment of RIP1, TRAF1 and TRAF2 (Kataoka et al., 2000). This pathway is believed to depend on processing of $cFLIP_L$ to the p43 fragment as non-cleavable mutant of $cFLIP_L$ does not induce it (Kataoka and Tschopp, 2004; Matsuda et al., 2014; Neumann et al., 2010). p43-FLIP has been found associated with NEMO after CD95 signalling (Neumann et al., 2010). One study reported that p22-FLIP, another cleavage product of $cFLIP_{L/S/R}$ can also directly interact with NEMO and activate IKK. p22-FLIP seems to be primarily important in NF-κB induction required for lymphocyte activation and DC maturation (Golks et al., 2006).

Akin to its role in apoptosis, the expression level of $cFLIP_L$ is found to be a major determinant of its function as inhibitor or activator of DR-induced NF-κB signalling. Neumann et al showed that $cFLIP_L$ mediates CD95-induced NF-κB activation when expressed at moderate levels. On the other hand, high concentrations of $cFLIP_L$ can occupy the DISC, preventing the procaspase-8 activation, p43-FLIP production and NF-κB activation (Neumann et al., 2010). This is in accordance with a number of other studies that propose $cFLIP_L$ downregulates CD95-induced NF-κB activity (Imamura et al., 2004; Kavuri et al., 2011; Kreuz et al., 2004). The reported inhibitory function of $cFLIP_S$ in TCR-induced NF-κB activation might be also explained by its capacity to effectively block procaspase-8 activation and the resultant generation of cFLIP cleavage products.

Regulatory roles of cFLIP isoforms have been also controversially discussed in regard with TRAIL-induced NF-κB activation (Kavuri et al., 2011; Song et al., 2007; Wachter et al., 2004). While both positive and negative roles have been ascribed to cFLIPs in this context, a recent study argued against involvement of these proteins in TRAIL-induced NF-κB signalling. Instead, FADD and caspase-8 were shown to mediate TRAIL-induced signalling to IKK (Grunert et al., 2012).

Among FLIP proteins, KSHV vFLIP is the most well-known inducer of NF-κB (Chaudhary et al., 1999; Chugh et al., 2005; Liu et al., 2002; Sun et al., 2003, 2006). Our group demonstrated direct, stable interaction between KSHV vFLIP and NEMO which leads to constitutive IKK complex activation (Field et al., 2003). Initially, it was suggested

that KSHV vFLIP binds to TRAF2 via a putative TRAF-binding motif and that this facilitates IKK activation by vFLIP (Guasparri et al., 2006). In contrast, later reports demonstrated that vFLIP could directly bind and activate NEMO independent of TRAF2 or TRAF3 (Matta et al., 2007). In KSHV-infected B cell lines, the IKK subunits alpha, beta and gamma, together with HSP90, are the only detectable proteins complexed with vFLIP; also NEMO immunoprecipitation depletes all detectable vFLIP from cell lysate (Field et al., 2003). KSHV vFLIP can also activate the alternative NF-κB pathway by upregulating the expression of p100 and its processing to p52. Non-canonical NF-κB induction by vFLIP is unique in that it does not require NIK and occurs through direct interaction between p100, vFLIP and IKK (Matta and Chaudhary, 2004).

Both viral FLIPs from MCV (MC159 and MC160) block TNF-induced NF-κB signalling; MC159 has been shown to do this by binding to NEMO (Nichols and Shisler, 2006; Randall et al., 2012). On the other hand, MC160 is not detectable in association with any of IKK subunits. However, expression of MC160 leads to substantial decrease in levels of IKKα/β and interactions between these subunits, suggesting that MC160 may exert its inhibitory function by dissociating the IKK complex (Nichols and Shisler, 2006). The vFLIPs from RRV and HSV do not activate NF-κB, in contrast to vFLIP form EHV (Chaudhary et al., 1999; Lee et al., 2009; Ritthipichai et al., 2012). The interaction of these viral FLIPs with NEMO has yet to be studied.

Detailed mechanisms of NF-κB activation by KSHV and cellular FLIPs will be discussed in chapters 3-5.

1.3.6 Regulation of MAPK pathways by FLIPs

The MAPK signalling network is involved in fundamental cellular processes such as growth, proliferation, differentiation and apoptosis. This pathway is built upon a three-tier kinase module where a MAPK becomes activated through phosphorylation by a MAPKK which, in turn, is induced by an upstream MAPKKK (Dhillon et al., 2007). Six distinct groups of MAPKs have been described so far in mammalian cells: extracellular signal-regulated kinase (ERK)1/2, ERK3/4, ERK5, ERK7/8, c-Jun N-terminal kinase (JNK)1/2/3 as well as the p38 isoforms α/β/γ [reviewed in (Arthur and Ley, 2013)]. While ERK1/2 are predominantly activated by growth factors, JNK and p38 kinases are induced in response to stress stimuli and cytokines (Pearson et al., 2001).

$cFLIP_L$, $cFLIP_S$ and p43-FLIP can all activate ERK1/2 via recruitment of the upstream MAPK3, Raf-1 which activates MAPK2 MEKK and then ERK (Kataoka et al., 2000; Koenig et al., 2014). In activated T cells, high levels of cFLIP leads to simultaneous activation of NF-κB and ERK, promoting IL-2 secretion and T-cell proliferation (Kataoka et al., 2000). Nevertheless, a recent study reported that high expressions of cFLIP proteins can inhibit CD95-induced ERK activation, through blocking the procaspase-8 processing (Kober et al., 2011). It is possible that, like their role in apoptosis, cFLIPs differentially regulate ERK in cell-, pathway- and signal strength-dependent manner.

Unlike ERK signalling, p38 and JNK appear to be preferentially inhibited by cFLIP isoforms. Gene silencing of cFLIP isoforms in keratinocytes enhances CD95- and TRAIL-induced p38 and JNK activation without affecting NF-κB activation (Kavuri et al., 2011). In addition, *cFLIP*$^{-/-}$ B-cells highly activate p38 and JNK signalling in response to LPS, while neither NF-κB nor ERK1/2 signalling is altered in these cells (Zhang et al., 2009b). Following TNFα activation, $cFLIP_L$, but not $cFLIP_S$, directly binds to MKK7, an activator of JNK (Nakajima et al., 2006). This stimulus-dependant binding inhibits the activation and interactions of MKK7 with its upstream kinases such as MEKK1, ASK1 (apoptosis-signal-regulating kinase1), and TAK1. As mentioned previously, $cFLIP_L$ is also targeted for degradation by JNK-induced E3 ubiquitin ligase Itch (Chang et al., 2006). Therefore, $cFLIP_L$ appears to operate as a molecular rheostat in TNFα-induced JNK signalling. While prolonged induction of JNK, which leads to cell death, is blocked by $cFLIP_L$, its degradation by Itch prevents full blockade of the pathway.

KSHV vFLIP was initially reported to activate JNK/AP-1 pathway in a TRAF2 dependent fashion, eventually leading to high expressions of cIL-6 (An et al., 2003). However, later studies failed to detect vFLIP-mediated JNK/AP-1 activation in either PEL or non-PEL cells (Sun et al., 2006; Ye et al., 2008). In marked contrast, vFLIP was demonstrated to suppress AP-1 activity -which is required for lytic KSHV replication- through NF-κB activation. This function of vFLIP is speculated to be central for maintaining the latent KSHV infection (Ye et al., 2008).

1.3.7 FLIPs as promising targets for anti-cancer therapies

Enhanced cFLIP expression has been observed in a wide variety of cancers including melanoma (Yang et al., 2007), glioblastoma (Panner et al., 2009), colorectal

(Longley et al., 2006; Wilson et al., 2007), pancreatic (Haag et al., 2011; Kauh et al., 2010), ovarian (El-Gazzar et al., 2010; Park et al., 2009), prostate (Zhang et al., 2007) and gastric carcinomas (McLornan et al., 2010). Importantly, the higher levels of cFLIP correlate with more aggressive tumours (Korkolopoulou et al., 2004; Ullenhag et al., 2007; Valente et al., 2006; Valnet-Rabier et al., 2005; Wang et al., 2007a). In fact, cFLIP has been considered as a prognosis marker which may contribute to characterisation of patients at higher risks (Bagnoli et al., 2010). In support of this notion, increased amounts of $cFLIP_L$ were identified as an independent maker of adverse clinical outcome in several malignancies such as ovarian, colon and endometrial carcinomas as well as Burkitt's lymphoma (Bagnoli et al., 2009; Safa et al., 2008).

Abnormal upregulation of cFLIP proteins renders cancer cells resistant to not only CD95 (Mezzanzanica et al., 2004) and TRAIL-induced cell death (Geserick et al., 2008; Li et al., 2007) but also to chemotherapeutic drugs (Rogers et al., 2007). Resistance to TRAIL-induced apoptosis is particularly important as this type of cell death is found to be highly selective for the killing of neoplastic cells rather than normal ones (Walczak et al., 1999). This is shown to be due to an impaired expression of decoy receptors in cancer cells (Pan et al., 1997; Sheridan et al., 1997). Alike cFLIPs, vFLIPs play crucial roles in apoptosis evasion and therefore, oncogenicity of the associated viruses. Thus, targeting FLIP proteins appears as an attractive anti-cancer therapy, especially if combined with conventional approaches such as TRAIL treatment and chemotherapy. Sensitising malignant cells to apoptosis by inhibiting FLIPs may also allow for administering lower doses of chemotherapeutic agents, decreasing the drug-induced systemic toxicity in cancer patients (Safa and Pollok, 2011).

Several strategic interventions have been utilised to inhibit FLIP variants which include (i) usage of compounds inhibiting transcription or translation of these proteins (ii) oligonucleotide- or RNAi-mediated silencing of FLIPs and (iii) targeting FLIPs for degradation. These therapeutic strategies and advantages and disadvantages of each method have been extensively reviewed in (Safa and Pollok, 2011; Shirley and Micheau, 2010).

1.4 HTLV-1 Tax: a functional analogue of the KSHV vFLIP

1.4.1 HTLV-1 biology

Human T-cell lymphotropic virus type 1 (HTLV-1) was discovered in Japan where it shows a high prevalence, about 10% of the population are infected (Yoshida, 2005). The virus was isolated and sequenced by the Gallo lab at the National Cancer Institute in the US and was the first human retrovirus to be identified (Poiesz et al., 1980). In Japan it is mainly transmitted neonatally by breastfeeding (Matsuoka and Jeang, 2007), and although it mainly infects T-cells, it enters cells by binding to a widely expressed glucose transporter GLUT-1 (Manel et al., 2003).

HTLV-1 causes an aggressive T-cell leukaemia, adult T-cell leukaemia (ATL), and is also associated with a progressive motor neuron disease known as HTLV-1 associated myelopathy/tropical spastic paraparesis (HAM/TSP) (Osame et al., 1987; Yoshida, 2005). ATL occurs with a long latency, up to 60 years, after infection with HTLV-1 (Matsuoka, 2003). Early in the disease infected T-cells are driven to proliferate by upregulation of the IL-2 receptor and secretion of IL-2 (Ballard et al., 1988; Wano et al., 1988). Then oligoclonal expansion of infected cells occurs. Finally, the aggressive leukemia develops, at this stage the cells have ceased to be dependent on autocrine IL-2; the transformed phenotype is dependent on secondary mutations, at least some caused by insertional mutagenesis induced by the viral genome (Grassmann et al., 2005). HTLV-1 is a complex retrovirus than encodes additional proteins along with those required for viral replication (Matsuoka and Jeang, 2007). The Rex protein is required for nuclear export of unspliced RNA, analogous to the Rev protein of HIV (Rimsky et al., 1988).

1.4.2 HTLV-1 Tax

The Tax protein is responsible for the stimulation of T cell proliferation by HTLV-1. Tax activates the NF-κB pathway (Ballard et al., 1988) and expression of Tax in T cells is sufficient to up-regulate both the IL-2 and its receptor, and drive cells to proliferate (Grassmann et al., 1989; Wano et al., 1988). Tax also upregulates HTLV-1 viral gene expression via recruitment of CREB to the LTR, enhancing viral replication (Yin and Gaynor, 1996; Zhao and Giam, 1992). Indeed Tax is a polyfunctional protein, interactions with a variety of host cellular proteins have been reported [reviewed in (Boxus et al., 2008)]. Later in infection Tax expression is lost and the HTLV-1 HBZ protein, encoded

by an antisense transcript, drives transformation; HBZ is also a transcriptional regulator with many opposite effects to Tax (Satou et al., 2006).

Tax is of particular relevance to this study because, like some vFLIP proteins, it binds directly to NEMO to activate IKK (Chu et al., 1999; Harhaj and Sun, 1999; Jin et al., 1999), explaining its ability to constitutively activate NF-κB pathway leading to upregulation of NF-κB-dependent genes. Nevertheless, how the Tax–IKK physical association leads to IKK activation is incompletely understood. Two regions of NEMO, distinct from that recognised by KSHV vFLIP, have been reported to be necessary for Tax activation of IKK (See 3.1.2) (Xiao and Sun, 2000; Xiao et al., 2000). Tax also activates the alternative NF-κB pathway in a similar manner to vFLIP, by enhancing p100 processing, dependent on IKKα and NEMO, but not NIK (Xiao et al., 2001b). Therefore, these proteins from unrelated viruses, which share no amino acid homology, represent a remarkable example of convergent evolution in the manner in which they activate the NF-κB pathway.

1.5 Aims of the thesis

Leading on from previous projects in our laboratory that demonstrated the necessity and dynamics of the vFLIP-NEMO interaction, I set out to achieve the following goals:

1) To identify the regions of NEMO required for activation of IKK by KSHV vFLIP, cellular FLIPs and HTLV-1 Tax
2) To determine how IKK is activated by KSHV vFLIP, cFLIPs and Tax

CHAPTER

2

MATERIALS AND METHODS

2.1 Materials

2.1.1 Molecular buffers and bacterial media

All buffers and bacterial media were prepared in double distilled H_2O (ddH_2O).

Table 2.1. Buffers and bacterial media.

Buffer/media	pH	Composition
Phosphate-buffered saline (PBS)	7.4	137 mM NaCl 2 mM KCl 10 mM sodium hydrogen phosphate (dibasic) 2 mM potassium hydrogen phosphate (dibasic)
Tris-EDTA (TE)	8.0	10 mM Tris-HCl 1 mM EDTA
Tris-acetate EDTA (TAE)	7.8	40 mM Tris-HCl 1 mM EDTA 20 mM sodium acetate
Elution buffer (EB)	8.5	10 mM Tris-HCl
Luria Bertani broth	7.5	1% bacto-tryptone 0.5% bacto-yeast extract 10% NaCl
Luria Bertani agar	7.5	LB broth plus bacto-agar 15g/L
Transformation buffer (TFB)-I	5.5	30 mM potassium acetate 100 mM rubidium chloride 10 mM calcium chloride 50 mM magnesium chloride 15% glycerol acetic acid to desired pH
TFB-II	6.5	10 mM MOPS 75 mM calcium chloride 10 mM rhubidium chloride 15% glycerol KOH to desired pH
6x gel loading buffer	6.8	0.25% bromophenol blue 0.25% xylene cyanol FF 30% glycerol in water

2.1.2 Antibodies

Table 2.2. Primary antibodies used for immunoblotting and immunoprecipitation.

Target	Clone	Manufacturer	Species/Isotype	Dilution
Atg3		CST	Rabbit, Polyclonal	1:1000
Caspase-8	C-20	Santa Cruz	Goat, Polyclonal	1:1000
cFLIP†	NF6	Enzo Life Sciences	Mouse, IgG1	1:2000
CYLD		Sigma	Rabbit, Polyclonal	1:1000
FADD	1/FADD	BD	Mouse, IgG1	1:1000
FLAG epitope	M2	Sigma	Mouse, IgG1	1:2000
GAPDH	14C10	CST	Rabbit, Monoclonal	1:4000
GST	B-14	Santa Cruz	Mouse, IgG1	1:1000
HA epitope	Y-11	Santa Cruz	Rabbit, Monoclonal	1:1000
HOIL-1		Walczack lab	Mouse, IgG2a	1:1000
HOIP		Sigma	Rabbit, Polyclonal	1:2000
IKKαβ	H470	Santa Cruz	Rabbit, Polyclonal	1:1000
MEKK3	40/MEKK3	BD	Mouse, IgG1	1:1000
NEMO	FL-419	Santa Cruz	Rabbit, Polyclonal	1:3000
pIKKα(S176/180)/ β(S177/181)	16A6	CST	Rabbit, Monoclonal	1:1000
pIKKα(S176)/β(S177)	C84E11	CST	Rabbit, Monoclonal	1:1000
pIκBα (S32)	14D4	CST	Rabbit, Monoclonal	1:1000
pIκBα (S32/36)	12C2	CST	Mouse, IgG1	1:700
RIP1	38/RIP1	BD	Mouse, IgG2a	1:1000
SHARPIN		Walczak lab	Mouse, IgG1	1:1000
TAK1	M-579	Santa Cruz	Rabbit, Polyclonal	1:1000
vFLIP	6/14	Collins lab	Rat, Monoclonal	1:300

Manufacturers: BD, Beckton Dickenson Transduction Laboratories, CST, Cell Signalling Technology.

† The anti-cFLIP(NF6) antibody has been raised against amino acids 1-194 of human cFLIP and therefore, recognises all of its isoforms and proteolytic fragments.

Table 2.3. HRP-conjugated secondary antibodies used for immunoblotting.

Target	Host	Manufacturer	Dilution
Goat IgG	Rabbit	Dako	1:2000
Mouse IgG	Sheep	GE Healthcare	1:10000
Mouse IgG (ligh chain-specific)	Mouse	Jackson Immunoresearch	1:20000
Rabbit IgG	Pig	Dako	1:3000
Rabbit IgG (Fc-specific)	Goat	Jackson Immunoresearch	1:20000
Rabbit IgG (ligh chain-specific)	Mouse	Jackson Immunoresearch	1:20000
Rat IgG	Rabbit	Dako	1:1000

Fc: Fragment crystallisable region of an antibody.

2.1.3 Primers

Table 2.4. Primers used for amplifying cDNAs of genes of interest.

Amplicon	Target Vector	Primer name	Primer sequence (5'→3')
$cFLIP_L$	pDual & pCDNA3	BglII-cFLIP-FW	agatctgccaccatgtctgctgaagtcatccat
		$cFLIP_L$-NotI-RS	gcggccgcttatgtgtaggagaggataagtttctttc
$cFLIP_S$	pDual & pCDNA3	BglII-cFLIP-FW	agatctgccaccatgtctgctgaagtcatccat
		$cFLIP_S$-NotI-RS	gcggccgctcacatggaacaatttccaagaattt
p22-FLIP	pDual & pCDNA3	BglII-cFLIP-FW	agatctgccaccatgtctgctgaagtcatccat
		p22-NotI-RS	ggggcggccgctcaatccttgagac
CYLD	pDual	BamHI-CYLD-FW	ggatccgccaccatgagttcaggcttatggagccaagaa aaag
		CYLD-NotI-RS	gcggccgcttatttgtacaaactcattgttggactctgg
FADD	pCAN	BamHI-FADD-FW	ggatccgacccgttcctggtgctgctgc
		FADD-NotI-RS	gcggccgctcaggacgcttcggaggtagatg
RIP1	pDual	AsiSI-RIP1-FW	gcgatcgcgccaccatgcaaccagacatgtccttgaatg
		RIP1-NotI-RS	gcggccgcttagttctggctgacgtaaatcaagctgctc
HA-RIP1	pCDNA3	KpnI-HA RIP1-FW	ggtaccgccaccatgtacccatacgacgtcccagactac gctggtcaaccagacatgtccttgaatgtca
		RIP1-NotI-RS	gcggccgcttagttctggctgacgtaaatcaagctgctc
IκBα(1-54)	pGEX-2T	BamHI-IκBα-FW	ggatccgccatgttccaggcg
		IκBαΔ54-EcoRI-RS	gaattctcagaggcggatctcctg

Luciferase	pDual	BamHI-Luc-FW	ggatccaccgccatggaagacgccaaaaacataaagaaagg
		Luc-NotI-RS	gcgggcgcttacaatttggactttccgcccttcttggcc
NEMO Δ254	pDual	AscI-SFFV-FW	ggcgcgccagtcctccgacagactg
		SalI-NEMOΔ254-RS	gtcgactcaccgctcactgcccaccacgctgctcttg
NEMO Δ271	pDual	AscI-SFFV-FW	ggcgcgccagtcctccgacagactg
		SalI-NEMOΔ271-RS	gtcgactctagtcactcggcctgctggagctgctg
vFLIP	pDual &	BamHI-vFLIP-FW	ggatccgccaccatggccacttacgag
	pCDNA3	vFLIP-NotI-RS	gcggccgcctatggtgtatggcgatagtg

Table 2.5. Primers used for site-directed mutagenesis

Mutation	**Primer Sequence (5'→3')**
cFLIP A56L	FW: tcggggacttgttggaactgctctac
	RS: gtagagcagttccaacaagtccccga
cFLIP K192/K195RR	FW: gaatgttctccaagcagcaatccaaagaagtctcagagatccttcaaataacttcagg
	RS: cctgaagttatttgaaggatctctgagacttctttggattgctgcttggagaacattc
cFLIP F114/L115AA	FW: tgtgcgagggatattaggtctttgatagctgcaagcaaggacactatagggtctc
	RS: gagaccctatagtgtccttgcttgcagctatcaaagacctaatatccctcgcaca
IKKβ S177/S181AA	FW: gctggatcagggcgctctttgcacagcattcgtggggac
	RS: gctggatcagggcgctctttgcacagcattcgtggggac
IKKβ S177/S181EE	FW: aggagctggatcagggcgaactttgcacagaattcgtggggaccctgc
	RS: gcagggtccccacgaattctgtgcaaagttcgccctgatccagctcct
RIP1 E620/D622AA	FW: gaaattgaccatgactatgcgcgagctggactgaaagaaaaggtt
	RS: aacctttttctttcagtccagctcgcgcatagtcatggtcaatttc
RIP1 G595/K596AA	FW: cccaatcagggaaaatctggcagcgcactggaaaaactgtgccc
	RS: gggcacagtttttccagtgcgctgccagattttccctgattggg
RIP1 K377R	FW: cccagcctgcagagtagactccaagacgaag
	RS: cttcgtcttggagtctactctgcaggctggg
vFLIP D102/E104RR	FW: cactgttctccacgtacgcgggcggctgtgtgcgaggg
	RS: ccctcgcacacagccgcccgcgtacgtggagaacagtg
vFLIP E104R	FW: ccacgtagacgggcggctgtgtgcgagg

	RS: cctcgcacacagccgcccgtctacgtgg
vFLIP F115/L116AA	FW: tgtgcgagggatattaggtctttgatagctgcaagcaaggacactatagggtctc
	RS: gagaccctatagtgtccttgcttgcagctatcaaagacctaatatccctcgcaca
vFLIP R12E	BamHI-vFLIP R12E- FW: ggatccgccaccatggccacttacgaggttct
	ctgtgaggtggcggagaaactgggcacgga

Table 2.6. Sequencing primers

Primer	Sequence
SFFV FW	cgagctctataaaagagctca
pDual seq RS	taaagcagcgtatccacatagcgtaaaagga
pSIREN shRNAFW	atttcttgggtagtttgcag
pSIREN shRNA RS	gggctgctaaagcgcatgc

2.1.4 Plasmids used in this study

Table 2.7. Mammalian and bacterial expression vectors used in this project.

Plasmid	Origin
pDual (SFFV) NEMO WT (Ub) mCherry	Akira Shimuzu, Collins lab
pDual (SFFV) NEMO F312A (Ub) mCherry	Akira Shimuzu, Collins lab
pDual (SFFV) NEMO F238/D242RR (Ub) mCherry	Akira Shimuzu, Collins lab
pDual (SFFV) NEMO D242V (Ub) mCherry	this study
pDual (SFFV) NEMO Δ271 (Ub) mCherry	this study
pDual (SFFV) NEMO Δ254 (Ub) mCherry	this study
pDual (SFFV) vFLIP (Ub) GFP	Akira Shimuzu, Collins lab
pDual (SFFV) FLAG-Tax (Ub) GFP	Akira Shimuzu, Collins lab
pDual (SFFV) $cFLIP_L$ (Ub) GFP	this study
pDual (SFFV) $cFLIP_S$ (Ub) GFP	this study
pDual (SFFV) p22-FLIP (Ub) GFP	this study
pDual (SFFV) CYLD (Ub) GFP	this study
pDual (SFFV) RIP1 WT (PGK) GFP	this study
pDual (SFFV) RIP1 WT (PGK) GFP	this study
pDual (SFFV) RIP1 K377R (PGK) GFP	this study
pDual (SFFV) RIP1 G595/K596AA (PGK) GFP	this study

pDual (SFFV) RIP1 E620/D622AA (PGK) GFP	this study
pDual (SFFV) empty (Ub) GFP	David Escors, UCL
pSIN (SFFV) GFP	David Escors, UCL
pSIN (CMV) NF-ϰB luciferase	this study
pSIN (CMV) NF-ϰB mCherry	this study
pHIV-SIREN GFP	David Escors, UCL
pHIV-SIREN $Puro^R$	Greg Towers, UCL
pHIV-SIREN $Hygro^R$	this study
pGL. IgK	this study
pGL. H2DK	this study
pRL.TK	David Guiliano, UEL
pNF-ϰB-H2DK-luciferase	Inna Lavrik, DKFZ, Germany
pCDNA3 empty	Pablo Rodriguez, UCL
pCDNA3 vFLIP	this study
pCDNA3 His-vFLIP	this study
pCDNA3 FLAG-vFLIP	this study
pCDNA3 vFLIP A57L	this study
pCDNA3 vFLIP F115/L116AA	this study
pCDNA3 vFLIP R12E	this study
pCDNA3 vFLIP R12E/E104R	this study
pCDNA3 vFLIP D102R/E104R	this study
pCDNA3 p22-FLIP WT	this study
pCDNA3 p22-FLIP A56L	this study
pCDNA3 p22-FLIP F114/L115AA	this study
pCDNA3 p22-FLIP K192/195RR	this study
pCDNA3 $cFLIP_S$ WT	this study
pCDNA3 $cFLIP_S$ A56L	this study
pCDNA3 $cFLIP_S$ F114/L115AA	this study
pCDNA3 $cFLIP_S$ K192/195RR	this study
pCDNA3 $cFLIP_L$ WT	this study
pCDNA3.1 FLAG-$cFLIP_L$ WT	Pascal Meier, ICR
pCDNA3 $cFLIP_L$ A56L	this study
pCDNA3 $cFLIP_L$ F114/L115AA	this study

pCDNA3 cFLIP$_S$ K192/195RR	this study
pCDNA3 cFLIP D196E/D376N	Inna Lavrik, DKFZ, Germany
pCDNA3 FLAG-Tax	this study
pCDNA3 Myc-NEMO WT	this study
pCDNA3 MycNEMO D242V	this study
pCDNA3 Myc NEMO F312A	this study
pCDNA3 Myc-NEMO F238/D242RR	this study
pCDNA3 HA-IKKα WT	this study
pCDNA3 HA-IKKα S176/S180AA	this study
pCDNA3 HA-IKKα S176/S180EE	this study
pCDNA3 HA-IKKβ WT	this study
pCDNA3 HA-IKKβ S177/S181AA	this study
pCDNA3 HA-IKKβ S177/S181EE	this study
pCDNA3.1 His-V5-HOIP	Henning Walczak, UCL
pCDNA3.1 FADD	Henning Walczak, UCL
pCDNA3 HA-FADD	this study
pCDNA3 HA-RIP1	this study
pGEX-2T IκBα (1-54)	this study
pGEX IκBα (1-73) S32/S36AA	Neil Perkins, Newcastle University

2.2 Molecular biology

2.2.1 Polymerase chain reaction (PCR)

To amplify DNA fragments for subcloning into an expression vector, PCR reactions were performed using the high fidelity Phusion® DNA polymerase (NEB), as described in Table 2.8. Phusion DNA Polymerase possesses 3´→5´ proof-reading activity and generates blunt end products which, following purification, can be ligated into pJET1.2/blunt cloning vector.

For colony screen PCRs, we used the goTaq® Green Master Mix (Promega, Madison, WI). The colony PCR is a convenient method to screen for the absence or presence of a plasmid DNA insert directly from the transformed *E.coli* colonies. This

method can also be used to determine the insert orientation following blunt-end DNA ligations. Table 2.9 summarises the reagents used for the PCRs with goTaq polymerase.

Table 2.8. Phusion polymerase reaction mixtures

Component	Stock Concentration	Volume added	Final concentration
Nuclease-free water	-	to 50 µl	
Phusion HF† or GC† buffer	x5	10 µl	x1
dNTPs	10 mM	1µl	200 µM
Forward Primer	10 µM	2.5 µl	0.5 µM
Reverse Primer	10 µM	2.5 µl	0.5 µM
DNA template	100 ng	1 µl	100 ng
Phusion DNA polymerase	2 units/µl	0.5 µl	1 unit/50 µl PCR
Total volume		**50 µl**	

†: As recommended by the manufacturer, HF buffer was used as the default buffer for high fidelity amplification, while GC buffer was used in PCRs with GC-rich template or those which did not work with HF.

Table 2.9. goTaq polymerase reaction mixtures

Component	Stock Concentration	Volume added	Final concentration
Nuclease-free water	-	to 25 µl	-
GoTaq Green Master Mix	x2	12.5 µl	x1
Forward Primer	10 µM	2.5 µl	1 µM
Revers Primer	10 µM	2.5 µl	1 µM
DNA template		A small amount of E.coli colony	
Total volume		**25 µl**	

Reactions were run in a Hybraid thermal cycler using parameters listed in Table 2.10 and Table 2.11.

Table 2.10. Cycling parameters for Phusion polymerase reactions

Cycle step	Cycles	Temperature	Time
Initial Activation	1	98 °C	30 seconds
Denaturation		98 °C	5-10 seconds
Annealing	25-30	~ 5°C below T_m of primers	10-30 seconds
Extension		72 °C	15-30 seconds/kb
Final Extension	1	72 °C	5-10 min
Hold	1	4 °C	∞

Table 2.11. Cycling parameters for goTaq polymerase reactions

Cycle step	Cycles	Temperature	Time
Initial Activation	1	95 °C	2 min
Denaturation		95 °C	30 seconds
Annealing	25-30	~ 5 °C below T_m of primers	30 seconds
Extension		72 °C	1 min/kb
Final Extension	1	72 °C	5-10 min
Hold	1	4 °C	∞

2.2.2 Site-directed mutagenesis

Mutations were introduced using either QuickChange® XL II Mutagenesis Kit (Agilent Technologies) according to the manufacturer's instructions, or by overlap extension PCR method (OE-PCR). Both methods are based on amplification of the unmutated template DNA using complementary primer pairs both harbouring the desired mutation in their middle part (one forward and one reverse primer, here referred to as sense and antisense).

The QuickChange XL-II mutagenesis relies on a single PCR reaction using mutation-containing primers and a plasmid DNA as template. Extension of the oligonucleotide primers by *Pfu* HF DNA polymerase generates a mutated plasmid

containing staggered nicks. DNA isolated from most strains of *E.coli* is dam methylated and therefore, susceptible to digestion with the restriction enzyme *DpnI*. Hence, treatment of the PCR mixture with *DpnI* results in digestion of the parental unmutated DNA; however, the mutated plasmid produced by the PCR is unmethylated and so, is preserved. The mutated plasmid can then be transformed into competent cells and amplified within bacteria.

In OE-PCRs, three PCR reactions are performed to generate a DNA fragment with the desired mutation. For this method, apart from the mutation-harbouring internal primers, two primers (FW: forward and RS: reverse) one for each end of the final product are required. First, two PCR reactions using FW+antisense and sense+RS oligos were performed to generate two overlapping DNA segments containing the mutation of interest at their 3'- and 5'-terminal part, respectively. Finally, a third PCR was carried out to adjoin the two segments into a full-length product using FW and RS primers and products of the initial PCRs as template. These PCR products were then cloned into pJET1.2/blunt cloning vector. Presence of the mutation (and also absence of undesired sequence alterations) was verified by DNA sequencing, before subcloning the mutated genes into expression vectors.

The primers used for site-direct mutagenesis were designed using the online QuickChange® Primer Design program; they are listed in Table 2.5.

2.2.3 Restriction digestions

All restriction enzymes and their optimal buffers were purchased from Promega (Madison, WI) or New England Biolabs (NEB; Ipswich, MA). Digestion reactions for DNA analysis were normally performed at 37 °C for at least two hours, in a total volume of 10 µl (1 µl DNA, 0.5 µl of each enzyme, 1 µl of 10x buffer and 7 µl water). For isolation of plasmid backbone or inserts for ligation, reactions were carried out in a final volume of 30 µl (3 µl DNA, 1 µl of each enzyme, 3 µl of 10x buffer and 23 µl water). The incubation time was reduced to 30 min when using High-Fidelity restriction enzymes.

To generate blunt-end DNA fragments from those with sticky-ends, the DNA was incubated with Klenow DNA polymerase at 37 °C for 30 minutes in a 30 µl reaction consisting of: 20µl gel-purified sticky end DNA, 1µl dNTP, 1 µl Klenow (NEB), 5µl water and 3 µl of x10 reaction buffer (10mM Tris-HCl, pH7.9, 50mM NaCl, 10mM $MgCl_2$ and 1mM DTT). The Klenow is a proteolytic fragment of *E.coli* DNA polymerase which

retains polymerisation and 3'→5' exonuclease activity, but has lost 5'→3' exonuclease activity. Hence, it fills in 5' overhangs and chews back 3' overhangs, generating a blunt-end DNA fragment (Jacobsen et al., 1974).

2.2.4 DNA ligations

For ligation of DNA fragments, Rapid DNA Ligation Kit® (Thermo Scientific) was used. Ligation reactions were carried at room temperature for 5-10 minutes, in a total volume of 20 µl using 1 µl T4 DNA ligase (5 U/µl) and 4 µl of 5x Rapid ligation buffer. Next, 2µl of the reaction mixture was used for transformation of the competent cells.

To minimise self-ligation of DNA fragments in reactions where both insert and vector were blunt-ended, we treated the backbone vector with calf intestinal alkaline phosphatase (CIAP) prior to ligation. This enzyme dephosphorylates 5'-ends of the vector, preventing them from binding to hydroxyl groups of the 3'-ends and therefore, minimising the re-circulation of the cut vectors. The dephosphorylation reactions were performed using 1µl of CIAP (1 U/µl, Promega) at 37 °C for 15 min, followed by further 15 min incubation at 56 °C to heat-inactivate the enzyme.

2.2.5 Annealing DNA oligonucleotides for subcloning into a plasmid

In order to introduce a short stretch of DNA into a plasmid, we designed overlapping oligonucleotides that once assembled could be directly cloned into the overhangs generated by restriction digest of the destination vector. For annealing the oligonucleotides, 2.5 µl of each (reverse and forward) form a 100 µM stock were mixed and diluted in 50 µl of annealing buffer (10mM Tris pH 8.0, 50mM NaCl and 1mM EDTA). The mixture was incubated at 95 °C for 5 min and then, allowed to cool down to room temperature on the bench for approximately 45 min. The annealed oligonucleotides were diluted 10 times using nuclease-free water. Finally, the annealed oligonucleotides were mixed with cut vector in ratios between 3:1 to 6:1, in a standard ligation reaction as described in section 2.2.4.

2.2.6 Agarose gel electrophoresis and recovery of DNA

Agarose gel electrophoreses were performed to separate, characterise and purify the DNA samples. DNA fragments were electrophoresed in 1% agarose gels (Invitrogen, Carlsbad, CA) containing 5 µg/ml ethidium bromide (Dutscher Scientific, Essex, UK), using TAE buffer as running buffer. Prior to loading, DNA samples were mixed with x6

TriTrack DNA loading dye (Thermo Scientific) and then, were run alongside 1kb Plus DNA ladder (Invitrogen, Carlsbad, CA) for the estimation of band sizes. Gels were finally visualised under UV illumination and analysed using the GeneSnap image acquisition software (SYNGENE, NJ, USA).

For DNA purification after electrophoresis, the bands of interest were excised form the gel and purified using Qiaquick Gel Extraction kit (Qiagen, Hilden, Germany) according to the manufacturer's instructions.

2.2.7 Preparation, transformation and growth of competent bacteria

For the generation of competent cells, we used the rhubidium chloride method. Briefly, XL10 gold *E.coli* (Agilent were streaked onto an LB-agar plate containing Tetracycline (10 μg/ml) and incubated overnight at 37 °C. A single colony was then picked and cultured overnight in 10 ml of LB medium with Tetracycline (10 μg/ml). Next, 100 ml of LB medium without antibiotics was inoculated with 1 ml of overnight culture and grown at 37 °C for approximately 90-120 min, until an OD600 of 0.5-0.6 was achieved. The bacterial suspension was then cooled on ice for 10 min and harvested at 3000 RPM and 4 °C for 10 min. The pellet was gently suspended in 50 ml of TFB-I buffer (See table 2.1) and left on ice for 5 min. Following this incubation, cells were spun down again as explained above, re-suspend in 4 ml of ice-cold TBF-II buffer and left on ice for additional 15 min. Finally, aliquots of 100 μl were prepared and stored at -80 °C until use.

For transformation, vials of competent bacteria were thawed on ice and inoculated with 100-500 ng of plasmid DNA or 2-5 μl of ligation reaction. After incubation on ice for 20 minutes, the bacteria were heat-shocked for 15 seconds at 42 °C (or 2 minutes at 37 °C) and put back on ice for an additional 2 minutes. The transformed cells were then streaked onto LB-agar plates containing selection antibiotics (Ampicillin 50 μg/ml, or Kanamycin 30 μg/ml) and grown overnight at 37°C.

2.2.8 DNA purification and quantification

Single colonies of transformed bacteria were picked from LB agar plates and grown overnight at 37 °C, in 4 ml (minipreps) or 100 ml (midipreps) of LB broth supplemented with appropriate selection antibiotics (usually Ampicillin 50 μg/ml). Plasmid DNA was purified using QiaPrep Spin Miniprep or Plasmid Midiprep kits (Qiagen) following the

manufacturer's protocol. The purified DNA was normally eluted in EB buffer or nuclease-free water and quantified using NanoDrop® 3300 spectrophotometer (Thermo Scientific, Wilmington, DE).

2.2.9 Extraction of cellular RNA and cDNA synthesis

The cDNAs encoding human IKKα and IKKβ, were amplified from cDNA synthesised from Jurkat T cells. To do this, we first isolated total cellular RNA using RNeasy mini kit (Qiagen) according to the manufacturer's instructions. Next, mRNA was reverse transcribed to cDNA using the qScript® II cDNA SuperMix (Quanta BioSciences). Reverse transcription-PCR reaction mixtures and parameters are shown below in Table 2.12. Finally, 2 µl of the cDNA/RNA sample was used as template to amplify IKKα and IKKβ cDNAs by means of a standard PCR reaction.

Table 2.12. RT-PCR reaction mixtures (top) and thermocycler parameters (bottom).

Component	Volume added
qScript cDNA SuperMix	4 µl
RNA template	1 µg (whatever the volume)
Nuclease-free water	to 20 µl
Total volume	20 µl

Cycle	Temperature	Time
Annealing	25°C	5 min
Elongation	42°C	30 min
Denaturation	85°C	5 min
Hold	4°C	∞

2.2.10 DNA sequencing

DNA sequences were verified, using standard or customised primers, at the University College London or Beckman Coulter sequencing services. The list of customised primers is given in Table 2.6.

2.3 Tissue culture

HEK293T cells were used for viral packaging, lentivector titrations and also testing of the transgene expression of cloned plasmids. They are highly transfectable cells derived from human embryonic kidney cells which stably expresses the large T antigen from simian virus 40. The expression of T antigen contributes to episomal maintenance and increased replication of vectors containing SV40 origin/promoter (DuBridge et al., 1987; Pear et al., 1993). This makes HEK293T ideal target cells for viral preparations, gene expression and protein production.

All adherent growing cell lines including HEK293T, HEK293 and mouse embryonic fibroblasts (MEF) were cultured in Dulbecco's modified Eagle's medium (DMEM)(Sigma), supplemented with 10% foetal bovine serum (FBS)(Gibco, Paisley, UK), 2 mM L-glutamine (Gibco), 100 U/ml Penicillin and 100 μg/ml Streptomycin (Gibco). These cells were grown at 37 ^{o}C in a 10% CO_2 incubator and passaged every 2-3 days, using Trypsin/EDTA (Sigma). The wild-type and MEKK3 KO MEFs were kindly provided by Prof. Philip Cohen (University of Dundee, Scotland).

Jurkat SVT35 cells and the 70Z/3 Pre-B cell line were cultured in Roswell Park Memorial Institute (RPMI) medium, supplemented with 10% FBS, 2 mM L-glutamine, 100 U/ml Penicillin, 100 μg/ml Streptomycin and 50 μM 2-Mercaptoethanol (Gibco). These cells were grown in a 5% CO2 incubator and passaged 1:10 (70Z/3) or 1:5 (Jurkat) every 3 days. The 70Z/3 and Jurkat SVT35 cells as well as their respective NEMO-deficient derivatives, 1.3E2 (Yamaoka et al., 1998) and JM4.5.2 cell (Harhaj et al., 2000), were kind gifts of Prof. Alain Isräel (Pasteur institute, Paris, France).

All cell lines were frozen in FBS containing 10% dimethyl sulfoxide (DMSO) at a density of 4-8 x10^6 cells/ml. Cell counting was performed either manually by use of a Neubauer chamber slide, or by using the Muse® cell analyser (Millipore).

2.4 Lentivectors

2.4.1 Lentiviral transfer plasmids

In this study, the pDual promoter lentivector backbone which has been previously described by our group (Arce et al., 2009; Rowe et al., 2009), was used. This construct incorporates two expression cassettes controlled by the spleen focus-forming virus (SFFV) and ubiquitin (Ub) promoters (Figure 2.1A). The SFFV promoter drives the

expression of a target gene (e.g, vFLIP or NEMO) while the Ub promoter initiates the expression of a fluorescent protein (emerald green fluorescent protein (eGFP) or mCherry).

The cDNA template of transgenes were amplified using reverse and forward primers with incorporated 5' *BamHI* and Kozak sequences (forward) and 3' *NotI* site (reverse), and then were subcloned into *BamHI-NotI* restriction sites under the control of the SFFV promoter. If the *BamHI* site was present within the gene of interest, the *BglII* site was used which gives compatible cohesive ends. If this was not applicable either, a pDual vector encoding *AsiSI* and *NotI* insertion sites (provided by Dr. Gary Britton), was used. Sequences of primers used for amplification of the transgenes have been listed in Table 2.4.

cDNA sources

cDNA templates were from the following sources: p22-FLIP and non-cleavable $cFLIP_L$ (Prof. Inna Lavrik, DKFZ, Germany), WT $cFLIP_L$ (Prof. Pascal Meier, ICR), RIP1 and FADD (Prof. Henning Walczak, UCL), CYLD (Addgene plasmid depositary), mCherry and firefly luciferase (Dr. David Escors). *E.coli* expressing plasmids encoding human $cFLIP_S$ cDNA (Clone ID: IHS1380-212917810) was obtained from Open Bioystems (Thermo Scientific). Human IKKα and IKKβ cDNAs were isolated from a cDNA pool synthesised from Jurkat cells.

2.4.2 Vector production

Lentivectors (LV) were generated by a 3-plasmid transient co-transfection of HEK293T cells using a transfer vector, a 2nd generation HIV-derived packaging plasmid (p8.91) and a plasmid expressing vesicular stomatitis virus-glycoprotein (VSV-G) envelope (pMD.G). The p8.91 and pMD.G vectors were obtained from Plasmid factory (Bielefeld, Germany) and have been described previously (Demaison et al., 2002) (Figure 2.1B and C).

One day prior to transfection, 10^7 HEK293T cells were seeded in 15 cm^2 dishes to reach a cell confluency of 70-80% the following day. Cells were then transfected using the FuGENE® HD transfection reagent (Promega) with the following mixture of components (per plate):

Table 2.13. Components of transfection mixture for LV production (amounts for a 15 cm plate)

Reagent	Quantity
LV transfer plasmid	3.75 μg
p8.91	2.5 μg
pMD.G	2.5 μg
FugeneHD	45 μl
Opti-MEM (Gibco)	500 μl

The mix was incubated at room temperature for 20 minutes and then added dropwise to cells in fresh DMEM. Twenty-four hours later the medium was changed and subsequently, three collections were made at day 2, 3 and 4 post-transfection. Supernatants containing lentiviral particles were then passed through 0.45 μm filters and concentrated 200-fold by ultra-centrifugation (20,000 RPM, at 4 °C for 2 hours) in a Sorvall centrifuge (Beckman Coulter). Viral pellets were then resuspended in ice-cold whole medium, incubated on ice for 1-2 hours and finally, aliquoted and stored at -80 °C, until use.

2.4.3 Viral titrations

Titration of LVs expressing a fluorescent protein (usually GFP or mCherry) was performed using flow cytometry technique, while for those lacking a fluorescent protein gene, quantitative PCR (qPCR) method was used.

2.4.3.1 LV titrations by flow cytometry

$2x10^5$ HEK293T cells were seeded in 24-well plates in 0.5 ml of DMEM, three to four hours before transduction. Cells were then transduced with serial dilutions (1 in 5, 25, 125, 625 and 3125) of the prepared lentiviral particles. Twenty-four hours later, plate wells were topped up with an additional ml of medium. Three days following transduction, cells were harvested, washed in PBS twice, pelleted in FACS tubes (1,500 RPM, at 4°C for 5 min) and resuspended in 300 μl of PBS. Subsequently, the percentage of fluorescent protein-expressing cells was quantified by flow cytometry using LSR-Fortessa® cell analyser (BD Biosciences) and BD Diva software. Dilutions which resulted in 10-30% transduction rate –which fall within the linear range of the titration graph- were used to calculate virus titrations using the following formula:

$$\frac{\#Cells \times transduction\,\% \times Dilution\ Factor}{Volume\ of\ Virus} \times 1000 = Infectious\ Units/ml$$

2.4.3.2 LV titrations by qPCR

This titration method calculates the number of integrated vector copies per cell. $2x10^5$ of HEK3293T cells were plated out in 24-well plates and transduced with 2-5 µl of LV. Three days post-infection, genomic DNA was extracted using DNeasy® Blood and Tissue kit (Qiagen) and quantified by Nanodrop. Standards containing 10^1 to10^5 copies of pHV per µl were prepared. We used primers and fluorescent Taqman probe which recognise the HIV leader sequence. Reactions were performed in duplicates using Realplex Eppendorf mastercycler. The PCR program included an initial step of 90 °C for 10 min, followed by 40 cycles of 90 °C for 1 min and 60 °C for 10 min. Finally, the number of cells was estimated from extracted gDNA concentration and then, based on the standard curve values, number of integrant copies per cell was calculated. The oligonucleotide sequences and the amount of reagents used for each reaction have been summarised in the following table.

Table 2.14. Components of qPCR reaction for titration of lentivectors.

Reagent	Quantity/rxn	Sequence
FW primer (GT248)	0.5 µl	5' tgtgtgcccgtctgttgtgt 3'
RS primer (GT 249)	0.5 µl	5' gagtcctgcgtcgagagagc 3'
Strong stop probe	0.25 µl	FAM 5'cagtggcgcccgaacaggga3' TAMRA
Quantitect Master Mix	12.5 µl	
ddH2O	8.25 µl	
Sample (Std or unkown)	2 µl	
Total	**25 µl**	

2.4.4 Cell transductions

Unless otherwise stated in the figures, cells were infected with lentiviral vectors at the following multiplicity of infection (MOI): HEK293/293T (10), Jurkat cells (20), MEFs (50) and 70Z/3 cells (100). At least 24 hours were allowed for the transgene expression before performing the functional assays.

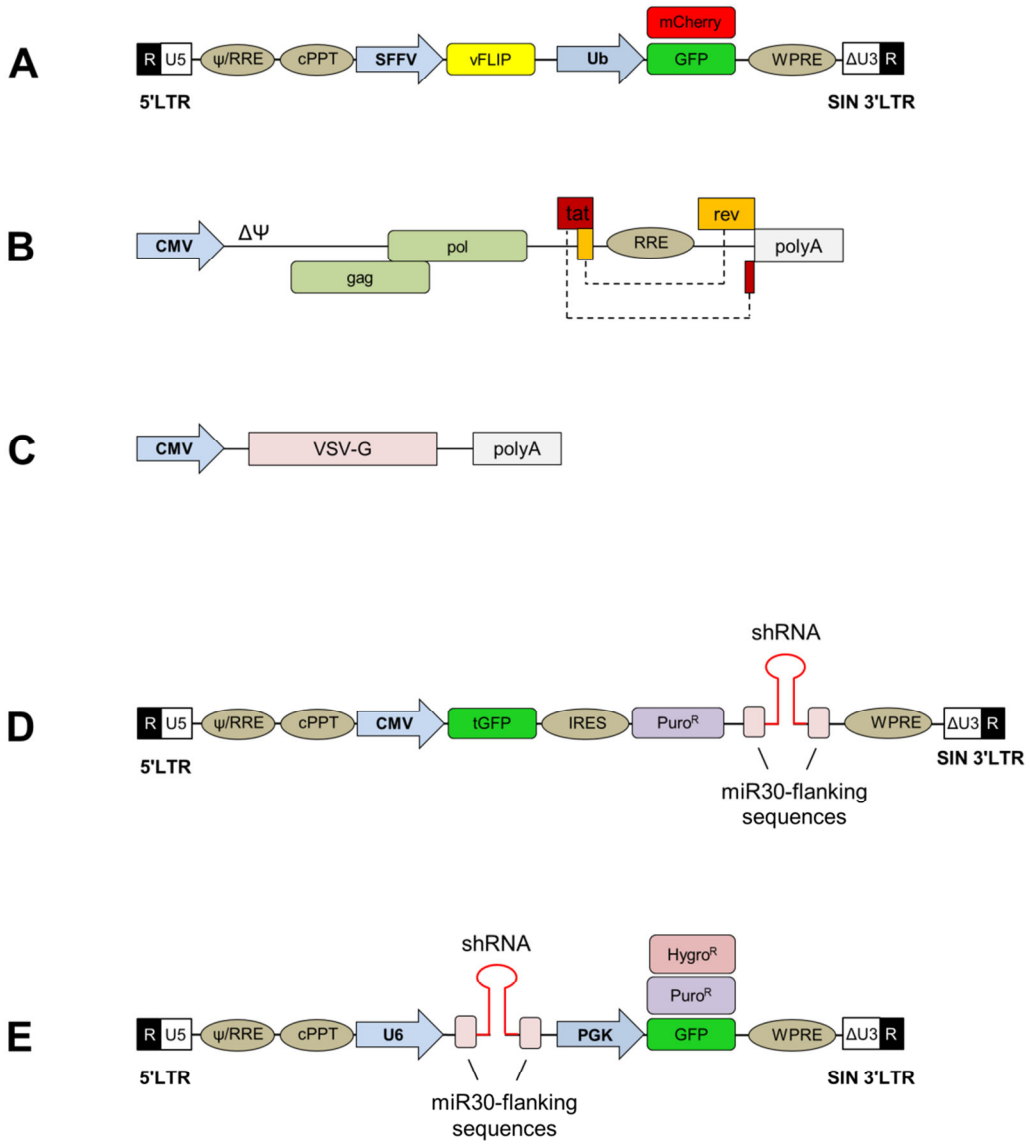

Figure 2.1. Lentiviral constructs. A) pDual vector. **B)** 2nd generation packaging plasmid. **C)** Envelope-expressing vector. **D)** pGIPZ. **E)** pHIV-SIREN. CMV: cytomegalovirus, cPPT: central polypurine tract, Hygro^R: hygromycin resistance gene, IRES: internal ribosome entry site, LTR: long terminal repeat, Puro^R: puromycin resistance gene, RRE: rev response element, SFFV: spleen focus-forming virus, tGFP: turbo GFP, Ub: ubiquitin. VSV-G: vesicular stomatitis virus-glycoprotein, WPRE: woodchuck hepatitis virus post-transcriptional regulatory element, Ψ: packaging signal.

2.5 Generation of stable knock-down cell lines

Short hairpin RNA (shRNA)-expressing lentivectors were produced using pGIPZ lentiviral plasmids (UCL Open Biosystems shRNA library). Alternatively, custom shRNA-encoding sequences were designed and cloned into pHIV-SIREN lentivector backbone (modified from pSIREN RetroQ, Clonetech).

2.5.1 pGIPZ

pGIPZ plasmids contain CMV promoter driving the transcription of turboGFP marker gene which is followed by an IRES (Internal Ribosome Entry Site), Puromycin resistance gene and an shRNA-encoding sequence within a microRNA30 context (Figure 2.1D). HEK293T cells were transduced with shRNA lentivectors (normally 5-7 targeting viruses for each protein) at an MOI of 50 and 48 hours later, Puromycin was added to medium at 1μg/ml concentration to select infected cells. A non-silencing and a GAPDH-targeting lentivectors were produced and tested alongside gene-specific shRNAs as negative and positive controls, respectively. Finally, the knockdown of protein expression was analysed by immunoblotting.

2.5.2 pHIV-SIREN

If pGIPZ constructs did not result in a successful knockdown or a different selection marker was needed, customised shRNA expressing oligonucleotide pairs were designed using Clonetech's online shRNA target finder and shRNA designer softwares and then, subcloned into the pHIV-SIREN backbone. Upon hybridisation, oligonucleotides designed by this software produce 5' *EcoRI* and 3' *BamHI* sticky ends which can be then ligated into the compatible sites within the destination vector.

The pHIV-SIREN is a bicistronic lentiviral construct designed to express a shRNA using the human U6 promoter and a selection marker gene (GFP, or Puromycin, or Hygromycin) driven by the phosphoglycerate kinase (PGK) promoter (Figure 2.1E). Selection of cells with HygromycinB (HygroGold®, Source Biosciences) was performed for two weeks at a concentration of 200 μg/ml. Cells transduced with GFP-expressing LVs were isolated by fluorescence-activated cell sorter (FACS).

2.5.3 shRNA sequences

Table 2.15. shRNA-targeted sequences.

Targeted Gene	Ref Seq	shRNA#	Clone number	Sequence (5'→3')	
Atg3 (Hs)	NM_022488.4	1	V2LHS_201190	cattgaccatattcatcaa	●
		2	V2LHS_14033	ggacttatatgtttatgca	●
		3	V2LHS_11836	cagccttacttgtttaata	
		4	V3LHS_319838	aagctgtcattccaacaat	
		5	V3LHS_319835	tggaaaataaggacaatat	
Caspase-8 (Hs)	NM_001228.4	1	V2LHS_112731	gtcatcctgggagaaggaa	
		2	V2LHS_112733	cctactttcacactaagaa	
		3	V2LHS_112730	gagctgctcttccgaatta	
		4	V3LHS_320399	gggtggttattgaaagtaa	●
		5	V3LHS_398368	tgcacagtagagcaaatct	●
		6	V3LHS_398369	gcaacaaggatgacaagaa	
FADD (Hs)	NM_003824.3	1	V2LHS_16975	caggacgaattgagataat	●
		2	V2LHS_16973	cgggatctcgtatctttaa	
		3	V3LHS_388202	ccgatgtcatggaactcag	
		4	V3LHS_412699	tgcaattctacagtttctt	
		5	V3LHS_388204	aggctggctcgtcagctca	
		6	V3LHS_388203	tgaccgagctcaagttcct	
		7	V3LHS_412698	aagatcttgtctccactaa	●
HOIL-1 (Hs)	NM_006462.4		pHIV-SIREN	ccacaacactcatctgtcaaa	●
HOIP (Hs)	NM_017999.4	1	V3LHS-399213	agctgctgtgctatgttcc	●
		2	V3LHS-399214	agcacggaggtgatgtgtc	
		3	V3LHS-399210	tggcgtggtgtcaagttta	
		4	V3LHS-399212	tgccgagtgatagagcaga	
MEKK3 (Hs)	NM_203351.1	1	pHIV-SIREN	cctggatatgagaccatga	●
		2	pHIV-SIREN	gagtgacgtcagaatcaag	
		3	V2LHS_1970	gcattgaactcaatcatga	
		4	V2LHS_151699	caaatgtcatgctgcctta	
		5	V2LHS_151695	ctgaccatcttcatggagt	●
		6	V3LHS_329522	tcggtgaaagaccagttga	
		7	V3LHS_329524	agacacaggtcactcaaat	

		8	V3LHS_329521	accaagatgatcttgataa	
		9	V3LHS_329520	agaatcaagttcgagcaca	
RIP1 (Hs)	NM_003804.3	1	V2LHS_241668	cagttgataatgtgcataa	
		2	V2LHS_17422	accaacagatgaatctata	
		3	V3LHS_638037	agagtaaactccaagacga	●
		4	V3LHS_638038	acagagaagtcggatgtgt	
		5	V3LHS_638034	agctgctaagtaccaagct	
		6	V3LHS_638036	tgggcgatatttgcaaata	
		7	V3LHS_645251	tgaagtggacgcctcactt	
		8	V3LHS_638040	accactagtctgacggata	●
		9	V3LHS_340514	gcgagatggactgaaagaa	
SHARPIN (Hs)		1	pHIV-SIREN	gtgttctcagagctcggtttc	
		2	pHIV-SIREN	ctgtccttcctgcaccttcat	●
		3	pHIV-SIREN	tggaaacttgacggagaga	
TAK1 (Hs)	NM_003188.3	1	V2LHS-153758	cagatgagccattacagta	
		2	V2LHS-201931	cctttggagttgtttgcaa	●
		3	V2LHS-201612	cgcccttcaatggaggaaa	
		4	V2LHS-202210	cgtgtgaaccatcctaata	●
		5	V3LHS-370925	agagtgaatctggacgttt	
		6	V3LHS-370924	agcttttagatgaaaacaa	
		7	V3LHS-370923	aggtagtaattacagtgaa	●
TAK1 (Mm)	NM_172688.3	1	pHIV-SIREN	cctgaacttcgaagagatc	
		2	pHIV-SIREN	cgaagagatcgactacaag	
		3	pHIV-SIREN	ctgagaggaaggctttcat	
		4	pHIV-SIREN	gcctgaatccagtatgtct	●
GAPDH (Hs)	NM_0012897 45.1			ccctcatttcctggtatgacaa	●
non-silencing				atctcgcttgggcgagagtaa	●

Hs: Homo sapiens, Mm: Mus musculus, RefSeq#: Reference sequence number

● indicates the shRNAs resulting in the highest knockdown efficiency.

2.6 Western blotting

Cells were washed twice with ice-cold PBS and then lysed by adding PBS-T lysis buffer (PBS containing 1% Triton X100 and 5% Glycerol, supplemented with complete protease inhibitor cocktail (Roche Diagnostics)) and incubating on ice for 10-15 min. After this, whole cell lysates were clarified by centrifugation at 13,000 RPM, 4 ^{o}C for 20 minutes. The supernatants were transferred to new tubes and quantified for total protein concentration using bicinchoninic acid (BCA) colorimetric assay (Pierce® BCA protein assay kit, Thermo Scientific, Rockford, IL). After adjusting samples for equal protein concentrations, they were mixed with 4x Laemmli sample buffer and boiled at 95 ^{o}C for 5 minutes.

30-50 μg of the prepared samples were subjected to electrophoresis in a 4% SDS-polyacrylamide stacking gel, followed by an 8-12% SDS-polyacrylamide separating gel at 120 Volts for 2 hours. The separated proteins were transferred to polyvinylidene difluoride (PVDF) membrane using semi-dry transfer system and subsequently blocked with 5% skimmed milk in PBS-T (PBS with 0.1% Tween20) for an hour. Next, it was incubated overnight at 4 ^{o}C with appropriate dilution of a primary antibody in PBS-T containing 5% BSA and 0.1% Na_3N. The membrane was washed in PBS-T five times for 5 minutes and incubated with horseradish peroxidase (HRP)-conjugated secondary antibody in PBS-T with 5% non-fat milk for an hour at room temperature. After thoroughly washing the membrane as stated above, it was incubated with LumiGLO® ECL (Cell Signalling Technology) for a minute and then, drained and exposed to Hyperfilm ECL (Amersham).

For reprobing with another antibody, membrane was incubated with stripping buffer for up to 45 minutes at 55 ^{o}C to denature both primary and secondary antibodies. This was followed by multiple washing steps with dH_2O and PBS-T. Membrane was then blocked for one hour and the immunoblotting procedure was continued as explained above. The buffers and antibodies used for immunoblotting have been summarised in Table 2.14 and Table 2.2, respectively.

Table 2.16. Western blot buffers and gel reagents

Buffer/gel	Composition
Laemmli sample buffer	50 mM Tris, pH6.8 10% Glycerol 2% SDS 5% 2-Mercapthoethanol 0.2 mg/ml Brumophenol blue 0.1 M DTT
Running buffer	25 mM Tris, pH8.5 200 mM Glycine 0.1% SDS
Transfer buffer	100 mM Tris, pH6.8 200 mM Glycine 20% Methanol
Stripping buffer	62.5 mM Tris-HCl, pH6.8 2% SDS 100 mM 2-Mercaptoethanol
4% stacking polyacrylamide gel	125 mM Tris-HCl, pH6.8 4% Acrylamide/bis 10% SDS 0.1% TEMED 1% Ammonium persulphate (APS)
10% separating polyacrylamide gel	125 mM Tris-HCl, pH8.8 10% Acrylamide/bis 10% SDS 0.1% TEMED 1% APS

2.7 Immunoprecipitation

After washing twice with ice-cold PBS, cells were lysed with PBS-E lysis buffer (PBS containing 1% TritonX100, 2 μM EDTA and complete Protease inhibitor cocktail) and incubated on ice for 15 minutes. The cell lysate were clarified as mentioned above and pre-cleared by incubating with beads for an hour at 4 ^{o}C. The pre-cleared lysate was

incubated with 1:100 dilutions of the desired antibody (test or isotype-matched control) plus 20 µl of ProteinA or G slurry beads at 4 °C for 2 hours while rotating. Next, beads were pelleted by centrifugation at 2,000 RPM for 2 min and washed twice with the high salt wash buffer (recipe in Table 2.17) followed by two additional washes with the PBS-E solution. Immune complexes were dissociated by adding 20 µl of 2x Laemmli buffer and boiling at 95 °C for 5 minutes. Finally, co-immunoprecipitation results were analysed by western blotting.

2.8 *In vitro* IKK kinase assay

Cytoplasmic extracts were prepared using kinase lysis buffer (see Table 2.17) and quantified for protein concentration using BCA method. 500-1000 µg of lysates were incubated with 20 µl Protein A sepharose beads and 1 µg anti-NEMO (sc-8330, Santa Cruz) for at least 2 hours at 4 °C. Beads were then washed in 0.5 ml of high salt wash buffer three times, 5 minutes each, followed by two more washes with kinase wash buffer. After removing all the residual wash buffer, 40 µl kinase reaction buffer plus 2 µg GST-IκBα (1-54) and 0.5 µl p^{32}γ-ATP was added to each sample and tubes were immediately incubated at 30 °C for 30 min. Reactions were stopped by adding 15µl 4x Lammeli buffer and incubating the tubes at 95 °C for 5 min. The samples were separated by 10% SDS-PAGE which was then dried out on a filter paper and exposed to a storage phosphor screen (GE Healthcare) for 15-30 minutes. To visualise the radiolabelled bands, the storage phosphor screen was scanned using Typhoon PhosphorImager (GE Healthcare) and the intensity of bands were quantified by ImageQuant TL 7.0 software (GE Healthcare).

Table 2.17. Composition of kinase assay buffers.

Buffer	Composition
Kinase lysis buffer	20 mM Tris-HCl, pH7.5 150 mM NaCl 1% Triton X-100 5% Glycerol 1 mM PMSF Protease inhibitor cocktail
High salt wash buffer	25 mM Tris-HCl, pH7.6 500 mM NaCl

	1 mM EGTA 1 mM DTT 1% Triton X-100 5% Glycerol 1 mM Na_3VO_4 10 mM β-glycerophosphate 5 mM NaF 1 mM PMSF
Kinase wash buffer	20 mM HEPES, pH7.6 50 mM NaCl 20 mM β-glycerophosphate 0.5 mM DTT 1 mM PMSF
Kinase reaction buffer	20 mM HEPES, pH7.6 50 mM NaCl 10 mM $MgCl_2$ 2 mM DTT 20 μM ATP 0.1 mM Na_3VO_4

2.8.1 Expression and purification of GST-IκBα(1-54)

First, IκBα(1-54) was PCR-amplified using the primers FW: 5'ggatccgccatgttccaggcg3' and RS: 5'gaattctcagaggcggatctcctg3', containing *BamHI* and *EcoRI* restriction sites (underlined), respectively. The PCR product was cloned into pJET1.2, sequence-verified and then digested and subcloned into the pGEX-2T vector (kindly provided by Dr. Pablo Rodriguez, UCL Cancer Institute).

Next, BL21 bacteria (NEB) were transformed with pGEX-2T-IκBα, streaked onto ampicillin LB-agar plates and grown overnight. A single colony was picked and grown at 37 °C in 100mL LB-broth containing 50 μg/ml ampicillin and 2% glucose until an absorbance of 0.4 to 0.5 at 600nm was reached. The bacterial culture was then induced by addition of 2mM isopropyl-β-thiogalactopyranoside (IPTG) for 3 hours at 37 °C. To act as a negative control, 5 ml of culture was be removed before induction and grown along with the induced culture. After incubation time, cultures were harvested by centrifugation

at 4,000 RPM for 10 minutes. The pelleted bacteria were then resuspended in B-PER Bacterial Protein Extraction Reagent (Pierce, ThermoSceintific), at 4 ml per gram of bacterial pellet, to lyse and release the GST fusion protein. Subsequently, the lysates were ultra-centrifuged at 20,000 RMP for 20 min at 4 °C to remove the bacterial debris. The supernatant was removed for purification with the pellet being resuspended in PBS for SDS-PAGE analysis after protein purification.

The supernatant was transferred to a 1 ml Glutathione Spin Column (Pierce) and the GST-IκBα was purified following the manufacturer's instructions (the protocol states that 3 fractions of eluted protein are produced with a possible 10 mg of protein being purified). Following the elution of the GST-IκBα from the spin column, the elution fractions, lysate, lysate supernatant and flow-through samples were subjected to SDS-PAGE and coomassie stained to determine the presence of the protein (Figure 2.2) After confirming the presence of GST-fusion proteins, the samples were dialysed to remove glutathione and other sample contaminants, using the 10 kDa molecular weight cut-off Vivaspin® columns (Millipore) and a dialysis buffer (20mM Tris-HCl, pH8.0, 100mM NaCl, 0.2mM EDTA, 10mM β-glycero-3-phosphate and 10% glycerol). Finally, the protein samples were adjusted to a concentration of 1 µg/µl and stored at -80 °C until use.

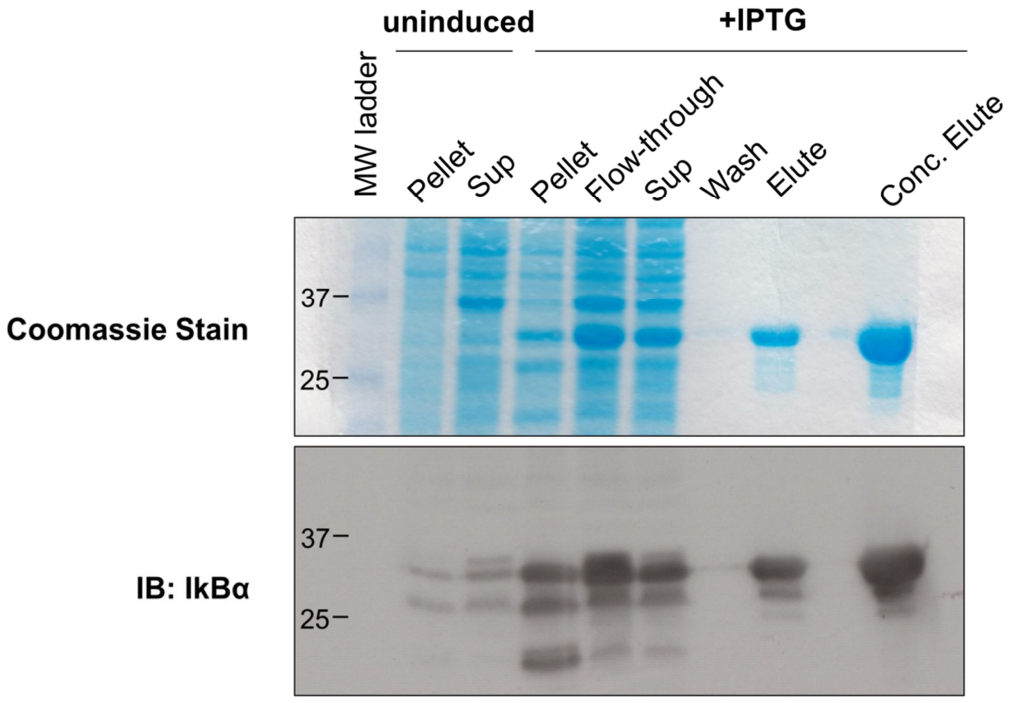

Figure 2.2. Expression and purification of the GST-IκBα.

2.9 *In vitro* IκBα phosphorylation assay

Resting HEK293T cells were lysed in HTX lysis buffer (10mM HEPES pH7.4, 10mM $MgCl_2$, 1mM $MnCl_2$, 0.1mM EGTA, 0.5% Triton X100) supplemented with complete protease inhibitor cocktail (Roche) and the S100 fractions were prepared by sequential centrifugation at 1,000 and 100,000g for 5 and 45 minutes, respectively. The cleared lysates were then incubated with recombinant FLIP and ATP generating system (10x stock: 10mM ATP, 20mM HEPES pH7.2, 10mM $MgCl_2$, 350mM creatinine phosphate and 500 μg/ml creatinine kinase) for 10 min at 37 °C. The reactions were terminated by adding 5x Laemmli buffer and boiling at 95 °C. Eventually, rec-FLIP-induced IKK activation rate was detected by immunoblotting for downstream indicators such as pIkBα and pIKKα/β. Levels of total IKKα/β served as control for equal protein loading.

2.9.1 Purification and expression of recombinant vFLIP, p22-FLIP and GB1-p22FLIP

Recombinant vFLIP was overexpressed and purified as described in Bagnéris et al (Bagnéris et al., 2008). For the production of recombinant p22-FLIP (and GB1-p22-FLIP), $cFLIP_S$ was first PCR amplified from a human thymus cDNA library (Clontech) using the primers 5'ttgctagcatgtctgctgaagtc3' and 5'ttctcgagtcacatggaacaatttc3' containing *NheI* and *XhoI* restriction sites respectively (underlined). Following digestion, the product was then ligated into the pETM442 vector (described in (Bagnéris et al., 2008)) to provide an N-terminal 6His-NusA tobacco etch virus (TEV) protease cleavable solubility tag to aid expression and purification. The resulting pETM442-$cFLIP_S$ vector was then used as the template for production of pETM442-p22-FLIP which was generated by the introduction of a stop codon at D196 using the primers 5'tccaaaagagtctcaagtagccttcaaataacttcaggat3' and 5'atcctgaagttatttgaaggctacttgagactcttttgga3'. GB1-p22-FLIP was produced by subcloning p22-FLIP into the *EcoRI* and *XhoI* restriction sites of a modified pET15b vector (kind gift from Prof Paul Driscoll, NIMR) to produce pET15-GB1-p22-FLIP (containing a 6His-GB1 solubility tag). The original pET15b vector was modified by inclusion of the coding sequence for the 56 amino acid B1 domain of *E.coli* protein G (GB1) 5' to the multiple cloning site (MCS), the addition of an *EcoRI* restriction site directly 3' to GB1 and removal of the MCS *EcoRI* site. This enabled subcloning of p22-FLIP 3' to GB1 into the

new *EcoRI* and existing *XhoI* sites. pETM442-p22-FLIP and pET15-GB1-p22-FLIP were then transformed into BL21(DE3) star® cells (Invitrogen).

The cultures were then inoculated into LB medium containing ampicillin (100 μg/ml) at a ratio of 1:100 and grown to an OD600 of between 0.6-0.8. They were subsequently induced with 1mM IPTG and the temperature reduced to 16°C overnight. Cells were harvested by centrifugation and the pellets either frozen at -80°C or re-suspended in a buffer comprising 25mM Tris-HCl pH 8.5, 200mM NaCl (buffer A) supplemented with an EDTA free protease inhibitor complex tablet (Roche) and DNase I (10 μg/ml). The purification protocols used for p22-FLIP and GB1-p22-FLIP were near identical. Resuspended pellets from 8L cultures of both proteins were sonicated on ice and the lysates clarified by centrifugation (46,000g for 1 hour). Supernatants were subsequently filtered through a 0.45 μm filter prior to loading on HisTrap FF columns (GE Healthcare) pre-equilibrated with buffer A. These were then washed with buffer B (A and 20mM imidazole) and eluted with buffer C (A and 500mM imidazole). For p22-FLIP, the 6His-NusA tag originating from the pETM442-p22-FLIP construct was removed by incubating 6His-NusA-p22-FLIP with TEV protease overnight while dialysing in buffer A (to remove the imidazole) and the solution reapplied to a 5ml HisTrap FF column pre-equilibrated in buffer A. p22-FLIP was eluted from the column using buffer A and 40mM imidazole. Fractions having greater than 95% purity as judged by SDS-PAGE gels were subsequently pooled and frozen at -80°C. Following elution from the 5ml HisTrap column, GB1-p22-FLIP appeared to be over 95% pure. To improve stability, however, GB1-p22-FLIP was subsequently dialysed into a buffer containing 5mM L-arginine, 300mM NaCl, 5mM TCEP and 25mM Imidazole prior to concentration using a 6ml, 10 kDa molecular weight cut-off Vivaspin concentrator (Millipore) and storage at -80 °C.

2.10 Immune complex dephosphorylation

Immunoprecipitated complexes were dephosphorylated using the Lambda protein phosphatase (LPP). This is an Mn^{2+}-dependent phosphatase with activity towards phosphorylated serine, threonine and tyrosine residues (Zhuo et al., 1993). Reactions were performed at 30 °C for 30 minutes, in a final volume of 50 μl using varying amounts of LPP (NEB) and Protein MetalloPhosphatase reaction buffer (50mM HEPES pH7.5, 10 mM NaCl, 2 mM DTT, 0.01% Brij35 and 1 mM $MnCl_2$). Subsequently, the reactions were

terminated by adding 25 mM Na_3VO_4 (Gordon, 1991) and 20 mM NaF, followed by cooling the samples on ice.

2.11 Luciferase gene reporter assays

Depending on the transfectability of the tested cell types, NF-κB luciferase assays were performed either by transfections or by viral transductions. 70Z/3, MEFs and Jurkat cells were mainly transduced while for HEK293 and HEK293T cells both transductions and transfections were utilised.

2.11.1 NF-κB reporter luciferase assays by transfection

One day prior to transfection, $2x10^5$ of HEK293 or 10^5 of HEK293T cells were seeded in 24-well plates in total volume of 500 µl. Then, cells were transfected with 400 ng of NF-κB luciferase plasmid (pGL.IgK or pGL H2DK), 100 ng of pRL.TK as internal control and 500 ng of pCDNA3 vectors encoding a transactivator gene. Twenty-four hours later the medium was removed, cells were resuspended in 100 µl of medium and transferred into an optical bottom 96-well plate. Luciferase activity was then measured using Dual-Glo® luciferase assay kit (Promega, Madison, WI). First, NF-κB-induced firefly luciferase activity was quantified by adding 50 µl of Dual-Glo luciferase reagent, this signal then was quenched by adding 50 µl of Stop and Glo reagent which also produces stabilised signal from Renilla luciferase. Firefly luciferase activity levels were normalised to that of Renilla which is driven by thymidine kinase promoter of herpes simplex virus and serves as transfection efficiency control.

2.11.2 NF-κB reporter luciferase assays by transduction

HEK293/293T, Jurkat, MEFs and 70Z/3 cells were transduced with NF-κB luciferase lentivectors at MOIs of 10, 50, 100 and 500, respectively to generate the stable NF-κB-reporter cell lines. These cells were passaged at least 2-3 times before performing assays. Next, to assess NF-κB activity, $5x10^4$ cells were seeded in optical bottom 96-well plate and transduced with test lentivectors at MOIs of 10, 20, 50 and 100 for HEK293/293T, Jurkat, MEFs and 70Z/3 cells, respectively. Forty-eight hours later, 50 µl BrightGlo® luciferase substrate (Promega) was added to each well and NF-κB-induced luminescence was detected using Varioskan Flash multimode reader (Thermo Scientific).

2.12 Statistical analysis

Statistical differences between two groups were analysed by the two-tailed unpaired student's *t* -test using the GraphPad Prism v4.03 software package (Graphpad Sotware, La Jolla, CA). The calculated *P*-values are given in the figures. All experiments were performed in triplicates, on at least three independent occasions (unless otherwise stated). The quantitative data are presented as mean±SD.

CHAPTER

3

The Role of NEMO in IKK Activation by KSHV vFLIP and Cellular FLIPs

3.1 Introduction

Constitutive activation of NF-κB signalling is linked to cancer development and progression by providing an inflammatory environment for tumour cells and conferring resistance to apoptosis (DiDonato et al., 2012). The oncoproteins KSHV vFLIP and HTLV-1 Tax stably bind to NEMO and constitutively activate the IKK complex, contributing to the neoplastic character of the associated viruses. Cellular FLIPs, which share a high degree of sequence homology with KSHV vFLIP (Figure 1.4), are also strong inducers of the NF-κB cascade (Hu et al., 2000). These proteins become upregulated in a variety of malignancies and are promising targets for cancer therapies (Shirley and Micheau, 2010). Much is known about the role of cFLIPs in the regulation of cell death pathways; however, how they activate NF-κB remains elusive. Potential similarities to vFLIP-induced activation have been suggested, but not investigated.

The crystal structure of the vFLIP-NEMO complex has been solved and multiple lines of evidence exist that indicate the necessity of binding to NEMO for the vFLIP-mediated induction of IKK (Bagnéris et al., 2008; Field et al., 2003; Liu et al., 2002). It is not clear how this interaction leads to activation. In this chapter, we aimed to explore the role of NEMO in FLIP-induced IKK activation with a particular emphasis on the ubiquitin binding function of NEMO. The UBAN domain of NEMO is indispensable for cytokine-induced IKK activation and has been shown to undergo conformational changes upon binding to linear ubiquitin oligomers (Bloor et al., 2008; Rahighi et al., 2009). Our initial working hypothesis was that vFLIP binding to NEMO may cause similar conformational changes, leading to changes in proximity or conformation of the catalytic IKKα and IKKβ, in favour of the activation. Therefore, we first set out to determine whether FLIP proteins required ubiquitination and the ubiquitin binding activities of the NEMO to stimulate IKK, or whether binding to NEMO was sufficient to bypass these processes.

In the following sections, I provide a brief description of the key IKK-dependent functions of the NEMO and also, a summary of the current knowledge on the interaction of NEMO with vFLIP, Tax and cellular FLIPs.

3.1.1 Molecular control of IKKs by NEMO

3.1.1.1 NEMO mediates the Ub-dependent activation of IKK

Activation of the canonical NF-κB pathway is contingent upon non-degradative polyubiquitination. NEMO plays a crucial role in ubiquitin-mediated activation of the IKK complex as it specifically recognises polyubiquitin chains through its UBAN domain and also, becomes ubiquitinated itself (Tokunaga et al., 2009; Wu et al., 2006a). Cells expressing NEMO mutants defective in Ub-binding exhibit impaired activation of IKKα/β in response to IL-1 and TNFα (Ea et al., 2006; Windheim et al., 2008; Wu et al., 2006a). Importantly, similar mutations of the UBAN domain of NEMO are found in patients afflicted with EDA-ID and IP, emphasising the essential role of this domain *in vivo* (Hubeau et al., 2011; Smahi et al., 2000).

Initially it was thought that the UBAN specifically binds to K63-linked ubiquitin chains (Wu et al., 2006a); later studies, however, demonstrated that it displays 100-fold higher affinity for linearly-linked ubiquitin chains (Rahighi et al., 2009; Xu et al., 2011). Consistent with these findings, full-length NEMO mutants engineered to selectively bind to K63-linked polyubiquitin only weakly activate NF-κB (Kensche et al., 2012). One further study, however, demonstrated that despite the much higher preference of NEMO C-terminus for linear ubiquitin oligomers, its immobilisation – which may be reminiscent of cellular IKK oligomerisation - enhances its affinity towards K63 linkages (Hadian et al., 2011). Therefore, in cells, both types of these linkages may function in a certain spatio-temporal order to achieve the maximal levels of NF-κB activation.

As previously mentioned, activation of the IKKs seems to occur through an induced proximity which results from dense organisation of the signalling components or structural changes induced by binding of adapter proteins. NEMO-mediated ubiquitin binding has been proposed to participate in both processes.

Upon receptor-mediated activation of the NF-κB, K63-linked ubiquitin chains synthesised by E3 ligases such as TRAF2/5 and cIAP1/2 (in TNFα signalling), and TRAF6 (in IL-1 signalling), provide a recruitment platform for TAB2/TAK1 and NEMO/IKK complex. These K63 ubiquitin chains also recruit LUBAC (Emmerich et al., 2013) to generate linear polyubiquitin oligomers on the NEMO and other substrates such as RIP1 (Gerlach et al., 2011), resulting in further stabilisation of the signalling complex. UBAN-mediated attachment to ubiquitin chains is suspected to enable NEMO

to facilitate co-localisation of IKKs with TAK1, leading to phosphorylation and activation of the IKKα/β (Clark et al., 2013).

Alternatively, binding of NEMO to ubiquitin have been suggested to cause IKK activation via other mechanisms. Crystal structure studies by Rahighi et al., showed that binding of linear di-ubiquitin molecules to the UBAN domain, induces an straightening of this coil-coiled region (Rahighi et al., 2009). It was proposed that this conformational change may then transmit to the N-terminal regions of NEMO, resulting in the re-orientation of the catalytic IKKs, favouring activation by autophosphorylation. Relevant to this notion, site-specific mutations can be introduced to NEMO (such as K270A in murine NEMO) which overcome the need for ubiquitin binding and constitutively activate IKK in the absence of any proinflammatory stimuli (Bloor et al., 2008). Such mutations may mimic the conformational alterations induced by the binding of the ubiquitin oligomers. That said, whether structural changes to NEMO translate to allosteric effects on IKKα/β, remains to be demonstrated.

3.1.1.2 Post-translational modifications of NEMO fine-tune the IKK activity

In addition to ubiquitination, other post-translational modifications such as phosphorylation and SUMOylation, also play crucial roles in modulating the function of NEMO (Perkins, 2006). Following NF-κB stimulation, IKKβ phosphorylates NEMO at several amino acids, located near the N-terminus and the C-terminus (Carter et al., 2003; Palkowitsch et al., 2008; Prajapati and Gaynor, 2002). Notably, phosphorylation of serine68 of NEMO, which resides within the IKKα/β-binding domain, disrupts the NEMO dimerisation and NEMO-IKKβ interaction (Palkowitsch et al., 2008). Accumulating evidence suggest that this modification together with the simultaneous authophosphorylation of IKKβ at its C-terminal NBD (Delhase, 1999; Schomer-Miller et al., 2006), serve as an intrinsic regulatory mechanism preventing hyperactivation of the IKKα/β following stimulation.

SUMOylation of NEMO is another important post-translational modification, found to be critical for its role in the nuclear-initiated NF-κB activation (Miyamoto, 2011). In cells, a subset of NEMO exists as an unbound form that shuttles between nucleus and cytoplasm. This form of NEMO appears to be essential for connecting the nuclear DNA damage events to cytoplasmic activation of IKK. Upon genotoxic stress, nuclear NEMO becomes SUMOylated by the SUMO E3 ligase, PIASy (protein inhibitor of activated

STAT y) at the lysines 277 and 309 (Huang et al., 2003; Mabb et al., 2006; Stilmann et al., 2009). This marks NEMO for cIAP1-mediated monoubiquitination at the same lysine residues, leading to its nuclear export and subsequent activation of TAK1, IKK and NF-κB, in a manner that requires ELKS (Huang et al., 2003; Wu et al., 2006b). Interestingly, SUMO-fused mutants of NEMO localise in the nucleus, indicating the importance of SUMOylation in determining the subcellular localisation of NEMO (McCool and Miyamoto, 2012). Taken together, these findings underscore the significance of the post-translational modifications of NEMO in producing a highly regulated and signal-specific NF-κB signalling.

3.1.1.3 NEMO ensures the substrate-specificity of the IKKβ

Most studies on NEMO have focused on its well-known role in the activation of IKKα/β. Nevertheless, a recent study showed that constitutively active IKKβ fails to activate NF-κB in the absence of NEMO, suggesting that NEMO may have additional roles (Schröfelbauer et al., 2012). Further investigations by Schrofelbauer et al., revealed that NEMO directs the substrate-specificity of IKKβ towards IκBα, through its ZF domain. Not surprisingly, various in-frame deletions and point mutations of the ZF domain are associated with the disease, EDA-ID (Cordier et al., 2008).

IKKα and IKKβ are pleiotropic enzymes which target a broad spectrum of NF-κB-related (e.g. IκBs, p65, and p105) and NF-κB-unrelated substrates (e.g. β-catenin, FOXO3 and p53) (Hinz and Scheidereit, 2014). Mutations of NEMO that fail to recruit IκBα, result in an increased phosphorylation of p65 and p105 (Schröfelbauer et al., 2012). This raises the possibility that NEMO may use distinct regions to target the activity of catalytic IKKs to other substrates. In support of this notion, panr2 mice that harbour a L153P mutation in NEMO exhibit severe defects in phosphorylation of p65 and p105, despite normal phosphorylation and degradation of IκBα (Siggs et al., 2010). Taken together, these findings indicate that NEMO is necessary not only for the activation of the IKK complex but also to ensure the substrate-selectivity of the enzymatic subunits.

3.1.1.4 NEMO serves as a docking site for various IKK-regulating proteins

Activation of IKK is a transient event which depends on dynamic regulatory processes to produce an optimal signal. The balance towards activation or deactivation is determined by selective recruitment of the upstream co-factors to the IKK complex machinery. In this regard, the elongated coiled-coil structure of NEMO provides a

docking platform for numerous regulatory proteins. Tables 3.1 gives a summary of such proteins which directly or through an adapter protein, interact with NEMO and modulate IKK activity.

Apart from the functions mentioned here, NEMO regulates a plethora of other NF-κB dependent (e.g. interferon production) and NF-κB independent mechanisms which have been reviewed in (Clark et al., 2013).

Table 3.1. NEMO-interacting proteins.

Interactor	Interaction region	Function	Reference
A20	aa 95-218	inh	(Zhang et al., 2000)
ABIN1	aa 50-100	inh	(Mauro et al., 2006)
ABIN2	aa 174-306	inh	(Liu et al., 2004)
ActI/CIKS	aa 1-150	inh	(Li et al., 2000; Mauro et al., 2003; Qian et al., 2004)
ATM	n.d	act	(Wu et al., 2006b)
CARMA1,3	n.d	act	(Stilo et al., 2004)
CBP	n.d	inh	(Verma et al., 2004)
CSN3	aa 297-419	inh	(Hong et al., 2001; Rual et al., 2005)
CYLD	ZF	inh	(Kovalenko et al., 2003; Saito et al., 2004; Trompouki et al., 2003)
EHV2 vCLAP	aa 300-419	act	(Poyet et al., 2001)
ELKS	n.d	act	(Ducut Sigala et al., 2004)
HIF-2α	aa 50-358	act	(Bracken et al., 2005)
HSP70	aa 25-320	inh	(Ran et al., 2004)
Htt	aa 1-134	act	(Khoshnan et al., 2004)
NLRX1	UBAN	inh	(Xia et al., 2011)
p47	K63 and linear Ub chains bound to NEMO	inh	(Shibata et al., 2012)
PAN1	n.d	inh	(Bruey et al., 2004)
PARP1	aa 1-126	act	(Stilmann et al., 2009)
PIASy	aa 1-120	act	(Huang et al., 2003; Mabb et al., 2006)
PIDD	n.d	act	(Janssens et al., 2005)
PP2A	aa 121-179	act	(Kray et al., 2005)
PP2Cβ	n.d	inh	(Prajapati et al., 2004)

RIP1	UBAN	act	(Wu et al., 2006a; Zhang et al., 2000)
SRC3	n.d	act	(Amazit et al., 2007)
TANK	aa 200-250 (mNEMO)	act	(Bonif et al., 2006; Chariot et al., 2002)
TFG	LZ	act	(Miranda et al., 2006)
TRAF1/2	n.d	act	(Devin et al., 2001; Henn et al., 2007)
TRUSS	n.d	act	(Soond et al., 2003)
Ubiquitin	UBAN	act	(Bloor et al., 2008; Ea et al., 2006; Wu et al., 2006a)
ZNF216	n.d	act	(Huang et al., 2004a)

n.d: not determined, inh: inhibition, act: activation, mNEMO: murine NEMO.

3.1.2 Interactions of the Tax, vFLIP and cFLIPs with NEMO

It is now well-established that the persistent activation of the canonical IKKs by Tax and vFLIP requires stable assembly with NEMO (Chu et al., 1999; Field et al., 2003; Harhaj and Sun, 1999). Although the mechanism by which these interactions lead to NF-κB activation is still a matter of mystery (See 5.1 for the suggested mechanisms). Using co-immunoprecipitation assays, Tax has been shown to interact with two distinct but highly homologous motifs in NEMO: one in the N-terminus (aa 100-140) and the other, near the C-terminus (aa 312-340) (Figure 3.1A) (Xiao et al., 2000). The region of Tax responsible for binding to NEMO is localised to a leucine rich repeat (LRR) motif, containing amino acid residues 105-141. Site-specific mutations of the LRR domain which disrupt binding to NEMO, such as those in the Tax M22 mutant (T130A, L131S), abrogate Tax-induced IKK activation. Strikingly, in-frame fusion of the M22 to NEMO restores its NF-κB activating function, further emphasising the necessity of interaction with NEMO for Tax-mediated IKK activation (Xiao and Sun, 2000; Xiao et al., 2000).

vFLIP, despite employing a similar mode of IKK activation which depends on physical interaction with NEMO, appears to target a different region of NEMO. Studies conducted in our laboratory have mapped the vFLIP-binding region of NEMO to its HLX-2 domain (residues 192-252) (Bagnéris et al., 2008; Field et al., 2003). Subsequent crystal structure studies determined that this region of NEMO forms a parallel intermolecular coiled -coil recognised by two vFLIP molecules that interact through their respective DED1 motifs (Fig 3.1B and C) (Bagnéris et al., 2008). Interactions of the NEMO helices with DED1 is facilitated by the presence of two deep adjacent clefts, of

which, cleft1 mediates the majority of the interprotein contacts (Fig 3.1C). Mutating the key amino acids of the cleft1-HLX2 interface (e.g. A57L in vFLIP and D242R in NEMO) results in complete abolition of the complex formation.

While some homologues of the KSHV vFLIP (e.g. p22-cFLIP) are similarly potent activators of the IKK, others fail to stimulate this complex (e.g. MC159L). This raises the possibility that the ability of FLIPs to activate IKK may depend on the conservation of structural properties affecting the FLIP-NEMO interface. In support of this concept, structural alignment of the KSHV vFLIP and MC159L suggested that the sequence differences in the latter, result in obscuring cleft2 and complete closure of cleft1, thereby abrogating the NEMO binding (Figure 3.1D). In the case of p22-FLIP, however, there are no amino acid substitutions that would lead to major steric clashes and hence drastic remodelling of cleft1 and cleft2. Therefore, FLIP-mediated activation of the canonical NF-κB pathway may strongly rely on the preservation of the NEMO contacts mediated by clefts of the DED1 motif (Figure 3.1D)(Bagnéris et al., 2008).

Among cFLIP variants, the proteolytic fragments p43-FLIP and p22-FLIP, have been reported to directly interact with NEMO (Golks et al., 2006; Neumann et al., 2010). p43-FLIP is generated by procapase-8 cleavage of the $cFLIP_L$ at the DISC following CD95 stimulation (Neumann et al., 2010), however, p22-FLIP can be catalysed from all isoforms ($cFLIP_{L/S/R}$) and differs form p43-FLIP in that it can be also produced in non-apoptotic cells. Therefore, p22-FLIP is believed to be the final cleavage product of cFLIP proteins, serving as the mediator of NF-κB activation, in a manner similar to that of KSHV vFLIP (Bagnéris et al., 2008; Golks et al., 2006). Nevertheless, there exists no experimental data demonstrating whether p22-FLIP (or any other cFLIP variant) targets the same vFLIP-binding region of the NEMO and whether this possible interaction is necessary for cFLIP-induced IKK activation.

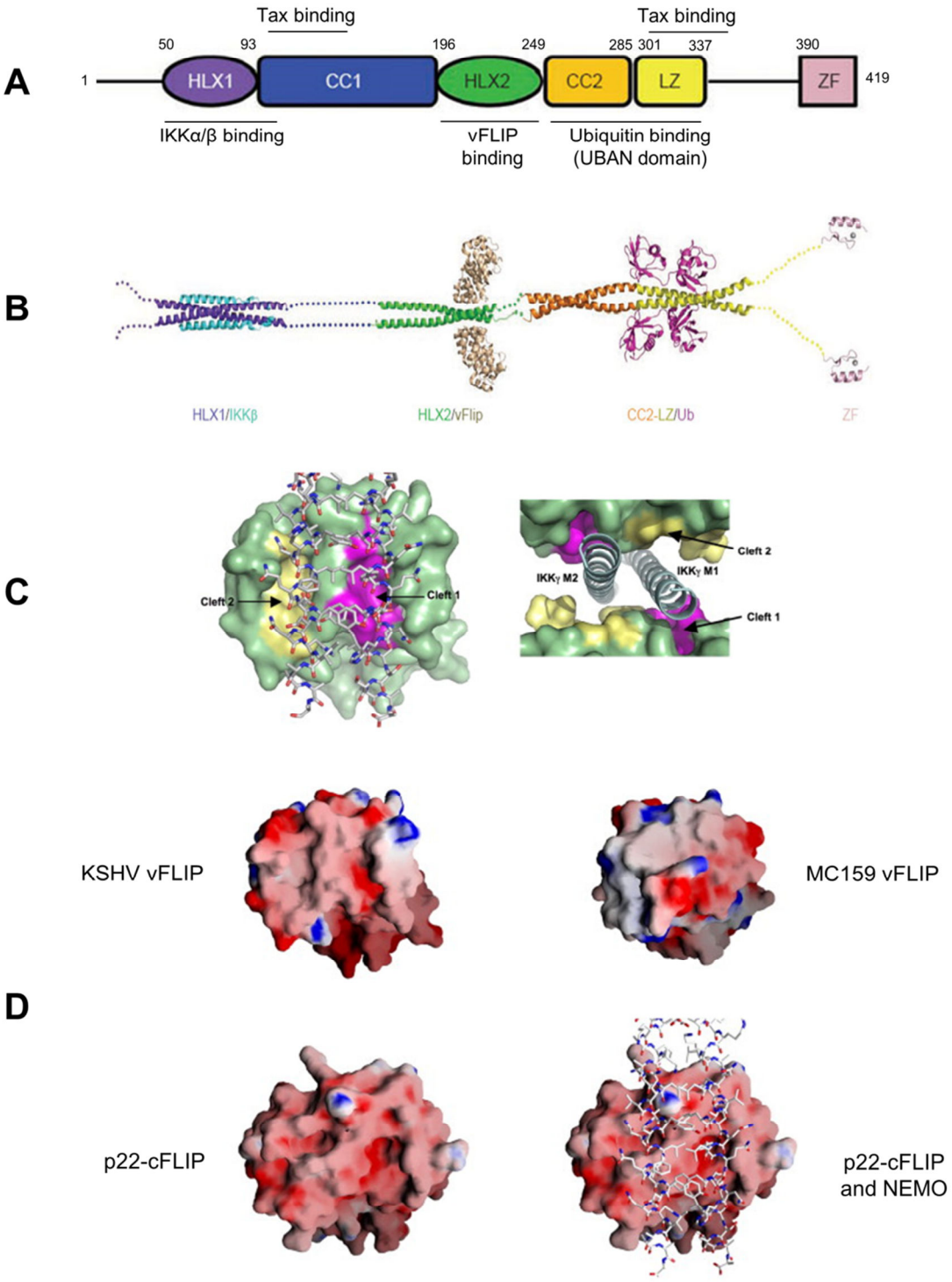

Figure 3.1. Structure of NEMO and its complexes. A) Domain organisation of the NEMO and its interaction sites with IKKα/β, vFLIP, ubiquitin and Tax. CC: colied coil, HLX: helical domain, LZ: leucine zipper, ZF: zinc finger. **B)** Crystal structures of NEMO fragments. Three-dimensional structure of the full-length NEMO is not available

yet; however, the crystal structures of several NEMO fragments have been resolved. These include: N-terminal kinase binding domain of NEMO in complex with IKKβ (Rushe et al., 2008), HLX2 in complex with KSHV vFLIP (Bagnéris et al., 2008), CC2-LZ fragment in complex with linear di-ubiquitin (Rahighi et al., 2009) and ZF domain (Cordier et al., 2008). **C)** The KSHV vFLIP-NEMO interface. Left panel: KSHV vFLIP depicted as green surface contains two adjacent vertical clefts in its DED1 motif. Cleft1 and cleft2, highlighted in magenta and yellow, respectively, are found to form a complementary binding surface for NEMO helices. Right panel: two vFLIP molecules are seen in complex with a central region of two parallel alpha helices of NEMO. Both clefts of the vFLIP are pivotal to the recognition of the NEMO dimer, although, the majority of interprotein contacts are mediated by cleft1. **D)** Structural comparisons of KSHV vFLIP, MC159 vFLIP and p22-FLIP. Analysis of the electrostatic potential surfaces of these proteins shows that the cleft1 and cleft2 are absent in MC159 vFLIP. However, homology model of p22-FLIP suggests that two binding clefts are conserved in this protein and that the analogous interactions to those observed with KSHV vFLIP are possible with NEMO. Reproduced from (Zheng et al., 2011) and (Bagnéris et al., 2008) with a permission from the publishers.

3.2 Aims of the chapter

- Identify the domains of NEMO that are required for IKK activation by vFLIP and cellular FLIPs
- Examine whether cellular FLIPs physically interact with NEMO and if they do, which region of the NEMO is targeted
- Examine the importance of linear ubiquitination in FLIP-induced activation of IKK

3.3 Results

3.3.1 Generation of a NF-κB reporter luciferase assay system

In order to establish a cell-based NF-κB activation assay, we generated a lentiviral vector (LV) that allows for NF-κB-dependent transcription of the firefly luciferase under the control of the minimal CMV promoter and four repeats of an NF-κB binding site (Figure 3.2A). First, to test the specificity of the system, we transduced cells with the lentivectors encoding GFP, or vFLIP, or NF-κB luciferase with and without vFLIP or GFP (each MOI=10). Forty-eight hours later, cells were lysed and activity of the firefly luciferase was measured using Bright-Glo detection system. As shown in Figure 3.2B, the IKK activator vFLIP robustly induced expression of luciferase by more than 100-fold increase (compared to unstimulated cells), whereas the GFP control failed to induce any luciferase activity. Next, to examine the sensitivity of our reporter system, we transduced HEK293T cells with increasing MOIs (0.5, 1, 2, 4, 8, 16 and 32) of both NF-κB luciferase and vFLIP lentivectors. Figure 3.3C and D show that the levels of luciferase activity correlated well with MOIs of the vFLIP LV, except in the condition where MOI of 32 was used for the NF-κB luciferase LV. Since the transductions of vFLIP and NF-κB luciferase were performed simultaneously, this could be due to a competition in viral entry between the two LVs at high MOIs. In all the luciferase experiments discussed later, I first transduced cells with NF-κB luciferase LV to produce a reporter cell line and then, activation assays were performed after at least two cell passages.

Collectively, the data presented in Figure 3.2 show that our LV-based NF-κB activation assay is highly sensitive and specific. An important advantage of this LV-based system is that it allows for genetic engineering of poorly transfectable cells (e.g. MEFs) that cannot be assessed using conventional reporter assays based on transient transfection. Furthermore, working with stable reporter cells can circumvent the problem with variations in transfection efficiency that may mask the NF-κB-dependent signal.

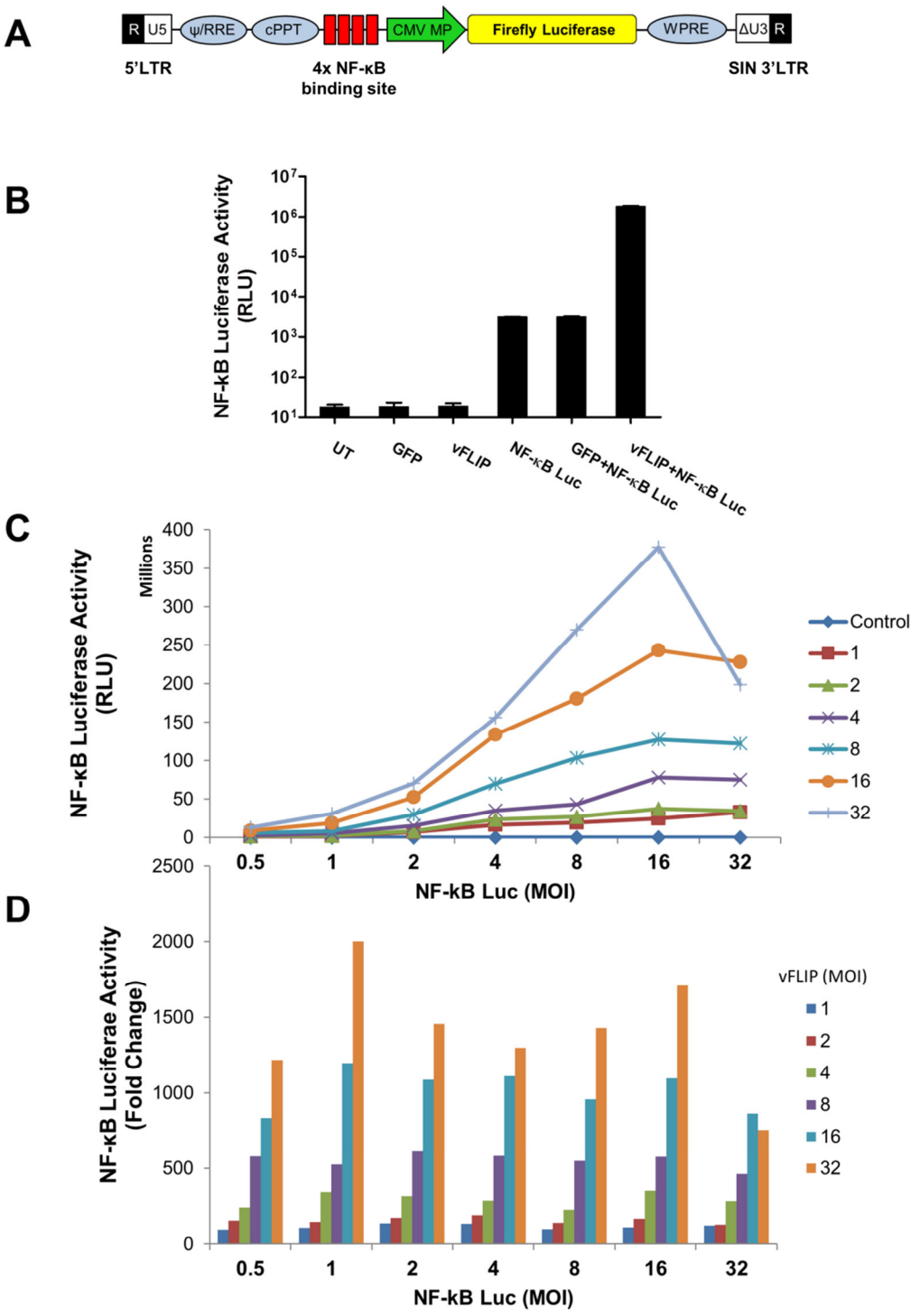

Figure 3.2. Generation of a cell-based NF-κB reporter luciferase assay. A) Schematic representation of the lentiviral construct (pSIN NF-κB Luc) used for the NF-κB reporter luciferase assays. CMV MP: minimal promoter of cytomegalovirus, cPPT: central polypurine tract, LTR: long terminal repeat, NF-κB RE: NF-κB response element, RRE: rev response element, SIN: self-inactivating, WPRE: woodchuck post-transcription regulatory element. **B)** NF-κB reporter luciferase assay to check the specificity of the

system. HEK293T cells, seeded in 96-well plates ($2x10^4$/well) were transduced with lentiviral vectors encoding GFP, or vFLIP, or NF-κB luciferase with and without GFP or vFLIP. The NF-κB dependent luciferase activity was measured 48 hours post-transduction. **C)** NF-κB reporter luciferase assay to check the sensitivity of the system. The same number of HEK293T cells, as described in (B), were transduced with LVs encoding NF-κB reporter luciferase and vFLIP over a broad range of MOI (0.5, 1, 2, 4, 8, 16, 32) for each lentivector. Cells were lysed 48 hours following transduction and the luciferase activities were measured using Bright GLO luminescence detection kit (Promega). The results are represented as RLU (relative luminesce units). **D)** as in (C), but the results have been represented as normalised fold change values, calculated by dividing of the RLU of activated cells to RLU of the control cells.

3.3.2 Unlike vFLIP and Tax, cellular FLIPs require Ub-binding function of NEMO to activate NF-κB signalling

To determine which functions of NEMO were necessary for IKK activation by the FLIP proteins, we used the NEMO null cell line 1.3E2 - a derivative of the mouse preB cell line 70Z/3- harbouring an NF-κB responsive luciferase gene. These cells were reconstituted with wild-type NEMO, a point mutant which does not bind linear ubiquitin (F312A, (Rahighi et al., 2009)), or a F238R/D242R mutant suggested by structural studies to disrupt vFLIP binding (Bagnéris et al., 2008). To do this, we used lentiviral vectors expressing wild type or mutant NEMO together with an mCherry fluorescent protein (See Figure 2.1A). Cells were transduced so that approximately 50% were mCherry positive. We then isolated cell clones, expanded those that were mCherry positive and performed immunoblotting to establish that the transduced cells expressed NEMO (Figure 3.3A). Cells were then infected with a second lentiviral vector expressing cFLIP variants (p22-FLIP, $FLIP_S$, $FLIP_L$), or vFLIP, or Tax together with eGFP. After 48 hrs eGFP was monitored and cells with transduction rates over 80% were used to measure luciferase activity.

Figure 3.3C shows that both vFLIP and Tax could activate IKK in the absence of its ubiquitin binding function, unlike the control Toll-like receptor agonist lipopolysaccharide (Figure 3.3B). In contrast, $cFLIP_L$, $cFLIP_S$, and their proteolytic product p22-FLIP all require the ubiquitin binding function of NEMO to activate IKK (Figure 3.3D). To our surprise, all cFLIP variants were able to activate vFLIP-binding

deficient NEMO, suggesting that cellular FLIPs either target different motifs of NEMO, or bind to it indirectly, or function at some upstream step (Figure 3.3D). Activation of F238/D242RR mutant by Tax, which binds to distinct regions of NEMO, and also LPS further showed that this mutation specifically inhibits vFLIP and does not impair other activatory mechanisms (Figure 3.3C).

As previously mentioned, the Ala57 residue of vFLIP plays an important role in binding to NEMO and an A57L mutation reportedly impairs NF-κB inducing activity of the protein. The LAE sequence harbouring this alanine is conserved in both KSHV and cellular FLIPs (marked with * in Figure 3.4A). To test if this residue was also important for the function of cFLIPs, I generated equivalent A56L mutants of all three isoforms and performed an NF-κB activation assay on 293T cells. The mutation resulted in almost complete inactivation of all FLIPs (Figure 3.4C). However, western blot analysis showed low levels of protein expression for vFLIP, p22-FLIP and $FLIP_S$, indicating that this mutation renders the proteins unstable (Figure 3.4B). This observation makes the relevant results inconclusive; nevertheless, similar protein levels in the case of WT and mutant $FLIP_L$ suggests that the conserved L57 residue may play a role in NF-κB induction by cFLIP variants.

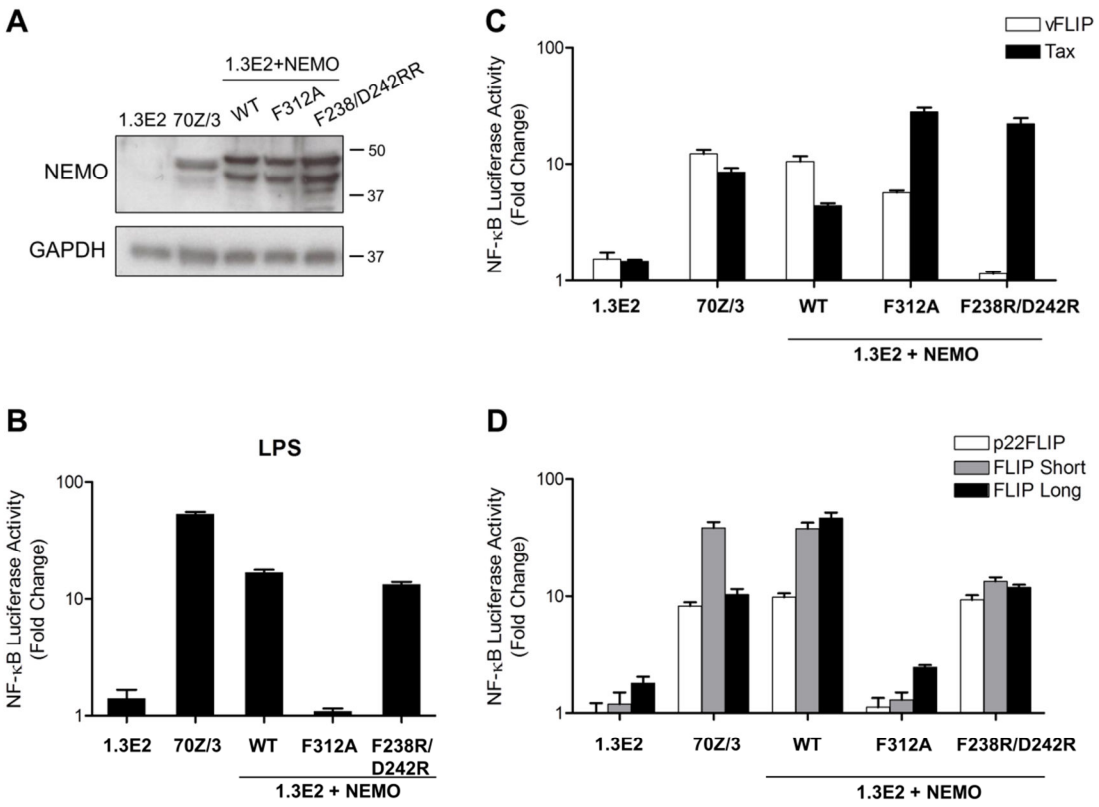

Figure 3.3. Mutational studies on NEMO reveal differential NF-ϰB activation mechanisms for the KSHV vFLIP and cellular FLIP isoforms. A) Immunoblot showing the expression of NEMO in 1.3E2 cells, 70Z/3 cells and 1.3E2 cells reconstituted with wild-type or mutant NEMO. The blot was re-probed for GAPDH to ensure even protein loading. **B)** To generate stable NF-ϰB reporter cell lines, cells were transduced with lentiviral vectors encoding NF-ϰB responsive luciferase gene (MOI=500). The transduced cells were passaged multiple times prior to NF-ϰB luciferase assays. Subsequently, the luciferase reporter assays were performed 6 hours after stimulation with LPS (10 μg/ml) or **C)** 48 hours following transduction with lentivectors encoding vFLIP, Tax (MOI=50) and **D)** cFLIP variants (MOI=100). Data are representative of three independent experiments performed in triplicates. Error bars indicate SD of the mean values.

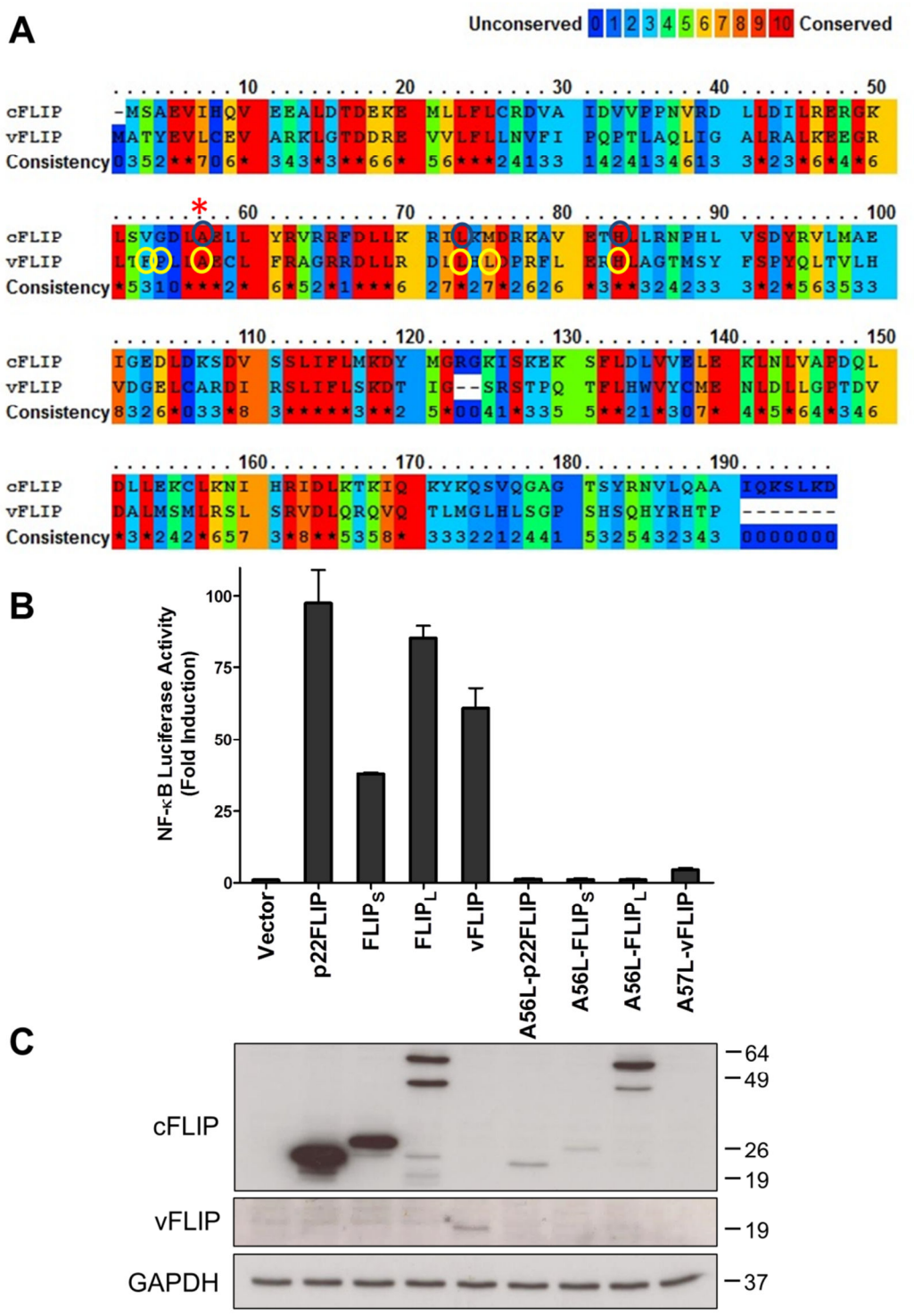

Figure 3.4. NF-ϰB activation by A57L vFLIP and A56L cFLIP isoforms. A) Sequence alignment of the KSHV vFLIP and cFLIP. Amino acid sequences of the proteins were retrieved from NCBI protein database and aligned using PRALINE multiple sequence alignment software. Accession numbers of the KSHV vFLIP and $cFLIP_S$ are AAD46498.1 and NP_001120656.1, respectively. Amino acid residues of vFLIP predicted by structural studies to be important for vFLIP-NEMO interaction have

been shown inside yellow circles. The equivalent conserved residues of cFLIP are depicted inside blue circles. Ala57 of KSHV vFLIP (indicated by *) which is essential for binding to NEMO and its adjacent amino acids (56-58, LAE) are highly conserved in cellular FLIPs. **B)** HEK293T were seeded in 24-well plates cells ($2x10^5$/well) 24 hours prior to transfection. Each well was transfected with 400 ng NF-κB firefly luciferase plasmid (pGL.IgK), 100ng Renilla luciferase plasmid (pRL.TK) as internal control and 300ng of pCDNA3 vectors encoding WT, or A57L vFLIP, or A56L cFLIP isoforms. NF-κB induction levels were measured after 24 hours using Dual-GLO kit (Promega). **B)** Western blot showing the expression of the WT and mutants versions of the vFLIP and cFLIP variants. The mutations severely lower the stability of both viral and cellular FLIPs. Quantitative data are representative of three independent experiments, performed in triplicates.

3.3.3 cFLIPs generate an active IKK without stable interaction with NEMO

Activation of the vFLIP-binding deficient NEMO by cFLIPs suggested that these proteins may target a distinct domain of NEMO or function upstream of this protein. Therefore, we next sought to determine whether cFLIP isoforms associate with NEMO and generate a constitutively active IKK. To do this, we transfected HEK293T cells with expression plasmids for $FLIP_S$, $FLIP_L$, a non-cleavable version of $cFLIP_L$ ($cFLIP_L$ D196E/D376N) and p22-FLIP as well as vFLIP as a positive control for IKK direct interaction. We then immunoprecipitated the IKK complex using an anti-NEMO antibody and measured its ability to phosphorylate recombinant IκB. As can be seen in Figure 3.5 panel A, in each case the cFLIP isoforms generated an activated IKK. The level of activation was comparable or greater than that generated by vFLIP, though less than the transient activation observed following TNFα treatment.

We then examined whether the cFLIP isoforms were found associated with the activated kinase and found no evidence for the presence of cFLIP isoforms in the IKK immune-precipitates, though vFLIP was clearly present as revealed by both anti-NEMO and anti-FLIP immunoprecipitations (Figure 3.5B). This is in contrast to the previous reports that showed p22-FLIP and p43-FLIP fragments stably associated with IKK (Golks et al., 2006; Neumann et al., 2010). Clearly, differences in the experimental conditions could explain these differing results; however, our data demonstrate that the cFLIP isoforms can generate an active IKK without remaining physically associated with the IKK complex.

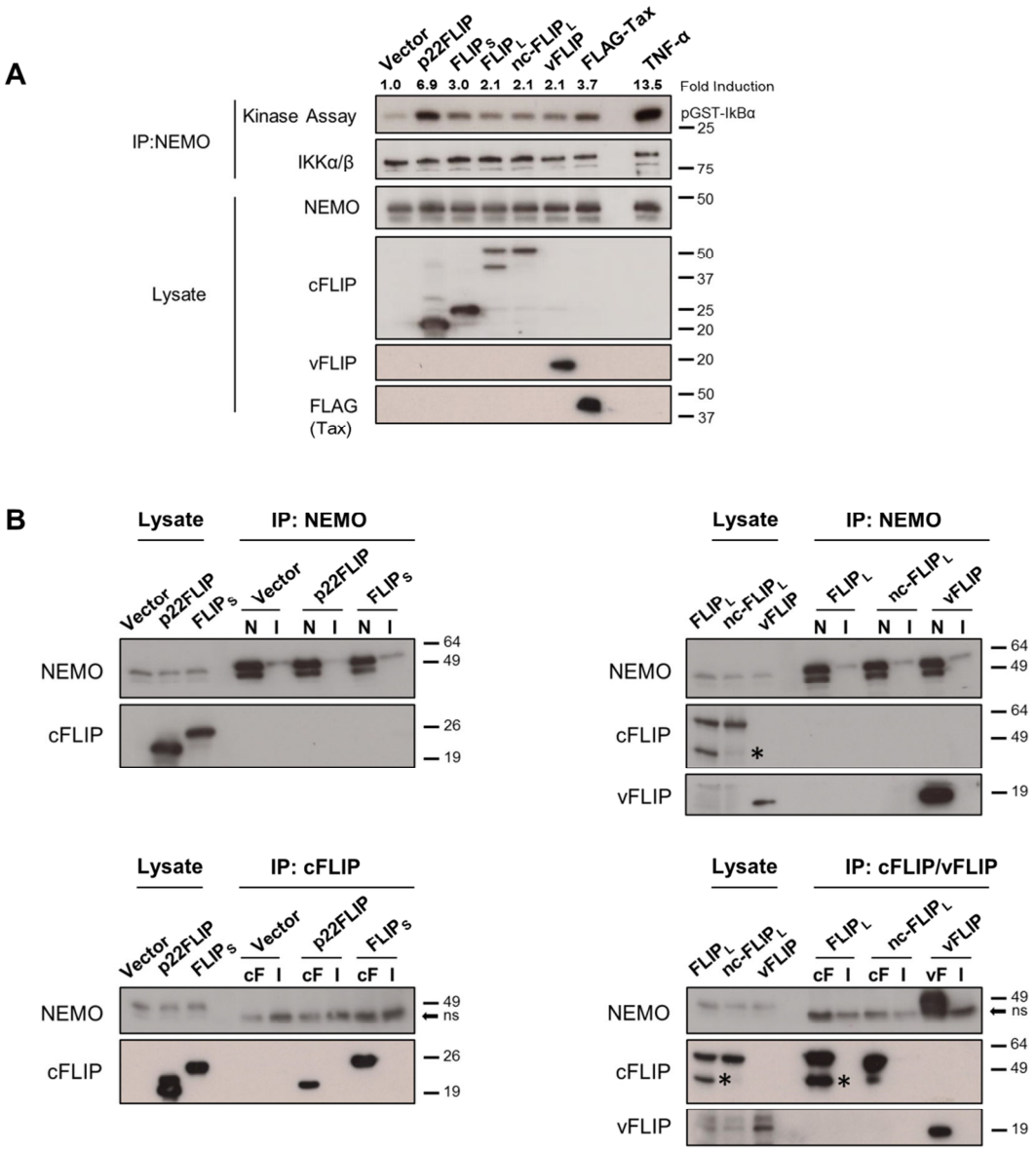

Figure 3.5. Cellular FLIPs constitutively activate IKK complex without stable association with NEMO. A) *In vitro* kinase assays to determine the activation of IKK. HEK293T cells seeded in 6-well plates ($5x10^5$ cells/well) were transfected with pCDNA3 vectors encoding p22FLIP, $FLIP_S$, $FLIP_L$, non-cleavable $FLIP_L$, vFLIP or Tax. Forty-eight hours later, whole cell lysates were extracted and subjected to immunoprecipitation (IP) with anti-NEMO or immunoblotting (IB) with the indicated antibodies. *In vitro* kinase assay was then performed on immuno-isolated IKK complexes using GST-IκBα (1-54) and γ^{32}P-ATP as substrates. Extract of cells treated with TNFα (10ng/ml) for 5 min was used as a positive control. Relative band intensity of phosphorylated GST-IκB was quantified by ImageQuant TL Plus7.0 and normalised to the corresponding immunoprecipitated IKKα/β levels. **B)** cFLIP variants are not found in complex with NEMO. HEK293T cells seeded in 15 cm^2 dishes were transfected with pCDNA3 constucts, using FuGene HD transfection reagent. Cells were lysed 48 hrs later and the

extracts were immunoprecipitated with 2 μg of antibodies against NEMO, cFLIP and vFLIP, or their isotype-matched controls. The immunoprecipitates were subject to 10% SDS-PAGE and were analysed by western blotting. Data shown are representative of at least four independent repeats. * indicates the position of p43-FLIP bands. cF: cFLIP, I: isotype control, N: NEMO, ns: non-specific, vF: vFLIP.

3.3.4 $cFLIP_L$ requires LUBAC to activate IKK

As cFLIP isoforms required the ubiquitin binding function of NEMO to activate IKK (Figure 3.3), we examined the effect of ubiquitination pathways on their action. Linear ubiquitin chain binding to NEMO is crucial for IKK activation by TNFα and these are generated by the trimeric LUBAC, composed of HOIL-1, HOIP and SHARPIN (Iwai et al., 2014). We therefore generated HEK293 cells that were stably transduced with lentiviral vectors containing short hairpin RNAs targeting HOIL-1, HOIP and SHARPIN (Figure 3.6A). Cells transduced with scramble non-targeting shRNA served as control. As previously reported LUBAC was required for IKK activation by TNFα (Figure 3.6B) but was dispensable for activation by vFLIP (Tolani et al., 2014) and Tax (Figure 3.6C). A clear blockade of $cFLIP_L$ and nc-$cFLIP_L$ induced activation of IKK was observed in the LUBAC knock-down cells. However, $cFLIP_S$ and p22-FLIP were unaffected by LUBAC knock-down (Figure 3.6C).

Lack of inhibition in the LUBAC KD cells, led us to hypothesise that $cFLIP_S$ and p22-FLIP may specifically require binding of K63-linked ubiquitin chains to NEMO. CYLD is a deubiquitinase (Komander et al., 2009) which can remove ubiquitin chains with K63 as well as linear linkages and has been shown to target several components of IKK signalling such as NEMO, RIP1, TRAF2 and TRAF6, resulting in inhibition of NF-κB signalling (See 1.2.3.3). Therefore, we overexpressed CYLD in our scramble and LUBAC KD HEK293 cells (Figure 3.7A). Upregulation of CYLD caused a significant decrease in TNFα-induced NF-κB activation in LUBAC KD cells, but not control cells (Figure 3.7B). As seen in Figure 3.7C, $cFLIP_L$ was once again inhibited in the CYLD overexpressed cells, while p22-FLIP, $cFLIP_S$ and vFLIP were unaffected. Nevertheless, in the case of $cFLIP_S$-induced activation, a statistically significant but not considerable decrease could be detected in the CYLD transduced/LUBAC KD cells when compared to control cells. The lack of requirement for ubiquitin signalling by $cFLIP_S$ and p22-FLIP required further investigation as the ubiquitin binding function of NEMO was clearly required. This conundrum will be addressed and discussed later in this thesis.

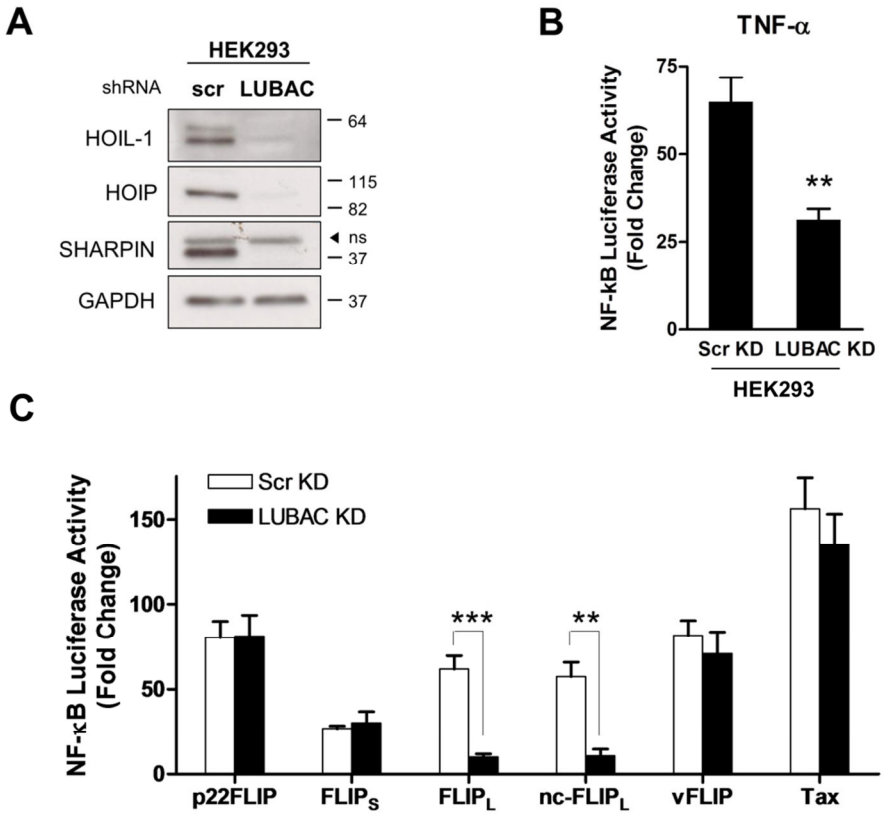

Figure 3.6. Effects of knocking down LUBAC on the NF-*κ*B activation ability of the Tax, vFLIP and cellular FLIPs. A) HEK293 cells were transduced with lentiviral vectors encoding either scramble control shRNA (scr) or shRNAs targeting HOIL-1, HOIP and SHARPIN, sequentially. Generation of LUBAC KD cells was confirmed with western blotting against each component of the complex and the housekeeping protein, GAPDH. ns; non-specific **B)** TNFα-induced NF-*κ*B activation which was measured 6 hours after stimulation at 10 ng/ml concentration is inhibited in LUBAC KD cells. **C)** Subconfluent monolayers of scramble and LUBAC KD HEK293 cells seeded in 24 well-plates ($2x10^5$/well) were co-transfected with an NF-*κ*B−firefly Luc reporter construct (300ng/well) and a Renilla Luc reporter vector (normalisation control,100ng/well) along with an empty or transactivator expressing pCDNA3 vectors (500ng/well). The luciferase reporter assay was performed 24 hrs post-transfection as described in "section 2.11.1". Values shown are the mean±SD of fold changes in the luciferase activity, from one representative experiment out of three, performed in triplicates; ** denotes $p<0.01$ and ***, $p<0.001$.

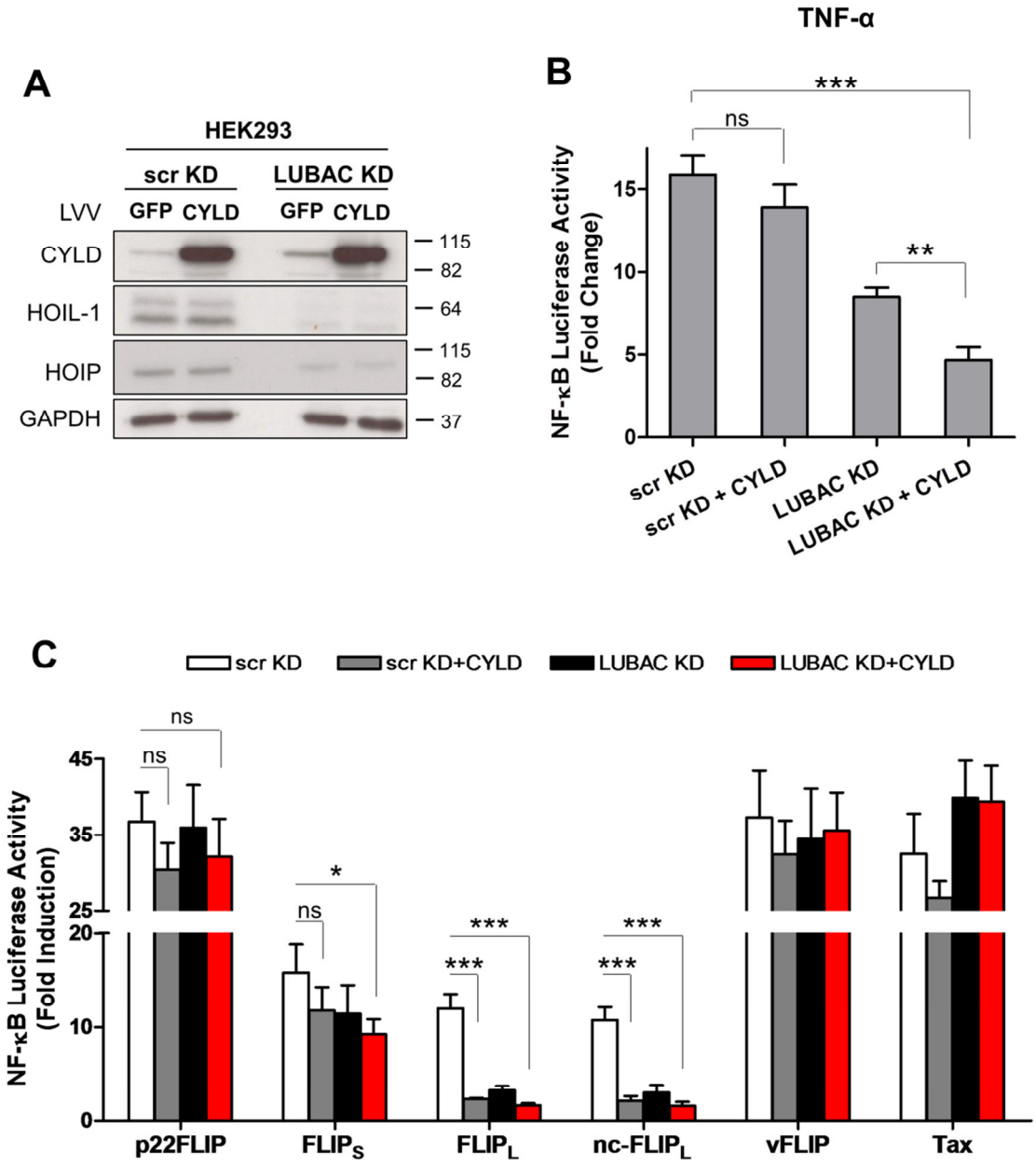

Figure 3.7. Only cFLIP$_L$ is inhibited in CYLD-overexpressing HEK293 cells. A) Immunoblot showing the expression of the ectopically expressed CYLD in scramble KD and LUBAC KD HEK293 cells. Cells transduced with GFP-encoding lentivectors were used as control. **B)** Effects of CYLD overexpression on NF-*κ*B activation levels induced by TNFα or **C)** cFLIPs, vFLIP and Tax were measured using NF-*κ*B reporter luciferase assay, as described in Figure 3.6. Results shown are representative of three independent experiments, performed in triplicates. Mean values were compared by two-tailed unpaired Student's *t*-test; ns: not statistically significant, * $p<0.05$, ** $p<0.01$ and *** $p<0.001$.

3.3.5 The UBAN domain of NEMO is dispensable for vFLIP activation of IKK

The C-terminal ubiquitin binding region of NEMO ends right before the vFLIP-binding site and one of the two Tax-binding regions of NEMO, resides within the N-terminal region far from the UBAN domain (Figure 3.1A). Given that vFLIP and Tax did not require ubiquitin binding function of NEMO, we sought to examine whether the absence of the UBAN domain would have any impact on the capacity of these oncoproteins to activate the canonical IKK signalling. To do this, we generated C-terminally truncated mutants of NEMO which terminated at positions Glu271 (Δ271) and Arg254 (Δ254) (Figure 3.8A). While the first of these two, lacks the essential ubiquitination and ubiquitin-binding residues, the whole putative UBAN domain (CC2-LZ) is deleted in the second one. NEMO deficient 1.3E2 cells were reconstituted with WT or truncated mutants of NEMO (Figure 3.8B) and analysed using the NF-κB luciferase reporter assay.

As shown in Figure 3.8D, both vFLIP and Tax induced near WT levels of activation in cells expressing the truncated NEMO mutants. In sharp contrast, neither LPS (Figure 3.8C) nor any of the cFLIP variants (Figure 3.8E) were able to stimulate IKK in the absence of the UBAN domain. Taking advantage of a NEMO deficient Jurkat cell line, known as JM4.5.2 cells we tried to reproduce these findings and showed that, similarly, vFLIP could fully activate Δ271 or Δ254 NEMO reconstituted Jurkat cells (Figure 3.8G). The same findings were evident in the case of Tax (Figure 3.8H). In keeping with these results, subsequent immunoprecipitation studies showed that the interaction of vFLIP with NEMO remains intact in the absence the UBAN domain, in contrast to the F238/D242RR point mutation which results in complete disruption of the complex (Figure 3.9). Surprisingly, we failed to detect significant activation of NF-κB by any of the cFLIP isoforms in the Jurkat cells, indicating that these proteins may induce IKK in a cell type-specific manner (Figure 3.8I).

In conclusion, our findings confirm that the N-terminal region of NEMO is alone sufficient for activation of IKK by vFLIP and its functional analogue, Tax. These results are consistent with those of Tolani et al who report a similar result with vFLIP inducing a NEMO-estrogen receptor fusion protein in which NEMO was truncated at Gly251 (Tolani et al., 2014).

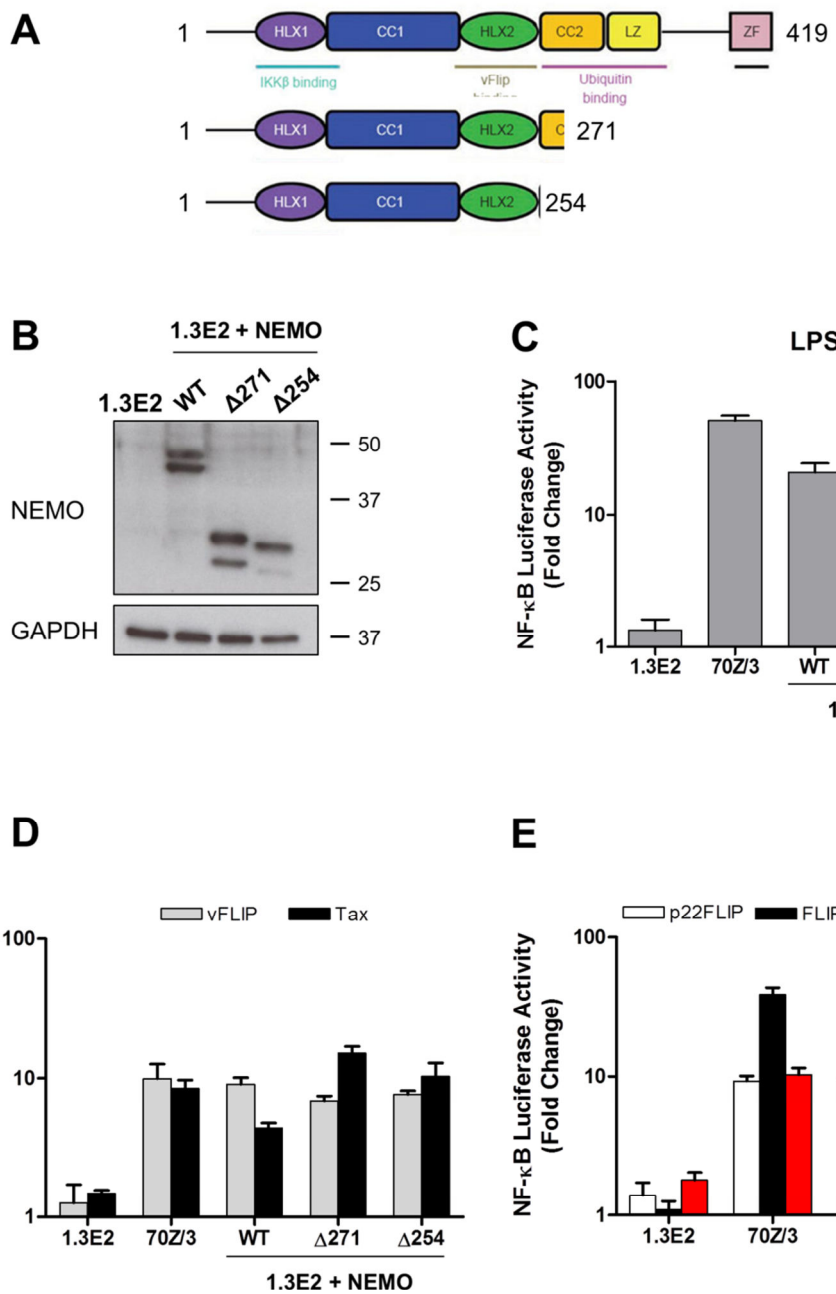
A
1
HLX1
CC1
HLX2
CC2
LZ
ZF
419
IKKβ binding
vFlip
Ubiquitin binding
271
254
B
1.3E2 + NEMO
1.3E2
WT
Δ271
Δ254
NEMO
GAPDH
50
37
25
37
C
LPS
NF-κB Luciferase Activity (Fold Change)
100
10
1
1.3E2
70Z/3
WT
Δ271
Δ254
1.3E2 + NEMO
D
vFLIP
Tax
NF-κB Luciferase Activity (Fold Change)
100
10
1
1.3E2
70Z/3
WT
Δ271
Δ254
1.3E2 + NEMO
E
p22FLIP
FLIP Short
FLIP Long
NF-κB Luciferase Activity (Fold Change)
100
10
1
1.3E2
70Z/3
WT
Δ271
1.3E2 + NEMO

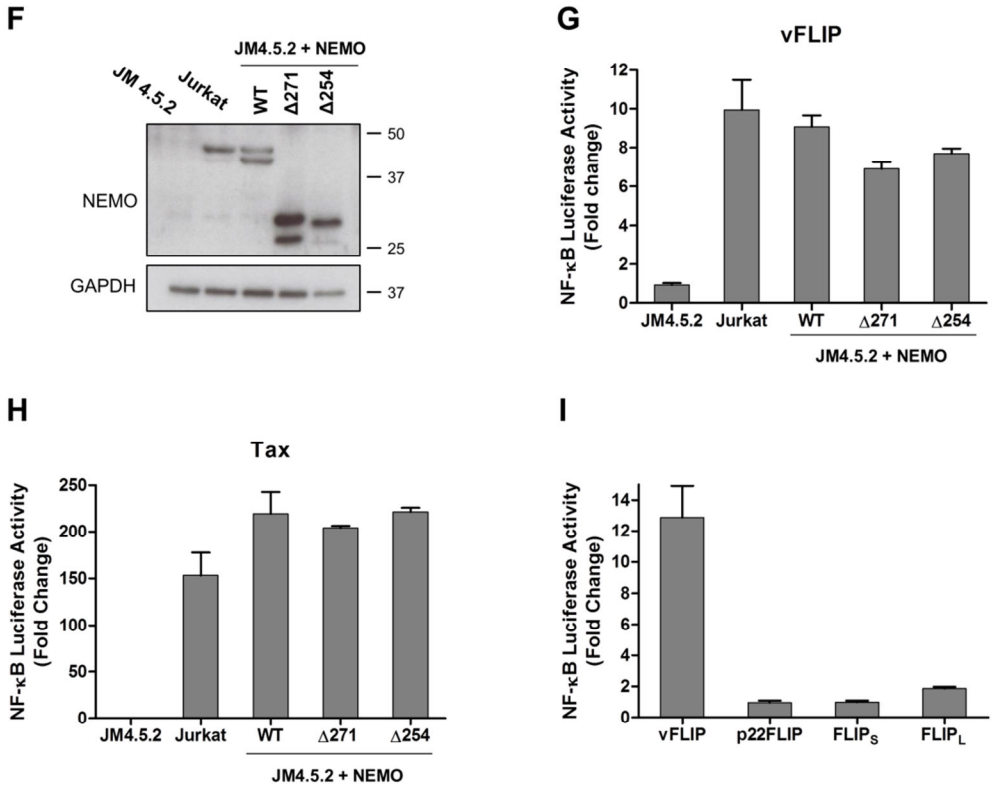

Figure 3.8. The UBAN domain of NEMO is dispensable for IKK activation by vFLIP and Tax. A) Schematic representation of the NEMO mutants truncated to include amino acids 1-271 (NEMO Δ271) or amino acids 1-254 (NEMO Δ254). **B)** Immunoblot showing the expression of NEMO in 1.3E2 cells reconstituted with either NEMO full-length, or NEMO Δ271, or NEMO Δ254. **C)** Cells were transduced with NF-κB luciferase LV (MOI=500) to generate stable NF-κB reporter cell lines. Subsequently, the luciferase reporter assays were performed 6 hours after stimulation with LPS (10 μg/ml) or **D)** 48 hours following transduction with lentivectors encoding vFLIP, Tax (MOI=50) and E) cFLIP variants (MOI=100). **F)** Western blot analysis of NEMO expression in Jurkat cells and JM.4.5.2 cells stably expressing WT or UBAN-deficient mutants of NEMO. **G)** Stable NF-κB sensor cell lines were produced by transducing cells with NF-κB luciferase encoding LVs (MOI=50). NF-κB dependent luciferase activates were measured 48 hours after transduction with LVs expressing vFLIP and **H)** Tax (MOI=20), or **I)** cFLIP variants (MOI=50). Data are representative of three independent experiments performed in triplicates. Error bars indicate SD of the mean values.

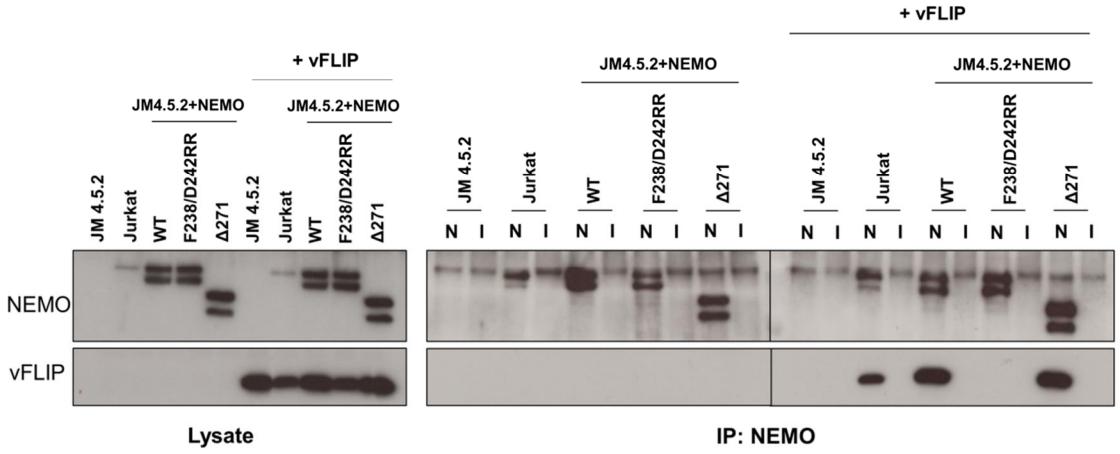

Figure 3.9. vFLIP binds to UBAN-deficient mutant of NEMO. JM4.5.2, Jurkat and JM.4.5.2 cells stably expressing NEMO WT, NEMO F238/D242RR, or NEMO Δ271 were transduced with vFLIP-encoding LVs (MOI=20). Cells were lysed 72 hours later and the extracts (300 μg/sample) were immunoprecipitated with 0.5 μg of anti-NEMO antibody or an isotype-matched control. The immunoprecipitates were subject to 12% SDS-PAGE and were analysed by western blotting against the indicated antibodies. Data shown are representative of two independent repeats. I: isotype-matched control, N: NEMO.

3.4 Discussion

NEMO functions as the signal integration hub of the canonical IKK signalling. By direct binding to this regulatory subunit, KSHV vFLIP and Tax persistently activate NF-ϰB signalling; however, how this interaction results in signal transmission to activate the catalytic subunits IKKα and IKKβ, is not clear. Due to structural similarities between vFLIP and cFLIP isoforms, these proteins have been suggested to adopt a similar mechanism of IKK activation.

Here it is shown that in fact all cFLIP variants can constitutively activate IKK, but unlike vFLIP and Tax, none of them physically associate with the NEMO. These results disagree with two previous studies, both originating from the same group, showing an stable interaction of p22-FLIP and p43-FLIP fragments with NEMO (Golks et al., 2006; Neumann et al., 2010). It is worth mentioning that those experiments have been mainly performed under conditions of overexpressing both cFLIP and IKK; except one experiment which showed a weak interaction of endogenous p43-FLIP and NEMO following CD95 stimulation (Neumann et al., 2010). Therefore, it is possible that the detected cFLIP constitutes a small subset of the protein interacting indirectly with NEMO within a complex or it is only an artefact of protein overexpression. Related to the latter possibility, including isotype-matched controls in our co-immunoprecipiation studies showed that the interactions detected after long exposures of membranes to X-ray films, were of non-specific nature. Although differences in experimental settings may explain for these discrepancies, our findings indicate that cFLIPs are able to generate an active IKK without stable interaction with the NEMO subunit.

Importantly, we also show that cellular FLIPs differ from KSHV vFLIP in that they depend on the ubiquitin function of NEMO. Interestingly, different isoforms were found to require distinct ubiquitination pathways. By shRNA-mediated knock-down of LUBAC complex, we could demonstrate that linear ubiquitin chains are indispensable for activity of the $cFLIP_L$, but not p22-FLIP or $cFLIP_S$. It has been shown that $cFLIP_L$, but not $cFLIP_S$, interacts with and requires TRAF2 to activate NF-ϰB (Kataoka and Tschopp, 2004; Kataoka et al., 2000). A recent study described that, in IL-1 signalling, LUBAC becomes recruited to IKK signalling machinery through K63-linked polyubiquitin catalysed by upstream E3 ligases (Emmerich et al., 2013). It is possible that TRAF2 mediates the LUBAC-dependent activation of IKK by the long isoform of cFLIP.

Our findings that p22-FLIP and $cFLIP_S$ do not need LUBAC to activate NF-κB implied that these proteins must require another type of non-degradative polyubiuquitin - most likely K63-linked Ub oligomers- as the LUBAC is the only E3 ubiquitin ligase known to generate linear chains. Moreover, F312A mutation of the NEMO - which disrupts the IKK activation by cFLIPs - is shown to block binding to K63-linked ubiquitin chains (Ea et al., 2006). To investigate whether p22FLIP and $cFLIP_S$ specifically required K63-linked polyubiquitin binding to NEMO, we overexpressed CYLD which is known to cleave ubiquitin chains with K63-linkges from a number of IKK signalling components including NEMO. Surprisingly, we failed to suppress the activity of the short cFLIP forms by overexpression of CYLD. One possible reason for this could be that the K63-ubiquinated protein used by these cFLIP variants is not a substrate of CYLD. Alternatively, binding to NEMO may render the ubiquitinated intermediate protein inaccessible to deubiquitination by the CYLD. In support of this concept, it was recently shown that in TNF-R signalling, binding to NEMO protects ubiquitinated RIP1 from CYLD-mediated deubiquitination, resulting in prevention of the initiation of necroptotic pathways (O'Donnell et al., 2012).

Although, we have clearly shown that ubiquitin binding function of NEMO is essential for the activity of cFLIP isoforms, it remains to be determined which ubiquitinatd proteins mediate this process. cFLIP isoforms are found to be a target of ubiquitination, themselves. Ubiquitination of $cFLIP_S$ at lysines 192 and 195 has been described to be responsible for the rapid turnover this isoform (Poukkula et al., 2005). Hence, it is tempting to speculate that cFLIP isoforms may undergo other types of non-degradative polyubiquitination, leading to a transient interaction with UBAN domain of NEMO or recruitment of intermediate signalling components. In an attempt to investigate this possibility, we generated K192/K195RR mutants of cFLIP isoforms and compared their activity with wild-type forms (Figure 3.10A). The mutations resulted in a partial decrease, but not complete loss of activity for both cFLIP long and short but led to a marked increase in the activity of p22-FLIP variant (Figure 3.10B), making the relevant results difficult to interpret. Obviously, a systemic approach to test this concept would require a series of site-directed mutagenesis to engineer Arg replacements at each of the cFLIP lysines. Moreover, given the availability of specific antibodies against distinct polyubiquitin linkages, cFLIP proteins can be immuno-isolated and directly probed for the possibility of ubiquitination by non-degradative Ub oligomers.

In this study, we have provided evidence indicating that ubiquitination and ubiquitin-binding function of NEMO are dispensable for vFLIP-induced mechanism of IKK activation. Moreover, we demonstrated that the absence of UBAN domain does not have any adverse impact on the NEMO binding ability of the vFLIP. These findings agree with a recent study by the Chaudhary lab which showed that the vFLIP-mediated NF-κB activities are not impaired in cells derived from mice lacking *TRAF6*, *HOIL-1* genes or cpdm mice which harbour a mutation in the *SHARPIN* gene (Matta et al., 2012). Our results are also compatible with those of Tolani et al – published at the time of writing this thesis- who reported that N-terminal 251 residues of NEMO are sufficient to support vFLIP-induced stimulation of NF-κB (Tolani et al., 2014).

It has to be noted that although these experiments show the lack of requirement for UBAN domain by the vFLIP, they do not completely rule out any involvement of the C-terminal region in vFLIP-induced transcriptional activities of the NF-κB. Hence, one could speculate that the C-terminal region of NEMO contributes to controlling the magnitude and duration of the vFLIP-induced responses or plays a role in modulating the expression of a subset of NF-κB responsive genes.

Clearly, vFLIP and Tax bind to distinct regions of NEMO and share no obvious sequence homology. Nevertheless, our data indicate that Tax has similarly evolved to stimulate NEMO without involvement of the ubiquitination or ubiquitin binding of NEMO. This is in agreement with the study showing Tax can activate of IKK in cells expressing a truncated NEMO mutant containing aa1-255 (Xiao and Sun, 2000). Together, these observations raise the possibility that binding to vFLIP and Tax may mimic ubiquitin-induced conformational changes on NEMO that lead to IKK activation. However, it has been shown that Tax fused to IKKα and β, can activate NF-κB pathway in the absence of NEMO (Xiao and Sun, 2000). Similarly, in frame fusion of NEMO to Tax mutants defective in NEMO-binding, is sufficient to activate IKK (Xiao et al., 2000). Therefore, given that Tax can self-dimerise (Fryrear et al., 2009; Jin and Jeang, 1997; Tie et al., 1996), it is logical to suppose that it may use NEMO as a scaffold to bring the IKKα/β subunits into close proximity, leading to activation by cross-phophorylation. This model can be also considered for vFLIP since dimeric interactions between vFLIP molecules are present within vFLIP-NEMO signalosome (see chapter5). Alternatively, these oncoproteins may function by directly recruiting upstream IKK-activating kinase. This model of activation will be addressed in the next chapters.

In summary, the study presented here shows that Tax, vFLIP and cellular FLIPs require distinct regions of NEMO to induce IKK. While Tax and vFLIP activate the NF-κB pathway independently of the ubiquitin-mediated signalling induced by cytokines, all cFLIP variants require ubiquitin-binding function of NEMO for their activation of IKK. These findings provide a basis for further identification of the IKK signalling components and mechanisms utilised by KSHV vFLIP and different isoforms of cFLIP.

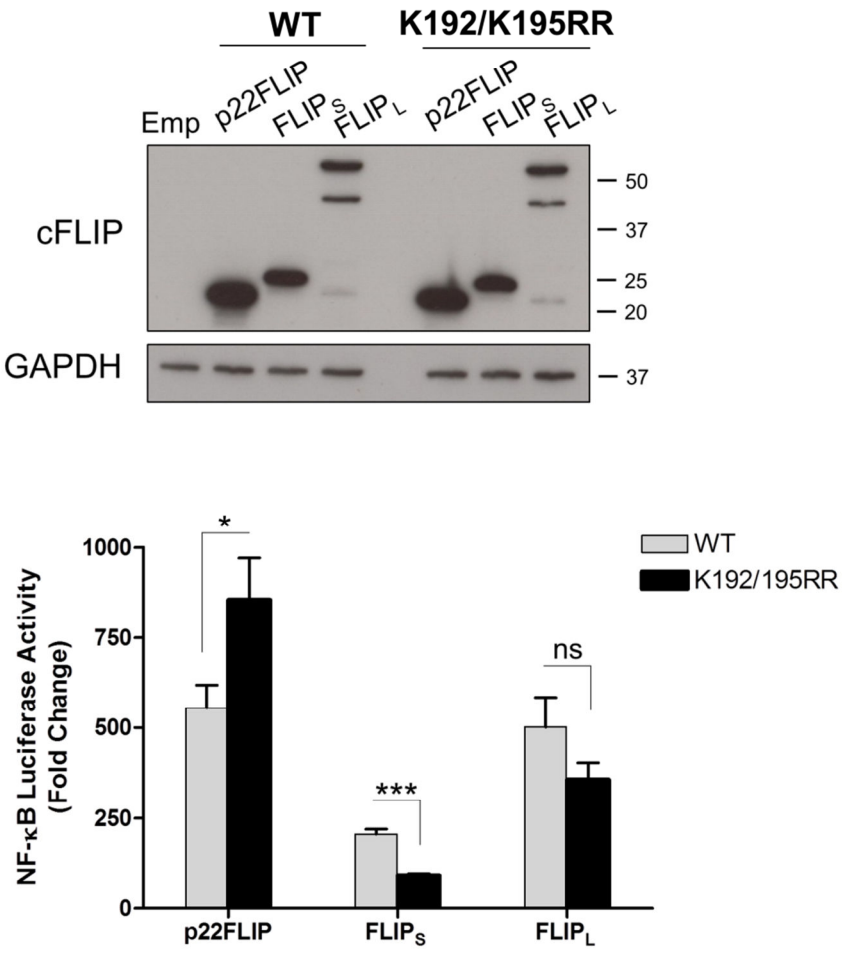

Figure 3.10. Effect of the K192/195RR mutations on the NF-ϰB inducing ability of the cFLIP variants. A) Western blot comparing the expression levels of the WT and K192/K195RR mutants of cFLIP isoforms. **B)** HEK293T cells were seeded in 24-well plates ($2x10^5$ cells well) 16 hours prior to transfections. Subsequently, each well was transfected with 400ng NF-ϰB firefly luciferase plasmid (pGL.IgK), 100ng Renilla luciferase plasmid (pRL.TK) as internal control and 300 ng of pCDNA3 vectors encoding WT, or muatnt versions of the cFLIP isoforms. NF-ϰB induction levels were measured after 24 hours using the Promega Dual-GLO luciferase assay system. Results shown are representative of two independent experiments, performed in triplicates. Error bars indicate SD of the mean values which were compared by two-tailed unpaired Student's *t*-test; ns: not statistically significant, * $p<0.05$ and *** $p<0.001$.

CHAPTER

4

The Role of Signalling Intermediates Upstream of IKK in NF-κB Signalling by KSHV vFLIP and Cellular FLIPs

4.1 Introduction

In the previous chapter of this thesis, we established that the ubiquitination and ubiquitin binding function of the NEMO are essential requirements for the cFLIP-induced NF-κB activation. Furthermore, it was demonstrated that cellular FLIPs, unlike the KSHV vFLIP, do not stably associate with the NEMO subunit of the IKK complex. Together, these findings suggested a possible mechanism whereby cellular FLIPs act indirectly on the IKK complex via intermediate signalling components. Such intermediate adaptors may recruit E3 ligases required for NEMO ubiquitination, or connect the IKK complex to upstream IKK-Ks, or serve as ubiquitination substrates which bind to the UBAN domain of NEMO. In this chapter, we sought to investigate which adaptor proteins were required for IKK activation by cFLIPs and whether these components were also important for the activity of vFLIP and Tax. Due to reasons outlined below, the targets chosen to study were Atg3, RIP1, caspase-8 and FADD as well as the IKK-activating kinases TAK1 and MEKK3.

4.1.1 Caspase-8, FADD and RIP1

Cellular FLIPs appear in complex with FADD, caspase-8 and RIP1 within several death receptor-induced signalling cascades: a cytoplasmic complex containing $cFLIP_L$, RIP1, FADD, caspase-8 and TRADD is induced by TNFR signalling (Micheau and Tschopp, 2003); a complex containing RIP1, FADD, caspase-8 and NEMO has been detected after TRAIL triggering (Varfolomeev et al., 2005) and a cFLIP/RIP1/FADD/caspase-8 complex has been found after Fas signalling (Lavrik et al., 2008). Moreover, inhibition or depletion of the cIAPs in tumour cells leads to assembly of the cytoplasmic ripoptosome complex which contains FADD, caspase-8, RIP1 and cellular FLIPs (Feoktistova et al., 2011; Tenev et al., 2011a). Individual overexpressions of RIP1, caspase-8 or FADD, all result in strong activation of the NF-κB pathway and there is evidence showing an interaction between these proteins and IKK complex (Biton and Ashkenazi, 2011; Chaudhary et al., 2000; Poyet et al., 2000; Zhang et al., 2000). Therefore, we hypothesised that when overexpressed, cFLIP proteins may require a similar multi-protein complex to induce the NF-κB signalling. Consistent with this idea, it has been shown that recruitment of cFLIP to the TRAIL-induced DISC complex, results in the translocation of DISC components from lipid rafts to non-rafts, further recruitment of the RIP1 and switching the outcome of DISC signals from

caspase-initiated apoptosis to activation of the ERK and NF-κB pathways (Song et al., 2007).

4.1.2 Atg3

Cellular FLIPs and KSHV vFLIP have been also shown to directly bind to the autophagy pathway protein, Atg3. This association blocks autophagosome biogenesis through preventing the Atg3-LC3 interaction, required for processing of LC3 to its active form, LC3-II (See 1.3.4). The Atg3-interacting regions of KSHV vFLIP have been localised to DED1 α2 helix (aa 20-29) and DED2 α4 helix (aa 128-139), which are distinct from motifs responsible for binding to NEMO and TRAFs (Field et al., 2003; Guasparri et al., 2006; Lee et al., 2009). FLIP mutants defective in binding to FADD, TRAFs or NEMO are capable of blocking rapamycin-induced autophagy as efficiently as the WT versions (Lee et al., 2009). Therefore, it has been concluded that authophagy-inhibiting ability of FLIP proteins must be separable from their anti-apoptotic or NF-κB inducing activities. Nevertheless, deletion of Atg3-binding regions of the KSHV vFLIP, completely abrogates both its NF-κB activation and anti-apoptotic capacity (Lee et al., 2009). These results raise the possibly that interaction with Atg3 may play a role in FLIP-induced activation of IKK.

4.1.3 TAK1 and MEKK3

Alongside ubiquitination events, phosphorylation of the catalytic IKKs by IKK-phosphorylating kinases is another major step in the activation of the NF-κB pathway. Two members of the MAPK family, TAK1 and MEKK3, are the most prominent of IKK-Ks that, alone or together, play pivotal roles in the inflammatory stimuli-induced IKK signalling (See 1.2.1). Although several studies have examined the function of these IKK-Ks in the Tax-induced pathway (Gohda et al., 2007; Suzuki et al., 2007; Wu and Sun, 2007), it remains to be determined whether they play a role in the activation of IKK by vFLIP and cFLIP variants.

4.2 Aims of the chapter

- Determine the role of Atg3, FADD, caspase-8 and RIP1 in FLIP-induced activation of IKK
- Examine whether the activation of IKKs by vFLIP and cFLIP isoforms depends on upstream MAP3Ks, TAK1 and MEKK3.

4.3 Results

4.3.1 $cFLIP_S$ and p22-FLIP activate IKK via a FADD-RIP1 complex

To further probe the mechanism of action of cellular FLIPs we generated HEK293T cells that were knocked-down for the molecules reported to be present in complexes with cFLIP isoforms or vFLIP. As previously mentioned, Atg3 has been reported to interact directly with vFLIP and cFLIPs (Lee et al., 2009), FADD interacts with cFLIP isoforms (reviewed in (Krueger et al., 2001)), and RIP1 interacts with FADD (Park et al., 2013). In order to identify shRNAs that would efficiently down-regulate the expression of these candidate proteins, at least five different target-specific LVs were generated for each gene, using shRNA-encoding lentiviral plasmids obtained from UCL Open Biosystem RNAi library. Subsequently, HEK293T cells were transduced with the LVs at an MOI of 50 and analysed by western blotting for expression levels of the targeted proteins, using GAPDH levels as internal control. Cells infected with LVs encoding scramble shRNA served as negative control. From each set, two shRNAs that yielded most efficient silencing were used to produce stably knocked-down cell lines for the experiments (Figure 4.1 A). The list of sequences targeted by each shRNA has been given in Table 2.15.

As Figure 4.1C shows, FADD and RIP1 were both required for $cFLIP_S$ and p22-FLIP activation of IKK, while Atg3 and caspase-8 were dispensable. On the other hand, none of the silenced proteins appeared to play a role in NF-κB activation by TNFα, $cFLIP_L$, vFLIP or Tax (Figure 4.1B and C). Our findings agree with those of the Chaudhary lab showing that vFLIP, despite physically binding to RIP1, does not require it for the activation of IKK (Liu et al., 2002; Matta and Chaudhary, 2004).

A hydrophobic stretch of amino acids in the DED2 motif of the murine $cFLIP_R$ has been identified as critical for its interaction with FADD, and hence, its DISC recruitment and anti-apoptotic function (Figure 4.2A) (Ueffing et al., 2008). Interestingly, this hydrophobic patch - which contains residues F119, L120, L146, L148 and L154 on its surface - is highly conserved in both KSHV vFLIP and human cFLIP isoforms (Figure 4.2B). We mutated the critical amino acids in this hydrophobic stretch (Figure 4.2C), which resulted in blocking IKK activation by $cFLIP_S$ and p22-FLIP and also $cFLIP_L$, but not vFLIP (Figure 4.3D). We then demonstrated that this mutation prevented interaction of the cFLIP isoforms with FADD, while FADD and RIP1 were present in these cells as

a pre-assembled complex (Figure 4.3). These data provide an explanation for the lack of inhibition of $cFLIP_S$ and p22-FLIP by CYLD, as ubiquitinated RIP1 bound to IKK has been reported to be protected from deubiquitination (O'Donnell et al., 2012). While mutation of the putative FADD binding domain in $cFLIP_L$ prevented activation of IKK (Figure 4.2C), $cFLIP_L$ did not require FADD or RIP1 for its action (Figure 4.1C), suggesting that this region interacts with a different effector to trigger LUBAC activity. This effector may be TRAF2, which has been reported to interact with the N-terminal region of $cFLIP_L$, and to be required for NF-κB activation (Kataoka and Tschopp, 2004). Our finding that RIP1 was not required for $cFLIP_L$ activation differs from the report of its role in TCR-triggered NF-κB activation, where RIP1 was required (Kataoka et al., 2000).

FADD and cFLIP isoforms interact via their DEDs; while FADD-RIP1 interaction is mediated through their respective DDs. Therefore, considering our findings, one could speculate that FADD functions as an adaptor protein connecting p22-FLIP or $FLIP_S$ to RIP1 which, following its ubiquitination, can bind to the IKK complex, facilitating its activation. To test this hypothesis, I generated lentiviral constructs encoding WT RIP1, or a point mutant of RIP1 reported to block its polyubiquitination (K377R)(Ea et al., 2006), or RIP1 mutants suggested to be deficient in FADD-binding (G595/K596AA and E620/D622AA)(Park et al., 2013). These LVs were then used to reconstitute a *RIP1*$^{-/-}$ MEF cell line (data not shown) for further studies. However, cFLIP did not induce NF-κB activation in these cells and other RIP1 deficient cell lines were not available, so I was unable to perform further experiments.

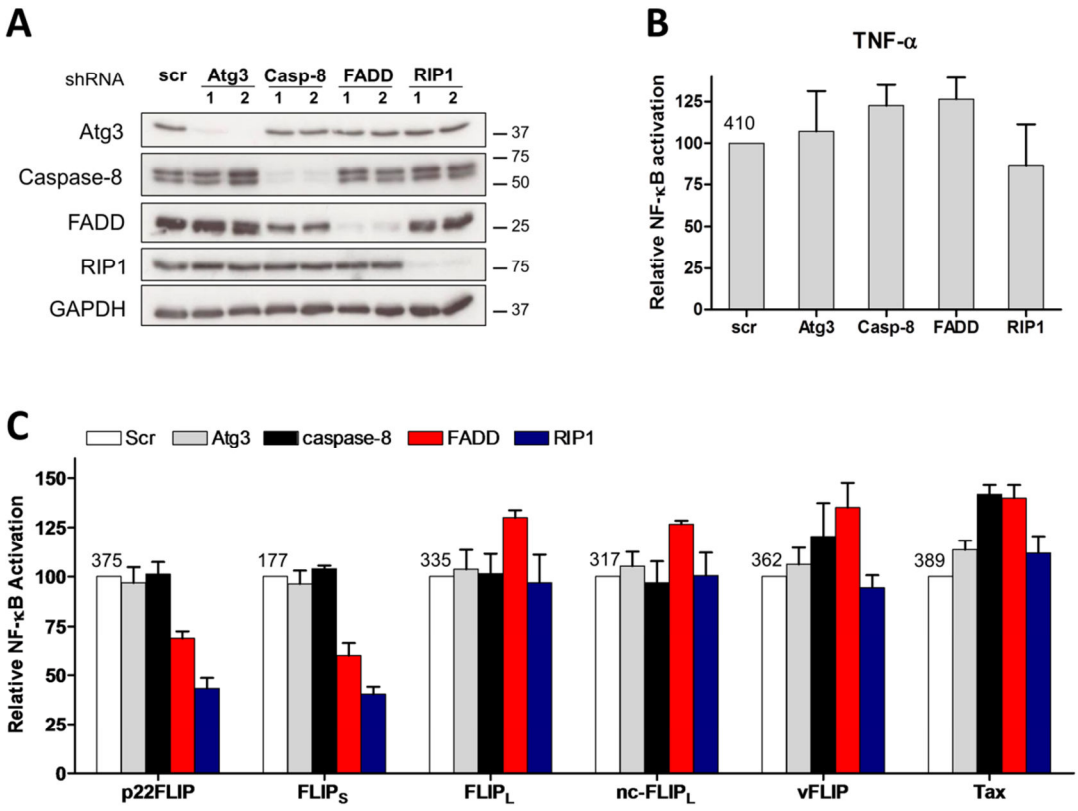

Figure 4.1. FADD and RIP1 are required for NF-κB activation by cFLIP$_S$ and p22-FLIP. A) Stable gene knockdown of Atg3, caspase-8, FADD and RIP1 in HEK293T cells was validated by western blotting. From five independent shRNAs used to silence each protein, two that yielded most efficient knockdowns were chosen for the experiments. Immunoblots were re-probed for GAPDH levels to ensure equal protein loading. **B)** Control and knockdown cells were transduced with NF-κB Luc lentivectors (MOI=10) to develop stable NF-κB reporter cell lines. Luciferase reporter assays were performed 6 hours following stimulation with TNFα (10ng/ml) or **C)** 48 hours after transduction with LVs encoding cFLIP variants (MOI=50), vFLIP and Tax (MOI=10). Values shown are the mean±SD of the relative luciferase activity from five independent experiments; numbers represent the absolute activation fold.

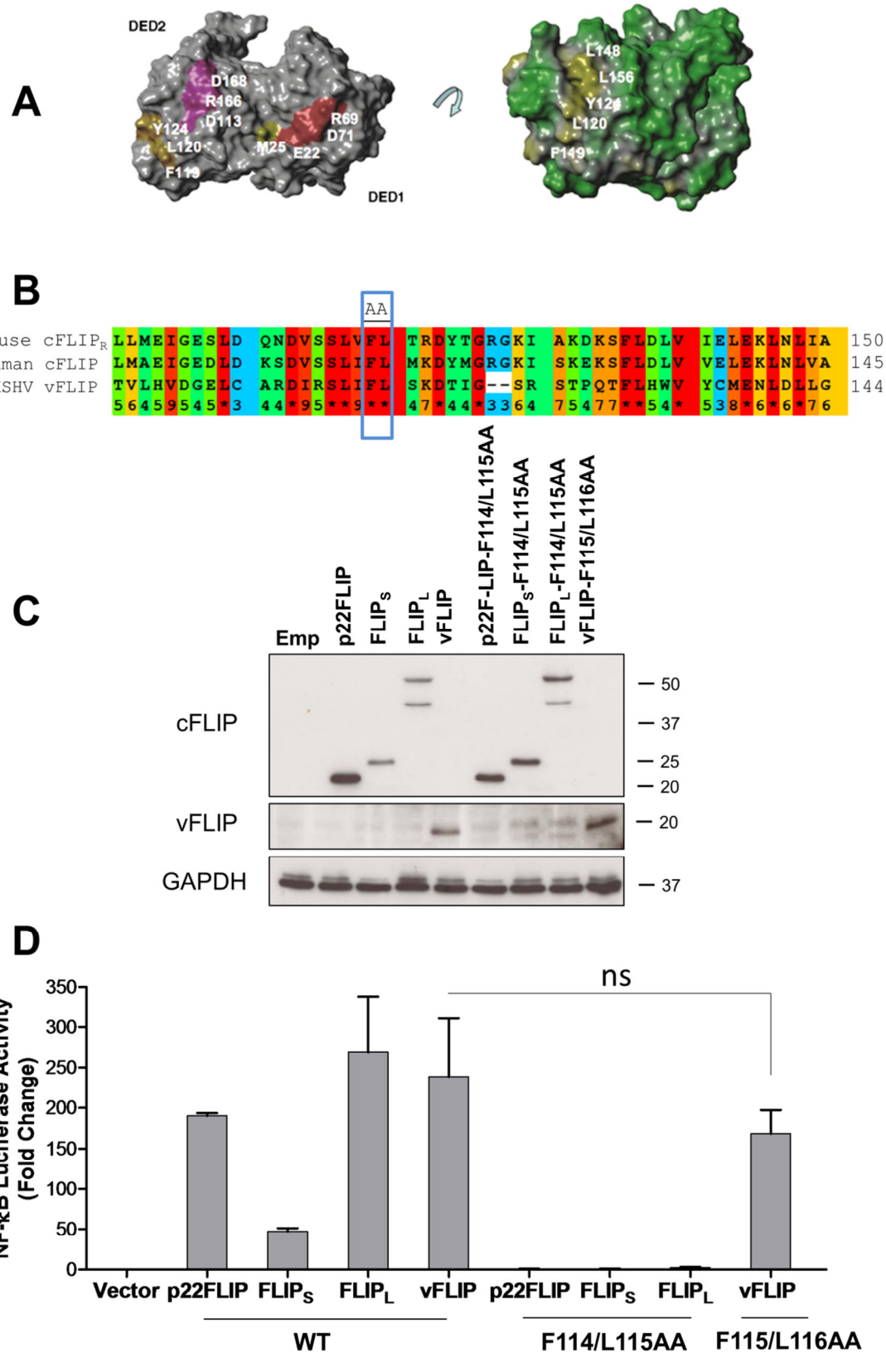
A
DED2
D168
R166
D113
Y124
L120
F119
M25
E22
R69
D71
DED1
L148
L156
Y124
L120
P149
B
AA
Mouse cFLIP$_R$ LLMEIGESLD QNDVSSLVFL TRDYTGRGKI AKDKSFLDLV IELEKLNLIA 150
Human cFLIP LMAEIGEDLD KSDVSSLIFL MKDYMGRGKI SKEKSFLDLV VELEKLNLVA 145
KSHV vFLIP TVLHVDGELC ARDIRSLIFL SKDTIG--SR STPQTFLHWV YCMENLDLLG 144
5645954 5*3 44*95**9** 47*44*3364 75477**54* 538*6*6*76
C
Emp
p22FLIP
FLIP$_S$
FLIP$_L$
vFLIP
p22F-LIP-F114/L115AA
FLIP$_S$-F114/L115AA
FLIP$_L$-F114/L115AA
vFLIP-F115/L116AA
cFLIP
vFLIP
GAPDH
50
37
25
20
20
37
D
NF-κB Luciferase Activity (Fold Change)
350
300
250
200
150
100
50
0
ns
Vector
p22FLIP
FLIP$_S$
FLIP$_L$
vFLIP
p22FLIP
FLIP$_S$
FLIP$_L$
vFLIP
WT
F114/L115AA
F115/L116AA

Figure 4.2. A hydrophobic stretch of amino acids on the surface of DED2 is indispensable for NF-κB activation by cellular FLIP isoforms, but not KSHV vFLIP. A) Electrostatic surface representation of the murine $cFLIP_R$. Left panel: hydrophobic and charged motifs on the surface of DED1 and DED2. Motifs coloured in red and magenta are hydrophilic, and motifs shown in yellow and gold are hydrophilic. Right panel: The hydrophobic amino acids present on the surface of DED2 (highlighted in yellow). The hydrophilic regions are shown in green (reproduced form (Ueffing et al., 2008)). **B)** Sequence alignment of the murine $cFLIP_R$, human cFLIP and KSHV vFLIP. The amino acids which form the hydrophobic patch of the DED2 in murine $cFLIP_R$ (F114, L115, L146, L148 and L154) are fully conserved in both KSHV vFLIP and human cFLIP. Sequence alignment was performed by PRALINE software. **C)** Immunoblot showing the expression of F114/L115AA cFLIP mutant, F115/L116AA vFLIP mutant and their WT versions in HEK293T cells. **D)** Subconfluent monolayers HEK293T cells seeded in 24-well plates ($2x10^5$/well) were co-transfected with an NF-κB firefly Luc reporter construct (300ng/well) and a Renilla Luc reporter vector (normalisation control,100 ng/well) together with empty or transactivator expressing pCDNA3 vectors (500 ng/well). The luciferase reporter assay was performed 24 hours post-transfection using Dual-Glo luciferase assay system.

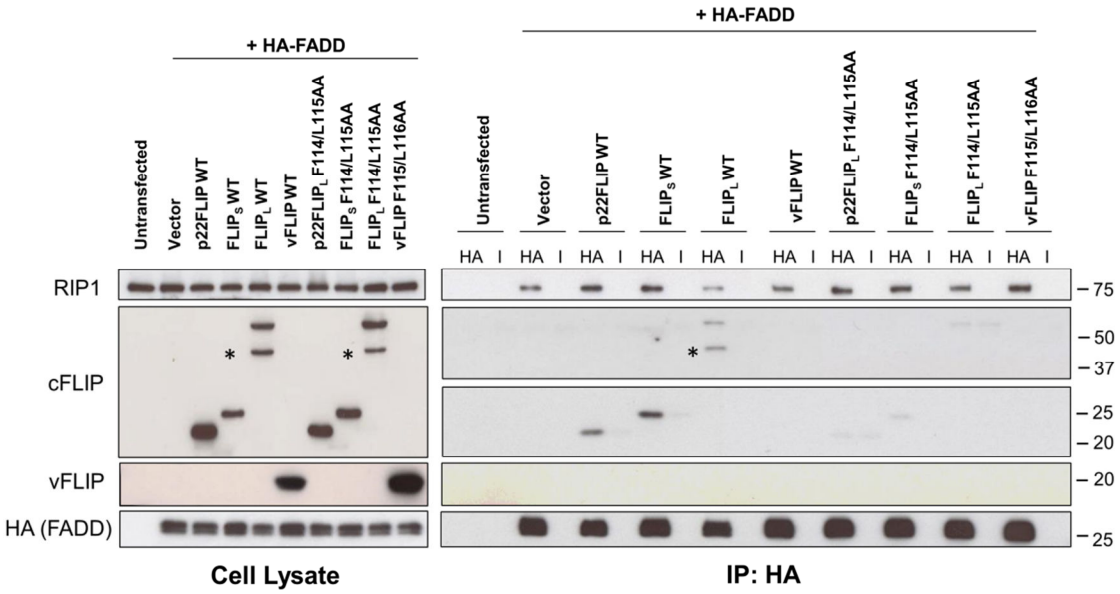

Figure 4.3. Unlike KSHV vFLIP, cellular FLIPs associate with a pre-assembled FADD-RIP1 complex. HEK293T cells, seeded in 6-well plates ($5x10^5$/well) were transfected with 1 μg of HA-FADD vector together with 1 μg of pCDNA3 constructs expressing WT or mutant versions of the p22-FLIP, $cFLIP_S$, $cFLIP_L$ and vFLIP. Forty-eight hours later, cell lysates were extracted and immunoprecipitated with 0.5 μg of anti-HA or an isotype-matched control antibody. Cell lysates and the immunoprecipitates were then analysed by western blotting with the indicated antibodies. * indicates the position of p43-FLIP bands. Results shown are representative of three independent experiments.

4.3.2 Processing to p22-FLIP and p43-FLIP fragments is not necessary for NF-κB activation by $cFLIP_L$

Golks et al., demonstrated that p22-FLIP fragment can be generated by procaspase-8 cleavage of either $cFLIP_L$, or $cFLIP_S$ isoform. They also reported that inhibition of capsase-8 by zVAD-fmk (Benzyloxycarbonyl-Val-Ala-Asp(OMe)-fluoro- methylketone) results in a decrease of NF-κB activation by p43-FLIP and $FLIP_L$, but not p22-FLIP. Furthermore, overexpression of p22-FLIP in HEK293T cells was shown to cause much stronger NF-κB activation than that observed with $cFLIP_L$. Therefore, it was concluded

that cFLIP variants have to be cleaved to p22-FLIP to be capable of inducing the IKK complex (Golks et al., 2006).

Surprisingly, in contrast to the findings of Golk et al., we observed a similar level of activation with non-cleavable $cFLIP_L$ as with wild-type. Moreover, we found no evidence that caspase-8 was required for NF-κB activation by cFLIP variants (Figure 4.1C). Together, our data suggested that, in contrast to the current view in the field, p22-FLIP might not be simply an active isoform of the cFLIP proteins but is likely to activate IKK in a manner distinct from its precursor $cFLIP_L$.

As the previous report had used a different NF-κB luciferase construct to measure NF-κB activation, we sought to determine whether this could explain the discrepancies in the results. To do this, we generated two different NF-κB luciferase reporter plasmids: one with H2DK response element from MHC class I gene (used in Golk et al.'s report) and one with NF-κB binding sites from immunoglobulin kappa light chain (Igk) gene (Figure 4.4A). We also replaced the murine c-Fos promoter, used in the previous report, with minimal promoter of the cytomegalovirus (CMV), as there is evidence that expression of $cFLIP_L$, but not $cFLIP_S$, strongly blocks c-Fos upregulation (Siegmund et al., 2001). Figure 4.4C shows that the non-cleavable $cFLIP_L$ was no different in activity from wild-type with either reporter construct; this agrees with our kinase assay results (Figure 3.5A).

Overall, our findings indicate that processing to p22-FLIP or p43-FLIP is not required for NF-κB activation capacity of the $cFLIP_L$. We have shown that $cFLIP_L$ requires LUBAC while p22-FLIP and $cFLIP_S$ depend on a FADD-RIP1 complex to stimulate IKK. Therefore, it is plausible to assume that, $cFLIP_L$ cleavage to generate p22-FLIP may switch the mechanism of NF-κB activation at the protein level, without a need for *de novo* synthesis of the $cFLIP_S$ isoform.

It is worth mentioning that upon vFLIP transduction of Jurkat cells, we observed a strong induction of p22-FLIP production (Figure 4.4D). However, as shown in the previous chapter, p22-FLIP overexpression does not activate the NF-κB pathway in these cells (Figure 3.8I). Thus, it is likely that p22-FLIP also plays a role in cellular mechanisms other than the NF-κB signalling.

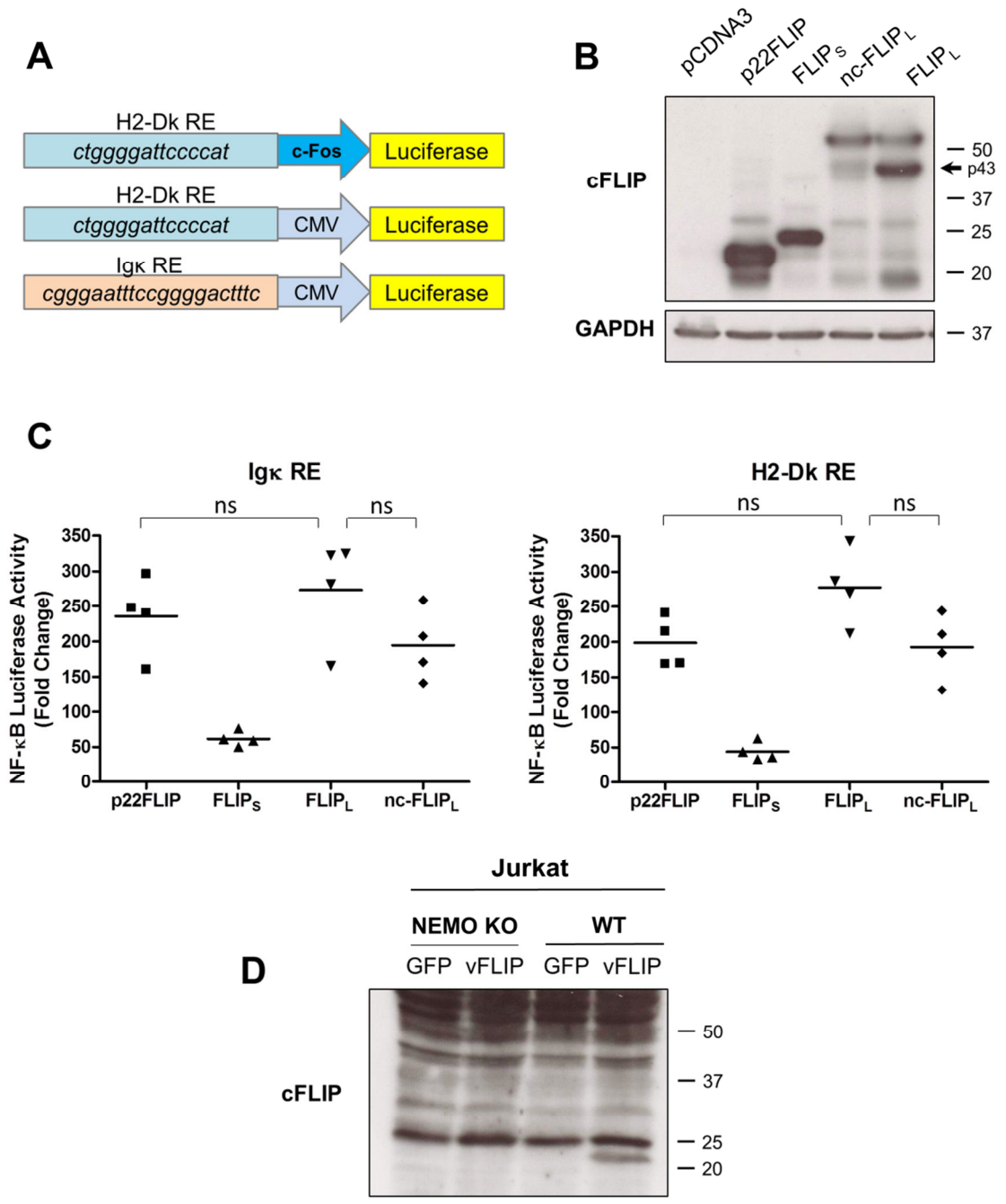

Figure 4.4. Non-cleavable mutant of cFLIP$_L$ activates NF-κB pathway in levels comparable to that of wild-type cFLIP$_L$ and p22-FLIP. A) Schematic representation of the NF-κB reporter vectors. Two different NF-κB luciferase plasmids were constructed to compare the activaties of the cFLIP variants: one with 4 repeats of NF-κB response element of immunoglobin kappa light chain (IgK) gene and another with 4 repeats of an NF-κB binding site of the mouse MHC classI H2DK gene. **B)** Immunoblot comparing the expression levels of p22-FLIP, cFLIP$_S$, cFLIP$_L$ and nc-FLIP$_L$. **C)** NF-κB luciferase assay comparing the NF-κB activation levels induced by WT- or nc-FLIP$_L$. The luciferase reporter assays were performed as described in Figure 4.3D. Results shown are representative of four independent experiments and the values represent mean±SD of triplicates within an experiment; ns: statistically not significant. **D)** WT and NEMO KO Jurkat cells were transduced with LVs encoding GFP or vFLIP. Forty-eight hours later, cells were lysed and analysed for cFLIP expression levels by western blotting.

4.3.3 Cellular FLIP variants require TAK1 to induce IKK

As discussed previously, the kinase TAK1 has been identified as a critical activator of IKK, phosphorylating the activation loops of the kinase subunits in response to a variety of signals (Shambharkar et al., 2007; Wang et al., 2001), and the kinase MEKK3 has also been reported to fulfil this role in some circumstances (Huang et al., 2004b; Yang et al., 2001a). In order to investigate the role of these IKK-Ks in FLIP-induced NF-κB activation, we produced HEK293T cells with stably knocked-down TAK1 or MEKK3 (Figure 4.4A). To prevent the possible compensative effect of these kinases on each other, we also generated double TAK1/MEKK3 KD cells (DKD)(Figure 4.5A).

As shown in Figure 4.5B, silencing of TAK1 in HEK293T cells severely disrupted the TNFα-mediated activation of the NF-κB, while MEKK3 was not required. TAK1 was clearly necessary for activation of IKK by all the cFLIP variants, though both kinases were dispensable for vFLIP and Tax activation (Figure 4.5C). The requirement for TAK1 in the cFLIP-mediated pathways suggests that the active kinase identified in Figure 3.5A has been phosphorylated and activated by TAK1. The lack of a requirement for TAK1 in vFLIP activation has been reported (Matta et al., 2012) although its role in Tax activation of IKK has been controversial (Suzuki et al., 2007; Wu and Sun, 2007). Interestingly, we could detect a partial decrease for NF-κB activation by both vFLIP and Tax in the double knock-down cells, suggesting that these kinases may have important but redundant roles. Since, even in the DKD cells, activity of these oncoproteins is not completely abrogated, another possibility is that these IKK-Ks contribute to the magnitude of IKK signalling but not its initiation.

To further confirm these experimental data in a different cell line, we acquired a *MEKK3* $^{-/-}$ MEF cell line and additionally knocked-down TAK1 in these cells (Figure 4.6A). For the KD of the murine TAK1, three different shRNAs were designed and cloned into LVs, of which shRNA No.3 resulted in the most efficient TAK1 silencing and was used for the experiments. Similar to what seen in HEK293T cells, none of the kinases were required for Tax-mediated activation and only a small, but statistically significant decrease could be detected when both kinases were lacking (Figure 4.6B). On the other hand, in MEFs, activation of the vFLIP was inhibited in part by the knockdown of TAK1. This discrepancy between the results obtained with HEK293T and MEFs suggests that the IKK-Ks might function in a cell type-specific manner. Nevertheless, whether the action of IKK-Ks is an absolute requirement for vFLIP activation of IKK or it is merely required for signal amplification remains an important unanswered question. This question has been addressed in Chapter5.

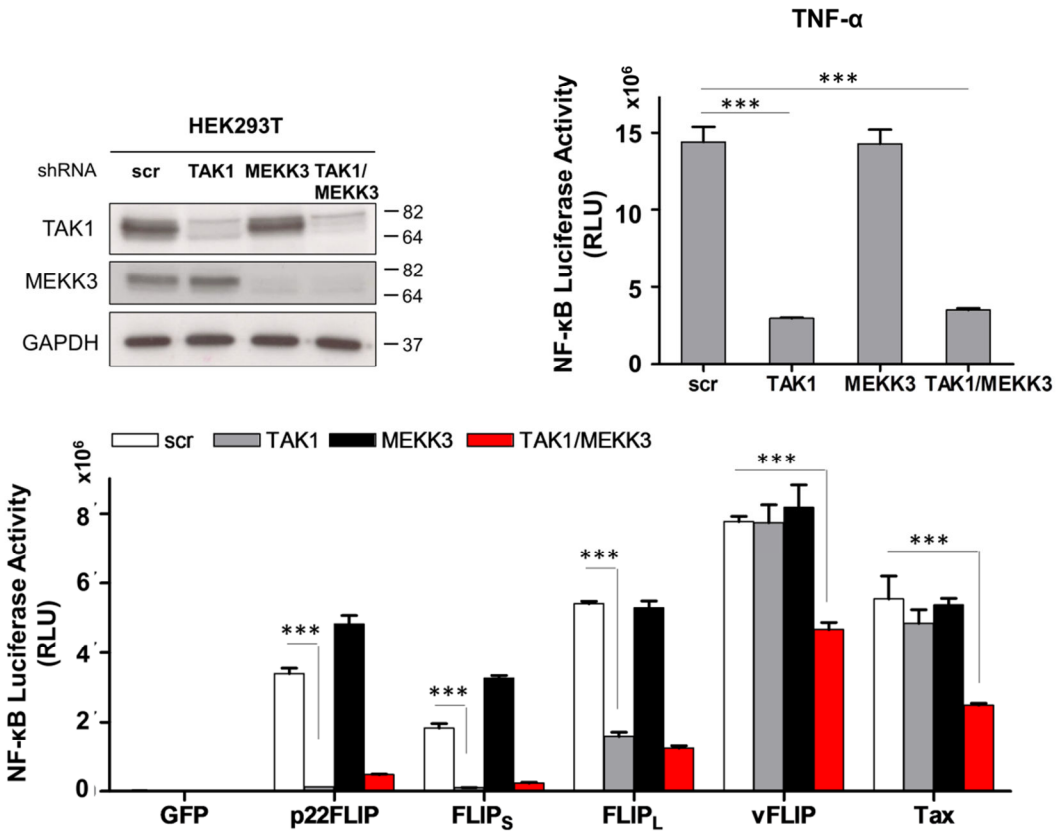

Figure 4.5. Cellular FLIPs require TAK1 for the activation of the NF-ϰB pathway. **A)** shRNA-mediated stable silencing of TAK1, or MEKK3 or both kinases in the HEK293T cells was validated with western blotting. **B)** Cells were further transduced with NF-ϰB Luc LV at an MOI of 10 to develop NF-ϰB sensor version of the cell lines. Luciferase reporter assays were then performed 6 hours following stimulation with TNFα (10ng/ml) or **C)** Forty-eight hours following transduction with control (eGFP) or test lentivectors (MOI=10). Results shown are mean ±SD of a representative experiment out of three, performed in triplicates. The two-tailed Student's *t*-test was used to determine the statistical differences between two groups; *** denotes $p<0.001$.

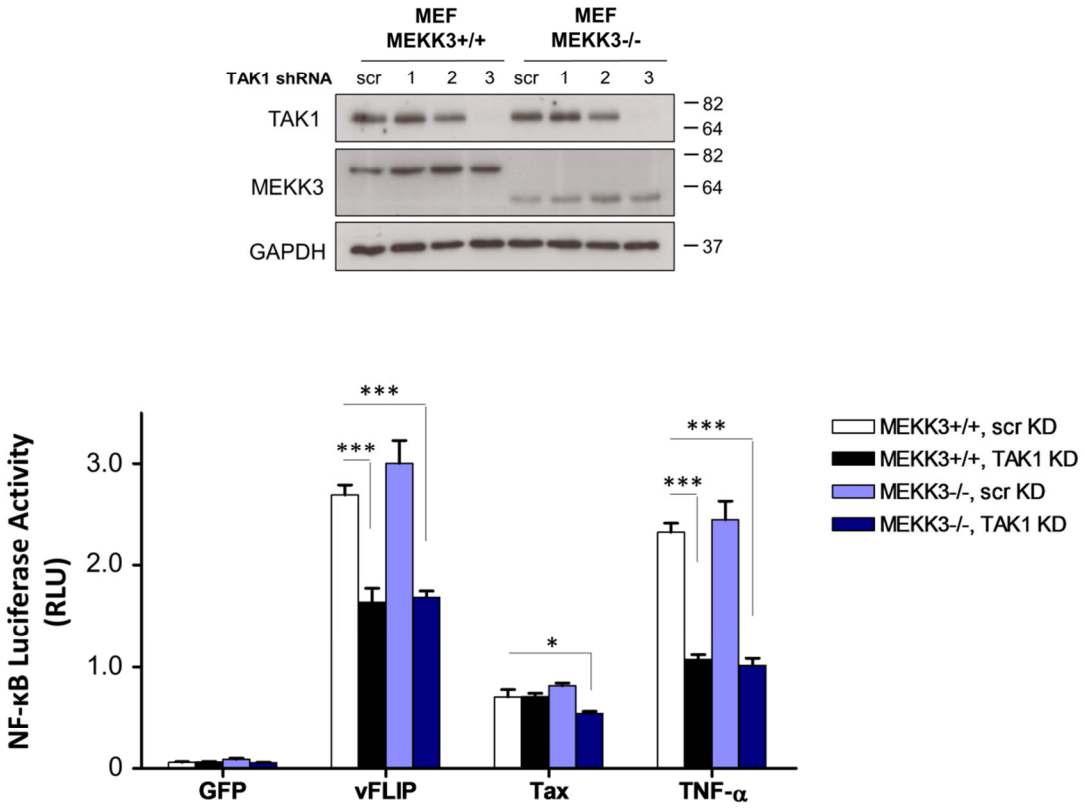

Figure 4.6. Analysis of vFLIP-, Tax- and TNFα-induced NF-κB activation in WT or TAK1 KD versions of the *MEKK3*$^{+/+}$ and *MEKK3*$^{-/-}$ mouse embryonic fibroblasts. A) Successful knockdown of TAK1 in WT and MEKK3 KO MEFs was validated by western blotting. **B)** MEFs were transduced with NF-κB luciferase LV at an MOI of 50 to generate NF-κB sensor cell lines. Luciferase reporter assays were performed using Bright-Glo detection system 6 hours following stimulation with TNFα (10 ng/ml) or 48 hours after transduction with LVs expressing GFP, or vFLIP, or Tax (MOI=20). Results shown are representative of two independent experiments, performed in triplicates. The two-tailed Student's *t*-test was used to determine the statistical differences between two groups; * $p<0.05$ and *** $p<0.001$.

4.4 Discussion

The data presented here show that all cFLIP variants can activate IKK via the ubiquitin binding domain of NEMO. The $cFLIP_L$ isoform requires the LUBAC ubiquitination complex, but does not require caspase-8 or $cFLIP_L$ cleavage. In contrast, $cFLIP_S$ and the cleavage product p22-FLIP form a stable complex with FADD and RIP1, which are required for IKK activation. This evidence for different pathways of NF-κB activation demonstrates that p22-FLIP is not simply the effector of $cFLIP_L$, though $cFLIP_L$ cleavage to generate p22-FLIP may switch the mechanism of NF-κB activation.

These $cFLIP_S$/FADD/RIP1 or p22-FLIP/FADD/RIP1 complexes are reminiscent of a cytoplasmic complex, termed the ripoptosome, induced by treatments of human tumour cells that deplete or inhibit cIAP proteins (Feoktistova et al., 2011; Tenev et al., 2011b). This depletion leads to the formation of a RIP1/FADD/procaspase-8 complex. cIAPs inhibit formation of this complex by ubiquitinating RIP1. In the absence of FLIP proteins, procaspase-8 molecules homodimerise in the ripoptosome, promoting cell death by apoptosis. Recruitment of $cFLIP_L$ to this complex leads to partial caspase-8 activation resulting in cell survival (Oberst et al., 2010). $cFLIP_S$, on the other hand, has been reported to block caspase-8 activation and facilitate cell death through necroptosis (Feoktistova et al., 2011). As previously mentioned, cFLIPs have also been reported to associate with and regulate a ripoptosome-like complex formed following TNF, TRAIL and Fas signalling (Lavrik et al., 2008; Micheau and Tschopp, 2003; Varfolomeev et al., 2005).

Our data shows that constitutive expression of cFLIP variants leads to formation of a FLIP/FADD/RIP1 complex that leads to NF-κB activation. The relationship between other complexes and this NF-κB activating complex remains to be determined, but we have clearly shown that caspase-8 is not required for NF-κB activation by any of the cFLIP variants. This is in contrast to some previous studies showing that caspase-8 is indispensable for $cFLIP_L$-mediated activation of NF-κB, especially following the Fas-signalling (Golks et al., 2006; Hu et al., 2000; Kataoka and Tschopp, 2004). There is evidence, however, that after cleaving $cFLIP_L$ to p43-FLIP, caspase-8 is not required for downstream steps of FasL-induced IKK activation (Matsuda et al., 2014; Neumann et al., 2010). Taken together, we conclude that caspase-8 is not a part of IKK-inducing complex used by different cFLIP variants, but it is required for signalling pathways which depend on cFLIP cleavage to induce or amplify IKK signalling (e.g, TCR and FasL signalling in T

cells mediated by p22- and p43-FLIP fragments) (Dohrman et al., 2005; Golks et al., 2006; Koenig et al., 2014; Neumann et al., 2010).

FADD-RIP1 and FADD-cFLIP bindings are mediated via homotypic DD and DED interactions, respectively (Lavrik et al., 2005; Park et al., 2013). Thus, it is likely that FADD acts as an adaptor protein connecting the short forms of cFLIP to ubiquitinated RIP1 which then can bind to and induce IKK complex. Interestingly, mutating the FADD binding domain of cFLIP resulted in complete blockade of their NF-κB activation while FADD knockdown had much milder effect. It is possible that residual amounts of FADD in the KD cells are sufficient to mediate $cFLIP_S$ and p22-FLIP induced signalling. Another explanation for this could be that other DD (death domain)-containing proteins such as TRADD may partially compensate for the lack of FADD. Indeed, TRADD is a known binding partner of both FADD (Hsu et al., 1996b) and RIP1 (Hsu et al., 1996a). We have provided evidence that FADD functions downstream of short forms of cFLIP to stimulate IKK, though further research is needed to determine the exact role of FADD in this context.

To our surprise, mutation of the putative FADD binding domain in $cFLIP_L$ prevented activation of IKK, whilst this isoform did not require FADD for its action, suggesting that this domain interacts with a different effector to trigger LUBAC activity. This effector may be TRAF2, which has been reported to interact with the N-terminal region of $cFLIP_L$, and to be required for its NF-κB activation (Kataoka and Tschopp, 2004). Nevertheless, whether $cFLIP_L$ could directly associate with a subunit of LUBAC remains to be tested.

We found that, unlike cFLIPs, KSHV vFLIP does not associate with FADD. Due to its sequence similarities to cellular FLIP, vFLIP was initially thought to protect cells from death receptor induced apoptosis through preventing caspase-8 activation at the DISC (Bertin et al., 1997; Hu et al., 1997a). Consistent with this idea, overexpression of vFLIP was shown to protect HeLa cells from Fas-induced apoptosis (Bélanger et al., 2001). Similarly, RNAi-mediated silencing of vFLIP was found to sensitise BC3 cells to Fas-mediated apoptosis (Guasparri et al., 2004). However, since NF-κB activation also protects against cell death by up-regulating a multitude of pro-survival genes (Luo et al., 2005), it was not clear whether the cytoprotective role of vFLIP is due to its ability to directly block caspase-8 activation or because of its NF-κB activation capacity. Interestingly, emerging evidence indicates that vFLIP is unable to protect NEMO

deficient cells from DR-induced cell death, suggesting that vFLIP is primarily an inducer of NF-κB rather than a caspase-8 inhibitor (Tolani et al., 2014; and data from an unpublished study by Chris Davis, Collins lab). Our results showing a lack of interaction between FADD and vFLIP further supports this concept as binding to FADD is essential for cFLIP-mediated inhibition of caspase-8 activity. Nevertheless, one study reported that vFLIP can directly bind to procaspase-8 and reduce its cleavage into its active p10 and p18 fragments (Bélanger et al., 2001).

The role of RIP1 in FLIP-induced IKK activation remains controversial. It was initially reported that RIP1 interacts with $cFLIP_L$ via its C-terminal caspase-like domain (Kataoka et al., 2000). Although, in a marked contrast, a recent study showed that under physiological conditions RIP1 interacts with caspase-8, but not $cFLIP_L$, and in fact, the C-terminal p12 domain of $cFLIP_L$ inhibits this interaction (Matsuda et al., 2014). Matusda et al., showed that NF-κB activation induced by c-$FLIP_L$ or its uncleavable form (D376A) could not be inhibited by overexpressing death domian of RIP1 (aa 559–671). On the other hand, FasL-induced NF-κB signalling which depends on p43-FLIP was repressed by RIP1(559-671). Similarly, we have shown that RIP1 is indispensable for activation of IKK by the catalytic p22-FLIP fragment, but not full-length $cFLIP_L$. Therefore, one could infer that $cFLIP_L$ processing to either p22-FLIP or p43-FLIP acts as a critical switch point between RIP1-independent and RIP1-dependent FLIP-induced NF-κB activation pathways.

Despite using different signalling intermediates, all cFLIP variants converge on TAK1 to phosphorylate and activate IKK. In TNF signalling, recruitment of TAK1 to IKK occurs through K63 ubiquitin chains bound to TRAF2 or RIP1 (Ea et al., 2006; Ishitani et al., 2003). Considering that we and others have shown the requirement of cFLIP variants for both proteins (p22-FLIP and $cFLIP_S$ for RIP1, and $cFLIP_L$ and p43-FLIP for TRAF2 (Kataoka and Tschopp, 2004; Koenig et al., 2014)), it would be important to examine whether these proteins mediate the co-localisation of TAK1 and IKK within cFLIP-induced signalling.

In contrast to cFLIPs, neither vFLIP nor Tax required TAK1 or MEKK3 to induce IKK. This strongly suggested a mechanism of activation which is independent of IKK-activating kinases. Nevertheless, partial decrease of their NF-κB activation in double MEKK3/TAK1 knockdown cells indicates that IKK-Ks may play a role in achieving optimal levels of activation in cells. It is also possible that these viral oncoproteins are able

to use several IKKs interchangeably. These concepts have been further addressed in the next chapter.

In summary, data presented here show that KSHV vFLIP and different variants of cellular FLIPs, despite their similar tandem DEDs, activate NF-κB by remarkably divergent mechanisms. This could have multiple applications when designing specific therapeutics for blocking pathological NF-κB activation in viral and non-viral tumourigenesis, while avoiding the deleterious effects on normal cellular functions.

CHAPTER

5

Probing the Mechanism of IKK Activation of the KSHV vFLIP

5.1 Introduction

Results in Chapters 3 and 4 demonstrated that vFLIP does not require ubiquitin signalling or the IKK kinases TAK1 or MEKK3 to achieve IKK activation. Clearly, however, an as yet unidentified IKK kinase might be involved (Figure 5.1A). Furthermore, the phosphatase PP2A was reported to interact with a similar region of NEMO to vFLIP, and Tax was reported to interact with PP2A in the IKK complex and inhibit its activity (Fu et al., 2003; Hong et al., 2007). One hypothesis might be that vFLIP binding to NEMO would either inhibit PP2A binding, or inhibit PP2A activity (Figure 5.1B). Furthermore, the ubiquitin binding proteins A20 and ABIN1 are known to interact with NEMO and inhibit IKK activity (Mauro et al., 2006; Zhang et al., 2000). In the case of A20 this is believed to be a direct binding to NEMO that prevents TAK1 recruitment, rather than dependent on the deubiquitination activity of A20 (Skaug et al., 2011). Therefore, a further hypothesis might be that vFLIP binding prevents A20 and/or ABIN1 interaction with NEMO, thereby blocking IKK inhibition. One approach to testing whether vFLIP recruits an upstream activator or blocks an inhibitor would be to test shRNA knockdown of candidate activators or inhibitors on the activity of vFLIP. However, this would be time consuming and likely require combinations of shRNAs. We therefore started to examine the activation of an immunoprecipitated IKK complex by recombinant vFLIP in this Chapter. This is a first step towards attempting activation of recombinant IKK by recombinant vFLIP which would provide conclusive proof that vFLIP acts independently of other activators or inhibitors.

In this chapter we also considered how vFLIP might activate IKK by direct binding to NEMO. When our group published the structure of vFLIP bound to a small fragment of NEMO, we proposed that this interaction might cause a major conformational change in NEMO leading to activation (Bagnéris et al., 2008) (Figure 5.1C). In our present experiments we considered this possibility and also whether the kinase subunits required T loop phosphorylation which has been reported for chronic activation of IKK by Tax (Carter et al., 2001). This activating phosphorylation could be the result of trans-autophosphorylation by the kinase subunits. Such trans-autophosphorylation can be observed with isolated, monomeric IKKβ *in vitro* (Hauenstein et al., 2014), so vFLIP binding to NEMO would need to enhance the likelihood of such an event.

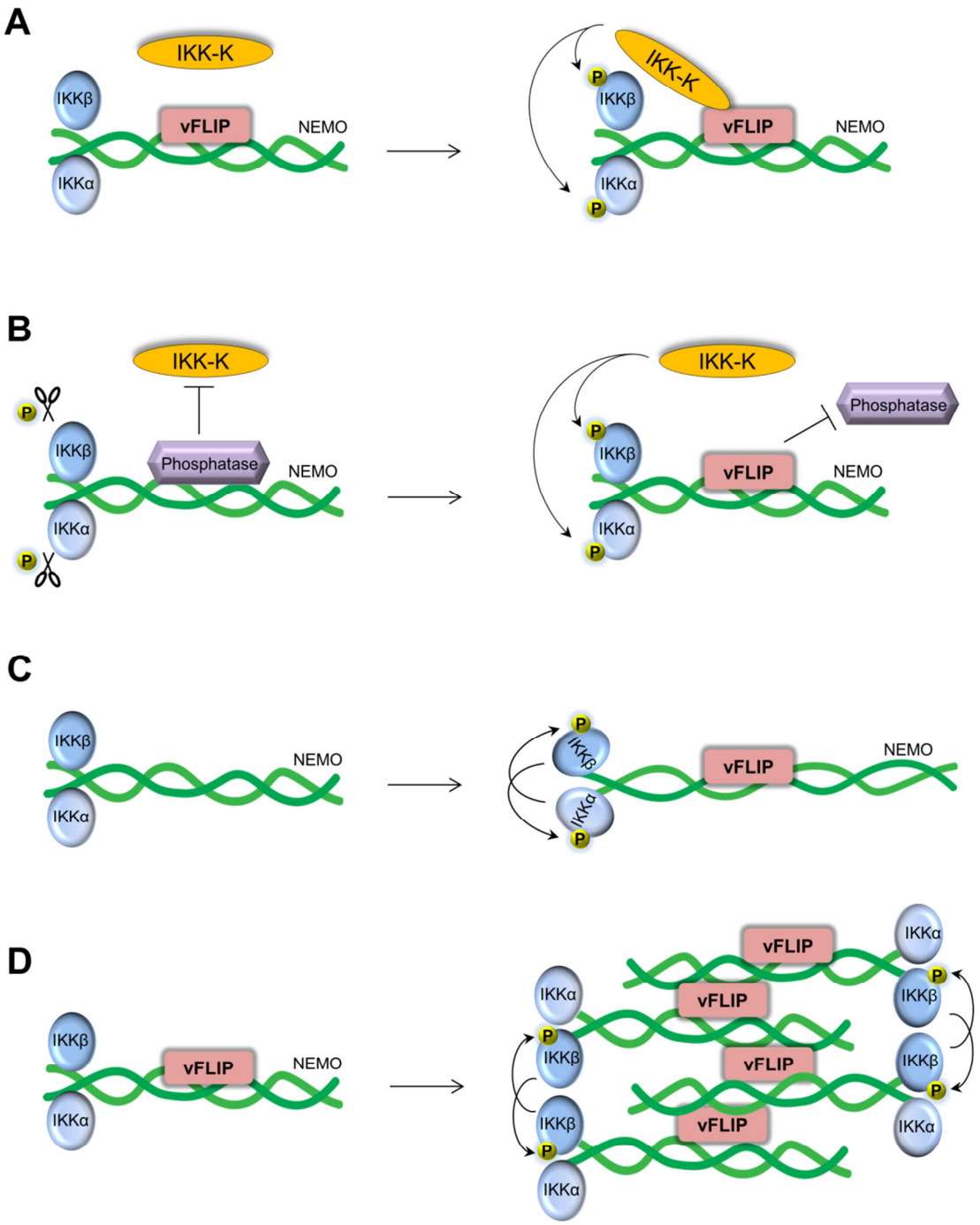

Figure 5.1. Possible mechanisms underlying vFLIP-mediated activation of IKK. A) vFLIP may function as a signalling adaptor to recruit upstream IKK-Ks to phosphorylate IKKs. **B)** vFLIP may block binding and function of proteins which repress activation of IKK (e.g., phosphatase or deubiquitinases), leading to its constitutive activation. **C)** vFLIP binding to NEMO may cause conformational changes which can then transmit to IKKα/β-binding regions of NEMO, affecting spatial conformation of the catalytic IKKs, favouring their activation by trans-autophosphorylation. **D)** Recognition of vFLIP by NEMO may induce multimerisation or re-orientation of the IKK complexes, positioning the catalytic IKKs for trans-autophosphorylation.

5.2 Aims of the chapter

- Examine whether vFLIP can directly activate IKK, independent of the upstream signalling mediators.
- Examine whether the phosphorylation of the catalytic IKKs is required for vFLIP-mediated IKK signalling.
- Investigate the possible mechanism of IKK activation by vFLIP.

5.3 Results

5.3.1 Recombinant vFLIP, but not p22-FLIP, can activate IKK when added to cell lysates

So far, we have demonstrated that vFLIP and p22-FLIP exhibit very different requirements for ubiquitination, signalling intermediates and IKK-Ks in their activation of IKK. In order to further probe the mechanism of action of these proteins, we set up an *in vitro* IKK activation assay, originally established by Mukherjee et al (Mukherjee et al., 2006). This assay is initiated by the addition of a purified activator of the IKK signalling pathway to S100 extract of resting cells in the presence of an ATP-regenerating system, followed by termination of the reaction by addition of SDS sample buffer. The activation of IKK complex is then assessed by immunoblotting for the phosphorylated form of the endogenous IκBα.

Here, we produced recombinant vFLIP and p22-FLIP proteins and added them to S100 lysates of the HEK293T cells, in a concentration range of 0.25 μM to 2 μM. Figure 5.2 shows that recombinant vFLIP induced phosphorylation of the kinase subunits of IKK, and that IKK became activated in the lysate as IκBα was phosphorylated. This occurred within 10 minutes of incubation with the lysate; in contrast recombinant p22-FLIP could not activate IKK under these conditions (Figure 5.2). Similar direct activation of the IKK kinase in cell lysates supplemented with recombinant Tax has been reported (Mukherjee et al., 2008). Taken together with our previous results showing the requirement for several signalling intermediates by the p22-FLIP, it is conceivable that p22-FLIP activation of IKK relies on signalling complexes which are usually restrained by the cellular architecture.

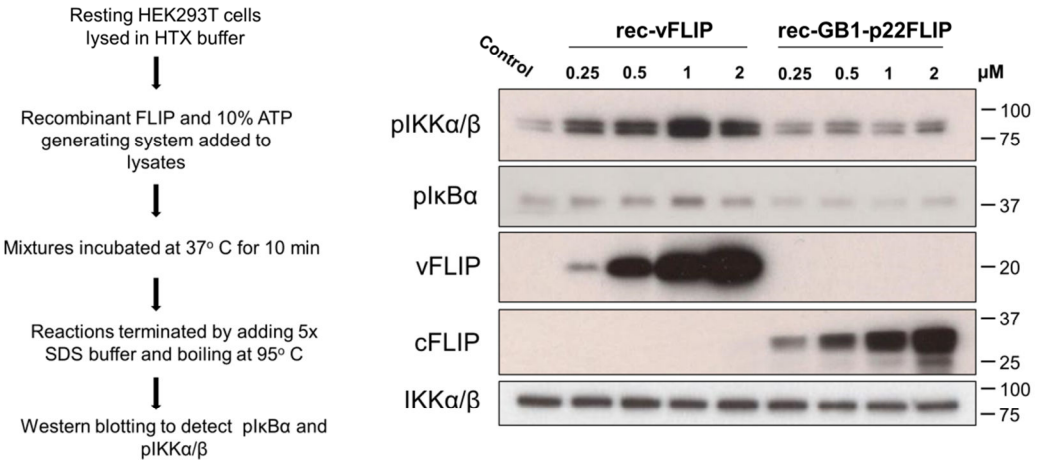

Figure 5.2. Recombinant KSHV vFLIP activates IKK when added to cell lysate. A) IKK activation by rec-vFLIP or rec-p22FLIP was analysed using an *in vitro* IκBα phosphorylation assay. Briefly, resting HEK293T cells were lysed in HTX buffer (See section 2.9) and the S100 fractions were extracted. The lysates were then incubated with an ATP-generating buffer and increasing concentrations of recombinant vFLIP or p22-FLIP at 37 °C for 10 min. Activation of the IKK complex was detected by immunoblotting against pIκBα and pIKKα/β. The blot was re-probed for total IKKα/β to ensure equal loading of protein.

5.3.2 Recombinant vFLIP can activate immuno-isolated IKK complexes in a cell-free assay system

We next sought to examine whether the vFLIP-induced activation of IKK in cell lysates was a consequence of direct and specific action of the recombinant vFLIP on the IKK complex. This is relevant as we have previously shown that, in KSHV-infected cells, the subunits of the IKK complex and HSP90 are the only detectable proteins in complex with vFLIP. Furthermore, studies by ourselves and other groups aimed at identifying a signalling constituent upstream of the IKK complex that would be necessary for vFLIP-mediated activation of IKK has been unsuccessful.

To test this hypothesis, we immunoprecipitated the IKK complex from unstimulated HEK293T cells using an anti-NEMO antibody and then, incubated them with varying concentrations of rec-vFLIP under two different conditions: one group were incubated at room temperature for one hour, while the other group were incubated overnight at 4 ^{o}C. Subsequently, the immune complexes were thoroughly washed with kinase wash buffer and subjected to the IKK kinase assay using GST-IκBα(1-54) and γ^{32}P-ATP as substrates. Due to technical problems, I was unable to perform this experiment with recombinant-cFLIP.

As Figure 5.3 shows, in both incubation conditions, rec-vFLIP was able to activate the immunoprecipitated IKK complex and the levels of pGST-IκBα correlated well with the concentrations of the added recombinant vFLIP. These data strongly suggest that vFLIP can directly activate the IKK complex without a requirement for upstream MAP3Ks. Nevertheless, in the previous chapter, we observed that silencing of the IKK-Ks could partially inhibit vFLIP-mediated NF-κB activation in some settings. Therefore, we conclude that, in cells, IKK-Ks are more likely required for maximal IKK signalling following its direct MAP3K-independent activation by the vFLIP.

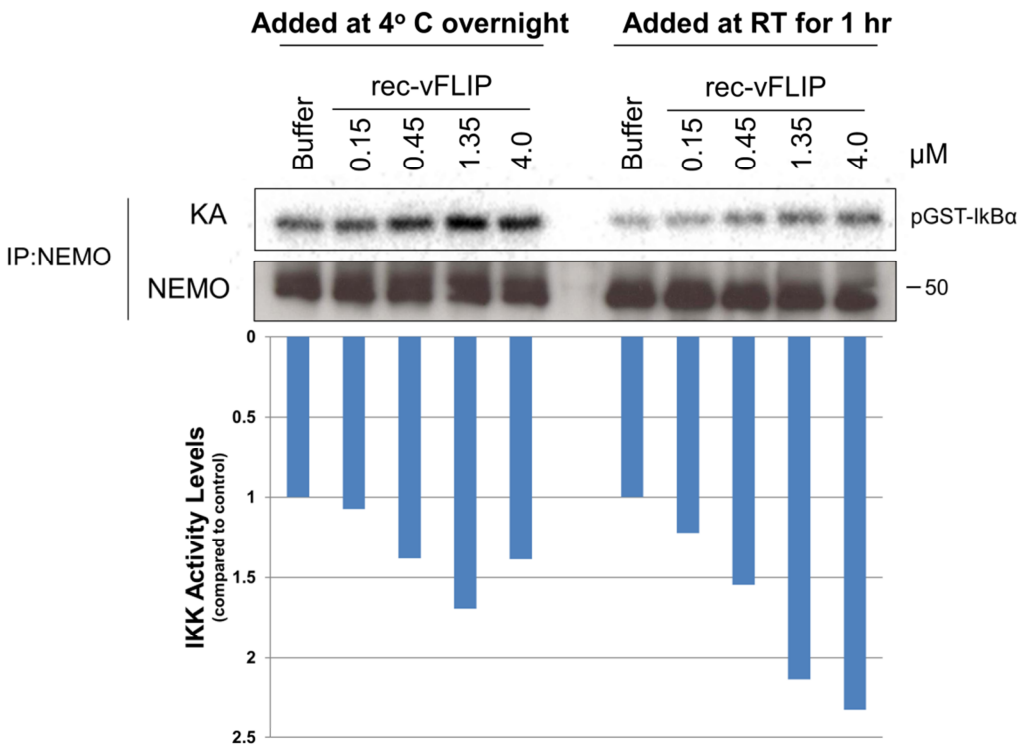

Figure 5.3. Direct *in vitro* activation of the IKK complex by recombinant vFLIP. IKK complex from unstimulated HEK293T cells ($2x10^6$/reaction) was immunoprecipitaed using an antibody against NEMO (0.5 μg/sample). The isolated complexes were then washed twice with kinase lysis buffer and once with kinase wash buffer (KWB). Next, the IKK-bound beads were divided into equal fractions, re-suspended with 500 μl of the KWB and incubated with increasing concentrations of recombinant vFLIP (0.15-4.0 μM) for 1 hour at room temperature, or overnight at 4 °C. Finally, *in vitro* IKK kinase assays were performed on immunoprecipitated complexes as previously described using γ^{32}p-ATP and GST-IκBα(1–54) as substrates. Relative band intensity of phosphorylated GST-IκBα was measured by ImageQuant TL Plus7.0 software (GE Healthcare). A value of 1.0 represents band intensity obtained in the control experiment. Data shown are representative of two independent experiments.

5.3.3 Phosphorylation of the IKKs at the activation loop is crucial for vFLIP-induced IKK activation

It is now well-established that phosphorylation of the IKKα/β at their activation loop (residues S176 and S180 for IKKα, and residues S177 and S181 for IKKβ) is an essential step for their activation following inflammatory stimuli (Ling et al., 1998; Mercurio et al., 1997; Régnier et al., 1997; Woronicz et al., 1997; Zandi et al., 1997). The phosphorylation of T-loop is believed to cause conformational changes that render the catalytic domains of IKKα/β active (Hayden and Ghosh, 2008). Nevertheless, tumour-specific somatic mutations of IKKβ have been recently reported which result in its constitutive activation independently of the T-loop phosphorylation (Kai et al., 2014). For example, K171E or K171T mutation of IKKβ, originally found in malignancies such as splenic marginal zone B-cell lymphoma (Rossi et al., 2011, 2012) and multiple myeloma (Chapman et al., 2011), were recently shown to render the IKKβ constitutively active without a requirement for activation loop phosphorylation. It has been proposed that these mutations mimic the structural alterations induced by the T-loop phosphorylation (Kai et al., 2014).

Considering this information and that vFLIP can activate the IKK complex in the absence of upstream kinases, we asked whether phosphorylation of the catalytic IKKs were required for their activation by the vFLIP? In other words, could vFLIP-binding to NEMO cause activatory conformational changes on IKKα/β which bypass the requirement for the T-loop phosphorylation? To test this hypothesis, we examined whether dephosphorylation of the vFLIP-bound IKK complex would inhibit its catalytic capacity.

To this end, we immunoprecipitated the active IKK complexes from vFLIP and p22-FLIP-transduced HEK293T cells and washed them thoroughly with high salt wash buffer. The immune complexes were then treated with increasing concentrations of lambda protein phosphatase (LPP or λPP), an Mn^{2+}-dependent protein phosphatase with activity towards serine, threonine and tyrosine residues (Zhuo et al., 1993). The *in vitro* phosphatase assay was terminated by adding high concentrations of Na_3VO_4 (25mM). Subsequently, the immunoprecipitates were washed three times to remove any remaining LPP and subjected to IKK kinase assay.

As shown in Figure 5.4A, pre-treatment with LPP led to a marked decrease in the activity of both cFLIP and vFLIP-activated IKKs; the kinase activity levels inversely

correlated with the amount of LPP used. This implies that both activators require the phosphorylataion of the T-loop of the catalytic IKKs to switch on the IKK complex. However, a major caveat to this assumption is that LPP may also remove phosphate groups from other phospho-acceptor residues in the IKKα, β and γ, with yet unidentified activatory roles.

As mentioned previously, mutation of the IKK activation loop serines to alanine (IKKβ S177/S181AA) impedes the kinase activity while their replacement with phosphomimetic glutamate residues (IKKβ S177/S181EE) renders the kinase constitutively active (Mercurio et al., 1997). In extension to the previous experiment, we also tested whether mutations of the T-loop phosphorylation sites would alter the vFLIP-induced IKK activity. To do this, we overexpressed vFLIP in HEK293T cells in combination with either WT IKKβ, or IKKβ SSAA, or IKKβ SSEE. Empty vector-transfected and TNFα-treated cells were used as negative and positive controls, respectively. NF-κB activity was then measured by means of a co-transfected NF-κB-responsive luciferase reporter system.

Similar to the result with TNFα stimulation, vFLIP-induced NF-κB activation was lower when co-expressed with IKKβ SSAA, as compared with the WT IKKβ, while it was higher when co-transfected with the active mutant, IKKβ SSEE (Figure 5.4B). Overall, these data suggest that vFLIP-mediated activation of the IKK relies on phosphorylation of the activation loop serines.

It has to be noted that even the overexpression of the IKKβ SSAA causes a considerable NF-κB activation in cells. This is presumably caused by enforced oligomerisation or re-orientation of the endogenous IKKα/β by the overexpressed mutant counterparts. Therefore, precise investigation of this hypothesis would require usage of double IKKα/β KO cells to overcome the problem of inducing high basal NF-κB activation which may mask the vFLIP-induced signals.

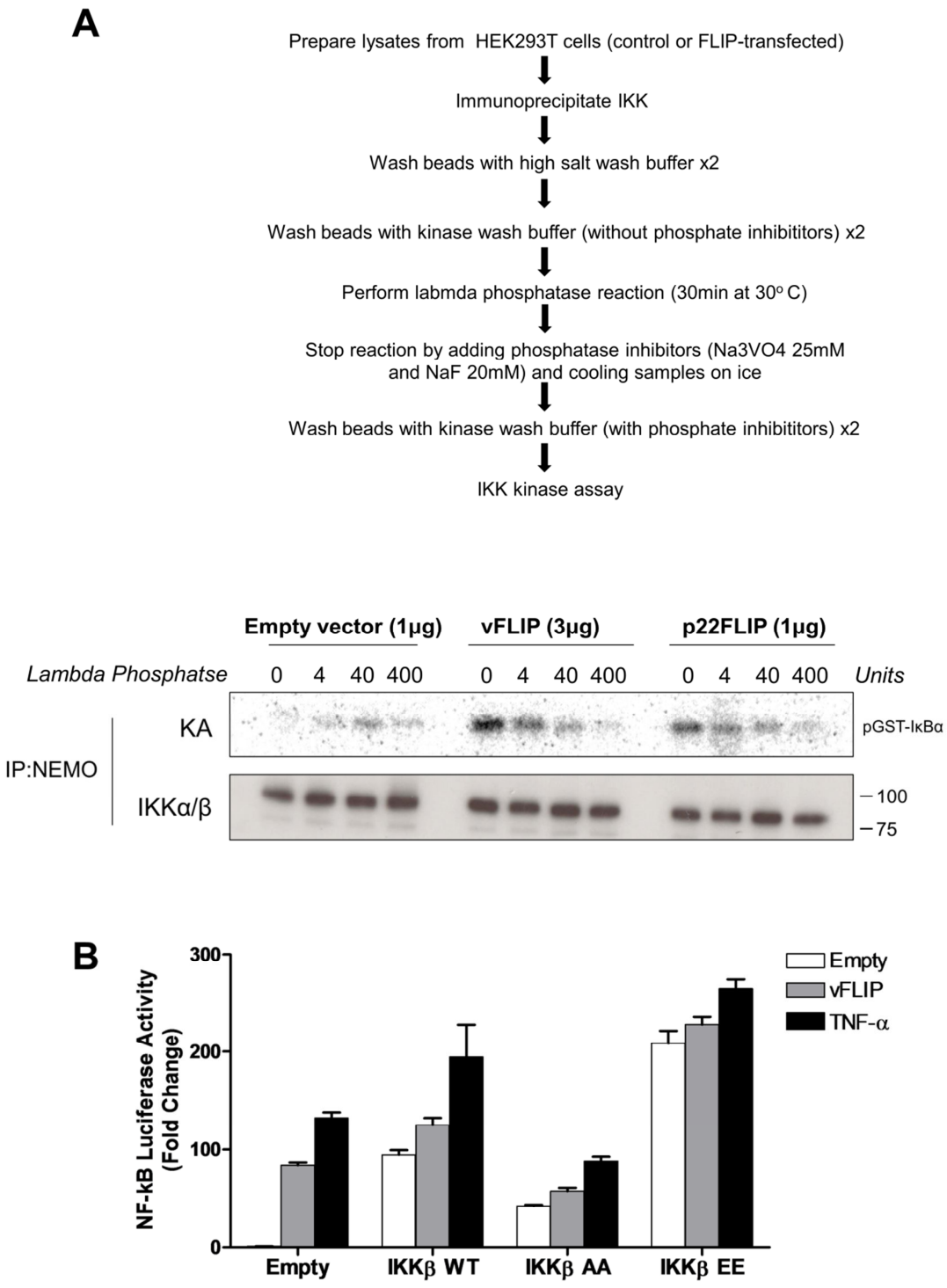

Figure 5.4. Phosphorylation of the IKKs at their activation loop is required for vFLIP-mediated activation of the IKK complex. A) HEK293T cells seeded in 6-well plates ($2x10^6$/well) were transfected with either 1µg of an empty expression vector, 3µg of pCDNA3-vFLIP, or 1µg of pCDNA3-p22FLIP. Forty-eight hours later, cells were lysed in 1ml of kinase lysis buffer and immunoprecipitated with an antibody against NEMO (0.5µg/sample). The immune complexes were then washed twice with high salt wash

buffer and two additional times with kinase wash buffer lacking the phosphatase inhibitors. Next, the anti-NEMO immunoprecipitates were incubated in phosphatase reaction buffer (total volume of 50 µl) containing increasing concentrations of LPP (4, 40 and 400 U) for 30 min at 30 °C. The reactions were terminated by adding high concentrations of Na_3VO_4 (25 mM) and NaF (20 mM). Finally, the immune complex were washed twice with kinase wash buffer and subjected to IKK kinase assay. **B)** HEK293T cells were transiently transfected with 1µg of an empty vector or pCDNA3-vFLIP in combination with 300ng of WT or mutant versions of IKKβ. NF-κB activity was measured 24 hours later by means of a co-transfected NF-κB reporter system (400ng of pGL.IgK and 100ng of pRL.TK). The results shown are representative of two independent experiments. IKKβAA: IKKβ S177/S181AA, and IKKβEE: IKKβ S177/S181EE.

5.3.4 Dimeric vFLIP-vFLIP interactions within the vFLIP-IKK signalosome are crucial for vFLIP activation of IKK

We previously demonstrated that vFLIP can directly activate IKK, in the absence of upstream kinases. It was also shown that that vFLIP is able to activate C-terminally truncated NEMO (NEMO Δ254). Together, this led us to hypothesise that binding to vFLIP, might induce conformational changes in the NEMO which then transmit to the N-terminal IKKα/β binding regions, leading to changes in proximity or conformation of the catalytic IKKs, favouring their activation by trans-autophosphorylation. To investigate this hypothesis, we collaborated with Tracey Barrett (School of Crystollography, Birkbeck College) and Chris Kay (Institute of Structural and Molecular Biology, UCL) who compared the solution structure of free and vFLIP-bound NEMO using electron paramagnetic resonance (EPR). The EPR data revealed that apart from a localised twisting near the vFLIP-binding region, NEMO does not undergo major structural alterations in response to binding, excluding the induction of conformational changes as a potential mechanism of vFLIP-mediated IKK activation (manuscript submitted).

In addition to conformational change-induced activation, oligomerisation of IKK has been also proposed as a means of its activation (See 1.2). The recent crystal structure of the human IKKβ suggested a head-to-head orientation of kinase domains for trans-autophosphorylation that arises through oligomerisation (Figure 5.5A). We, therefore, wondered whether vFLIP could lock IKKβ subunits into this configuration, promoting

their oligomerisation-induced activation. To address this question, Tracey Barrett re-analysed the X-ray diffraction data from the vFLIP-NEMO crystals. She found that vFLIP-NEMO complexes pack against one another throughout the crystal to generate higher order oligomers whose configuration could bring the catalytic IKKs into close proximity, leading to their cross-phosphorylation (Figure 5.5B).

A close inspection of their arrangement suggests that these oligomers are stabilised by both vFLIP-vFLIP and vFLIP-NEMO interactions (Figure 5.6A and B). The latter interactions occur at two distinct vFLIP-NEMO interfaces: here referred to as interface1 and interface2 (Figure 5.6C). In chapter 3, we demonstrated that mutations such as NEMO F238/D242RR which disrupt the interface1 interactions completely abolish the formation of vFLIP-NEMO complexes and the subsequent IKK activation.

To gain further insights into the mechanism of IKK activation used by vFLIP, we introduced mutations in vFLIP that would disrupt interactions involved in its dimerisation interface (D102R and E104R), or the vFLIP-NEMO interface2 (R12E) or both (R12E/E104R). As shown in Figure 5.7A, while none of these mutations affected the ability of vFLIP to form complex with NEMO, they all showed a considerably reduced capacity to activate IKK, as revealed by immunoblotting against pIκBα. Consistently, the NF-κB luciferase activities induced by vFLIP mutants were significantly lower as compared with the WT vFLIP (Figure 5.7B). In summary, these preliminary data demonstrate the importance of vFLIP-vFLIP and vFLIP-NEMO interactions that are required for the assembly of the higher order oligomers, suggesting the multimerisation-induced IKK activation as a possible mechanism of action utilised by the KSHV vFLIP.

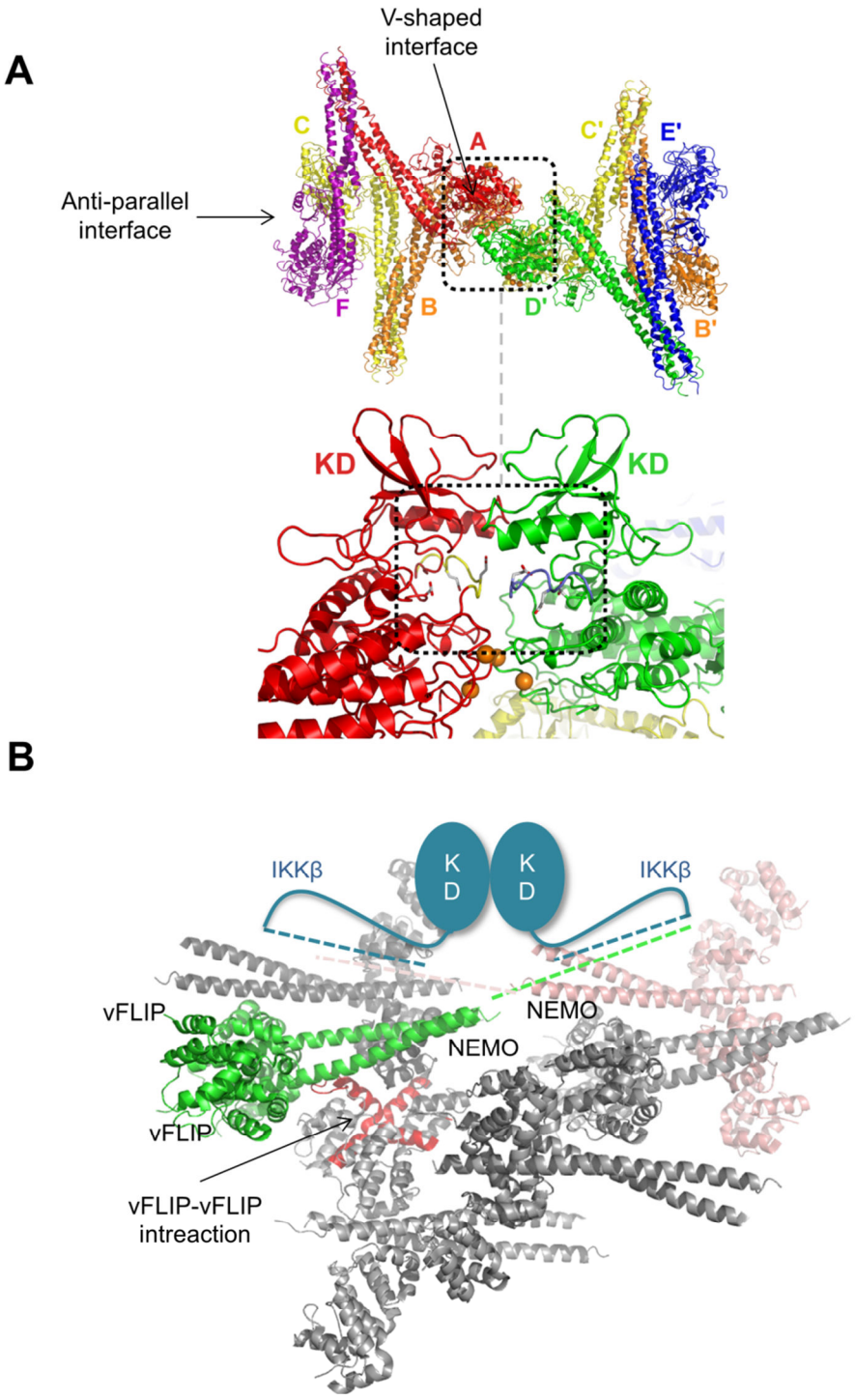

Figure 5.5. Multimerisation of the vFLIP-NEMO complexes within the crystal. A) Human IKKβ dimers adopt open conformations that permit higher order oligomerisation within the crystal. A separate colour has been assigned to ribbon diagram of each IKKβ subunit. Association of two neighbouring IKKβ dimers gives rise to two unique intersubunit interfaces: (i) the V-shaped interface and (ii) the anti-parallel interface. Within the higher order complex, neighbouring tetrameric IKKβ assemblies interact

symmetrically in a way that they contact one another through their V-shaped interfaces and two kinase domains (KD) are positioned within close proximity to one another, facilitating for their trans-autophosphorylation . Reproduced from (Polley et al., 2013). **B)** Within the vFLIP-NEMO crystal, there is an oligomer consistent with the head-to-head orientation of IKKβ subunits observed in (A). Courtesy of Dr. Tracey Barret.

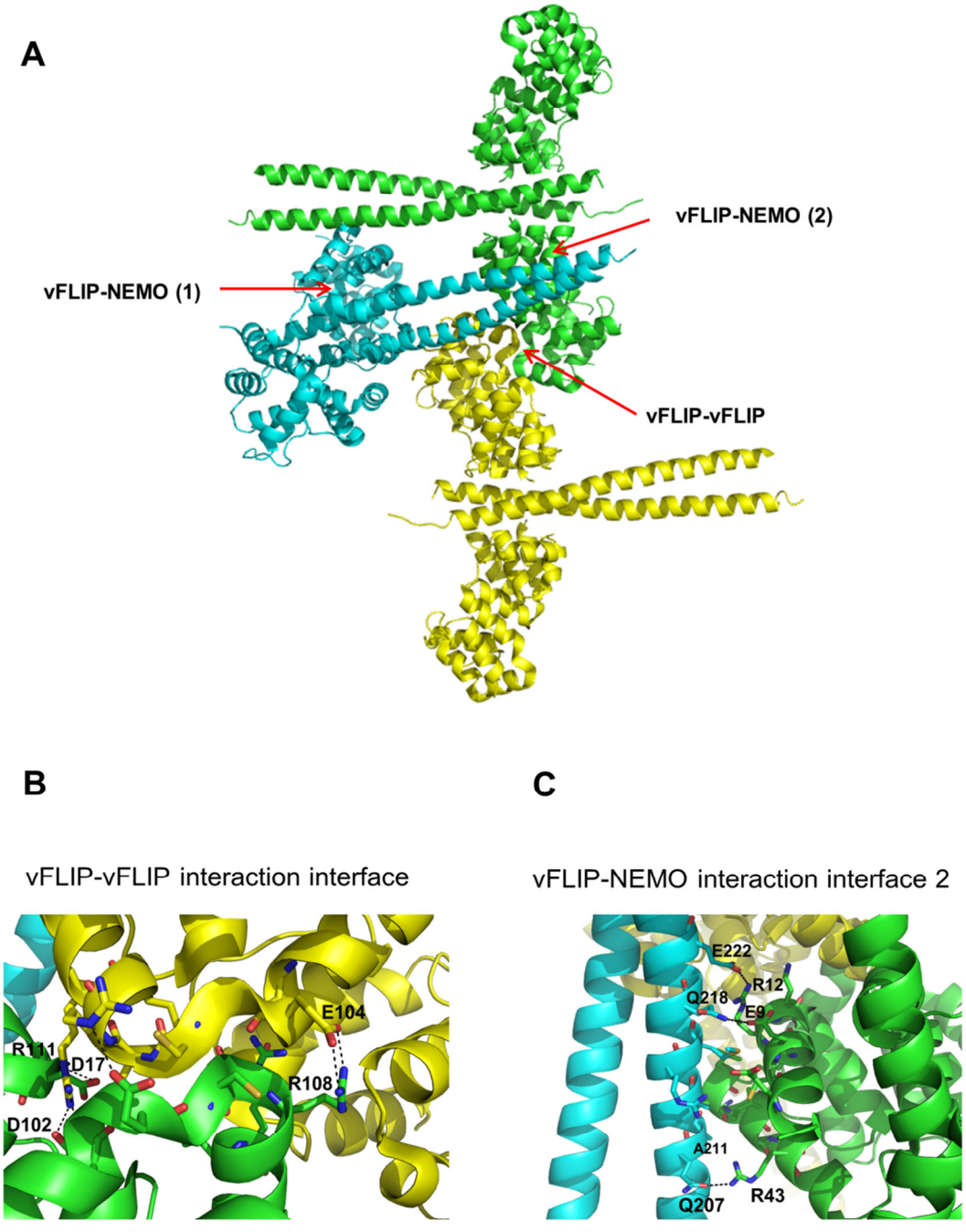

Figure 5.6. Interactions involved in the formation of higher order vFLIP-NEMO assemblies. A) Three interaction interfaces are detected within the vFLIP-NEMO crystals. These include two vFLIP-NEMO contact regions (here referred to as interface 1 and 2) and a dimeric vFLIP-vFLIP contact interface. The vFLIP-NEMO interaction interface1 has been discussed previously in Section 3.1.2. **B)** The vFLIP-vFLIP interactions are mediated by salt bridges between R108, D102 and D17 of one monomer with E104 and R111 of a second vFLIP monomer (form an adjacent vFLIP-NEMO complex). This interaction region is in a close proximity to vFLIP-NEMO interaction interface2 . **C)** The intermolecular contacts within the vFLIP-NEMO interaction interface (2) include a network of salt bridges between E222, Q208 and Q217 of NEMO and R12, R43 and E9 of vFLIP, respectively.

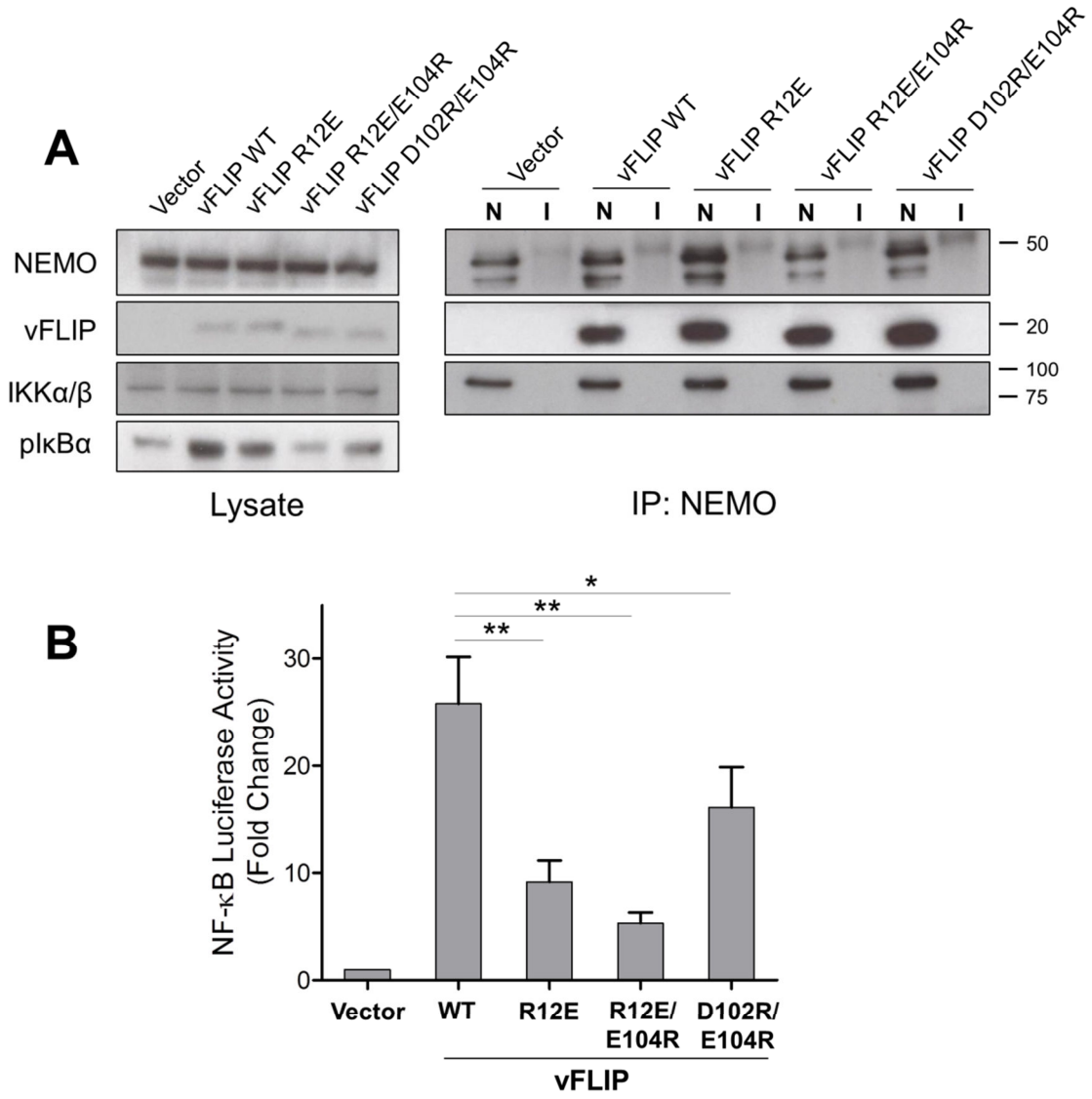

Figure 5.7. Mutations in the vFLIP-vFLIP and vFLIP-NEMO(2) interaction interfaces impair the vFLIP-induced activation of IKK. A) HEK293T cells seeded in 6-well plates ($2x10^6$ cells/well) were transfected with 1μg of pCDNA3 vectors encoding WT vFLIP or the mutant versions: vFLIP R12E, or R12E/E104R, or D102/E104RR. Forty-eight hours later, whole cell lysates were extracted and subjected to immunoprecipitation (IP) with anti-NEMO (N) or an isotype-matched control IgG (I), followed by immunoblotting (IB) with the indicated antibodies. While none of the mutations affected the ability of vFLIP to form complex with NEMO, they all showed a considerably reduced capacity to activate IKK, as revealed by reduced levels of IκBα phosphorylation. B) $2x10^5$ HEK293T cells were co-transfected with an NF-κB luciferase reporter construct (300ng/well) and a Renilla Luc reporter vector (100ng/well) along with an empty vector or pCDNA3 vectors (500ng/well) expressing the WT and mutant versions of the vFLIP. NF-κB activity was measured 24 hours later, as described previously. Results shown are representative of three independent experiments, performed in triplicates. Error bars indicate SD of the mean values compared by two-tailed unpaired Student's t-test; * $p<0.05$, ** $p<0.01$ and *** $p<0.001$.

5.3.5 A stapled peptide derived from HLX2 region of NEMO can efficiently block vFLIP-binding to IKK and its subsequent activation

The crystal structure of the vFLIP-NEMO complex revealed that a very important aspect of the vFLIP-mediated IKK activation is the recognition of α-helical structure of the NEMO HLX2 by two clefts in the vFLIP DED2 (see 3.1.2). It was then evident that further characterisation of the biochemical and structural traits of the complex would require strategies to simulate the vFLIP-NEMO interactions. In order to achieve this goal, Tracey Barrett in collaboration with David Selwood (Division of Medicine, UCL) designed a stapled peptide containing the minimal vFLIP-binding sequence of the NEMO (amino acids 226-247) (Figure 5.8A). Stapled peptides (SP) incorporate a hydrocarbon cross-linker or "staple" which forces them to maintain their natural α-helical shape. Therefore, these peptides retain their ability to bind to target proteins and serve as valuable molecular tools to interrogate the native protein-protein interactions (Bernal and Katz, 2014; Walensky et al., 2004).

Structural studies by Tracey Barrett's group indicated that interactions between stapled NEMO peptide and vFLIP directly mimetic of those involving NEMO and extend to conservation of the NEMO-NEMO dimer interface (Figure 5.8B and C). In keeping with these findings, preliminary ITC (isothermal titration calorimetry) data suggested a vFLIP-binding affinity for stapled peptide comparable to that of NEMO. It was also shown that the stapled NEMO helix could competitively inhibit formation of vFLIP-NEMO complexes in solution (Tracey Barrett, unpublished data). Based on these findings, we set out to investigate whether this peptide could also block the vFLIP-induced IKK activation.

To test this, we extracted cell lysates of the WT or vFLIP-expressing Jurkat cells and incubated them with stapled NEMO peptide (50 μM) or DMSO (as negative control) at 4 ^{o}C overnight. We then immunoprecipitated IKK from cell extracts using an anti-NEMO antibody and measured its ability to phosphorylate recombinant IκBα. Figure 5.9 shows that stapled peptide not only disrupted the vFLIP-NEMO binding in cell lysates but also repressed the vFLIP-induced, but not basal, IKK activities.

Because of their enhanced cell permeability and resistance to protease degradation, stapled peptides may be cell permeable and are therefore possible therapeutics. More experiments are required to confirm that the stapled NEMO peptide does not have any non-specific effects on physiological cytokine-induced IKK signalling. In addition, the in

vivo efficacy of the peptide remains to be examined. Nevertheless, our preliminary data suggests that this peptide could have therapeutic potential against KS-induced tumours. Clearly also the peptide is a useful experimental tool as we can demonstrate that removal of vFLIP from the IKK complex reverses its activation.

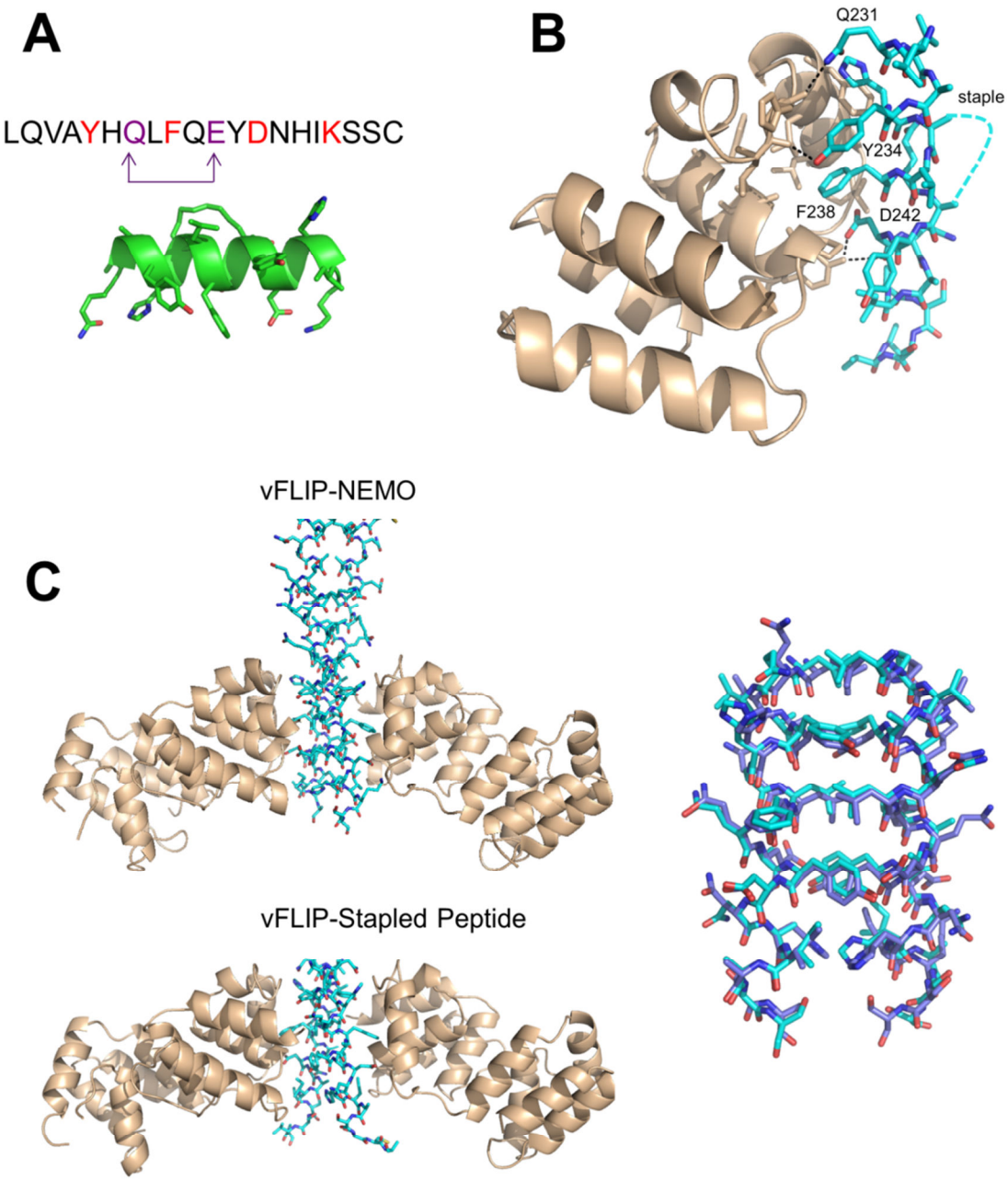

Figure 5.8. Crystal structure of the stapled NEMO peptide. A) Primary sequence and α-helical structure of the NEMO SP. The all-hydrocarbon staple has been incorporated into the peptide sequence at the *i*, *i+4* positions, highlighted in violet. **B)** The GB1-vFLIP-NEMO interface. GB1-vFLIP is represented as stick model and NEMO is shown

as brown ribbon representation. **C)** Interactions between SP and vFLIP directly mimic of those involving NEMO (right panel) and extend to conservation of the NEMO-NEMO dimer interface. This is revealed by superimposition of vFLIP-bound SP and NEMO dimers (left panel).

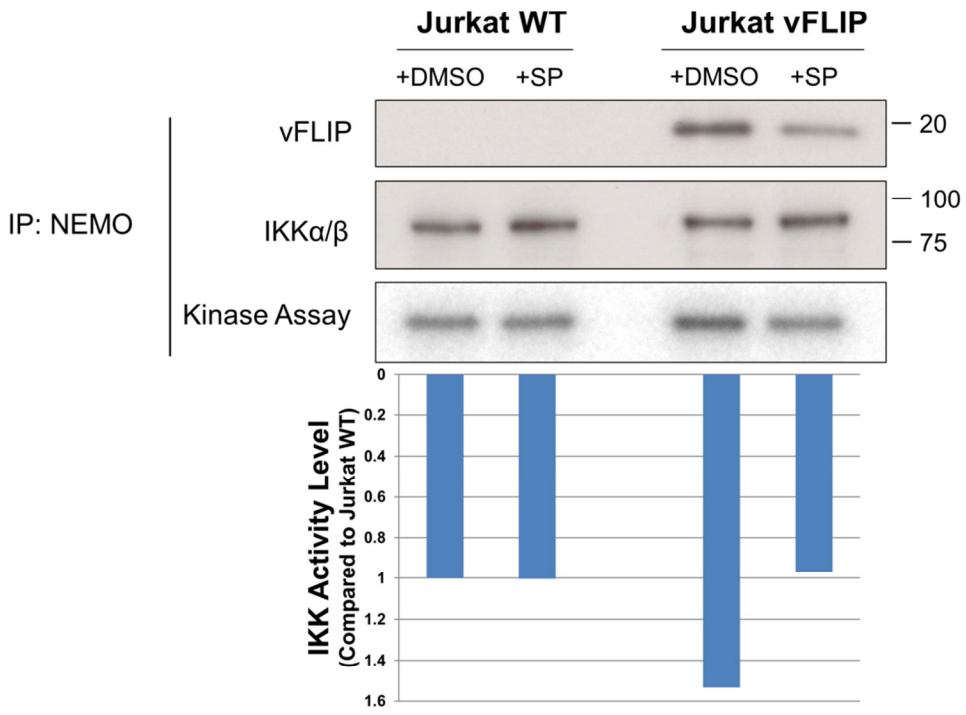

Figure 5.9. The stapled NEMO peptide efficiently inhibits the vFLIP-induced IKK activation by blocking the interaction of vFLIP with NEMO. Cytoplasmic extracts of wild-type or vFLIP-expressing Jurkat cells ($2x10^6$) were prepared and incubated with the staple peptide (SP) or DMSO at 4 °C overnight. Subsequently, IKK complexes were immunoprecipitated using an anti-NEMO antibody (0.5µg/sample) and subjected to an *in vitro* kinase assay as described previously. The same membrane was immunoblotted using the indicated antibodies to assess the vFLIP-NEMO interactions and to ensure of equal protein loading. The relative activities of the IKK complex are expressed as the intensity of the pGST-IκBα band, normalised to the levels of IKK complex as detected by the anti-IKKα/β antibody.

5.4 Summary

The results in this chapter suggest a possible mechanism for vFLIP activation of IKK. We propose that vFLIP binding to NEMO causes oligomerisation of IKK complexes leading to trans-autophosphorylation of the kinase subunits and activation. This is not implausible as direct activation of IKK by addition of free ubiquitin chains has been reported, which could reflect a similar mechanism (Xia et al., 2009). A recent study demonstrates that TAK1 phosphorylation of S177 primes IKK for trans-autophosphorylation on S181 in the T-loop (Zhang et al., 2014). Further analysis will be necessary to determine whether vFLIP activation causes both S177 and S181 phosphorylation.

There is also a wealth of further information that can be obtained from using the *in vitro* activation system where recombinant vFLIP can be added to purified IKK. A more suitable purification system for the kinase would involve a cleavable tag, and the kinase purity could then be established using Mass Spectrometry. Some specificity analyses using vFLIP and NEMO mutants are necessary. It will also be possible to measure the rate of activation, the conditions required for activation (pH, temperature, ionic composition) and also whether the stapled peptide can reverse vFLIP activation of purified IKK. One might predict that the latter will not occur rapidly if the kinase is sufficiently pure as a phosphatase will be required. As stated in the introduction it may be possible eventually to reconstitute a recombinant kinase of IKKα/β, NEMO and HSP90 and then examine activation by recombinant vFLIP.

Finally, the demonstration that the vFLIP-NEMO interaction can be inhibited by a stapled peptide is an encouraging start to the development of a therapy for Kaposi's sarcoma. The next steps will be to examine whether the existing peptide is cell permeable, and if so whether it reduces the viability of KS transformed B cell lines.

CHAPTER

6

CONCLUSIONS AND FUTURE PERSPECTIVES

6.1 Insight into vFLIP activation of IKK

My experiments demonstrated that vFLIP activation of IKK does not require the upstream kinases TAK1 or MEKK3. This led to the hypothesis that vFLIP binding to NEMO might cause a conformational change in the kinase complex leading to intramolecular autophosphorylation of the IKKα/β subunits. We then collaborated with Dr. Tracey Barrett and Prof. Chris Kay to solve the solution structure of NEMO, in the absence or presence of vFLIP, by electron paramagnetic resonance (EPR) (manuscript submitted). This showed that NEMO remains a parallel alpha-helical coiled-coil when vFLIP binds, with vFLIP causing only local perturbation in the structure. Polley et al., then published a structure for human IKKβ, which showed that this kinase subunit of IKK can form oligomers in the crystal and in solution (Polley et al., 2013). They demonstrated the presence of kinase domain interactions within these oligomers, that were important both for phosphorylation of the activation loop *in trans*, and kinase activation (Polley et al., 2013). This led Dr. Tracey Barrett to revisit the X-ray diffraction data from the vFLIP/NEMO crystals. She found signals corresponding to vFLIP-vFLIP interactions, causing oligomerisation of the vFLIP-NEMO complexes. The parallel configuration of these oligomers could bring IKKα/β subunits into proximity similar to that detected by Polley et al, which could lead to intermolecular activation by phosphorylation of the activation loop *in trans*. My preliminary data shows that mutation of residues that are involved in the vFLIP-vFLIP interactions inhibits vFLIP activation of IKK *in vivo*.

This provides a logical new hypothesis to be further tested. Previous work from our lab and others showed that IKK was detected in cell lysate as a high molecular weight complex by gel filtration (Field et al., 2003). Our lab showed that vFLIP is incorporated in a saturable manner into this complex and that vFLIP does not change the size of the complex (Field et al., 2003). When vFLIP was immunoprecipitated and the proteins in the IP were identified we found only vFLIP, IKKα, β and γ and HSP90 (Field et al., 2003). While these experiments were not quantitative, similar amounts of the five proteins were detected. Therefore it seems logical that IKK exists as a multimer: perhaps some level of intermolecular activation by autophosphorylation occurs in the basal state, accounting for its basal activity. When vFLIP is incorporated into this multimer it brings at least some of the IKK subunits into an optimal configuration for intermolecular activation by phosphorylation of the activation loop *in trans*.

To further test this hypothesis I intend to further analyse vFLIP mutants in the predicted dimerisation surfaces for their ability to dimerise, bind to IKK and activate IKK *in vitro* and *in vivo*. I can also analyse the IKKβ dimerisation mutants reported by Polley et al., for their ability to respond to vFLIP. These data may also be extended to HTLV-1 Tax. While purification of recombinant Tax has not been possible, I have demonstrated that Tax does not require TAK1 or MEKK3 to activate IKK and that it can act on an N-terminal fragment of NEMO. Tax dimerisation has been reported (Fryrear et al., 2009; Jin and Jeang, 1997; Tie et al., 1996) and it would therefore be interesting to examine Tax dimerisation mutants for their ability to activate IKK. Finally, in the long term, it would be of great value to reconstitute a recombinant IKK that can respond to vFLIP.

6.2 Insight into cFLIP activation of IKK

It has been reported that a proteolytic fragment of both $cFLIP_L$ and $cFLIP_S$, p22-cFLIP, could bind directly to NEMO and activate IKK (Golks et al., 2006). Indeed when our lab, with collaborators, published the crystal structure of vFLIP bound to NEMO they proposed that p22-cFLIP might bind to the same site (Bagnéris et al., 2008). My experiments showed a different and complex mechanism of activation of IKK by cFLIP family members. One common feature between all of them was that they required ubiquitin recognition by the ubiquitin-binding domain of NEMO and also the upstream kinase TAK1.

Activation of IKK by overexpression of $cFLIP_L$ required the linear ubiquitination complex LUBAC. This is a similar mechanism in essence to that utilised by TLRs and cytokines (Emmerich et al., 2013; Gerlach et al., 2011; Sasaki et al., 2013). The recent publication of Fujita et al suggests that LUBAC interacts specifically with NEMO, leading to NEMO's linear ubiquitination (Fujita et al., 2014). It has not yet been established how this leads to TAK1 activation of IKK in molecular terms, though ubiquitin chains can directly activate TAK1 (Xia et al., 2009). I found that the activity of IKK immunoprecipitated from TNF-treated cells appeared higher than that of vFLIP expressing cells (Figure 3.5A). Perhaps the LUBAC/TAK1 activation pathway results in transient phosphorylation of all the IKK enzymes with the high molecular weight multimer, whereas vFLIP does not?

In the case of $cFLIP_S$ and p22-cFLIP I found a novel activation mechanism of IKK, involving a FLIP/FADD/RIP1 complex. One question that remains is whether these FLIP variants cause ubiquitination of RIP1, and if so, by what mechanism? I will start to address this by immunoprecipitating RIP1 (as in Figure 4.3) and immunoblotting with antibodies against K63 and linear ubiquitin linkages. If this is the case then it provides an explanation for why cFLIPs and p22-cFLIP cause activation of IKK via ubiquitin recognition by the ubiquitin-binding domain of NEMO, but again does not address how TAK1 is recruited. Note that I also found that the activity of IKK immunoprecipitated from p22-FLIP expressing cells appeared higher than that of vFLIP expressing cells (Figure 3.5A), again suggesting more optimal phosphorylation of the IKKα/β activation loop.

RIP1 is a kinase which forms filamentous structures, together with RIP3 kinase, which are involved in TNF-induced cell necroptosis (He et al., 2009; Zhang et al., 2009a). However, a soluble complex between the recombinant death domains of FADD and RIP1 has also been prepared (Park et al., 2013). Presumably $cFLIP_S$ and p22-cFLIP could interact with FADD via DED homotypic interactions, perhaps in a trimeric complex with RIP1. Further mutational analysis of the three proteins could be used to determine whether this is the case. It could also be possible to prepare a recombinant RIP1/FADD/cFLIP complex which could be ubiquitinated then used to activate IKK in cell lysate. This might provide a physiological *in vitro* method of ubiquitin-dependent IKK activation.

6.3 Therapeutic importance of our findings in viral and non-viral tumours

The expression of cFLIP proteins is tightly regulated in normal cells. At the transcriptional level cFLIP isoforms are upregulated by NF-κB activation, so they positively regulate their own expression (Kreuz and Siegmund, 2001; Micheau et al., 2001). $cFLIP_S$ is particularly more prone to ubiquitination and displays a considerably shorter half-life compared to $cFLIP_L$ (Poukkula et al., 2005); the stability of $cFLIP_R$ is similar to $cFLIP_S$ (Golks et al., 2005). p22-FLIP is more stable than $cFLIP_S$ as it lacks this C-terminal sequence (Golks et al., 2006). By using over-expression of cFLIP in our experiments we have over-ridden some of these control mechanisms, there is however evidence for overexpression of cFLIP isoforms in tumour cells (See 1.3.7), which is the situation that we have mimicked.

Upregulation of cFLIP expression has been reported in many types of human solid tumours and lymphomas, and there is evidence that the level of cFLIP may determine clinical outcome (Ullenhag et al., 2007; Valente et al., 2006; Valnet-Rabier et al., 2005). cFLIP inhibition or down-regulation has therefore been proposed as a potential cancer therapy, with the assumption that this will operate by sensitising tumour cells to Fas, TRAIL- or TNF-induced cell death [reviewed in (Safa and Pollok, 2011)]. However, tumour cells may also be dependent on cFLIP activation of NF-κB for their survival (DiDonato et al., 2012; Karin et al., 2002). Indeed, it is now well-established that the tumourigenic capacity of the KSHV substantially relies on the vFLIP-mediated constitutive activation of IKK, leading to upregulation of NF-κB-dependent survival genes (Ballon et al., 2011; Guasparri et al., 2004; Keller et al., 2006).

Accumulating evidence indicate that in different malignancies, different cFLIP isoforms are overexpressed [reviewed in (Shirley and Micheau, 2010)]. While, for example, $cFLIP_L$ is mainly upregulated in B-cell chronic lymphocytic leukaemia (B-CLL), tissue samples from lung adenocarcinoma patients show increased levels of $cFLIP_S$, but not $cFLIP_L$ (MacFarlane et al., 2002; Olsson et al., 2001; Salon et al., 2006). Hence, understanding the isoform-specific mechanism of action of the FLIP proteins is critical for designing novel targeted therapeutics against the associated tumours.

Specific inhibitors of IKK (In particular IKKβ) that can selectivity block NF-κB activation are being developed by multiple pharmaceutical companies (Karin et al., 2004). However, due to global effects of the NF-κB pathway in cellular functions, the clinical utility of such therapeutic agents is likely to be limited by their potential toxicity. For instance, *in vivo* administration of ML120B, a small molecule selective inhibitor of IKKβ, resulted in a rapid depletion of T and B cells (Nagashima et al., 2006). Taken together, therefore, we believe that our dissection of the different mechanisms of NF-κB activation by cFLIP variants and KSHV vFLIP (Figure 6.1) will allow the development of reagents to inhibit these pathways selectively and thereby assess their role in FLIP-driven tumourigenesis.

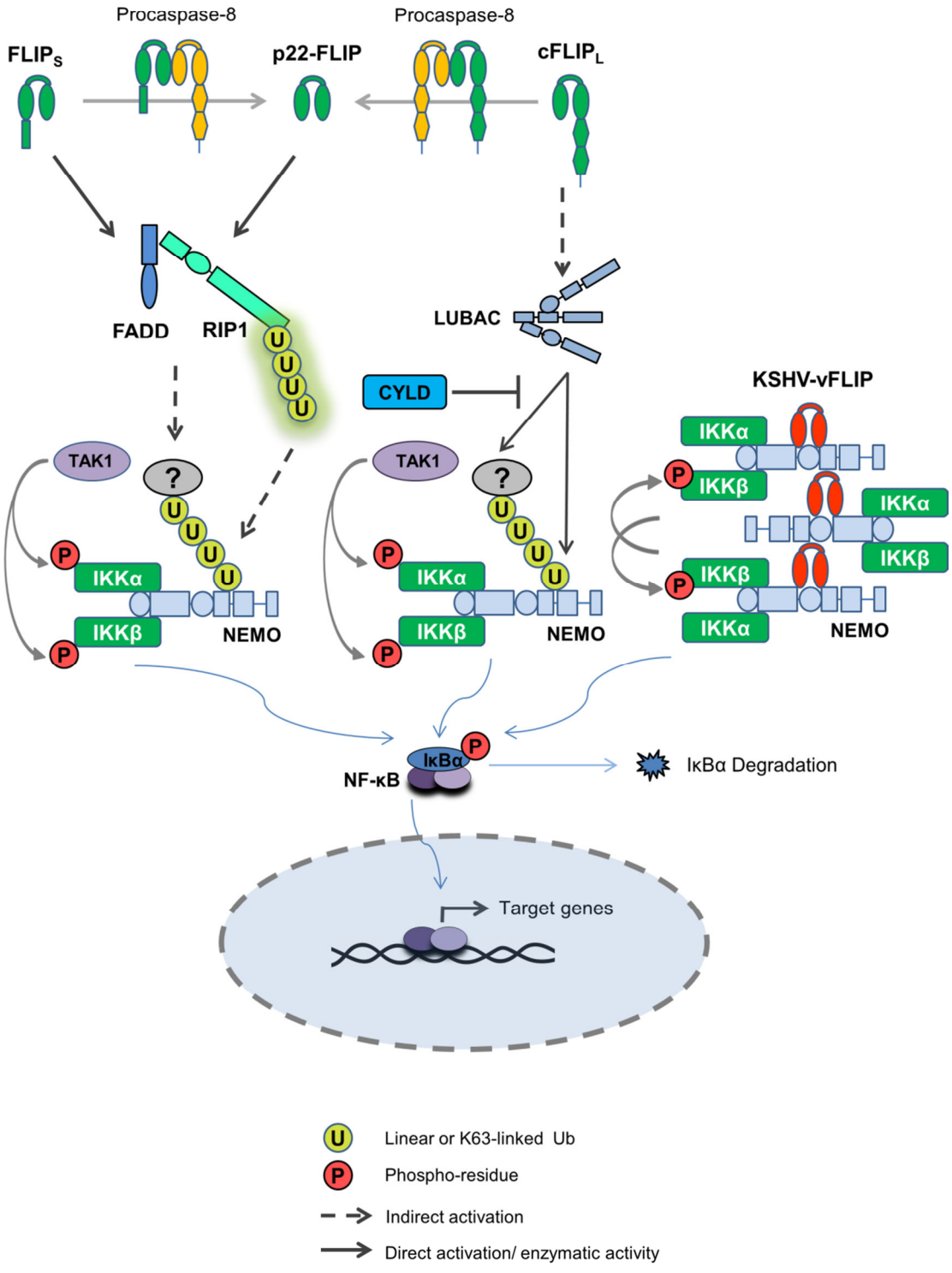

Figure 6.1. Our working model of IKK activation by the KSHV vFLIP and cellular FLIPs. All cFLIP isoforms critically depend on UBAN domain of NEMO and the IKK-activating enzyme, TAK1 for their activation of IKK. p22-FLIP can be generated by procaspase-8 cleavage of both $cFLIP_L$ and $cFLIP_S$ isoforms. The short variants of cFLIP,

$cFLIP_S$ and p22-FLIP, associate with a preformed RIP1/FADD complex to signal to IKK. It is possible that RIP1-bound non-degradative polyubiquitin chains connect these cFLIP variants to UBAN domain of NEMO. Alternatively, the RIP1/FADD/cFLIP complexes may recruit E3 ligases which can then ubiquitinate NEMO or another unidentified protein that is capable of binding to and activating the NEMO UBAN. In contrast to short variants, $cFLIP_L$-mediated activation of IKK depends on LUBAC and can be inhibited by the activity of the deubiquitinase, CYLD. KSHV vFLIP, unlike cellular FLIPs, does not require intermediate signalling components upstream of IKK. Instead, vFLIP-induced activation of IKK is most likely to occur through oligomerisation and re-orientation of IKK complexes, leading to formation of higher order complexes which would allow for trans-autophosphortylation of the catalytic IKKα/β subunits.

BIBLIOGRAPHAY

Ahmad, A., Groshong, J.S., Matta, H., Schamus, S., Punj, V., Robinson, L.J., Gill, P.S., and Chaudhary, P.M. (2010). Kaposi sarcoma-associated herpesvirus-encoded viral FLICE inhibitory protein (vFLIP) K13 cooperates with Myc to promote lymphoma in mice. Cancer Biol. Ther. *10*, 1033–1040.

Al-Muhsen, S., and Casanova, J.-L. (2008). The genetic heterogeneity of mendelian susceptibility to mycobacterial diseases. J. Allergy Clin. Immunol. *122*, 1043–1051; quiz 1052–1053.

Amazit, L., Pasini, L., Szafran, A.T., Berno, V., Wu, R.-C., Mielke, M., Jones, E.D., Mancini, M.G., Hinojos, C.A., O'Malley, B.W., et al. (2007). Regulation of SRC-3 intercompartmental dynamics by estrogen receptor and phosphorylation. Mol. Cell. Biol. *27*, 6913–6932.

An, J., Sun, Y., Sun, R., and Rettig, M.B. (2003). Kaposi's sarcoma-associated herpesvirus encoded vFLIP induces cellular IL-6 expression: the role of the NF-kappaB and JNK/AP1 pathways. Oncogene *22*, 3371–3385.

Arce, F., Rowe, H.M., Chain, B., Lopes, L., and Collins, M.K. (2009). Lentiviral vectors transduce proliferating dendritic cell precursors leading to persistent antigen presentation and immunization. Mol. Ther. *17*, 1643–1650.

Arsenescu, R., Bruno, M.E.C., Rogier, E.W., Stefka, A.T., McMahan, A.E., Wright, T.B., Nasser, M.S., de Villiers, W.J.S., and Kaetzel, C.S. (2008). Signature biomarkers in Crohn's disease: toward a molecular classification. Mucosal Immunol. *1*, 399–411.

Arthur, J.S.C., and Ley, S.C. (2013). Mitogen-activated protein kinases in innate immunity. Nat. Rev. Immunol. *13*, 679–692.

Bagnéris, C., Ageichik, A. V, Cronin, N., Wallace, B., Collins, M., Boshoff, C., Waksman, G., and Barrett, T. (2008). Crystal structure of a vFlip-IKKgamma complex: insights into viral activation of the IKK signalosome. Mol. Cell *30*, 620–631.

Bagnoli, M., Ambrogi, F., Pilotti, S., Alberti, P., Ditto, A., Barbareschi, M., Galligioni, E., Biganzoli, E., Canevari, S., and Mezzanzanica, D. (2009). c-FLIPL expression defines two ovarian cancer patient subsets and is a prognostic factor of adverse outcome. Endocr. Relat. Cancer *16*, 443–453.

Bagnoli, M., Canevari, S., and Mezzanzanica, D. (2010). Cellular FLICE-inhibitory protein (c-FLIP) signalling: a key regulator of receptor-mediated apoptosis in physiologic context and in cancer. Int. J. Biochem. Cell Biol. *42*, 210–213.

Ballard, D.W., Böhnlein, E., Lowenthal, J.W., Wano, Y., Franza, B.R., and Greene, W.C. (1988). HTLV-I tax induces cellular proteins that activate the kappa B element in the IL-2 receptor alpha gene. Science *241*, 1652–1655.

Ballon, G., Chen, K., and Perez, R. (2011). Kaposi sarcoma herpesvirus (KSHV) vFLIP oncoprotein induces B cell transdifferentiation and tumorigenesis in mice. J. Clin. ….

Baud, V., and Karin, M. (2009). Is NF-kappaB a good target for cancer therapy? Hopes and pitfalls. Nat. Rev. Drug Discov. *8*, 33–40.

Behrends, C., and Harper, J.W. (2011). Constructing and decoding unconventional ubiquitin chains. Nat. Struct. Mol. Biol. *18*, 520–528.

Bélanger, C., Gravel, A., Tomoiu, A., Janelle, M.E., Gosselin, J., Tremblay, M.J., and Flamand, L. (2001). Human herpesvirus 8 viral FLICE-inhibitory protein inhibits Fas-mediated apoptosis through binding and prevention of procaspase-8 maturation. J. Hum. Virol. *4*, 62–73.

Berlin, A.L., Paller, A.S., and Chan, L.S. (2002). Incontinentia pigmenti: A review and update on the molecular basis of pathophysiology. J. Am. Acad. Dermatol. *47*, 169–190.

Bernal, F., and Katz, S.G. (2014). Synthesis of stabilized alpha-helical peptides. Methods Mol. Biol. *1176*, 107–114.

Bernassola, F., Karin, M., Ciechanover, A., and Melino, G. (2008). The HECT Family of E3 Ubiquitin Ligases: Multiple Players in Cancer Development. Cancer Cell *14*, 10–21.

Bertin, J., Armstrong, R.C., Ottilie, S., Martin, D. a, Wang, Y., Banks, S., Wang, G.H., Senkevich, T.G., Alnemri, E.S., Moss, B., et al. (1997). Death effector domain-containing herpesvirus and poxvirus proteins inhibit both Fas- and TNFR1-induced apoptosis. Proc. Natl. Acad. Sci. U. S. A. *94*, 1172–1176.

Bertrand, M.J.M., Milutinovic, S., Dickson, K.M., Ho, W.C., Boudreault, A., Durkin, J., Gillard, J.W., Jaquith, J.B., Morris, S.J., and Barker, P. a (2008). cIAP1 and cIAP2 facilitate cancer cell survival by functioning as E3 ligases that promote RIP1 ubiquitination. Mol. Cell *30*, 689–700.

Besse, A., Lamothe, B., Campos, A.D., Webster, W.K., Maddineni, U., Lin, S.-C., Wu, H., and Darnay, B.G. (2007). TAK1-dependent signaling requires functional interaction with TAB2/TAB3. J. Biol. Chem. *282*, 3918–3928.

Bhoj, V.G., and Chen, Z.J. (2009). Ubiquitylation in innate and adaptive immunity. Nature *458*, 430–437.

Bignell, G.R., Warren, W., Seal, S., Takahashi, M., Rapley, E., Barfoot, R., Green, H., Brown, C., Biggs, P.J., Lakhani, S.R., et al. (2000). Identification of the familial cylindromatosis tumour-suppressor gene. Nat. Genet. *25*, 160–165.

Biton, S., and Ashkenazi, A. (2011). NEMO and RIP1 control cell fate in response to extensive DNA damage via TNF-α feedforward signaling. Cell *145*, 92–103.

Blonska, M., Shambharkar, P.B., Kobayashi, M., Zhang, D., Sakurai, H., Su, B., and Lin, X. (2005). TAK1 is recruited to the tumor necrosis factor-alpha (TNF-alpha) receptor 1 complex in a receptor-interacting protein (RIP)-dependent manner and cooperates with MEKK3 leading to NF-kappaB activation. J. Biol. Chem. *280*, 43056–43063.

Bloor, S., Ryzhakov, G., Wagner, S., Butler, P.J.G., Smith, D.L., Krumbach, R., Dikic, I., and Randow, F. (2008). Signal processing by its coil zipper domain activates IKK gamma. Proc. Natl. Acad. Sci. U. S. A. *105*, 1279–1284.

Boatright, K.M., Deis, C., Denault, J.-B., Sutherlin, D.P., and Salvesen, G.S. (2004). Activation of caspases-8 and -10 by FLIP(L). Biochem. J. *382*, 651–657.

Bonif, M., Meuwis, M.-A., Close, P., Benoit, V., Heyninck, K., Chapelle, J.-P., Bours, V., Merville, M.-P., Piette, J., Beyaert, R., et al. (2006). TNFalpha- and IKKbeta-mediated TANK/I-TRAF phosphorylation: implications for interaction with NEMO/IKKgamma and NF-kappaB activation. Biochem. J. *394*, 593–603.

Bonizzi, G., and Karin, M. (2004). The two NF-kappaB activation pathways and their role in innate and adaptive immunity. Trends Immunol. *25*, 280–288.

Borrelli, S., Candi, E., Alotto, D., Castagnoli, C., Melino, G., Viganò, M. a, and Mantovani, R. (2009). p63 regulates the caspase-8-FLIP apoptotic pathway in epidermis. Cell Death Differ. *16*, 253–263.

Bosanac, I., Wertz, I.E., Pan, B., Yu, C., Kusam, S., Lam, C., Phu, L., Phung, Q., Maurer, B., Arnott, D., et al. (2010). Ubiquitin binding to A20 ZnF4 is required for modulation of NF-κB signaling. Mol. Cell *40*, 548–557.

Boxus, M., Twizere, J.-C., Legros, S., Dewulf, J.-F., Kettmann, R., and Willems, L. (2008). The HTLV-1 Tax interactome. Retrovirology *5*, 76.

Bracken, C.P., Whitelaw, M.L., and Peet, D.J. (2005). Activity of hypoxia-inducible factor 2alpha is regulated by association with the NF-kappaB essential modulator. J. Biol. Chem. *280*, 14240–14251.

Brechmann, M., Mock, T., Nickles, D., Kiessling, M., Weit, N., Breuer, R., Müller, W., Wabnitz, G., Frey, F., Nicolay, J.P., et al. (2012). A PP4 holoenzyme balances physiological and oncogenic nuclear factor-kappa B signaling in T lymphocytes. Immunity *37*, 697–708.

Bremm, A., Freund, S.M. V, and Komander, D. (2010). Lys11-linked ubiquitin chains adopt compact conformations and are preferentially hydrolyzed by the deubiquitinase Cezanne. Nat. Struct. Mol. Biol. *17*, 939–947.

Broemer, M., Krappmann, D., and Scheidereit, C. (2004). Requirement of Hsp90 activity for IkappaB kinase (IKK) biosynthesis and for constitutive and inducible IKK and NF-kappaB activation. Oncogene *23*, 5378–5386.

Bruey, J.M., Bruey-Sedano, N., Newman, R., Chandler, S., Stehlik, C., and Reed, J.C. (2004). PAN1/NALP2/PYPAF2, an inducible inflammatory mediator that regulates NF-kappaB and caspase-1 activation in macrophages. J. Biol. Chem. *279*, 51897–51907.

Brummelkamp, T.R., Nijman, S.M.B., Dirac, A.M.G., and Bernards, R. (2003). Loss of the cylindromatosis tumour suppressor inhibits apoptosis by activating NF-kappaB. Nature *424*, 797–801.

Budd, R.C., Yeh, W.-C., and Tschopp, J. (2006). cFLIP regulation of lymphocyte activation and development. Nat. Rev. Immunol. *6*, 196–204.

Cadwell, K., and Coscoy, L. (2005). Ubiquitination on nonlysine residues by a viral E3 ubiquitin ligase. Science *309*, 127–130.

Cao, Y., Bonizzi, G., Seagroves, T.N., Greten, F.R., Johnson, R., Schmidt, E. V, and Karin, M. (2001). IKKalpha provides an essential link between RANK signaling and cyclin D1 expression during mammary gland development. Cell *107*, 763–775.

Carter, R.S., Geyer, B.C., Xie, M., Acevedo-Suárez, C. a, and Ballard, D.W. (2001). Persistent activation of NF-kappa B by the tax transforming protein involves chronic phosphorylation of IkappaB kinase subunits IKKbeta and IKKgamma. J. Biol. Chem. *276*, 24445–24448.

Carter, R.S., Pennington, K.N., Ungurait, B.J., and Ballard, D.W. (2003). In vivo identification of inducible phosphoacceptors in the IKKgamma/NEMO subunit of human IkappaB kinase. J. Biol. Chem. *278*, 19642–19648.

Carter, R.S., Pennington, K.N., Arrate, P., Oltz, E.M., and Ballard, D.W. (2005). Site-specific monoubiquitination of IkappaB kinase IKKbeta regulates its phosphorylation and persistent activation. J. Biol. Chem. *280*, 43272–43279.

Cesarman, E. (2014). Gammaherpesviruses and Lymphoproliferative Disorders. Annu. Rev. Pathol. Mech. Dis. *9*, 349–372.

Chang, L., Kamata, H., Solinas, G., Luo, J.-L., Maeda, S., Venuprasad, K., Liu, Y.-C., and Karin, M. (2006). The E3 ubiquitin ligase itch couples JNK activation to TNFalpha-induced cell death by inducing c-FLIP(L) turnover. Cell *124*, 601–613.

Chapman, M. a, Lawrence, M.S., Keats, J.J., Cibulskis, K., Sougnez, C., Schinzel, A.C., Harview, C.L., Brunet, J.-P., Ahmann, G.J., Adli, M., et al. (2011). Initial genome sequencing and analysis of multiple myeloma. Nature *471*, 467–472.

Chariot, A., Leonardi, A., Muller, J., Bonif, M., Brown, K., and Siebenlist, U. (2002). Association of the adaptor TANK with the I kappa B kinase (IKK) regulator NEMO connects IKK complexes with IKK epsilon and TBK1 kinases. J. Biol. Chem. *277*, 37029–37036.

Chaudhary, P.M., Jasmin, a, Eby, M.T., and Hood, L. (1999). Modulation of the NF-kappa B pathway by virally encoded death effector domains-containing proteins. Oncogene *18*, 5738–5746.

Chaudhary, P.M., Eby, M.T., Jasmin, A., Kumar, A., Liu, L., and Hood, L. (2000). Activation of the NF-kappaB pathway by caspase 8 and its homologs. Oncogene *19*, 4451–4460.

Chen, Z.J. (2012). Ubiquitination in signaling to and activation of IKK. Immunol. Rev. *246*, 95–106.

Chen, G., Cao, P., and Goeddel, D. V (2002). TNF-induced recruitment and activation of the IKK complex require Cdc37 and Hsp90. Mol. Cell *9*, 401–410.

Chen, Z.J., Bhoj, V., and Seth, R.B. (2006). Ubiquitin, TAK1 and IKK: is there a connection? Cell Death Differ. *13*, 687–692.

Chew, J., Biswas, S., Shreeram, S., Humaidi, M., Wong, E.T., Dhillion, M.K., Teo, H., Hazra, A., Fang, C.C., López-Collazo, E., et al. (2009). WIP1 phosphatase is a negative regulator of NF-kappaB signalling. Nat. Cell Biol. *11*, 659–666.

Cho, U.S., and Xu, W. (2007). Crystal structure of a protein phosphatase 2A heterotrimeric holoenzyme. Nature *445*, 53–57.

Cho, Y.S., Challa, S., Moquin, D., Genga, R., Ray, T.D., Guildford, M., and Chan, F.K.-M. (2009). Phosphorylation-driven assembly of the RIP1-RIP3 complex regulates programmed necrosis and virus-induced inflammation. Cell *137*, 1112–1123.

Choi, J., Nannenga, B., Demidov, O.N., Bulavin, D. V, Cooney, A., Brayton, C., Zhang, Y., Mbawuike, I.N., Bradley, A., Appella, E., et al. (2002). Mice deficient for the wild-type p53-induced phosphatase gene (Wip1) exhibit defects in reproductive organs, immune function, and cell cycle control. Mol. Cell. Biol. *22*, 1094–1105.

Chowdhury, D., Xu, X., Zhong, X., Ahmed, F., Zhong, J., Liao, J., Dykxhoorn, D.M., Weinstock, D.M., Pfeifer, G.P., and Lieberman, J. (2008). A PP4-phosphatase complex dephosphorylates gamma-H2AX generated during DNA replication. Mol. Cell *31*, 33–46.

Chu, Z.L., Shin, Y.A., Yang, J.M., DiDonato, J. a., and Ballard, D.W. (1999). IKKgamma mediates the interaction of cellular IkappaB kinases with the tax transforming protein of human T cell leukemia virus type 1. J. Biol. Chem. *274*, 15297–15300.

Chugh, P., Matta, H., Schamus, S., Zachariah, S., Kumar, A., Richardson, J. a, Smith, A.L., and Chaudhary, P.M. (2005). Constitutive NF-kappaB activation, normal Fas-induced apoptosis, and increased incidence of lymphoma in human herpes virus 8 K13 transgenic mice. Proc. Natl. Acad. Sci. U. S. A. *102*, 12885–12890.

Ciechanover, A., Elias, S., Heller, H., and Hershko, A. (1982). "Covalent affinity" purification of ubiquitin-activating enzyme. J. Biol. Chem. *257*, 2537–2542.

Clark, K., Nanda, S., and Cohen, P. (2013). Molecular control of the NEMO family of ubiquitin-binding proteins. Nat. Rev. Mol. Cell Biol. *14*, 673–685.

Cordier, F., Vinolo, E., Véron, M., Delepierre, M., and Agou, F. (2008). Solution structure of NEMO zinc finger and impact of an anhidrotic ectodermal dysplasia with immunodeficiency-related point mutation. J. Mol. Biol. *377*, 1419–1432.

Delhase, M. (1999). Positive and Negative Regulation of IB Kinase Activity Through IKK Subunit Phosphorylation. Science (80-.). *284*, 309–313.

Demaison, C., Parsley, K., Brouns, G., Scherr, M., Battmer, K., Kinnon, C., Grez, M., and Thrasher, A.J. (2002). High-level transduction and gene expression in hematopoietic repopulating cells using a human immunodeficiency [correction of imunodeficiency] virus type 1-based lentiviral vector containing an internal spleen focus forming virus promoter. Hum. Gene Ther. *13*, 803–813.

Deng, L., Wang, C., Spencer, E., Yang, L., Braun, A., You, J., Slaughter, C., Pickart, C., and Chen, Z.J. (2000). Activation of the IkappaB kinase complex by TRAF6 requires a dimeric ubiquitin-conjugating enzyme complex and a unique polyubiquitin chain. Cell *103*, 351–361.

Deshaies, R.J., and Joazeiro, C.A.P. (2009). RING domain E3 ubiquitin ligases. Annu. Rev. Biochem. *78*, 399–434.

Devin, A., Lin, Y., Yamaoka, S., Li, Z., Karin, M., and Liu Zg (2001). The alpha and beta subunits of IkappaB kinase (IKK) mediate TRAF2-dependent IKK recruitment to

tumor necrosis factor (TNF) receptor 1 in response to TNF. Mol. Cell. Biol. *21*, 3986–3994.

Dhillon, a S., Hagan, S., Rath, O., and Kolch, W. (2007). MAP kinase signalling pathways in cancer. Oncogene *26*, 3279–3290.

DiDonato, J. a, Hayakawa, M., Rothwarf, D.M., Zandi, E., and Karin, M. (1997). A cytokine-responsive IkappaB kinase that activates the transcription factor NF-kappaB. Nature *388*, 548–554.

DiDonato, J. a, Mercurio, F., and Karin, M. (2012). NF-κB and the link between inflammation and cancer. Immunol. Rev. *246*, 379–400.

Dikic, I., Wakatsuki, S., and Walters, K.J. (2009). Ubiquitin-binding domains - from structures to functions. Nat. Rev. Mol. Cell Biol. *10*, 659–671.

Djerbi, M., Darreh-Shori, T., Zhivotovsky, B., and Grandien, a (2001). Characterization of the human FLICE-inhibitory protein locus and comparison of the anti-apoptotic activity of four different flip isoforms. Scand. J. Immunol. *54*, 180–189.

Döffinger, R., Smahi, A., Bessia, C., Geissmann, F., Feinberg, J., Durandy, A., Bodemer, C., Kenwrick, S., Dupuis-Girod, S., Blanche, S., et al. (2001). X-linked anhidrotic ectodermal dysplasia with immunodeficiency is caused by impaired NF-kappaB signaling. Nat. Genet. *27*, 277–285.

Dohrman, A., Kataoka, T., Cuenin, S., Russell, J.Q., Tschopp, J., and Budd, R.C. (2005). Cellular FLIP (long form) regulates CD8+ T cell activation through caspase-8-dependent NF-kappa B activation. J. Immunol. *174*, 5270–5278.

DuBridge, R.B., Tang, P., Hsia, H.C., Leong, P.M., Miller, J.H., and Calos, M.P. (1987). Analysis of mutation in human cells by using an Epstein-Barr virus shuttle system. Mol. Cell. Biol. *7*, 379–387.

Ducut Sigala, J.L., Bottero, V., Young, D.B., Shevchenko, A., Mercurio, F., and Verma, I.M. (2004). Activation of transcription factor NF-kappaB requires ELKS, an IkappaB kinase regulatory subunit. Science *304*, 1963–1967.

Ea, C.-K., Deng, L., Xia, Z.-P., Pineda, G., and Chen, Z.J. (2006). Activation of IKK by TNFalpha requires site-specific ubiquitination of RIP1 and polyubiquitin binding by NEMO. Mol. Cell *22*, 245–257.

Efklidou, S., Bailey, R., Field, N., Noursadeghi, M., and Collins, M.K. (2008). vFLIP from KSHV inhibits anoikis of primary endothelial cells. J. Cell Sci. *121*, 450–457.

Eitelhuber, A.C., Warth, S., Schimmack, G., Düwel, M., Hadian, K., Demski, K., Beisker, W., Shinohara, H., Kurosaki, T., Heissmeyer, V., et al. (2011). Dephosphorylation of Carma1 by PP2A negatively regulates T-cell activation. EMBO J. *30*, 594–605.

El-Gazzar, A., Wittinger, M., Perco, P., Anees, M., Horvat, R., Mikulits, W., Grunt, T.W., Mayer, B., and Krainer, M. (2010). The role of c-FLIP(L) in ovarian cancer: chaperoning tumor cells from immunosurveillance and increasing their invasive potential. Gynecol. Oncol. *117*, 451–459.

Emmerich, C.H., Ordureau, A., Strickson, S., Arthur, J.S.C., Pedrioli, P.G. a, Komander, D., and Cohen, P. (2013). Activation of the canonical IKK complex by K63/M1-linked hybrid ubiquitin chains. Proc. Natl. Acad. Sci. U. S. A. *110*, 15247–15252.

Enesa, K., Zakkar, M., Chaudhury, H., Luong, L.A., Rawlinson, L., Mason, J.C., Haskard, D.O., Dean, J.L.E., and Evans, P.C. (2008). NF-kappaB suppression by the deubiquitinating enzyme Cezanne: a novel negative feedback loop in pro-inflammatory signaling. J. Biol. Chem. *283*, 7036–7045.

Ermolaeva, M.A., Michallet, M.-C., Papadopoulou, N., Utermöhlen, O., Kranidioti, K., Kollias, G., Tschopp, J., and Pasparakis, M. (2008). Function of TRADD in tumor necrosis factor receptor 1 signaling and in TRIF-dependent inflammatory responses. Nat. Immunol. *9*, 1037–1046.

Evans, P.C., Smith, T.S., Lai, M.-J., Williams, M.G., Burke, D.F., Heyninck, K., Kreike, M.M., Beyaert, R., Blundell, T.L., and Kilshaw, P.J. (2003). A novel type of deubiquitinating enzyme. J. Biol. Chem. *278*, 23180–23186.

Evans, P.C., Ovaa, H., Hamon, M., Kilshaw, P.J., Hamm, S., Bauer, S., Ploegh, H.L., and Smith, T.S. (2004). Zinc-finger protein A20, a regulator of inflammation and cell survival, has de-ubiquitinating activity. Biochem. J. *378*, 727–734.

Feoktistova, M., Geserick, P., Kellert, B., Dimitrova, D.P., Langlais, C., Hupe, M., Cain, K., MacFarlane, M., Häcker, G., and Leverkus, M. (2011). cIAPs block Ripoptosome formation, a RIP1/caspase-8 containing intracellular cell death complex differentially regulated by cFLIP isoforms. Mol. Cell *43*, 449–463.

Feoktistova, M., Geserick, P., Panayotova-Dimitrova, D., and Leverkus, M. (2012). Pick your poison: the Ripoptosome, a cell death platform regulating apoptosis and necroptosis. Cell Cycle *11*, 460–467.

Field, N., Low, W., Daniels, M., Howell, S., Daviet, L., Boshoff, C., and Collins, M. (2003). KSHV vFLIP binds to IKK-gamma to activate IKK. J. Cell Sci. *116*, 3721–3728.

Fryrear, K. a, Durkin, S.S., Gupta, S.K., Tiedebohl, J.B., and Semmes, O.J. (2009). Dimerization and a novel Tax speckled structure localization signal are required for Tax nuclear localization. J. Virol. *83*, 5339–5352.

Fu, D.-X., Kuo, Y.-L., Liu, B.-Y., Jeang, K.-T., and Giam, C.-Z. (2003). Human T-lymphotropic virus type I tax activates I-kappa B kinase by inhibiting I-kappa B kinase-associated serine/threonine protein phosphatase 2A. J. Biol. Chem. *278*, 1487–1493.

Fujita, H., Rahighi, S., Akita, M., Kato, R., Sasaki, Y., Wakatsuki, S., and Iwai, K. (2014). Mechanism underlying IκB kinase activation mediated by the linear ubiquitin chain assembly complex. Mol. Cell. Biol. *34*, 1322–1335.

Fukazawa, T., Fujiwara, T., Uno, F., Teraishi, F., Kadowaki, Y., Itoshima, T., Takata, Y., Kagawa, S., Roth, J. a, Tschopp, J., et al. (2001). Accelerated degradation of cellular FLIP protein through the ubiquitin-proteasome pathway in p53-mediated apoptosis of human cancer cells. Oncogene *20*, 5225–5231.

Fung, E.Y.M.G., Smyth, D.J., Howson, J.M.M., Cooper, J.D., Walker, N.M., Stevens, H., Wicker, L.S., and Todd, J.A. (2009). Analysis of 17 autoimmune disease-associated variants in type 1 diabetes identifies 6q23/TNFAIP3 as a susceptibility locus. Genes Immun. *10*, 188–191.

Gatza, M.L., and Marriott, S.J. (2006). Genotoxic stress and cellular stress alter the subcellular distribution of human T-cell leukemia virus type 1 tax through a CRM1-dependent mechanism. J. Virol. *80*, 6657–6668.

Gatza, M.L., Dayaram, T., and Marriott, S.J. (2007). Ubiquitination of HTLV-I Tax in response to DNA damage regulates nuclear complex formation and nuclear export. Retrovirology *4*, 95.

Gerlach, B., Cordier, S.M., Schmukle, A.C., Emmerich, C.H., Rieser, E., Haas, T.L., Webb, A.I., Rickard, J. a, Anderton, H., Wong, W.W.-L., et al. (2011). Linear ubiquitination prevents inflammation and regulates immune signalling. Nature *471*, 591–596.

Geserick, P., Drewniok, C., Hupe, M., Haas, T.L., Diessenbacher, P., Sprick, M.R., Schön, M.P., Henkler, F., Gollnick, H., Walczak, H., et al. (2008). Suppression of cFLIP is sufficient to sensitize human melanoma cells to TRAIL- and CD95L-mediated apoptosis. Oncogene *27*, 3211–3220.

Ghosh, S., and Hayden, M.S. (2008). New regulators of NF-kappaB in inflammation. Nat. Rev. Immunol. *8*, 837–848.

Ghosh, G., Wang, V.Y.-F., Huang, D.-B., and Fusco, A. (2012). NF-κB regulation: lessons from structures. Immunol. Rev. *246*, 36–58.

Ghosh, S., May, M.J., and Kopp, E.B. (1998). NF-kappa B and Rel proteins: evolutionarily conserved mediators of immune responses. Annu. Rev. Immunol. *16*, 225–260.

Gilmore, T.D. (2006). Introduction to NF-kappaB: players, pathways, perspectives. Oncogene *25*, 6680–6684.

Gingras, A.-C., Caballero, M., Zarske, M., Sanchez, A., Hazbun, T.R., Fields, S., Sonenberg, N., Hafen, E., Raught, B., and Aebersold, R. (2005). A novel, evolutionarily conserved protein phosphatase complex involved in cisplatin sensitivity. Mol. Cell. Proteomics *4*, 1725–1740.

Godfrey, A., Anderson, J., Papanastasiou, A., Takeuchi, Y., and Boshoff, C. (2005). Inhibiting primary effusion lymphoma by lentiviral vectors encoding short hairpin RNA. Blood *105*, 2510–2518.

Gohda, J., Irisawa, M., Tanaka, Y., Sato, S., Ohtani, K., Fujisawa, J., and Inoue, J. (2007). HTLV-1 Tax-induced NFkappaB activation is independent of Lys-63-linked-type polyubiquitination. Biochem. Biophys. Res. Commun. *357*, 225–230.

Golks, A., Brenner, D., Fritsch, C., Krammer, P.H., and Lavrik, I.N. (2005). c-FLIPR, a new regulator of death receptor-induced apoptosis. J. Biol. Chem. *280*, 14507–14513.

Golks, A., Brenner, D., Krammer, P.H., and Lavrik, I.N. (2006). The c-FLIP-NH2 terminus (p22-FLIP) induces NF-kappaB activation. J. Exp. Med. *203*, 1295–1305.

Goltsev, Y. V., Kovalenko, A. V, Arnold, E., Varfolomeev, E.E., Brodianskii, V.M., and Wallach, D. (1997). CASH, a novel caspase homologue with death effector domains. J. Biol. Chem. *272*, 19641–19644.

Gordon, J.A. (1991). Use of vanadate as protein-phosphotyrosine phosphatase inhibitor. Methods Enzymol. *201*, 477–482.

Grassmann, R., Dengler, C., Müller-Fleckenstein, I., Fleckenstein, B., McGuire, K., Dokhelar, M.C., Sodroski, J.G., and Haseltine, W.A. (1989). Transformation to continuous growth of primary human T lymphocytes by human T-cell leukemia virus type I X-region genes transduced by a Herpesvirus saimiri vector. Proc. Natl. Acad. Sci. U. S. A. *86*, 3351–3355.

Grassmann, R., Aboud, M., and Jeang, K.-T. (2005). Molecular mechanisms of cellular transformation by HTLV-1 Tax. Oncogene *24*, 5976–5985.

Green, D.R., and Evan, G.I. (2002). A matter of life and death. Cancer Cell *1*, 19–30.

Grunert, M., Gottschalk, K., Kapahnke, J., Gündisch, S., Kieser, A., and Jeremias, I. (2012). The adaptor protein FADD and the initiator caspase-8 mediate activation of NF-κB by TRAIL. Cell Death Dis. *3*, e414.

Guasparri, I., Keller, S. a, and Cesarman, E. (2004). KSHV vFLIP is essential for the survival of infected lymphoma cells. J. Exp. Med. *199*, 993–1003.

Guasparri, I., Wu, H., and Cesarman, E. (2006). The KSHV oncoprotein vFLIP contains a TRAF-interacting motif and requires TRAF2 and TRAF3 for signalling. EMBO Rep. *7*, 114–119.

Guicciardi, M.E., and Gores, G.J. (2009). Life and death by death receptors. FASEB J. *23*, 1625–1637.

Haag, C., Stadel, D., Zhou, S., Bachem, M.G., Möller, P., Debatin, K.-M., and Fulda, S. (2011). Identification of c-FLIP(L) and c-FLIP(S) as critical regulators of death receptor-induced apoptosis in pancreatic cancer cells. Gut *60*, 225–237.

Häcker, H., and Karin, M. (2006). Regulation and function of IKK and IKK-related kinases. Sci. STKE *2006*, re13.

Hadian, K., and Krappmann, D. (2011). Signals from the nucleus: activation of NF-kappaB by cytosolic ATM in the DNA damage response. Sci. Signal. *4*, pe2.

Hadian, K., Griesbach, R. a, Dornauer, S., Wanger, T.M., Nagel, D., Metlitzky, M., Beisker, W., Schmidt-Supprian, M., and Krappmann, D. (2011). NF-κB essential modulator (NEMO) interaction with linear and lys-63 ubiquitin chains contributes to NF-κB activation. J. Biol. Chem. *286*, 26107–26117.

Haglund, K., and Dikic, I. (2005). Ubiquitylation and cell signaling. EMBO J. *24*, 3353–3359.

Han, D.K., Chaudhary, P.M., Wright, M.E., Friedman, C., Trask, B.J., Riedel, R.T., Baskin, D.G., Schwartz, S.M., and Hood, L. (1997). MRIT, a novel death-effector domain-containing protein, interacts with caspases and BclXL and initiates cell death. Proc. Natl. Acad. Sci. U. S. A. *94*, 11333–11338.

Harhaj, E.W., and Dixit, V.M. (2011). Deubiquitinases in the regulation of NF-κB signaling. Cell Res. *21*, 22–39.

Harhaj, E.W., and Sun, S.C. (1999). IKKgamma serves as a docking subunit of the IkappaB kinase (IKK) and mediates interaction of IKK with the human T-cell leukemia virus Tax protein. J. Biol. Chem. *274*, 22911–22914.

Harhaj, E.W., Good, L., Xiao, G., Uhlik, M., Cvijic, M.E., Rivera-Walsh, I., and Sun, S.C. (2000). Somatic mutagenesis studies of NF-kappa B signaling in human T cells: evidence for an essential role of IKK gamma in NF-kappa B activation by T-cell costimulatory signals and HTLV-I Tax protein. Oncogene *19*, 1448–1456.

Hauenstein, A. V, Rogers, W.E., Shaul, J.D., Huang, D., Ghosh, G., and Huxford, T. (2014). Probing kinase activation and substrate specificity with an engineered monomeric IKK2. Biochemistry *53*, 2064–2073.

Hayden, M.S., and Ghosh, S. (2004). Signaling to NF-kappaB. Genes Dev. *18*, 2195–2224.

Hayden, M.S., and Ghosh, S. (2008). Shared principles in NF-kappaB signaling. Cell *132*, 344–362.

He, S., Wang, L., Miao, L., Wang, T., Du, F., Zhao, L., and Wang, X. (2009). Receptor interacting protein kinase-3 determines cellular necrotic response to TNF-alpha. Cell *137*, 1100–1111.

Henn, I.H., Bouman, L., Schlehe, J.S., Schlierf, A., Schramm, J.E., Wegener, E., Nakaso, K., Culmsee, C., Berninger, B., Krappmann, D., et al. (2007). Parkin mediates neuroprotection through activation of IkappaB kinase/nuclear factor-kappaB signaling. J. Neurosci. *27*, 1868–1878.

Hershko, A. (1983). Ubiquitin: roles in protein modification and breakdown. Cell *34*, 11–12.

Hershko, A., and Ciechanover, A. (1998). The ubiquitin system. Annu. Rev. Biochem. *67*, 425–479.

Hershko, A., Heller, H., Elias, S., and Ciechanover, A. (1983). Components of ubiquitin-protein ligase system. Resolution, affinity purification, and role in protein breakdown. J. Biol. Chem. *258*, 8206–8214.

Hicke, L. (2001). Protein regulation by monoubiquitin. Nat. Rev. Mol. Cell Biol. *2*, 195–201.

Hicke, L., Schubert, H.L., and Hill, C.P. (2005). Ubiquitin-binding domains. Nat. Rev. Mol. Cell Biol. *6*, 610–621.

Hinz, M., and Scheidereit, C. (2014). The IκB kinase complex in NF-κB regulation and beyond. EMBO Rep. *15*, 46–61.

Hinz, M., Arslan, S.Ç., and Scheidereit, C. (2012). It takes two to tango: IκBs, the multifunctional partners of NF-κB. Immunol. Rev. *246*, 59–76.

Hoeller, D., Hecker, C.-M., and Dikic, I. (2006). Ubiquitin and ubiquitin-like proteins in cancer pathogenesis. Nat. Rev. Cancer *6*, 776–788.

Hoffmann, a, Natoli, G., and Ghosh, G. (2006). Transcriptional regulation via the NF-kappaB signaling module. Oncogene *25*, 6706–6716.

Hong, S., Wang, L.-C., Gao, X., Kuo, Y.-L., Liu, B., Merling, R., Kung, H.-J., Shih, H.-M., and Giam, C.-Z. (2007). Heptad repeats regulate protein phosphatase 2a recruitment to I-kappaB kinase gamma/NF-kappaB essential modulator and are targeted by human T-lymphotropic virus type 1 tax. J. Biol. Chem. *282*, 12119–12126.

Hong, X., Xu, L.-G., Li, X., Zhai, Z., and Shu, H.-B. (2001). CSN3 interacts with IKKgamma and inhibits TNF- but not IL-1-induced NF-kappaB activation. FEBS Lett. *499*, 133–136.

Honma, K., Tsuzuki, S., Nakagawa, M., Tagawa, H., Nakamura, S., Morishima, Y., and Seto, M. (2009). TNFAIP3/A20 functions as a novel tumor suppressor gene in several subtypes of non-Hodgkin lymphomas. Blood *114*, 2467–2475.

Hsu, H., Xiong, J., and Goeddel, D. V (1995). The TNF receptor 1-associated protein TRADD signals cell death and NF-kappa B activation. Cell *81*, 495–504.

Hsu, H., Huang, J., Shu, H.-B., Baichwal, V., and Goeddel, D. V (1996a). TNF-Dependent Recruitment of the Protein Kinase RIP to the TNF Receptor-1 Signaling Complex. Immunity *4*, 387–396.

Hsu, H., Shu, H.B., Pan, M.G., and Goeddel, D. V. (1996b). TRADD-TRAF2 and TRADD-FADD interactions define two distinct TNF receptor 1 signal transduction pathways. Cell *84*, 299–308.

Hu, S., Vincenz, C., Buller, M., and Dixit, V.M. (1997a). A novel family of viral death effector domain-containing molecules that inhibit both CD-95- and tumor necrosis factor receptor-1-induced apoptosis. J. Biol. Chem. *272*, 9621–9624.

Hu, S., Vincenz, C., Ni, J., Gentz, R., and Dixit, V.M. (1997b). I-FLICE, a novel inhibitor of tumor necrosis factor receptor-1- and CD-95-induced apoptosis. J. Biol. Chem. *272*, 17255–17257.

Hu, W.H., Johnson, H., and Shu, H.B. (2000). Activation of NF-kappaB by FADD, Casper, and caspase-8. J. Biol. Chem. *275*, 10838–10844.

Huang, J., Teng, L., Li, L., Liu, T., Li, L., Chen, D., Xu, L.-G., Zhai, Z., and Shu, H.-B. (2004a). ZNF216 Is an A20-like and IkappaB kinase gamma-interacting inhibitor of NFkappaB activation. J. Biol. Chem. *279*, 16847–16853.

Huang, Q., Yang, J., Lin, Y., Walker, C., Cheng, J., Liu, Z., and Su, B. (2004b). Differential regulation of interleukin 1 receptor and Toll-like receptor signaling by MEKK3. Nat. Immunol. *5*, 98–103.

Huang, T.T., Wuerzberger-Davis, S.M., Wu, Z.-H., and Miyamoto, S. (2003). Sequential modification of NEMO/IKKgamma by SUMO-1 and ubiquitin mediates NF-kappaB activation by genotoxic stress. Cell *115*, 565–576.

Hubeau, M., Ngadjeua, F., Puel, A., Israel, L., Feinberg, J., Chrabieh, M., Belani, K., Bodemer, C., Fabre, I., Plebani, A., et al. (2011). New mechanism of X-linked anhidrotic ectodermal dysplasia with immunodeficiency: impairment of ubiquitin binding despite normal folding of NEMO protein. Blood *118*, 926–935.

Huxford, T., Hoffmann, A., and Ghosh, G. (2011). Understanding the logic of IκB:NF-κB regulation in structural terms. Curr. Top. Microbiol. Immunol. *349*, 1–24.

Ikeda, F., Deribe, Y.L., Skånland, S.S., Stieglitz, B., Grabbe, C., Franz-Wachtel, M., van Wijk, S.J.L., Goswami, P., Nagy, V., Terzic, J., et al. (2011). SHARPIN forms a linear ubiquitin ligase complex regulating NF-κB activity and apoptosis. Nature *471*, 637–641.

Imamura, R., Konaka, K., Matsumoto, N., Hasegawa, M., Fukui, M., Mukaida, N., Kinoshita, T., and Suda, T. (2004). Fas ligand induces cell-autonomous NF-kappaB activation and interleukin-8 production by a mechanism distinct from that of tumor necrosis factor-alpha. J. Biol. Chem. *279*, 46415–46423.

Inohara, N., Koseki, T., Hu, Y., Chen, S., and Núñez, G. (1997). CLARP, a death effector domain-containing protein interacts with caspase-8 and regulates apoptosis. Proc. Natl. Acad. Sci. U. S. A. *94*, 10717–10722.

Irmler, M., Thome, M., Hahne, M., Schneider, P., Hofmann, K., Steiner, V., Bodmer, J.L., Schröter, M., Burns, K., Mattmann, C., et al. (1997). Inhibition of death receptor signals by cellular FLIP. Nature *388*, 190–195.

Ishitani, T., Takaesu, G., Ninomiya-Tsuji, J., Shibuya, H., Gaynor, R.B., and Matsumoto, K. (2003). Role of the TAB2-related protein TAB3 in IL-1 and TNF signaling. EMBO J. *22*, 6277–6288.

Israël, A. (2010). The IKK complex, a central regulator of NF-kappaB activation. Cold Spring Harb. Perspect. Biol. *2*, a000158.

Iwai, K., and Tokunaga, F. (2009). Linear polyubiquitination: a new regulator of NF-kappaB activation. EMBO Rep. *10*, 706–713.

Iwai, K., Fujita, H., and Sasaki, Y. (2014). Linear ubiquitin chains: NF-κB signalling, cell death and beyond. Nat. Rev. Mol. Cell Biol. *15*, 503–508.

Jacobsen, H., Klenow, H., and Overgaard-Hansen, K. (1974). The N-terminal amino-acid sequences of DNA polymerase I from Escherichia coli and of the large and the small fragments obtained by a limited proteolysis. Eur. J. Biochem. *45*, 623–627.

Janssens, V., and Goris, J. (2001). Protein phosphatase 2A: a highly regulated family of serine/threonine phosphatases implicated in cell growth and signalling. Biochem. J. *353*, 417–439.

Janssens, S., Tinel, A., Lippens, S., and Tschopp, J. (2005). PIDD mediates NF-kappaB activation in response to DNA damage. Cell *123*, 1079–1092.

Jin, D.Y., and Jeang, K.T. (1997). HTLV-I Tax self-association in optimal trans-activation function. Nucleic Acids Res. *25*, 379–387.

Jin, D.Y., Giordano, V., Kibler, K. V., Nakano, H., and Jeang, K.T. (1999). Role of adapter function in oncoprotein-mediated activation of NF-kappaB. Human T-cell leukemia virus type I Tax interacts directly with IkappaB kinase gamma. J. Biol. Chem. *274*, 17402–17405.

Jin, W., Chang, M., Paul, E.M., Babu, G., Lee, A.J., Reiley, W., Wright, A., Zhang, M., You, J., and Sun, S.-C. (2008). Deubiquitinating enzyme CYLD negatively

regulates RANK signaling and osteoclastogenesis in mice. J. Clin. Invest. *118*, 1858–1866.

Kai, X., Chellappa, V., Donado, C., Reyon, D., Sekigami, Y., Ataca, D., Louissaint, A., Mattoo, H., Joung, J.K., and Pillai, S. (2014). IκB Kinase β (IKBKB) Mutations in Lymphomas That Constitutively Activate Canonical Nuclear Factor κB (NFκB) Signaling. J. Biol. Chem. *289*, 26960–26972.

Kaiser, W.J., Upton, J.W., Long, A.B., Livingston-Rosanoff, D., Daley-Bauer, L.P., Hakem, R., Caspary, T., and Mocarski, E.S. (2011). RIP3 mediates the embryonic lethality of caspase-8-deficient mice. Nature *471*, 368–372.

Kanayama, A., Seth, R.B., Sun, L., Ea, C.-K., Hong, M., Shaito, A., Chiu, Y.-H., Deng, L., and Chen, Z.J. (2004). TAB2 and TAB3 activate the NF-kappaB pathway through binding to polyubiquitin chains. Mol. Cell *15*, 535–548.

Karin, M., and Ben-Neriah, Y. (2000). Phosphorylation meets ubiquitination: the control of NF-[kappa]B activity. Annu. Rev. Immunol. *18*, 621–663.

Karin, M., Cao, Y., Greten, F.R., and Li, Z.-W. (2002). NF-kappaB in cancer: from innocent bystander to major culprit. Nat. Rev. Cancer *2*, 301–310.

Karin, M., Yamamoto, Y., and Wang, Q.M. (2004). The IKK NF-kappa B system: a treasure trove for drug development. Nat. Rev. Drug Discov. *3*, 17–26.

Kataoka, T., and Tschopp, J. (2004). N-terminal fragment of c-FLIP(L) processed by caspase 8 specifically interacts with TRAF2 and induces activation of the NF-kappaB signaling pathway. Mol. Cell. Biol. *24*, 2627–2636.

Kataoka, T., Budd, R.C., Holler, N., Thome, M., Martinon, F., Irmler, M., Burns, K., Hahne, M., Kennedy, N., Kovacsovics, M., et al. (2000). The caspase-8 inhibitor FLIP promotes activation of NF-kappaB and Erk signaling pathways. Curr. Biol. *10*, 640–648.

Kato, M., Sanada, M., Kato, I., Sato, Y., Takita, J., Takeuchi, K., Niwa, A., Chen, Y., Nakazaki, K., Nomoto, J., et al. (2009). Frequent inactivation of A20 in B-cell lymphomas. Nature *459*, 712–716.

Kauh, J., Fan, S., Xia, M., Yue, P., Yang, L., Khuri, F.R., and Sun, S.-Y. (2010). c-FLIP degradation mediates sensitization of pancreatic cancer cells to TRAIL-induced apoptosis by the histone deacetylase inhibitor LBH589. PLoS One *5*, e10376.

Kaunisto, a, Kochin, V., Asaoka, T., Mikhailov, a, Poukkula, M., Meinander, a, and Eriksson, J.E. (2009). PKC-mediated phosphorylation regulates c-FLIP ubiquitylation and stability. Cell Death Differ. *16*, 1215–1226.

Kavuri, S.M., Geserick, P., Berg, D., Dimitrova, D.P., Feoktistova, M., Siegmund, D., Gollnick, H., Neumann, M., Wajant, H., and Leverkus, M. (2011). Cellular FLICE-inhibitory protein (cFLIP) isoforms block CD95- and TRAIL death receptor-induced gene induction irrespective of processing of caspase-8 or cFLIP in the death-inducing signaling complex. J. Biol. Chem. *286*, 16631–16646.

Keller, S.A., Schattner, E.J., and Cesarman, E. (2000). Inhibition of NF-kappaB induces apoptosis of KSHV-infected primary effusion lymphoma cells. Blood *96*, 2537–2542.

Keller, S.A., Hernandez-Hopkins, D., Vider, J., Ponomarev, V., Hyjek, E., Schattner, E.J., and Cesarman, E. (2006). NF-kappaB is essential for the progression of KSHV- and EBV-infected lymphomas in vivo. Blood *107*, 3295–3302.

Kensche, T., Tokunaga, F., Ikeda, F., Goto, E., Iwai, K., and Dikic, I. (2012). Analysis of nuclear factor-κB (NF-κB) essential modulator (NEMO) binding to linear and lysine-linked ubiquitin chains and its role in the activation of NF-κB. J. Biol. Chem. *287*, 23626–23634.

Khoshnan, A., Ko, J., Watkin, E.E., Paige, L.A., Reinhart, P.H., and Patterson, P.H. (2004). Activation of the IkappaB kinase complex and nuclear factor-kappaB contributes to mutant huntingtin neurotoxicity. J. Neurosci. *24*, 7999–8008.

Kim, Y., Suh, N., Sporn, M., and Reed, J.C. (2002). An inducible pathway for degradation of FLIP protein sensitizes tumor cells to TRAIL-induced apoptosis. J. Biol. Chem. *277*, 22320–22329.

Kirisako, T., Kamei, K., Murata, S., Kato, M., Fukumoto, H., Kanie, M., Sano, S., Tokunaga, F., Tanaka, K., and Iwai, K. (2006). A ubiquitin ligase complex assembles linear polyubiquitin chains. EMBO J. *25*, 4877–4887.

Kober, a M.M., Legewie, S., Pforr, C., Fricker, N., Eils, R., Krammer, P.H., and Lavrik, I.N. (2011). Caspase-8 activity has an essential role in CD95/Fas-mediated MAPK activation. Cell Death Dis. *2*, e212.

Koenig, A., Buskiewicz, I. a, Fortner, K. a, Russell, J.Q., Asaoka, T., He, Y.-W., Hakem, R., Eriksson, J.E., and Budd, R.C. (2014). The c-FLIPL cleavage product p43FLIP promotes activation of extracellular signal-regulated kinase (ERK), nuclear factor κB (NF-κB), and caspase-8 and T cell survival. J. Biol. Chem. *289*, 1183–1191.

Komander, D. (2009). The emerging complexity of protein ubiquitination. Biochem. Soc. Trans. *37*, 937–953.

Komander, D. (2010). Mechanism, specificity and structure of the deubiquitinases. Subcell. Biochem. *54*, 69–87.

Komander, D., and Barford, D. (2008). Structure of the A20 OTU domain and mechanistic insights into deubiquitination. Biochem. J. *409*, 77–85.

Komander, D., Lord, C.J., Scheel, H., Swift, S., Hofmann, K., Ashworth, A., and Barford, D. (2008). The Structure of the CYLD USP Domain Explains Its Specificity for Lys63-Linked Polyubiquitin and Reveals a B Box Module. Mol. Cell *29*, 451–464.

Komander, D., Reyes-Turcu, F., Licchesi, J.D.F., Odenwaelder, P., Wilkinson, K.D., and Barford, D. (2009). Molecular discrimination of structurally equivalent Lys 63-linked and linear polyubiquitin chains. EMBO Rep. *10*, 466–473.

Koopal, S., Furuhjelm, J.H., Järviluoma, A., Jäämaa, S., Pyakurel, P., Pussinen, C., Wirzenius, M., Biberfeld, P., Alitalo, K., Laiho, M., et al. (2007). Viral oncogene-induced DNA damage response is activated in Kaposi sarcoma tumorigenesis. PLoS Pathog. *3*, 1348–1360.

Korkolopoulou, P., Goudopoulou, A., Voutsinas, G., Thomas-Tsagli, E., Kapralos, P., Patsouris, E., and Saetta, A. a (2004). c-FLIP expression in bladder urothelial

carcinomas: its role in resistance to Fas-mediated apoptosis and clinicopathologic correlations. Urology *63*, 1198–1204.

Korsmeyer, S.J., Wei, M.C., Saito, M., Weiler, S., Oh, K.J., and Schlesinger, P.H. (2000). Pro-apoptotic cascade activates BID, which oligomerizes BAK or BAX into pores that result in the release of cytochrome c. Cell Death Differ. *7*, 1166–1173.

Kovalenko, A., Chable-Bessia, C., Cantarella, G., Israël, A., Wallach, D., and Courtois, G. (2003). The tumour suppressor CYLD negatively regulates NF-kappaB signalling by deubiquitination. Nature *424*, 801–805.

Krammer, P.H., Arnold, R., and Lavrik, I.N. (2007). Life and death in peripheral T cells. Nat. Rev. Immunol. *7*, 532–542.

Kray, A.E., Carter, R.S., Pennington, K.N., Gomez, R.J., Sanders, L.E., Llanes, J.M., Khan, W.N., Ballard, D.W., and Wadzinski, B.E. (2005). Positive regulation of IkappaB kinase signaling by protein serine/threonine phosphatase 2A. J. Biol. Chem. *280*, 35974–35982.

Kreuz, S., and Siegmund, D. (2001). NF-Î°B inducers upregulate cFLIP, a cycloheximide-sensitive inhibitor of death receptor signaling. Mol. Cell. … *21*, 3964–3973.

Kreuz, S., Siegmund, D., Rumpf, J.-J., Samel, D., Leverkus, M., Janssen, O., Häcker, G., Dittrich-Breiholz, O., Kracht, M., Scheurich, P., et al. (2004). NFkappaB activation by Fas is mediated through FADD, caspase-8, and RIP and is inhibited by FLIP. J. Cell Biol. *166*, 369–380.

Krikos, A., Laherty, C.D., and Dixit, V.M. (1992). Transcriptional activation of the tumor necrosis factor alpha-inducible zinc finger protein, A20, is mediated by kappa B elements. J. Biol. Chem. *267*, 17971–17976.

Krueger, A., Baumann, S., Krammer, P.H., and Kirchhoff, S. (2001). FLICE-inhibitory proteins: regulators of death receptor-mediated apoptosis. Mol. Cell. Biol. *21*, 8247–8254.

Kulathu, Y., Akutsu, M., Bremm, A., Hofmann, K., and Komander, D. (2009). Two-sided ubiquitin binding explains specificity of the TAB2 NZF domain. Nat. Struct. Mol. Biol. *16*, 1328–1330.

Kundu, M., Pathak, S.K., Kumawat, K., Basu, S., Chatterjee, G., Pathak, S., Noguchi, T., Takeda, K., Ichijo, H., Thien, C.B.F., et al. (2009). A TNF- and c-Cbl-dependent FLIP(S)-degradation pathway and its function in Mycobacterium tuberculosis-induced macrophage apoptosis. Nat. Immunol. *10*, 918–926.

Kuwana, T., Bouchier-Hayes, L., Chipuk, J.E., Bonzon, C., Sullivan, B.A., Green, D.R., and Newmeyer, D.D. (2005). BH3 domains of BH3-only proteins differentially regulate Bax-mediated mitochondrial membrane permeabilization both directly and indirectly. Mol. Cell *17*, 525–535.

Kwak, Y.T. (2000). Analysis of Domains in the IKKalpha and IKKbeta Proteins That Regulate Their Kinase Activity. J. Biol. Chem. *275*, 14752–14759.

Lamothe, B., Besse, A., Campos, A.D., Webster, W.K., Wu, H., and Darnay, B.G. (2007). Site-specific Lys-63-linked tumor necrosis factor receptor-associated factor 6 auto-

ubiquitination is a critical determinant of I kappa B kinase activation. J. Biol. Chem. *282*, 4102–4112.

Laplantine, E., Fontan, E., Chiaravalli, J., Lopez, T., Lakisic, G., Véron, M., Agou, F., and Israël, A. (2009). NEMO specifically recognizes K63-linked poly-ubiquitin chains through a new bipartite ubiquitin-binding domain. EMBO J. *28*, 2885–2895.

Lavrik, I., Golks, A., and Krammer, P.H. (2005). Death receptor signaling. J. Cell Sci. *118*, 265–267.

Lavrik, I.N., Mock, T., Golks, A., Hoffmann, J.C., Baumann, S., and Krammer, P.H. (2008). CD95 stimulation results in the formation of a novel death effector domain protein-containing complex. J. Biol. Chem. *283*, 26401–26408.

Lee, D.-H., Pan, Y., Kanner, S., Sung, P., Borowiec, J.A., and Chowdhury, D. (2010). A PP4 phosphatase complex dephosphorylates RPA2 to facilitate DNA repair via homologous recombination. Nat. Struct. Mol. Biol. *17*, 365–372.

Lee, E.G., Boone, D.L., Chai, S., Libby, S.L., Chien, M., Lodolce, J.P., and Ma, A. (2000). Failure to regulate TNF-induced NF-kappaB and cell death responses in A20-deficient mice. Science *289*, 2350–2354.

Lee, F.S., Hagler, J., Chen, Z.J., and Maniatis, T. (1997). Activation of the IkappaB alpha kinase complex by MEKK1, a kinase of the JNK pathway. Cell *88*, 213–222.

Lee, F.S., Peters, R.T., Dang, L.C., and Maniatis, T. (1998). MEKK1 activates both IkappaB kinase alpha and IkappaB kinase beta. Proc. Natl. Acad. Sci. U. S. A. *95*, 9319–9324.

Lee, J.-S., Li, Q., Lee, J.-Y., Lee, S.-H., Jeong, J.H., Lee, H.-R., Chang, H., Zhou, F.-C., Gao, S.-J., Liang, C., et al. (2009). FLIP-mediated autophagy regulation in cell death control. Nat. Cell Biol. *11*, 1355–1362.

Leidal, A.M., Cyr, D.P., Hill, R.J., Lee, P.W.K., and McCormick, C. (2012). Subversion of autophagy by Kaposi's sarcoma-associated herpesvirus impairs oncogene-induced senescence. Cell Host Microbe *11*, 167–180.

Letai, A., Bassik, M.C., Walensky, L.D., Sorcinelli, M.D., Weiler, S., and Korsmeyer, S.J. (2002). Distinct BH3 domains either sensitize or activate mitochondrial apoptosis, serving as prototype cancer therapeutics. Cancer Cell *2*, 183–192.

Li, H.-Y., Liu, H., Wang, C.-H., Zhang, J.-Y., Man, J.-H., Gao, Y.-F., Zhang, P.-J., Li, W.-H., Zhao, J., Pan, X., et al. (2008a). Deactivation of the kinase IKK by CUEDC2 through recruitment of the phosphatase PP1. Nat. Immunol. *9*, 533–541.

Li, J., Mahajan, A., and Tsai, M.-D. (2006a). Ankyrin repeat: a unique motif mediating protein-protein interactions. Biochemistry *45*, 15168–15178.

Li, L., Hailey, D.W., Soetandyo, N., Li, W., Lippincott-Schwartz, J., Shu, H., and Ye, Y. (2008b). Localization of A20 to a lysosome-associated compartment and its role in NFkappaB signaling. Biochim. Biophys. Acta *1783*, 1140–1149.

Li, S., Wang, L., Berman, M. a, Zhang, Y., and Dorf, M.E. (2006b). RNAi screen in mouse astrocytes identifies phosphatases that regulate NF-kappaB signaling. Mol. Cell *24*, 497–509.

Li, W., Zhang, X., and Olumi, A.F. (2007). MG-132 sensitizes TRAIL-resistant prostate cancer cells by activating c-Fos/c-Jun heterodimers and repressing c-FLIP(L). Cancer Res. *67*, 2247–2255.

Li, X., Commane, M., Nie, H., Hua, X., Chatterjee-Kishore, M., Wald, D., Haag, M., and Stark, G.R. (2000). Act1, an NF-kappa B-activating protein. Proc. Natl. Acad. Sci. U. S. A. *97*, 10489–10493.

Lin, L., DeMartino, G.N., and Greene, W.C. (1998). Cotranslational biogenesis of NF-kappaB p50 by the 26S proteasome. Cell *92*, 819–828.

Lin, S.-C., Chung, J.Y., Lamothe, B., Rajashankar, K., Lu, M., Lo, Y.-C., Lam, A.Y., Darnay, B.G., and Wu, H. (2008). Molecular basis for the unique deubiquitinating activity of the NF-kappaB inhibitor A20. J. Mol. Biol. *376*, 526–540.

Ling, L., Cao, Z., and Goeddel, D. V (1998). NF-kappaB-inducing kinase activates IKK-alpha by phosphorylation of Ser-176. Proc. Natl. Acad. Sci. U. S. A. *95*, 3792–3797.

Linkermann, A., and Green, D.R. (2014). Necroptosis. N. Engl. J. Med. *370*, 455–465.

Liou, H.C., Sha, W.C., Scott, M.L., and Baltimore, D. (1994). Sequential induction of NF-kappa B/Rel family proteins during B-cell terminal differentiation. Mol. Cell. Biol. *14*, 5349–5359.

Liston, P., Roy, N., Tamai, K., Lefebvre, C., Baird, S., Cherton-Horvat, G., Farahani, R., McLean, M., Ikeda, J.E., MacKenzie, A., et al. (1996). Suppression of apoptosis in mammalian cells by NAIP and a related family of IAP genes. Nature *379*, 349–353.

Liu, F., Xia, Y., Parker, A.S., and Verma, I.M. (2012). IKK biology. Immunol. Rev. *246*, 239–253.

Liu, H.-H., Xie, M., Schneider, M.D., and Chen, Z.J. (2006). Essential role of TAK1 in thymocyte development and activation. Proc. Natl. Acad. Sci. U. S. A. *103*, 11677–11682.

Liu, L., Eby, M.T., Rathore, N., Sinha, S.K., Kumar, A., and Chaudhary, P.M. (2002). The human herpes virus 8-encoded viral FLICE inhibitory protein physically associates with and persistently activates the Ikappa B kinase complex. J. Biol. Chem. *277*, 13745–13751.

Liu, S., Misquitta, Y.R., Olland, A., Johnson, M. a, Kelleher, K.S., Kriz, R., Lin, L.L., Stahl, M., and Mosyak, L. (2013). Crystal structure of a human IκB kinase β asymmetric dimer. J. Biol. Chem. *288*, 22758–22767.

Liu, W., Yen, P., Chien, C., Fann, M., Su, J., and Chou, C. (2004). The inhibitor ABIN-2 disrupts the interaction of receptor-interacting protein with the kinase subunit IKKgamma to block activation of the transcription factor NF-kappaB and potentiate apoptosis. Biochem. J. *378*, 867–876.

Liu, Y., Shepherd, E.G., and Nelin, L.D. (2007). MAPK phosphatases--regulating the immune response. Nat. Rev. Immunol. *7*, 202–212.

Lo, Y.-C., Lin, S.-C., Rospigliosi, C.C., Conze, D.B., Wu, C.-J., Ashwell, J.D., Eliezer, D., and Wu, H. (2009). Structural basis for recognition of diubiquitins by NEMO. Mol. Cell *33*, 602–615.

Longley, D.B., Wilson, T.R., McEwan, M., Allen, W.L., McDermott, U., Galligan, L., and Johnston, P.G. (2006). c-FLIP inhibits chemotherapy-induced colorectal cancer cell death. Oncogene *25*, 838–848.

Luo, J.-L., Kamata, H., and Karin, M. (2005). The anti-death machinery in IKK/NF-kappaB signaling. J. Clin. Immunol. *25*, 541–550.

Mabb, A.M., Wuerzberger-Davis, S.M., and Miyamoto, S. (2006). PIASy mediates NEMO sumoylation and NF-kappaB activation in response to genotoxic stress. Nat. Cell Biol. *8*, 986–993.

Mace, P.D., Smits, C., Vaux, D.L., Silke, J., and Day, C.L. (2010). Asymmetric recruitment of cIAPs by TRAF2. J. Mol. Biol. *400*, 8–15.

MacFarlane, M., Harper, N., Snowden, R.T., Dyer, M.J.S., Barnett, G.A., Pringle, J.H., and Cohen, G.M. (2002). Mechanisms of resistance to TRAIL-induced apoptosis in primary B cell chronic lymphocytic leukaemia. Oncogene *21*, 6809–6818.

Maggirwar, S.B. (1995). Activation of NF-kappaB by Phosphatase Inhibitors Involves the Phosphorylation of IkappaBalpha at Phosphatase 2A-sensitive Sites. J. Biol. Chem. *270*, 18347–18351.

Malek, S., Chen, Y., Huxford, T., and Ghosh, G. (2001). IkappaBbeta, but not IkappaBalpha, functions as a classical cytoplasmic inhibitor of NF-kappaB dimers by masking both NF-kappaB nuclear localization sequences in resting cells. J. Biol. Chem. *276*, 45225–45235.

Malynn, B. a, and Ma, A. (2010). Ubiquitin makes its mark on immune regulation. Immunity *33*, 843–852.

Manel, N., Kim, F.J., Kinet, S., Taylor, N., Sitbon, M., and Battini, J.-L. (2003). The ubiquitous glucose transporter GLUT-1 is a receptor for HTLV. Cell *115*, 449–459.

Martinou, J.C., and Green, D.R. (2001). Breaking the mitochondrial barrier. Nat. Rev. Mol. Cell Biol. *2*, 63–67.

Massoumi, R., Chmielarska, K., Hennecke, K., Pfeifer, A., and Fässler, R. (2006). Cyld inhibits tumor cell proliferation by blocking Bcl-3-dependent NF-kappaB signaling. Cell *125*, 665–677.

Matsuda, I., Matsuo, K., Matsushita, Y., Haruna, Y., Niwa, M., and Kataoka, T. (2014). The C-terminal domain of the long form of cellular FLICE-inhibitory protein (c-FLIPL) inhibits the interaction of the caspase 8 prodomain with the receptor-interacting protein 1 (RIP1) death domain and regulates caspase 8-dependent nuclear factor κB (NF-κ. J. Biol. Chem. *289*, 3876–3887.

Matsuoka, M. (2003). Human T-cell leukemia virus type I and adult T-cell leukemia. Oncogene *22*, 5131–5140.

Matsuoka, M., and Jeang, K.-T. (2007). Human T-cell leukaemia virus type 1 (HTLV-1) infectivity and cellular transformation. Nat. Rev. Cancer *7*, 270–280.

Matta, H., and Chaudhary, P.M. (2004). Activation of alternative NF-kappa B pathway by human herpes virus 8-encoded Fas-associated death domain-like IL-1 beta-converting enzyme inhibitory protein (vFLIP). Proc. Natl. Acad. Sci. U. S. A. *101*, 9399–9404.

Matta, H., Mazzacurati, L., Schamus, S., Yang, T., Sun, Q., and Chaudhary, P.M. (2007). Kaposi's sarcoma-associated herpesvirus (KSHV) oncoprotein K13 bypasses TRAFs and directly interacts with the IkappaB kinase complex to selectively activate NF-kappaB without JNK activation. J. Biol. Chem. *282*, 24858–24865.

Matta, H., Gopalakrishnan, R., Graham, C., Tolani, B., Khanna, A., Yi, H., Suo, Y., and Chaudhary, P.M. (2012). Kaposi's sarcoma associated herpesvirus encoded viral FLICE inhibitory protein K13 activates NF-κB pathway independent of TRAF6, TAK1 and LUBAC. PLoS One *7*, e36601.

Mauro, C., Vito, P., Mellone, S., Pacifico, F., Chariot, A., Formisano, S., and Leonardi, A. (2003). Role of the adaptor protein CIKS in the activation of the IKK complex. Biochem. Biophys. Res. Commun. *309*, 84–90.

Mauro, C., Pacifico, F., Lavorgna, A., Mellone, S., Iannetti, A., Acquaviva, R., Formisano, S., Vito, P., and Leonardi, A. (2006). ABIN-1 binds to NEMO/IKKgamma and co-operates with A20 in inhibiting NF-kappaB. J. Biol. Chem. *281*, 18482–18488.

May, M.J. (2000). Selective Inhibition of NF-kappa B Activation by a Peptide That Blocks the Interaction of NEMO with the Ikappa B Kinase Complex. Science (80-.). *289*, 1550–1554.

May, M.J., Marienfeld, R.B., and Ghosh, S. (2002). Characterization of the Ikappa B-kinase NEMO binding domain. J. Biol. Chem. *277*, 45992–46000.

McCool, K.W., and Miyamoto, S. (2012). DNA damage-dependent NF-κB activation: NEMO turns nuclear signaling inside out. Immunol. Rev. *246*, 311–326.

McLornan, D.P., Barrett, H.L., Cummins, R., McDermott, U., McDowell, C., Conlon, S.J., Coyle, V.M., Van Schaeybroeck, S., Wilson, R., Kay, E.W., et al. (2010). Prognostic significance of TRAIL signaling molecules in stage II and III colorectal cancer. Clin. Cancer Res. *16*, 3442–3451.

Mercurio, F., Zhu, H., Murray, B.W., Shevchenko, A., Bennett, B.L., Li, J., Young, D.B., Barbosa, M., Mann, M., Manning, A., et al. (1997). IKK-1 and IKK-2: cytokine-activated IkappaB kinases essential for NF-kappaB activation. Science *278*, 860–866.

Mesri, E. a, Cesarman, E., and Boshoff, C. (2010). Kaposi's sarcoma and its associated herpesvirus. Nat. Rev. Cancer *10*, 707–719.

Mezzanzanica, D., Balladore, E., Turatti, F., Luison, E., Alberti, P., Bagnoli, M., Figini, M., Mazzoni, A., Raspagliesi, F., Oggionni, M., et al. (2004). CD95-mediated apoptosis is impaired at receptor level by cellular FLICE-inhibitory protein (long form) in wild-type p53 human ovarian carcinoma. Clin. Cancer Res. *10*, 5202–5214.

Micheau, O., and Tschopp, J. (2003). Induction of TNF receptor I-mediated apoptosis via two sequential signaling complexes. Cell *114*, 181–190.

Micheau, O., Lens, S., Gaide, O., Alevizopoulos, K., and Tschopp, J. (2001). NF-kappaB signals induce the expression of c-FLIP. Mol. Cell. Biol. *21*, 5299–5305.

Miranda, C., Roccato, E., Raho, G., Pagliardini, S., Pierotti, M.A., and Greco, A. (2006). The TFG protein, involved in oncogenic rearrangements, interacts with TANK and NEMO, two proteins involved in the NF-kappaB pathway. J. Cell. Physiol. *208*, 154–160.

Miyamoto, S. (2011). Nuclear initiated NF-κB signaling: NEMO and ATM take center stage. Cell Res. *21*, 116–130.

Mizushima, N., Levine, B., Cuervo, A.M., and Klionsky, D.J. (2008). Autophagy fights disease through cellular self-digestion. Nature *451*, 1069–1075.

Mukherjee, S., Keitany, G., Li, Y., Wang, Y., Ball, H.L., Goldsmith, E.J., and Orth, K. (2006). Yersinia YopJ acetylates and inhibits kinase activation by blocking phosphorylation. Science *312*, 1211–1214.

Mukherjee, S., Negi, V.S., Keitany, G., Tanaka, Y., and Orth, K. (2008). In vitro activation of the IkappaB kinase complex by human T-cell leukemia virus type-1 Tax. J. Biol. Chem. *283*, 15127–15133.

Musone, S.L., Taylor, K.E., Lu, T.T., Nititham, J., Ferreira, R.C., Ortmann, W., Shifrin, N., Petri, M.A., Kamboh, M.I., Manzi, S., et al. (2008). Multiple polymorphisms in the TNFAIP3 region are independently associated with systemic lupus erythematosus. Nat. Genet. *40*, 1062–1064.

Nagabhushana, A., Bansal, M., and Swarup, G. (2011). Optineurin is required for CYLD-dependent inhibition of TNFα-induced NF-κB activation. PLoS One *6*, e17477.

Nagashima, K., Sasseville, V.G., Wen, D., Bielecki, A., Yang, H., Simpson, C., Grant, E., Hepperle, M., Harriman, G., Jaffee, B., et al. (2006). Rapid TNFR1-dependent lymphocyte depletion in vivo with a selective chemical inhibitor of IKKbeta. Blood *107*, 4266–4273.

Nair, R.P., Duffin, K.C., Helms, C., Ding, J., Stuart, P.E., Goldgar, D., Gudjonsson, J.E., Li, Y., Tejasvi, T., Feng, B.-J., et al. (2009). Genome-wide scan reveals association of psoriasis with IL-23 and NF-kappaB pathways. Nat. Genet. *41*, 199–204.

Nakajima, A., Komazawa-Sakon, S., Takekawa, M., Sasazuki, T., Yeh, W.-C., Yagita, H., Okumura, K., and Nakano, H. (2006). An antiapoptotic protein, c-FLIPL, directly binds to MKK7 and inhibits the JNK pathway. EMBO J. *25*, 5549–5559.

Nanda, S.K., Venigalla, R.K.C., Ordureau, A., Patterson-Kane, J.C., Powell, D.W., Toth, R., Arthur, J.S.C., and Cohen, P. (2011). Polyubiquitin binding to ABIN1 is required to prevent autoimmunity. J. Exp. Med. *208*, 1215–1228.

Naumann, M., Wulczyn, F.G., and Scheidereit, C. (1993a). The NF-kappa B precursor p105 and the proto-oncogene product Bcl-3 are I kappa B molecules and control nuclear translocation of NF-kappa B. EMBO J. *12*, 213–222.

Naumann, M., Nieters, A., Hatada, E.N., and Scheidereit, C. (1993b). NF-kappa B precursor p100 inhibits nuclear translocation and DNA binding of NF-kappa B/rel-factors. Oncogene *8*, 2275–2281.

Neumann, L., Pforr, C., Beaudouin, J., Pappa, A., Fricker, N., Krammer, P.H., Lavrik, I.N., and Eils, R. (2010). Dynamics within the CD95 death-inducing signaling complex decide life and death of cells. Mol. Syst. Biol. *6*, 352.

Nichols, D.B., and Shisler, J.L. (2006). The MC160 protein expressed by the dermatotropic poxvirus molluscum contagiosum virus prevents tumor necrosis factor alpha-induced NF-kappaB activation via inhibition of I kappa kinase complex formation. J. Virol. *80*, 578–586.

Nijman, S.M.B., Luna-Vargas, M.P.A., Velds, A., Brummelkamp, T.R., Dirac, A.M.G., Sixma, T.K., and Bernards, R. (2005). A genomic and functional inventory of deubiquitinating enzymes. Cell *123*, 773–786.

Ninomiya-Tsuji, J., Kishimoto, K., Hiyama, A., Inoue, J., Cao, Z., and Matsumoto, K. (1999). The kinase TAK1 can activate the NIK-I kappaB as well as the MAP kinase cascade in the IL-1 signalling pathway. Nature *398*, 252–256.

O'Donnell, M.A., Hase, H., Legarda, D., and Ting, A.T. (2012). NEMO inhibits programmed necrosis in an NF*κ*B-independent manner by restraining RIP1. PLoS One *7*, e41238.

Oberst, A., Pop, C., Tremblay, A.G., Blais, V., Denault, J.-B., Salvesen, G.S., and Green, D.R. (2010). Inducible dimerization and inducible cleavage reveal a requirement for both processes in caspase-8 activation. J. Biol. Chem. *285*, 16632–16642.

Oberst, A., Dillon, C.P., Weinlich, R., McCormick, L.L., Fitzgerald, P., Pop, C., Hakem, R., Salvesen, G.S., and Green, D.R. (2011). Catalytic activity of the caspase-8-FLIP(L) complex inhibits RIPK3-dependent necrosis. Nature *471*, 363–367.

Oeckinghaus, A., and Ghosh, S. (2009). The NF-kappaB family of transcription factors and its regulation. Cold Spring Harb. Perspect. Biol. *1*, a000034.

Oeckinghaus, A., Hayden, M.S., and Ghosh, S. (2011). Crosstalk in NF-*κ*B signaling pathways. Nat. Immunol. *12*, 695–708.

Olsson, A., Diaz, T., Aguilar-Santelises, M., Osterborg, A., Celsing, F., Jondal, M., and Osorio, L.M. (2001). Sensitization to TRAIL-induced apoptosis and modulation of FLICE-inhibitory protein in B chronic lymphocytic leukemia by actinomycin D. Leukemia *15*, 1868–1877.

Osame, M., Igata, A., Matsumoto, M., and Tara, M. (1987). [HTLV-I-associated myelopathy]. Gan To Kagaku Ryoho. *14*, 2411–2416.

Oztürk, S., Schleich, K., and Lavrik, I.N. (2012). Cellular FLICE-like inhibitory proteins (c-FLIPs): fine-tuners of life and death decisions. Exp. Cell Res. *318*, 1324–1331.

Palkowitsch, L., Leidner, J., Ghosh, S., and Marienfeld, R.B. (2008). Phosphorylation of serine 68 in the IkappaB kinase (IKK)-binding domain of NEMO interferes with the structure of the IKK complex and tumor necrosis factor-alpha-induced NF-kappaB activity. J. Biol. Chem. *283*, 76–86.

Pan, G., Ni, J., Wei, Y.F., Yu, G., Gentz, R., and Dixit, V.M. (1997). An antagonist decoy receptor and a death domain-containing receptor for TRAIL. Science *277*, 815–818.

Panner, A., James, C.D., Berger, M.S., and Pieper, R.O. (2005). mTOR controls FLIPS translation and TRAIL sensitivity in glioblastoma multiforme cells. Mol. Cell. Biol. *25*, 8809–8823.

Panner, A., Nakamura, J.L., Parsa, A.T., Rodriguez-Viciana, P., Berger, M.S., Stokoe, D., and Pieper, R.O. (2006). mTOR-independent translational control of the extrinsic cell death pathway by RalA. Mol. Cell. Biol. *26*, 7345–7357.

Panner, A., Crane, C. a, Weng, C., Feletti, A., Parsa, A.T., and Pieper, R.O. (2009). A novel PTEN-dependent link to ubiquitination controls FLIPS stability and TRAIL sensitivity in glioblastoma multiforme. Cancer Res. *69*, 7911–7916.

Park, S.-J., Kim, M.-J., Kim, H.-B., Sohn, H.-Y., Bae, J.-H., Kang, C.-D., and Kim, S.-H. (2009). Trichostatin A sensitizes human ovarian cancer cells to TRAIL-induced apoptosis by down-regulation of c-FLIPL via inhibition of EGFR pathway. Biochem. Pharmacol. *77*, 1328–1336.

Park, Y.-H., Jeong, M.S., Park, H.H., and Jang, S.B. (2013). Formation of the death domain complex between FADD and RIP1 proteins in vitro. Biochim. Biophys. Acta *1834*, 292–300.

Pasparakis, M., Luedde, T., and Schmidt-Supprian, M. (2006). Dissection of the NF-kappaB signalling cascade in transgenic and knockout mice. Cell Death Differ. *13*, 861–872.

Pear, W.S., Nolan, G.P., Scott, M.L., and Baltimore, D. (1993). Production of high-titer helper-free retroviruses by transient transfection. Proc. Natl. Acad. Sci. U. S. A. *90*, 8392–8396.

Pearson, G., Robinson, F., Beers Gibson, T., Xu, B.E., Karandikar, M., Berman, K., and Cobb, M.H. (2001). Mitogen-activated protein (MAP) kinase pathways: regulation and physiological functions. Endocr. Rev. *22*, 153–183.

Perez, D., White, E., and Downregulating, S. (2003). E1A Sensitizes Cells to Tumor Necrosis Factor Alpha by Downregulating c-FLIP S E1A Sensitizes Cells to Tumor Necrosis Factor Alpha by. *77*.

Perkins, N.D. (2006). Post-translational modifications regulating the activity and function of the nuclear factor kappa B pathway. Oncogene *25*, 6717–6730.

Petroski, M.D., and Deshaies, R.J. (2005). Function and regulation of cullin-RING ubiquitin ligases. Nat. Rev. Mol. Cell Biol. *6*, 9–20.

Pickart, C.M. (2001). Mechanisms underlying ubiquitination. Annu. Rev. Biochem. *70*, 503–533.

Pickart, C.M., and Fushman, D. (2004). Polyubiquitin chains: Polymeric protein signals. Curr. Opin. Chem. Biol. *8*, 610–616.

Poiesz, B.J., Ruscetti, F.W., Gazdar, A.F., Bunn, P.A., Minna, J.D., and Gallo, R.C. (1980). Detection and isolation of type C retrovirus particles from fresh and cultured

lymphocytes of a patient with cutaneous T-cell lymphoma. Proc. Natl. Acad. Sci. *77*, 7415–7419.

Polley, S., Huang, D.-B., Hauenstein, A. V., Fusco, A.J., Zhong, X., Vu, D., Schröfelbauer, B., Kim, Y., Hoffmann, A., Verma, I.M., et al. (2013). A Structural Basis for IκB Kinase 2 Activation Via Oligomerization-Dependent Trans Auto-Phosphorylation. PLoS Biol. *11*, e1001581.

Pop, C., Oberst, A., Drag, M., Van Raam, B.J., Riedl, S.J., Green, D.R., and Salvesen, G.S. (2011). FLIP(L) induces caspase 8 activity in the absence of interdomain caspase 8 cleavage and alters substrate specificity. Biochem. J. *433*, 447–457.

Poukkula, M., Kaunisto, A., Hietakangas, V., Denessiouk, K., Katajamäki, T., Johnson, M.S., Sistonen, L., and Eriksson, J.E. (2005). Rapid turnover of c-FLIPshort is determined by its unique C-terminal tail. J. Biol. Chem. *280*, 27345–27355.

Poyet, J.L., Srinivasula, S.M., Lin, J.H., Fernandes-Alnemri, T., Yamaoka, S., Tsichlis, P.N., and Alnemri, E.S. (2000). Activation of the Ikappa B kinases by RIP via IKKgamma /NEMO-mediated oligomerization. J. Biol. Chem. *275*, 37966–37977.

Poyet, J.L., Srinivasula, S.M., and Alnemri, E.S. (2001). vCLAP, a caspase-recruitment domain-containing protein of equine Herpesvirus-2, persistently activates the Ikappa B kinases through oligomerization of IKKgamma. J. Biol. Chem. *276*, 3183–3187.

Prajapati, S., and Gaynor, R.B. (2002). Regulation of Ikappa B kinase (IKK)gamma /NEMO function by IKKbeta -mediated phosphorylation. J. Biol. Chem. *277*, 24331–24339.

Prajapati, S., Verma, U., Yamamoto, Y., Kwak, Y.T., and Gaynor, R.B. (2004). Protein phosphatase 2Cbeta association with the IkappaB kinase complex is involved in regulating NF-kappaB activity. J. Biol. Chem. *279*, 1739–1746.

Punj, V., Matta, H., Schamus, S., and Chaudhary, P.M. (2009). Integrated microarray and multiplex cytokine analyses of Kaposi's Sarcoma Associated Herpesvirus viral FLICE Inhibitory Protein K13 affected genes and cytokines in human blood vascular endothelial cells. BMC Med. Genomics *2*, 50.

Pyo, J.O., Nah, J., and Jung, Y.K. (2012). Molecules and their functions in autophagy. Exp. Mol. Med. *44*, 73–80.

Qian, Y., Qin, J., Cui, G., Naramura, M., Snow, E.C., Ware, C.F., Fairchild, R.L., Omori, S.A., Rickert, R.C., Scott, M., et al. (2004). Act1, a negative regulator in CD40- and BAFF-mediated B cell survival. Immunity *21*, 575–587.

Qing, G., Qu, Z., and Xiao, G. (2005). Stabilization of basally translated NF-kappaB-inducing kinase (NIK) protein functions as a molecular switch of processing of NF-kappaB2 p100. J. Biol. Chem. *280*, 40578–40582.

Rahighi, S., Ikeda, F., Kawasaki, M., Akutsu, M., Suzuki, N., Kato, R., Kensche, T., Uejima, T., Bloor, S., Komander, D., et al. (2009). Specific recognition of linear ubiquitin chains by NEMO is important for NF-kappaB activation. Cell *136*, 1098–1109.

Ran, R., Lu, A., Zhang, L., Tang, Y., Zhu, H., Xu, H., Feng, Y., Han, C., Zhou, G., Rigby, A.C., et al. (2004). Hsp70 promotes TNF-mediated apoptosis by binding IKK gamma and impairing NF-kappa B survival signaling. Genes Dev. *18*, 1466–1481.

Randall, C.M.H., Jokela, J. a, and Shisler, J.L. (2012). The MC159 protein from the molluscum contagiosum poxvirus inhibits NF-κB activation by interacting with the IκB kinase complex. J. Immunol. *188*, 2371–2379.

Rasper, D.M., Vaillancourt, J.P., Hadano, S., Houtzager, V.M., Seiden, I., Keen, S.L., Tawa, P., Xanthoudakis, S., Nasir, J., Martindale, D., et al. (1998). Cell death attenuation by "Usurpin", a mammalian DED-caspase homologue that precludes caspase-8 recruitment and activation by the CD-95 (Fas, APO-1) receptor complex. Cell Death Differ. *5*, 271–288.

Razani, B., Zarnegar, B., Ytterberg, a J., Shiba, T., Dempsey, P.W., Ware, C.F., Loo, J. a, and Cheng, G. (2010). Negative feedback in noncanonical NF-kappaB signaling modulates NIK stability through IKKalpha-mediated phosphorylation. Sci. Signal. *3*, ra41.

Razani, B., Reichardt, A.D., and Cheng, G. (2011). Non-canonical NF-κB signaling activation and regulation: principles and perspectives. Immunol. Rev. *244*, 44–54.

Régnier, C.H., Song, H.Y., Gao, X., Goeddel, D. V, Cao, Z., and Rothe, M. (1997). Identification and characterization of an IkappaB kinase. Cell *90*, 373–383.

Reiley, W., Zhang, M., Wu, X., Granger, E., and Sun, S. (2005). Regulation of the Deubiquitinating Enzyme CYLD by I κ B Kinase Gamma-Dependent Phosphorylation Regulation of the Deubiquitinating Enzyme CYLD by I B Kinase Gamma-Dependent Phosphorylation †.

Reiley, W.W., Zhang, M., Jin, W., Losiewicz, M., Donohue, K.B., Norbury, C.C., and Sun, S.-C. (2006). Regulation of T cell development by the deubiquitinating enzyme CYLD. Nat. Immunol. *7*, 411–417.

Reiley, W.W., Jin, W., Lee, A.J., Wright, A., Wu, X., Tewalt, E.F., Leonard, T.O., Norbury, C.C., Fitzpatrick, L., Zhang, M., et al. (2007). Deubiquitinating enzyme CYLD negatively regulates the ubiquitin-dependent kinase Tak1 and prevents abnormal T cell responses. J. Exp. Med. *204*, 1475–1485.

Rimsky, L., Hauber, J., Dukovich, M., Malim, M.H., Langlois, A., Cullen, B.R., and Greene, W.C. (1988). Functional replacement of the HIV-1 rev protein by the HTLV-1 rex protein. Nature *335*, 738–740.

Ritthipichai, K., Nan, Y., Bossis, I., and Zhang, Y. (2012). Viral FLICE inhibitory protein of rhesus monkey rhadinovirus inhibits apoptosis by enhancing autophagosome formation. PLoS One *7*, e39438.

Rogers, K.M. a, Thomas, M., Galligan, L., Wilson, T.R., Allen, W.L., Sakai, H., Johnston, P.G., and Longley, D.B. (2007). Cellular FLICE-inhibitory protein regulates chemotherapy-induced apoptosis in breast cancer cells. Mol. Cancer Ther. *6*, 1544–1551.

Rossi, D., Deaglio, S., Dominguez-Sola, D., Rasi, S., Vaisitti, T., Agostinelli, C., Spina, V., Bruscaggin, A., Monti, S., Cerri, M., et al. (2011). Alteration of BIRC3 and

multiple other NF-κB pathway genes in splenic marginal zone lymphoma. Blood *118*, 4930–4934.

Rossi, D., Trifonov, V., Fangazio, M., Bruscaggin, A., Rasi, S., Spina, V., Monti, S., Vaisitti, T., Arruga, F., Famà, R., et al. (2012). The coding genome of splenic marginal zone lymphoma: activation of NOTCH2 and other pathways regulating marginal zone development. J. Exp. Med. *209*, 1537–1551.

Rowe, H.M., Lopes, L., Brown, N., Efklidou, S., Smallie, T., Karrar, S., Kaye, P.M., and Collins, M.K. (2009). Expression of vFLIP in a lentiviral vaccine vector activates NF-{kappa}B, matures dendritic cells, and increases CD8+ T-cell responses. J. Virol. *83*, 1555–1562.

Rual, J.-F., Venkatesan, K., Hao, T., Hirozane-Kishikawa, T., Dricot, A., Li, N., Berriz, G.F., Gibbons, F.D., Dreze, M., Ayivi-Guedehoussou, N., et al. (2005). Towards a proteome-scale map of the human protein-protein interaction network. Nature *437*, 1173–1178.

Rushe, M., Silvian, L., Bixler, S., Chen, L.L., Cheung, A., Bowes, S., Cuervo, H., Berkowitz, S., Zheng, T., Guckian, K., et al. (2008). Structure of a NEMO/IKK-associating domain reveals architecture of the interaction site. Structure *16*, 798–808.

Ryter, S.W., Cloonan, S.M., and Choi, A.M.K. (2013). Autophagy: a critical regulator of cellular metabolism and homeostasis. Mol. Cells *36*, 7–16.

Safa, A.R., and Pollok, K.E. (2011). Targeting the Anti-Apoptotic Protein c-FLIP for Cancer Therapy. Cancers (Basel). *3*, 1639–1671.

Safa, A.R., Day, T.W., and Wu, C.-H. (2008). Cellular FLICE-like inhibitory protein (C-FLIP): a novel target for cancer therapy. Curr. Cancer Drug Targets *8*, 37–46.

Saito, K., Kigawa, T., Koshiba, S., Sato, K., Matsuo, Y., Sakamoto, A., Takagi, T., Shirouzu, M., Yabuki, T., Nunokawa, E., et al. (2004). The CAP-Gly domain of CYLD associates with the proline-rich sequence in NEMO/IKKgamma. Structure *12*, 1719–1728.

Salon, C., Eymin, B., Micheau, O., Chaperot, L., Plumas, J., Brambilla, C., Brambilla, E., and Gazzeri, S. (2006). E2F1 induces apoptosis and sensitizes human lung adenocarcinoma cells to death-receptor-mediated apoptosis through specific downregulation of c-FLIP(short). Cell Death Differ. *13*, 260–272.

Sasaki, Y., Sano, S., Nakahara, M., Murata, S., Kometani, K., Aiba, Y., Sakamoto, S., Watanabe, Y., Tanaka, K., Kurosaki, T., et al. (2013). Defective immune responses in mice lacking LUBAC-mediated linear ubiquitination in B cells. EMBO J. *32*, 2463–2476.

Sato, S., Sanjo, H., Takeda, K., Ninomiya-Tsuji, J., Yamamoto, M., Kawai, T., Matsumoto, K., Takeuchi, O., and Akira, S. (2005). Essential function for the kinase TAK1 in innate and adaptive immune responses. Nat. Immunol. *6*, 1087–1095.

Satou, Y., Yasunaga, J., Yoshida, M., and Matsuoka, M. (2006). HTLV-I basic leucine zipper factor gene mRNA supports proliferation of adult T cell leukemia cells. Proc. Natl. Acad. Sci. U. S. A. *103*, 720–725.

Scaffidi, C., Schmitz, I., Krammer, P.H., and Peter, M.E. (1999). The role of c-FLIP in modulation of CD95-induced apoptosis. J. Biol. Chem. *274*, 1541–1548.

Scheidereit, C. (2006). IkappaB kinase complexes: gateways to NF-kappaB activation and transcription. Oncogene *25*, 6685–6705.

Schmidt, C., Peng, B., Li, Z., Sclabas, G.M., Fujioka, S., Niu, J., Schmidt-Supprian, M., Evans, D.B., Abbruzzese, J.L., and Chiao, P.J. (2003). Mechanisms of proinflammatory cytokine-induced biphasic NF-kappaB activation. Mol. Cell *12*, 1287–1300.

Schmitz, I., Weyd, H., Krueger, A., Baumann, S., Fas, S.C., Krammer, P.H., and Kirchhoff, S. (2004). Resistance of short term activated T cells to CD95-mediated apoptosis correlates with de novo protein synthesis of c-FLIPshort. J. Immunol. *172*, 2194–2200.

Schomer-Miller, B., Higashimoto, T., Lee, Y.-K., and Zandi, E. (2006). Regulation of IkappaB kinase (IKK) complex by IKKgamma-dependent phosphorylation of the T-loop and C terminus of IKKbeta. J. Biol. Chem. *281*, 15268–15276.

Schröfelbauer, B., Polley, S., Behar, M., Ghosh, G., and Hoffmann, A. (2012). NEMO ensures signaling specificity of the pleiotropic IKKβ by directing its kinase activity toward IκBα. Mol. Cell *47*, 111–121.

Searles, R.P., Bergquam, E.P., Axthelm, M.K., and Wong, S.W. (1999). Sequence and genomic analysis of a Rhesus macaque rhadinovirus with similarity to Kaposi's sarcoma-associated herpesvirus/human herpesvirus 8. J. Virol. *73*, 3040–3053.

Sen, R., and Baltimore, D. (1986a). Multiple nuclear factors interact with the immunoglobulin enhancer sequences. Cell *46*, 705–716.

Sen, R., and Baltimore, D. (1986b). Inducibility of κ immunoglobulin enhancer-binding protein NF-κB by a posttranslational mechanism. Cell *47*, 921–928.

Sen, R., and Smale, S.T. (2009). Selectivity of the NF- B Response. Cold Spring Harb. Perspect. Biol. *2*, a000257–a000257.

Senftleben, U., Cao, Y., Xiao, G., Greten, F.R., Krähn, G., Bonizzi, G., Chen, Y., Hu, Y., Fong, a, Sun, S.C., et al. (2001). Activation by IKKalpha of a second, evolutionary conserved, NF-kappa B signaling pathway. Science *293*, 1495–1499.

Seymour, R.E., Hasham, M.G., Cox, G.A., Shultz, L.D., Hogenesch, H., Roopenian, D.C., and Sundberg, J.P. (2007). Spontaneous mutations in the mouse Sharpin gene result in multiorgan inflammation, immune system dysregulation and dermatitis. Genes Immun. *8*, 416–421.

Shambharkar, P.B., Blonska, M., Pappu, B.P., Li, H., You, Y., Sakurai, H., Darnay, B.G., Hara, H., Penninger, J., and Lin, X. (2007). Phosphorylation and ubiquitination of the IkappaB kinase complex by two distinct signaling pathways. EMBO J. *26*, 1794–1805.

Shembade, N., Harhaj, N.S., Liebl, D.J., and Harhaj, E.W. (2007). Essential role for TAX1BP1 in the termination of TNF-alpha-, IL-1- and LPS-mediated NF-kappaB and JNK signaling. EMBO J. *26*, 3910–3922.

Shembade, N., Ma, A., and Harhaj, E.W. (2010). Inhibition of NF-kappaB signaling by A20 through disruption of ubiquitin enzyme complexes. Science *327*, 1135–1139.

Shembade, N., Pujari, R., Harhaj, N.S., Abbott, D.W., and Harhaj, E.W. (2011). The kinase IKKα inhibits activation of the transcription factor NF-κB by phosphorylating the regulatory molecule TAX1BP1. Nat. Immunol. *12*, 834–843.

Sheridan, J.P., Marsters, S.A., Pitti, R.M., Gurney, A., Skubatch, M., Baldwin, D., Ramakrishnan, L., Gray, C.L., Baker, K., Wood, W.I., et al. (1997). Control of TRAIL-induced apoptosis by a family of signaling and decoy receptors. Science *277*, 818–821.

Shi, B., Tran, T., Sobkoviak, R., and Pope, R.M. (2009). Activation-induced degradation of FLIP(L) is mediated via the phosphatidylinositol 3-kinase/Akt signaling pathway in macrophages. J. Biol. Chem. *284*, 14513–14523.

Shibata, Y., Oyama, M., Kozuka-Hata, H., Han, X., Tanaka, Y., Gohda, J., and Inoue, J. (2012). p47 negatively regulates IKK activation by inducing the lysosomal degradation of polyubiquitinated NEMO. Nat. Commun. *3*, 1061.

Shintani, T., and Klionsky, D.J. (2004). Autophagy in health and disease: a double-edged sword. Science *306*, 990–995.

Shirley, S., and Micheau, O. (2010). Targeting c-FLIP in cancer. Cancer Lett. 1–10.

Shu, H.B., Halpin, D.R., and Goeddel, D. V (1997). Casper is a FADD- and caspase-related inducer of apoptosis. Immunity *6*, 751–763.

Siegmund, D., Mauri, D., Peters, N., Juo, P., Thome, M., Reichwein, M., Blenis, J., Scheurich, P., Tschopp, J., and Wajant, H. (2001). Fas-associated death domain protein (FADD) and caspase-8 mediate up-regulation of c-Fos by Fas ligand and tumor necrosis factor-related apoptosis-inducing ligand (TRAIL) via a FLICE inhibitory protein (FLIP)-regulated pathway. J. Biol. Chem. *276*, 32585–32590.

Siggs, O.M., Berger, M., Krebs, P., Arnold, C.N., Eidenschenk, C., Huber, C., Pirie, E., Smart, N.G., Khovananth, K., Xia, Y., et al. (2010). A mutation of Ikbkg causes immune deficiency without impairing degradation of IkappaB alpha. Proc. Natl. Acad. Sci. U. S. A. *107*, 3046–3051.

Sil, A.K., Maeda, S., Sano, Y., Roop, D.R., and Karin, M. (2004). IkappaB kinase-alpha acts in the epidermis to control skeletal and craniofacial morphogenesis. Nature *428*, 660–664.

Singhirunnusorn, P., Suzuki, S., Kawasaki, N., Saiki, I., and Sakurai, H. (2005). Critical roles of threonine 187 phosphorylation in cellular stress-induced rapid and transient activation of transforming growth factor-beta-activated kinase 1 (TAK1) in a signaling complex containing TAK1-binding protein TAB1 and TAB2. J. Biol. Chem. *280*, 7359–7368.

Skaug, B., Chen, J., Du, F., He, J., Ma, A., and Chen, Z.J. (2011). Direct, noncatalytic mechanism of IKK inhibition by A20. Mol. Cell *44*, 559–571.

Smahi, A., Courtois, G., Vabres, P., Yamaoka, S., Heuertz, S., Munnich, A., Israël, A., Heiss, N.S., Klauck, S.M., Kioschis, P., et al. (2000). Genomic rearrangement in

NEMO impairs NF-kappaB activation and is a cause of incontinentia pigmenti. The International Incontinentia Pigmenti (IP) Consortium. Nature *405*, 466–472.

Smale, S.T. (2012). Dimer-specific regulatory mechanisms within the NF-*κ*B family of transcription factors. Immunol. Rev. *246*, 193–204.

Solt, L.A., Madge, L.A., Orange, J.S., and May, M.J. (2007). Interleukin-1-induced NF-kappaB activation is NEMO-dependent but does not require IKKbeta. J. Biol. Chem. *282*, 8724–8733.

Song, J.H., Tse, M.C.L., Bellail, A., Phuphanich, S., Khuri, F., Kneteman, N.M., and Hao, C. (2007). Lipid rafts and nonrafts mediate tumor necrosis factor related apoptosis-inducing ligand induced apoptotic and nonapoptotic signals in non small cell lung carcinoma cells. Cancer Res. *67*, 6946–6955.

Soond, S.M., Terry, J.L., Colbert, J.D., and Riches, D.W.H. (2003). TRUSS, a novel tumor necrosis factor receptor 1 scaffolding protein that mediates activation of the transcription factor NF-kappaB. Mol. Cell. Biol. *23*, 8334–8344.

Srinivasula, S.M., Ahmad, M., Ottilie, S., Bullrich, F., Banks, S., Wang, Y., Fernandes-Alnemri, T., Croce, C.M., Litwack, G., Tomaselli, K.J., et al. (1997). FLAME-1, a novel FADD-like anti-apoptotic molecule that regulates Fas/TNFR1-induced apoptosis. J. Biol. Chem. *272*, 18542–18545.

Stefansson, B., and Brautigan, D.L. (2006). Protein phosphatase 6 subunit with conserved Sit4-associated protein domain targets IkappaBepsilon. J. Biol. Chem. *281*, 22624–22634.

Stilmann, M., Hinz, M., Arslan, S.C., Zimmer, A., Schreiber, V., and Scheidereit, C. (2009). A nuclear poly(ADP-ribose)-dependent signalosome confers DNA damage-induced IkappaB kinase activation. Mol. Cell *36*, 365–378.

Stilo, R., Liguoro, D., Di Jeso, B., Formisano, S., Consiglio, E., Leonardi, A., and Vito, P. (2004). Physical and functional interaction of CARMA1 and CARMA3 with Ikappa kinase gamma-NFkappaB essential modulator. J. Biol. Chem. *279*, 34323–34331.

Stokes, A., Wakano, C., Koblan-Huberson, M., Adra, C.N., Fleig, A., and Turner, H. (2006). TRPA1 is a substrate for de-ubiquitination by the tumor suppressor CYLD. Cell. Signal. *18*, 1584–1594.

Sun, S.-C. (2008). Deubiquitylation and regulation of the immune response. Nat. Rev. Immunol. *8*, 501–511.

Sun, S.-C. (2012). The noncanonical NF-*κ*B pathway. Immunol. Rev. *246*, 125–140.

Sun, Q., Zachariah, S., and Chaudhary, P.M. (2003). The human herpes virus 8-encoded viral FLICE-inhibitory protein induces cellular transformation via NF-kappaB activation. J. Biol. Chem. *278*, 52437–52445.

Sun, Q., Matta, H., Lu, G., and Chaudhary, P.M. (2006). Induction of IL-8 expression by human herpesvirus 8 encoded vFLIP K13 via NF-kappaB activation. Oncogene *25*, 2717–2726.

Sun, W., Li, H., Yu, Y., Fan, Y., Grabiner, B.C., Mao, R., Ge, N., Zhang, H., Fu, S., Lin, X., et al. (2009a). MEKK3 is required for lysophosphatidic acid-induced NF-kappaB activation. Cell. Signal. *21*, 1488–1494.

Sun, W., Yu, Y., Dotti, G., Shen, T., Tan, X., Savoldo, B., Pass, A.K., Chu, M., Zhang, D., Lu, X., et al. (2009b). PPM1A and PPM1B act as IKKbeta phosphatases to terminate TNFalpha-induced IKKbeta-NF-kappaB activation. Cell. Signal. *21*, 95–102.

Sun, W., Wang, H., Zhao, X., Yu, Y., Fan, Y., Wang, X., Lu, X., Zhang, G., Fu, S., and Yang, J. (2010). Protein phosphatase 2A acts as a mitogen-activated protein kinase kinase kinase 3 (MEKK3) phosphatase to inhibit lysophosphatidic acid-induced IkappaB kinase beta/nuclear factor-kappaB activation. J. Biol. Chem. *285*, 21341–21348.

Suzuki, S., Singhirunnusorn, P., Mori, A., Yamaoka, S., Kitajima, I., Saiki, I., and Sakurai, H. (2007). Constitutive activation of TAK1 by HTLV-1 tax-dependent overexpression of TAB2 induces activation of JNK-ATF2 but not IKK-NF-kappaB. J. Biol. Chem. *282*, 25177–25181.

Takaesu, G., Kishida, S., Hiyama, a, Yamaguchi, K., Shibuya, H., Irie, K., Ninomiya-Tsuji, J., and Matsumoto, K. (2000). TAB2, a novel adaptor protein, mediates activation of TAK1 MAPKKK by linking TAK1 to TRAF6 in the IL-1 signal transduction pathway. Mol. Cell *5*, 649–658.

Takaesu, G., Surabhi, R.M., Park, K.-J., Ninomiya-Tsuji, J., Matsumoto, K., and Gaynor, R.B. (2003). TAK1 is critical for IkappaB kinase-mediated activation of the NF-kappaB pathway. J. Mol. Biol. *326*, 105–115.

Tang, E.D., Inohara, N., Wang, C.-Y., Nuñez, G., and Guan, K.-L. (2003). Roles for homotypic interactions and transautophosphorylation in IkappaB kinase beta IKKbeta) activation [corrected]. J. Biol. Chem. *278*, 38566–38570.

Taylor, R.C., Cullen, S.P., and Martin, S.J. (2008). Apoptosis: controlled demolition at the cellular level. Nat. Rev. Mol. Cell Biol. *9*, 231–241.

Tenev, T., Bianchi, K., Darding, M., Broemer, M., Langlais, C., Wallberg, F., Zachariou, A., Lopez, J., MacFarlane, M., Cain, K., et al. (2011a). The Ripoptosome, a signaling platform that assembles in response to genotoxic stress and loss of IAPs. Mol. Cell *43*, 432–448.

Tenev, T., Bianchi, K., Darding, M., Broemer, M., Langlais, C., Wallberg, F., Zachariou, A., Lopez, J., MacFarlane, M., Cain, K., et al. (2011b). The Ripoptosome, a signaling platform that assembles in response to genotoxic stress and loss of IAPs. Mol. Cell *43*, 432–448.

Thome, M., Schneider, P., Hofmann, K., Fickenscher, H., Meinl, E., Neipel, F., Mattmann, C., Burns, K., Bodmer, J.L., Schröter, M., et al. (1997). Viral FLICE-inhibitory proteins (FLIPs) prevent apoptosis induced by death receptors. Nature *386*, 517–521.

Thomson, W., Barton, A., Ke, X., Eyre, S., Hinks, A., Bowes, J., Donn, R., Symmons, D., Hider, S., Bruce, I.N., et al. (2007). Rheumatoid arthritis association at 6q23. Nat. Genet. *39*, 1431–1433.

Tie, F., Adya, N., Greene, W.C., and Giam, C.Z. (1996). Interaction of the human T-lymphotropic virus type 1 Tax dimer with CREB and the viral 21-base-pair repeat. J. Virol. *70*, 8368–8374.

Tokunaga, F., Sakata, S., Saeki, Y., Satomi, Y., Kirisako, T., Kamei, K., Nakagawa, T., Kato, M., Murata, S., Yamaoka, S., et al. (2009). Involvement of linear polyubiquitylation of NEMO in NF-kappaB activation. Nat. Cell Biol. *11*, 123–132.

Tokunaga, F., Nakagawa, T., Nakahara, M., Saeki, Y., Taniguchi, M., Sakata, S., Tanaka, K., Nakano, H., and Iwai, K. (2011). SHARPIN is a component of the NF-κB-activating linear ubiquitin chain assembly complex. Nature *471*, 633–636.

Tolani, B., Matta, H., Gopalakrishnan, R., Punj, V., and Chaudhary, P.M. (2014). NEMO is essential for Kaposi's sarcoma-associated herpesvirus-encoded vFLIP K13-induced gene expression and protection against death receptor-induced cell death, and its N-terminal 251 residues are sufficient for this process. J. Virol. *88*, 6345–6354.

Tran, K., Merika, M., and Thanos, D. (1997). Distinct functional properties of IkappaB alpha and IkappaB beta. Mol. Cell. Biol. *17*, 5386–5399.

Trompouki, E., Hatzivassiliou, E., Tsichritzis, T., Farmer, H., Ashworth, A., and Mosialos, G. (2003). CYLD is a deubiquitinating enzyme that negatively regulates NF-kappaB activation by TNFR family members. Nature *424*, 793–796.

Tsao, D.H., McDonagh, T., Telliez, J.B., Hsu, S., Malakian, K., Xu, G.Y., and Lin, L.L. (2000). Solution structure of N-TRADD and characterization of the interaction of N-TRADD and C-TRAF2, a key step in the TNFR1 signaling pathway. Mol. Cell *5*, 1051–1057.

Ueffing, N., Keil, E., Freund, C., Kühne, R., Schulze-Osthoff, K., and Schmitz, I. (2008). Mutational analyses of c-FLIPR, the only murine short FLIP isoform, reveal requirements for DISC recruitment. Cell Death Differ. *15*, 773–782.

Ueffing, N., Singh, K.K., Christians, A., Thorns, C., Feller, A.C., Nagl, F., Fend, F., Heikaus, S., Marx, A., Zotz, R.B., et al. (2009). A single nucleotide polymorphism determines protein isoform production of the human c-FLIP protein. Blood *114*, 572–579.

Ullenhag, G.J., Mukherjee, A., Watson, N.F.S., Al-Attar, A.H., Scholefield, J.H., and Durrant, L.G. (2007). Overexpression of FLIPL is an independent marker of poor prognosis in colorectal cancer patients. Clin. Cancer Res. *13*, 5070–5075.

De Valck, D., Jin, D.Y., Heyninck, K., Van de Craen, M., Contreras, R., Fiers, W., Jeang, K.T., and Beyaert, R. (1999). The zinc finger protein A20 interacts with a novel anti-apoptotic protein which is cleaved by specific caspases. Oncogene *18*, 4182–4190.

Valente, G., Manfroi, F., Peracchio, C., Nicotra, G., Castino, R., Nicosia, G., Kerim, S., and Isidoro, C. (2006). cFLIP expression correlates with tumour progression and patient outcome in non-Hodgkin lymphomas of low grade of malignancy. Br. J. Haematol. *132*, 560–570.

Vallabhapurapu, S., and Karin, M. (2009). Regulation and function of NF-kappaB transcription factors in the immune system. Annu. Rev. Immunol. *27*, 693–733.

Vallabhapurapu, S., Matsuzawa, A., Zhang, W., Tseng, P.-H., Keats, J.J., Wang, H., Vignali, D. a a, Bergsagel, P.L., and Karin, M. (2008). Nonredundant and complementary functions of TRAF2 and TRAF3 in a ubiquitination cascade that activates NIK-dependent alternative NF-kappaB signaling. Nat. Immunol. *9*, 1364–1370.

Valnet-Rabier, M.-B., Challier, B., Thiebault, S., Angonin, R., Margueritte, G., Mougin, C., Kantelip, B., Deconinck, E., Cahn, J.-Y., and Fest, T. (2005). c-Flip protein expression in Burkitt's lymphomas is associated with a poor clinical outcome. Br. J. Haematol. *128*, 767–773.

Vanlangenakker, N., Vanden Berghe, T., and Vandenabeele, P. (2012). Many stimuli pull the necrotic trigger, an overview. Cell Death Differ. *19*, 75–86.

Varfolomeev, E., Maecker, H., Sharp, D., Lawrence, D., Renz, M., Vucic, D., and Ashkenazi, A. (2005). Molecular determinants of kinase pathway activation by Apo2 ligand/tumor necrosis factor-related apoptosis-inducing ligand. J. Biol. Chem. *280*, 40599–40608.

Varfolomeev, E., Goncharov, T., Fedorova, A. V, Dynek, J.N., Zobel, K., Deshayes, K., Fairbrother, W.J., and Vucic, D. (2008). c-IAP1 and c-IAP2 are critical mediators of tumor necrosis factor alpha (TNFalpha)-induced NF-kappaB activation. J. Biol. Chem. *283*, 24295–24299.

Vaux, D.L., and Flavell, R. a (2000). Apoptosis genes and autoimmunity. Curr. Opin. Immunol. *12*, 719–724.

Verma, U.N., Yamamoto, Y., Prajapati, S., and Gaynor, R.B. (2004). Nuclear role of I kappa B Kinase-gamma/NF-kappa B essential modulator (IKK gamma/NEMO) in NF-kappa B-dependent gene expression. J. Biol. Chem. *279*, 3509–3515.

Verschuren, E.W., Klefstrom, J., Evan, G.I., and Jones, N. (2002). The oncogenic potential of Kaposi's sarcoma-associated herpesvirus cyclin is exposed by p53 loss in vitro and in vivo. Cancer Cell *2*, 229–241.

Vince, J.E., Pantaki, D., Feltham, R., Mace, P.D., Cordier, S.M., Schmukle, A.C., Davidson, A.J., Callus, B.A., Wong, W.W.-L., Gentle, I.E., et al. (2009). TRAF2 must bind to cellular inhibitors of apoptosis for tumor necrosis factor (tnf) to efficiently activate nf-{kappa}b and to prevent tnf-induced apoptosis. J. Biol. Chem. *284*, 35906–35915.

Wachter, T., Sprick, M., Hausmann, D., Kerstan, A., McPherson, K., Stassi, G., Bröcker, E.-B., Walczak, H., and Leverkus, M. (2004). cFLIPL inhibits tumor necrosis factor-related apoptosis-inducing ligand-mediated NF-kappaB activation at the death-inducing signaling complex in human keratinocytes. J. Biol. Chem. *279*, 52824–52834.

Walczak, H., Miller, R.E., Ariail, K., Gliniak, B., Griffith, T.S., Kubin, M., Chin, W., Jones, J., Woodward, a, Le, T., et al. (1999). Tumoricidal activity of tumor necrosis factor-related apoptosis-inducing ligand in vivo. Nat. Med. *5*, 157–163.

Walensky, L.D., Kung, A.L., Escher, I., Malia, T.J., Barbuto, S., Wright, R.D., Wagner, G., Verdine, G.L., and Korsmeyer, S.J. (2004). Activation of apoptosis in vivo by a hydrocarbon-stapled BH3 helix. Science *305*, 1466–1470.

Wan, Y.Y., Chi, H., Xie, M., Schneider, M.D., and Flavell, R. a (2006). The kinase TAK1 integrates antigen and cytokine receptor signaling for T cell development, survival and function. Nat. Immunol. *7*, 851–858.

Wang, C., Deng, L., Hong, M., Akkaraju, G.R., Inoue, J., and Chen, Z.J. (2001). TAK1 is a ubiquitin-dependent kinase of MKK and IKK. Nature *412*, 346–351.

Wang, L., Du, F., and Wang, X. (2008). TNF-alpha induces two distinct caspase-8 activation pathways. Cell *133*, 693–703.

Wang, W., Wang, S., Song, X., Sima, N., Xu, X., Luo, A., Chen, G., Deng, D., Xu, Q., Meng, L., et al. (2007a). The relationship between c-FLIP expression and human papillomavirus E2 gene disruption in cervical carcinogenesis. Gynecol. Oncol. *105*, 571–577.

Wang, X., Herr, R. a, Chua, W.-J., Lybarger, L., Wiertz, E.J.H.J., and Hansen, T.H. (2007b). Ubiquitination of serine, threonine, or lysine residues on the cytoplasmic tail can induce ERAD of MHC-I by viral E3 ligase mK3. J. Cell Biol. *177*, 613–624.

Wano, Y., Feinberg, M., Hosking, J.B., Bogerd, H., and Greene, W.C. (1988). Stable expression of the tax gene of type I human T-cell leukemia virus in human T cells activates specific cellular genes involved in growth. Proc. Natl. Acad. Sci. U. S. A. *85*, 9733–9737.

Wen, K.W., and Damania, B. (2010). Kaposi sarcoma-associated herpesvirus (KSHV): molecular biology and oncogenesis. Cancer Lett. *289*, 140–150.

Wertz, I.E., O'Rourke, K.M., Zhou, H., Eby, M., Aravind, L., Seshagiri, S., Wu, P., Wiesmann, C., Baker, R., Boone, D.L., et al. (2004). De-ubiquitination and ubiquitin ligase domains of A20 downregulate NF-kappaB signalling. Nature *430*, 694–699.

Wilson, T.R., McLaughlin, K.M., McEwan, M., Sakai, H., Rogers, K.M.A., Redmond, K.M., Johnston, P.G., and Longley, D.B. (2007). c-FLIP: a key regulator of colorectal cancer cell death. Cancer Res. *67*, 5754–5762.

Windheim, M., Stafford, M., Peggie, M., and Cohen, P. (2008). Interleukin-1 (IL-1) induces the Lys63-linked polyubiquitination of IL-1 receptor-associated kinase 1 to facilitate NEMO binding and the activation of IkappaBalpha kinase. Mol. Cell. Biol. *28*, 1783–1791.

Witt, J., Barisic, S., Schumann, E., Allgöwer, F., Sawodny, O., Sauter, T., and Kulms, D. (2009). Mechanism of PP2A-mediated IKK beta dephosphorylation: a systems biological approach. BMC Syst. Biol. *3*, 71.

Woronicz, J.D., Gao, X., Cao, Z., Rothe, M., and Goeddel, D. V (1997). IkappaB kinase-beta: NF-kappaB activation and complex formation with IkappaB kinase-alpha and NIK. Science *278*, 866–869.

Wright, A., Reiley, W.W., Chang, M., Jin, W., Lee, A.J., Zhang, M., and Sun, S.-C. (2007). Regulation of early wave of germ cell apoptosis and spermatogenesis by deubiquitinating enzyme CYLD. Dev. Cell *13*, 705–716.

Wu, X., and Sun, S.-C. (2007). Retroviral oncoprotein Tax deregulates NF-kappaB by activating Tak1 and mediating the physical association of Tak1-IKK. EMBO Rep. *8*, 510–515.

Wu, C.-J., Conze, D.B., Li, T., Srinivasula, S.M., and Ashwell, J.D. (2006a). Sensing of Lys 63-linked polyubiquitination by NEMO is a key event in NF-kappaB activation [corrected]. Nat. Cell Biol. *8*, 398–406.

Wu, Z.-H., Shi, Y., Tibbetts, R.S., and Miyamoto, S. (2006b). Molecular linkage between the kinase ATM and NF-kappaB signaling in response to genotoxic stimuli. Science *311*, 1141–1146.

Xia, X., Cui, J., Wang, H.Y., Zhu, L., Matsueda, S., Wang, Q., Yang, X., Hong, J., Songyang, Z., Chen, Z.J., et al. (2011). NLRX1 negatively regulates TLR-induced NF-κB signaling by targeting TRAF6 and IKK. Immunity *34*, 843–853.

Xia, Z.-P., Sun, L., Chen, X., Pineda, G., Jiang, X., Adhikari, A., Zeng, W., and Chen, Z.J. (2009). Direct activation of protein kinases by unanchored polyubiquitin chains. Nature *461*, 114–119.

Xiao, G., and Sun, S. (2000). Activation of IKKa and IKKb through their fusion with HTLV-I Tax protein. 5198–5203.

Xiao, G., Harhaj, E.W., and Sun, S.C. (2000). Domain-specific interaction with the I kappa B kinase (IKK)regulatory subunit IKK gamma is an essential step in tax-mediated activation of IKK. J. Biol. Chem. *275*, 34060–34067.

Xiao, G., Harhaj, E.W., and Sun, S.C. (2001a). NF-kappaB-inducing kinase regulates the processing of NF-kappaB2 p100. Mol. Cell *7*, 401–409.

Xiao, G., Cvijic, M.E., Fong, A., Harhaj, E.W., Uhlik, M.T., Waterfield, M., and Sun, S.C. (2001b). Retroviral oncoprotein Tax induces processing of NF-kappaB2/p100 in T cells: evidence for the involvement of IKKalpha. EMBO J. *20*, 6805–6815.

Xiao, G., Fong, A., and Sun, S.-C. (2004). Induction of p100 processing by NF-kappaB-inducing kinase involves docking IkappaB kinase alpha (IKKalpha) to p100 and IKKalpha-mediated phosphorylation. J. Biol. Chem. *279*, 30099–30105.

Xu, G., Tan, X., Wang, H., Sun, W., Shi, Y., Burlingame, S., Gu, X., Cao, G., Zhang, T., Qin, J., et al. (2010). Ubiquitin-specific peptidase 21 inhibits tumor necrosis factor alpha-induced nuclear factor kappaB activation via binding to and deubiquitinating receptor-interacting protein 1. J. Biol. Chem. *285*, 969–978.

Xu, G., Lo, Y.-C., Li, Q., Napolitano, G., Wu, X., Jiang, X., Dreano, M., Karin, M., and Wu, H. (2011). Crystal structure of inhibitor of κB kinase β. Nature *472*, 325–330.

Yamaoka, S., Courtois, G., Bessia, C., Whiteside, S.T., Weil, R., Agou, F., Kirk, H.E., Kay, R.J., and Israël, a (1998). Complementation cloning of NEMO, a component of the IkappaB kinase complex essential for NF-kappaB activation. Cell *93*, 1231–1240.

Yang, B.F., Xiao, C., Roa, W.H., Krammer, P.H., and Hao, C. (2003). Calcium/calmodulin-dependent protein kinase II regulation of c-FLIP expression and phosphorylation in modulation of Fas-mediated signaling in malignant glioma cells. J. Biol. Chem. *278*, 7043–7050.

Yang, B.-F., Xiao, C., Li, H., and Yang, S.-J. (2007). Resistance to Fas-mediated apoptosis in malignant tumours is rescued by KN-93 and cisplatin via downregulation of c-FLIP expression and phosphorylation. Clin. Exp. Pharmacol. Physiol. *34*, 1245–1251.

Yang, J., Boerm, M., McCarty, M., Bucana, C., Fidler, I.J., Zhuang, Y., and Su, B. (2000). Mekk3 is essential for early embryonic cardiovascular development. Nat. Genet. *24*, 309–313.

Yang, J., Lin, Y., Guo, Z., Cheng, J., Huang, J., Deng, L., Liao, W., Chen, Z., Liu, Z., and Su, B. (2001a). The essential role of MEKK3 in TNF-induced NF-kappaB activation. Nat. Immunol. *2*, 620–624.

Yang, J., Fan, G.H., Wadzinski, B.E., Sakurai, H., and Richmond, a (2001b). Protein phosphatase 2A interacts with and directly dephosphorylates RelA. J. Biol. Chem. *276*, 47828–47833.

Yang, Y., Xia, F., Hermance, N., Mabb, A., Simonson, S., Morrissey, S., Gandhi, P., Munson, M., Miyamoto, S., and Kelliher, M. a (2011). A cytosolic ATM/NEMO/RIP1 complex recruits TAK1 to mediate the NF-kappaB and p38 mitogen-activated protein kinase (MAPK)/MAPK-activated protein 2 responses to DNA damage. Mol. Cell. Biol. *31*, 2774–2786.

Yao, J., Kim, T.W., Qin, J., Jiang, Z., Qian, Y., Xiao, H., Lu, Y., Qian, W., Gulen, M.F., Sizemore, N., et al. (2007). Interleukin-1 (IL-1)-induced TAK1-dependent Versus MEKK3-dependent NFkappaB activation pathways bifurcate at IL-1 receptor-associated kinase modification. J. Biol. Chem. *282*, 6075–6089.

Ye, F.-C., Zhou, F.-C., Xie, J.-P., Kang, T., Greene, W., Kuhne, K., Lei, X.-F., Li, Q.-H., and Gao, S.-J. (2008). Kaposi's sarcoma-associated herpesvirus latent gene vFLIP inhibits viral lytic replication through NF-kappaB-mediated suppression of the AP-1 pathway: a novel mechanism of virus control of latency. J. Virol. *82*, 4235–4249.

Yeh, P.Y., Yeh, K.-H., Chuang, S.-E., Song, Y.C., and Cheng, A.-L. (2004). Suppression of MEK/ERK signaling pathway enhances cisplatin-induced NF-kappaB activation by protein phosphatase 4-mediated NF-kappaB p65 Thr dephosphorylation. J. Biol. Chem. *279*, 26143–26148.

Yin, M.J., and Gaynor, R.B. (1996). Complex formation between CREB and Tax enhances the binding affinity of CREB for the human T-cell leukemia virus type 1 21-base-pair repeats. Mol. Cell. Biol. *16*, 3156–3168.

Yoshida, M. (2005). Discovery of HTLV-1, the first human retrovirus, its unique regulatory mechanisms, and insights into pathogenesis. Oncogene *24*, 5931–5937.

You, M., Flick, L.M., Yu, D., and Feng, G.S. (2001). Modulation of the nuclear factor kappa B pathway by Shp-2 tyrosine phosphatase in mediating the induction of interleukin (IL)-6 by IL-1 or tumor necrosis factor. J. Exp. Med. *193*, 101–110.

Zandi, E., Rothwarf, D.M., Delhase, M., Hayakawa, M., and Karin, M. (1997). The IkappaB kinase complex (IKK) contains two kinase subunits, IKKalpha and IKKbeta, necessary for IkappaB phosphorylation and NF-kappaB activation. Cell *91*, 243–252.

Zarnegar, B.J., Wang, Y., Mahoney, D.J., Dempsey, P.W., Cheung, H.H., He, J., Shiba, T., Yang, X., Yeh, W.-C., Mak, T.W., et al. (2008). Noncanonical NF-kappaB activation requires coordinated assembly of a regulatory complex of the adaptors cIAP1, cIAP2, TRAF2 and TRAF3 and the kinase NIK. Nat. Immunol. *9*, 1371–1378.

Zhang, D.-W., Shao, J., Lin, J., Zhang, N., Lu, B.-J., Lin, S.-C., Dong, M.-Q., and Han, J. (2009a). RIP3, an energy metabolism regulator that switches TNF-induced cell death from apoptosis to necrosis. Science *325*, 332–336.

Zhang, H., Rosenberg, S., Coffey, F.J., He, Y.-W., Manser, T., Hardy, R.R., and Zhang, J. (2009b). A role for cFLIP in B cell proliferation and stress MAPK regulation. J. Immunol. *182*, 207–215.

Zhang, H., Zhou, X., McQuade, T., Li, J., Chan, F.K.-M., and Zhang, J. (2011). Functional complementation between FADD and RIP1 in embryos and lymphocytes. Nature *471*, 373–376.

Zhang, J., Stirling, B., Temmerman, S.T., Ma, C.A., Fuss, I.J., Derry, J.M.J., and Jain, A. (2006). Impaired regulation of NF-kappaB and increased susceptibility to colitis-associated tumorigenesis in CYLD-deficient mice. J. Clin. Invest. *116*, 3042–3049.

Zhang, J., Clark, K., Lawrence, T., Peggie, M.W., and Cohen, P. (2014). An unexpected twist to the activation of IKKβ: TAK1 primes IKKβ for activation by autophosphorylation. Biochem. J. *461*, 531–537.

Zhang, S.Q., Kovalenko, A., Cantarella, G., and Wallach, D. (2000). Recruitment of the IKK signalosome to the p55 TNF receptor: RIP and A20 bind to NEMO (IKKgamma) upon receptor stimulation. Immunity *12*, 301–311.

Zhang, X., Zhang, L., Yang, H., Huang, X., Otu, H., Libermann, T. a, DeWolf, W.C., Khosravi-Far, R., and Olumi, A.F. (2007). c-Fos as a proapoptotic agent in TRAIL-induced apoptosis in prostate cancer cells. Cancer Res. *67*, 9425–9434.

Zhao, Q. (1999). Mitogen-activated Protein Kinase/ERK Kinase Kinases 2 and 3 Activate Nuclear Factor-kappa B through Ikappa B Kinase-alpha and Ikappa B Kinase-beta. J. Biol. Chem. *274*, 8355–8358.

Zhao, L.J., and Giam, C.Z. (1992). Human T-cell lymphotropic virus type I (HTLV-I) transcriptional activator, Tax, enhances CREB binding to HTLV-I 21-base-pair repeats by protein-protein interaction. Proc. Natl. Acad. Sci. U. S. A. *89*, 7070–7074.

Zhao, L., Yue, P., Khuri, F.R., and Sun, S.-Y. (2013). mTOR complex 2 is involved in regulation of Cbl-dependent c-FLIP degradation and sensitivity of TRAIL-induced apoptosis. Cancer Res. *73*, 1946–1957.

Zheng, C., Yin, Q., and Wu, H. (2011). Structural studies of NF-κB signaling. Cell Res. *21*, 183–195.

Zhong, H., May, M.J., Jimi, E., and Ghosh, S. (2002). The phosphorylation status of nuclear NF-kappa B determines its association with CBP/p300 or HDAC-1. Mol. Cell *9*, 625–636.

Zhuo, S., Clemens, J.C., Hakes, D.J., Barford, D., and Dixon, J.E. (1993). Expression, purification, crystallization, and biochemical characterization of a recombinant protein phosphatase. J. Biol. Chem. *268*, 17754–17761.